20 May 2003
Amended 5 July 2004

BACKGROUND DOCUMENTS TO EN 1992-1-2
Eurocode 2: Design of concrete structures –
Part 1-2: General rules – Structural fire design

Background documentation consists of this main document, annexes listed hereafter and references to commonly available documents.

PROJECT TEAM MEMBERS:

Dr. Yngve Anderberg	Fire Safety Design AB	Sweden	Permanently invited
Dr.Ing. Nils Erik Forsén	Multiconsult AS	Norway	
Mr. Tauno Hietanen	Confederation of Finnish Construction Industries RT	Finland	Convenor
Mr. José Maria Izquierdo	INTEMAC	Spain	
Mr. Alain Le Duff	CSTB	France	
Dr.-Ing. Ekkehard Richter	Institut für Baustoffe, Massivbau und Brandschutz der TU Braunschweig	Germany	
Mr. Robin T. Whittle	Ove Arup & Partners 13, Fitzroy Street	United Kingdom	Technical secretary

Ex-officio:

Prof.Dr. Horst Bossenmayer	Deutsches Institut für Bautechnik	Germany	TC 250 chairman
Dr.-Ing. H.-U. Litzner	Deutscher Beton- und Bautechnik Verein E.V.	Germany	TC 250/SC 2 chairman
Mr. Kruppa	CTICM	France	TC 250 Horizontal Group Fire convenor

ANNEXES:

General documents and documents related to sections 1 and 2:

BDA 1.1 CEN/TC 250/SC 2 N 195 *Background document for ENV 1992-1-2: 1995.*
BDA 1.2 CEN/TC 250 HGF N 221 *Insulation criteria for "natural" fire development situation - Note to FRG*

Documents related to Section 3 Material properties:

BDA 3.1 CEN/TC 250/SC 2/PT N 150 *Background documentation for thermal conductivity of concrete*
BDA 3.2 CEN/TC 250/SC 2/PT N 176 *Comparison of thermal properties 100 mm slab*
BDA 3.3 CEN/TC 250/SC 2/PT N 178 *Thermal properties of concrete – Additional comparison and response*
BDA 3.4 CEN/ TC 250 HGF N 219 *Special meeting on thermal properties of concrete, Delft 15 May 2002*
BDA 3.5 *Background document for the new proposal of the lower limit for thermal conductivity, CERIB/DPO/DCO/FR, 03/06/02*
BDA 3.6 *Temperature comparisons CERIB/DPO/DCO/FR*
BDA 3.7 *EC 4 Background document for thermal laws of concrete EC4-1-2/75, Observations and remarks, Tauno Hietanen, 2002-05-08*
BDA 3.8 *New proposal for the mechanical properties of prestressing steel (wires and strands) at elevated temperatures, CERIB, 2003-06-13*
BDA 3.9 *Common new proposal from the University of Liege and CERIB for the general and simplified models for the mechanical properties of prestressing steel (wires and strands) at elevated temperatures, September 12th 2003*

Documents related to Section 4 Design procedures

BDA 1.1 See above

Documents related to Section 5 Tabulated data

BDA 5.1 *Comparison of fire resistance of columns in Tabulated data to test results*

BDA 5.2 *Background for Tabulated data Method A for columns*

BDA 5.3 *Comparison of Belgian simplified calculation methods and ENV 1992-1-2 Tabulated data to circular column test results*

BDA 5.4 CEN/TC 250/SC 2/PT Doc N 35 *Flat slabs under fire, redistribution of the internal forces and punching tests, Prof. Kordina, Abstract 1993*

Documents related to Section 6 High strength concrete

BDA 6.1 *Mechanical behaviour of HPC at high temperature, Pirre Pimienta, Izabela Hager*

BDA 6.2 Tunnel fire safety, Kees Both, TNO

DRAFTS AND ASSESSMENTS

ENV 1992-1-2: 1995 Eurocode 2: Design of concrete structures – Part 1-2: General rules – Structural fire design

Assessment of comments on ENV 1992-1-2: 1995
TC 250/SC 2 N 283 (= PT Doc N 40, 1999-07-08)

prEN 1992-1-2, 1st informal draft , January 2000
TC 250/SC 2 N 316 (= PT Doc N 72)

Assessment of comments on 1st informal draft
TC 250/SC 2 PT Doc N 132, 2001-07-10 rev

prEN 1992-1-2, 1st draft , October 2000
TC 250/SC 2 N 351

Assessment of comments on 1st draft
TC 250/SC 2 PT Doc N 139, 2001-07-10 rev

prEN 1992-1-2, 2nd draft , July 2001
TC 250/SC 2 N 404

Written comments were not asked, discussion at PT + NTC meeting 12/13 September 2001 in Paris

prEN 1992-1-2, Final draft , December 2001
TC 250/SC 2 N 418

Comments were discussed at PT + NTC meeting 11/12 March in Berlin

prEN 1992-1-2, Revised Project Team Final draft , April 2002
TC 250/SC 2 N 447

Comments were discussed at TC 250/SC 2 meeting 1/2 July 2002 in Milan.

FOREWORD

Foreword follows TC 250 document N 250 giving general guidance for all Eurocodes, and especially Annex K Model clauses for fire parts, and recommendations of TC 250 Horizontal Group Fire.

Table 0.1 has been added to explain the use of alternative methods, and it is specific for concrete structures.

SECTION 1 GENERAL

Section 1 follows TC 250 document N 250 giving general guidance for all Eurocodes, and especially Annex K Model clauses for fire parts, and recommendations of TC 250 Horizontal Group Fire.

SECTION 2 BASIS OF DESIGN

Section 2 follows TC 250 document N 250 giving general guidance for all Eurocodes, and especially Annex K Model clauses for fire parts, and recommendations of TC 250 Horizontal Group Fire.

2.1.3 Parametric fire exposure

Background for the temperature limits for insulation criteria is given in TC 250 Horizontal Group Fire Document N 221.

Reference:
BDA 1.2 CEN/TC 250 HGF N 221 *Insulation criteria for "natural" fire development situation - Note to FRG*

2.2 Actions

2.2 (2) Resulting emissivity has been changed to surface emissivity due to changes in EN 1991-1-2 (introduction of plate thermometer in testing).

2.3 Design values of material properties

Recommended values for partial safety factors = 1,0 are based on work done in Horizontal Group Fire during ENV preparation. Higher probability of failure can be accepted in fire situation than in Ultimate Limit State design at normal temperature. Safety factors 1,0 were calibrated to give approximately same results as fire tests.

Reference:
BDA 1.1 CEN/TC 250/SC 2 N 195 *Background document for ENV 1992-1-2: 1995.*

2.4.2 Member analysis

Clarification for load level and reduction:

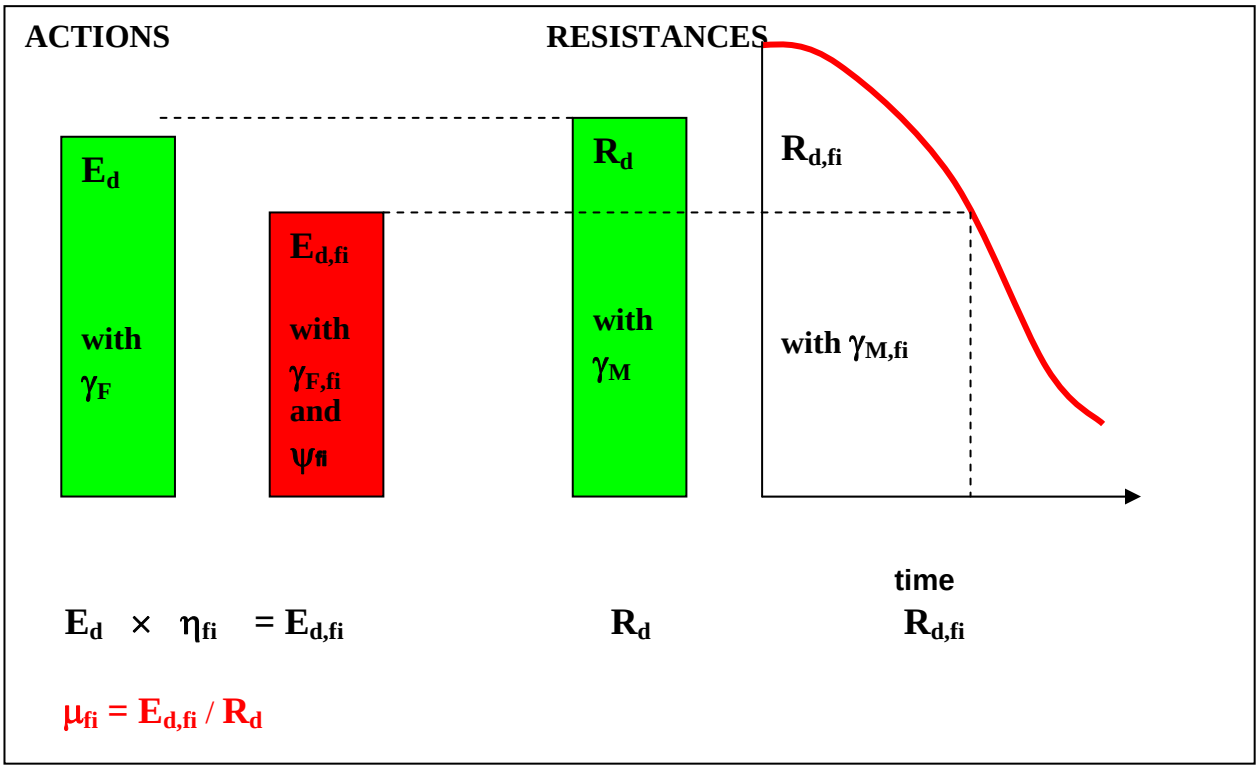

$\mathbf{E_d}$ and $\mathbf{R_d}$ are known from normal temperature design.

η_{fi} is defined in 2.4.2, with three possibilities
- calculate accurate value, see EN 1991-1-2 section 4
- calculate by using simplified equations in 2.4.2(3)
- use the safe side recommended value $\eta_{fi} = 0,7$ (Note in 2.4.2(3))

η_{fi} does not take into account if the structure is fully loaded ($E_d = R_d$) or not ($E_d < R_d$)

μ_{fi} takes into account if the structure is not fully loaded ($E_d < R_d$)

Tabulated data is based on **reference load level** $\eta_{fi} = 0,7$, see 5.2(3), safe side value assuming that the structure is fully loaded, unless otherwise stated in the relevant clauses.

SECTION 3 MATERIAL PROPERTIES

3.1 General

Lightweight aggregate concrete:

Material properties are not given, due to wide range of lightweight aggregates and concrete properties.

This does not exclude use of lightweight aggregates, see e.g. Scope and Tabulated Data 5.1(2).

3.2.2 Strength and deformation properties of concrete

The relative concrete strength at 100°C was changed (compared to ENV) to 1,00, and a small corresponding modification was made at 200°C. The reason for this change was to be in line with Part 1 of Eurocode 2, where material properties are valid up to 100°C.

Further justification can be found e.g. in CEB N° 208 *Fire design of concrete structures, July 1991*, Fig. 7.2.5 where recommended practical design curve for compressive strength has the full strength up to 200°C.

3.2.3 Strength and deformation properties of reinforcing steel

A new class X was introduced, as requested in Finnish comments, PT document N 180. There is requirement in Finland to test reinforcing steel strength at elevated temperatures, and strength reduction in class X is derived from the Finnish requirements.

3.2.4 Strength and deformation properties of prestressing steel

A new class A was introduced, justified in Annexes BDA 3.8 and BDA 3.9.

References:

BDA 3.8 *New proposal for the mechanical properties of prestressing steel (wires and strands) at elevated temperatures, CERIB, 2003-06-13*

BDA 3.9 *Common new proposal from the University of Liege and CERIB for the general and simplified models for the mechanical properties of prestressing steel (wires and strands) at elevated temperatures, September 12th 2003*

3.3 Thermal and physical properties of concrete

Specific heat and thermal conductivity of concrete have been changed. In 1st draft October 2000 specific heat and thermal conductivity were taken from the Swedish design handbook. Background documents for these values are comparisons of measured and calculated temperatures in Project Team documents:

References:

BDA 3.1 PT N 150 *Background documentation for thermal conductivity of concrete*
BDA 3.2 PT N 176 *Comparison of thermal properties 100 mm slab*
BDA 3.3 PT N 178 *Thermal properties of concrete – Additional comparison and response*

However, convenor of Project Team EN 1994-1-2 *Fire design of steel-concrete-composite structures* could not accept the new thermal properties, arguing that the ENV properties give good results for composite structures, and a lot of new calculations would be required if the thermal properties were changed.

After discussions in TC 250 Horizontal Group Fire, a special meeting was held and the outcome of the meeting was confirmed by TC 250 resolution in May 2002. The result was to give a range for thermal conductivity, where the lower limit is calibrated to temperatures measured in concrete structures, and the upper limit is calibrated to temperatures measured in steel-concrete composite structures.

The agreement is given in HGF document N 219 (= TC 250 N 528-rev)

Reference:

BDA 3.4 TC 250 HGF N 219 *Special meeting on thermal properties of concrete, Delft 15 May 2002*

Additional calibrations for the lower limit are given documents from CERIB (F):

Reference:

BDA 3.5 *Background document for the new proposal of the lower limit for thermal conductivity, CERIB/DPO/DCO/FR, 03/06/02*

Reference:

BDA 3.6 *Temperature comparisons CERIB/DPO/DCO/FR*

Calibrations for steel-concrete composite structures are given in TC 250/SC 4/PT 1-2 internal document N75. Observations and remarks on this document are presented in:

Reference:

BDA 3.7 *EC 4 Background document for thermal laws of concrete EC4-1-2/75, Observations and remarks, Tauno Hietanen, 2002-05-08*

Summary of conclusions in the reference documents

- The proposed “prEN” curves (Swedish thermal conductivity) are in good agreement in comparison to measured temperatures and temperatures given in CEB 145 in Documents BDA 3.1 and BDA 3.2.
- According to French (CSTB) slab tests the proposed “prEN” curves are in good agreement with measured temperatures near the exposed surface where the reinforcement is located, but deeper in the cross-section they give lower temperatures than measured, and higher surface temperatures than measured, BDA 3.3

- This indicates that a small increase of thermal conductivity will give optimum results. New proposal from France , calibrated in BDA 3.5 gives very good agreement.
- The lower limit of thermal conductivity is therefore recommended for concrete structures. Temperature profiles in Annex A of EN 1992-1-2 are based on the lower limit.
- For steel-concrete composite structures EN 1994-1-2 will recommend the upper limit. It seems to give better agreement with measured temperatures, but the scatter of temperatures is large. A possible clarification may be differences in modelling the thermal transfer, and composite structures being more complicated to model.

SECTION 4 DESIGN PROCEDURES

4.2 Simplified calculation method

Two methods are given:

1. 500°C isotherm method , developed in Sweden, and included in CEB Bulletin

Reference: CEB N° 208 *Fire design of concrete structures, July 1991*

2. Zone method, developed in Denmark, and included in ENV 1992-1-2

Reference:
BDA 1.1 CEN/TC 250/SC 2 N 195 *Background document for ENV 1992-1-2: 1995.*

4.2.4.3 Strength reduction of steel

In figures 4.2a and 4.2b the strength reduction depends on the strain. If 2 % steel strain is possible in the structure (e.g. in most beams and slabs) strength reduction $f_{sy,\theta}/f_{yk}$ in Tables 3.2a and 3.2b may be used.

If 2 % steel strain can not be achieved (e.g. some beams with high reinforcement ratio, or compression reinforcement) a safe side assumption is made: strength corresponding 0,2 % proof strain is given in figures 4.2a and 4.2b, as shown in the figures BD 4.1 to 4.3 below.

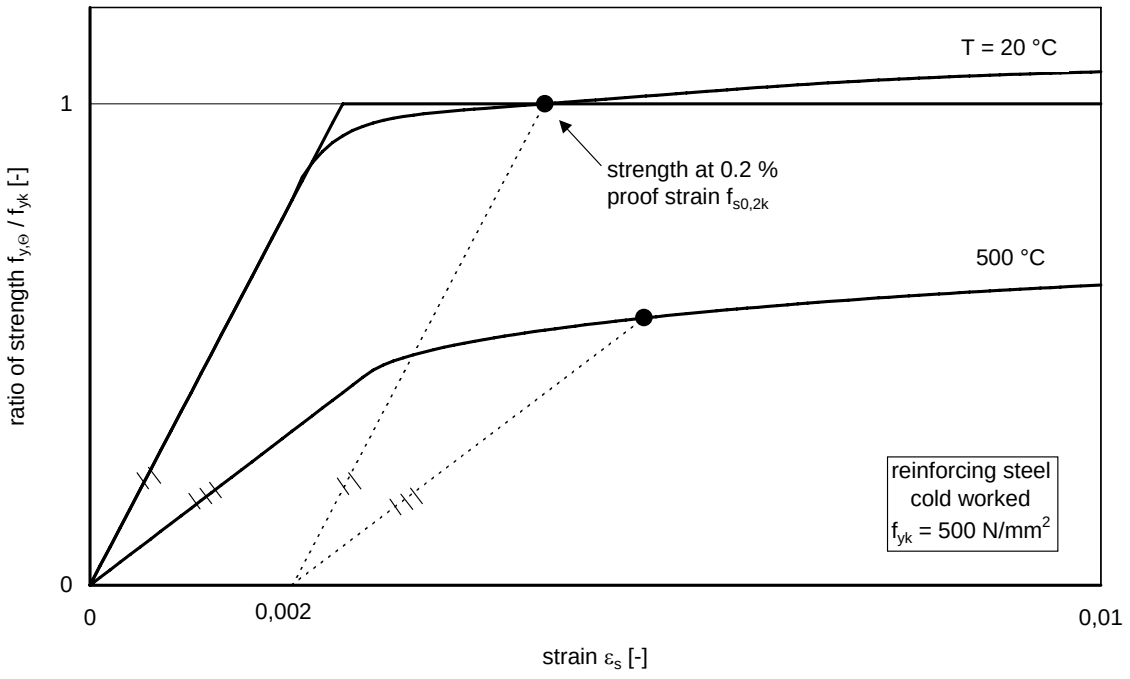

Figure BD 4.1: Principle model for determination of strength at 0.2% proof strain

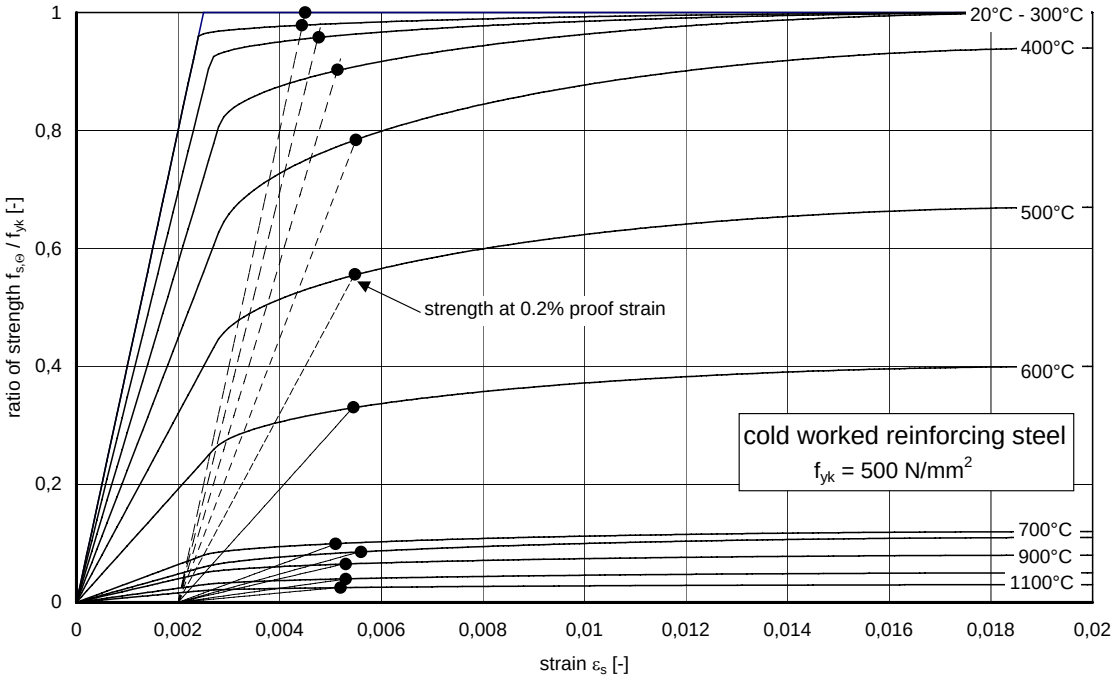

Figure BD 4.2: Strength at 0.2% proof strain of cold worked reinforcing steel

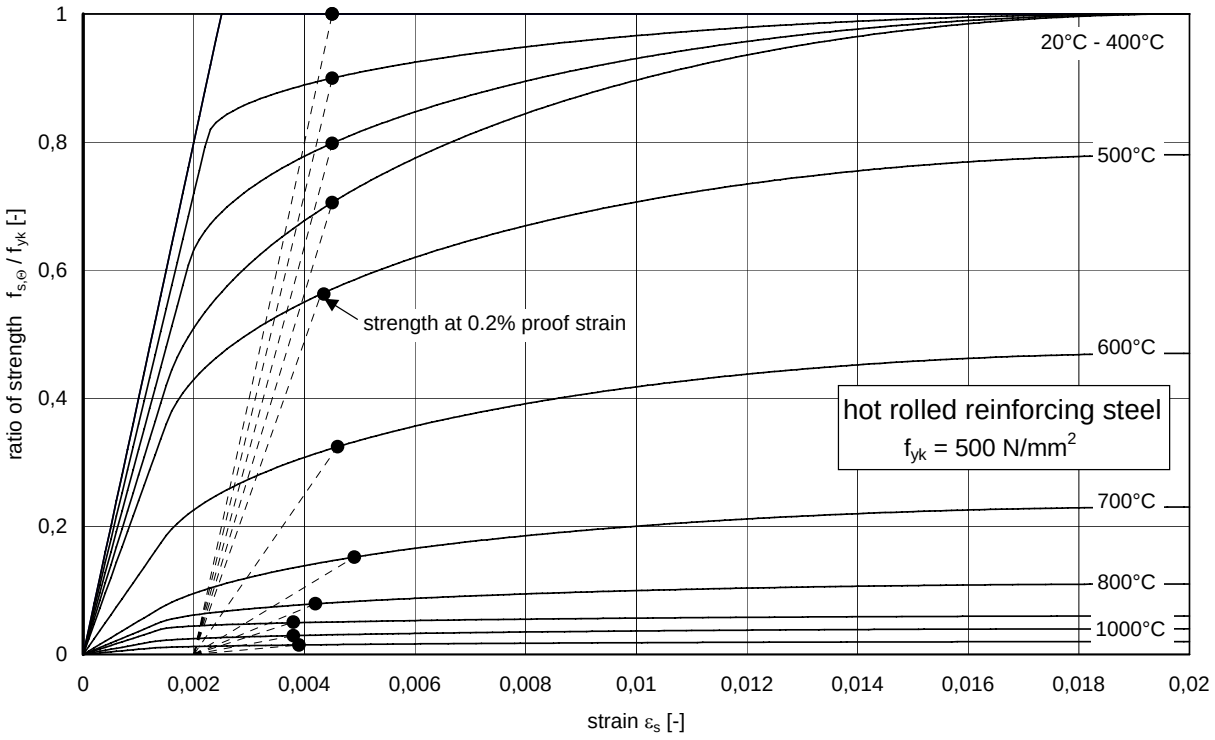

Figure BD 4.3: Strength at 0.2% proof strain of hot rolled reinforcing steel

SECTION 5 TABULATED DATA

5.2 GENERAL DESIGN RULES

Reference load level

5.2(3) See background for 2.4.2.

When tabulated data is used for CE-marking of products like precast concrete elements, reference load level for R-classification should be given, if deviating from $\eta_{fi} = 0,7$.

It may also be practical to give several fire resistance times for different load levels, e.g. Resistance to fire: R60 for $\eta_{fi} = 0,7$
R90 for $\eta_{fi} = 0,5$

Reference curves for critical temperature

Reference curve 1 for reinforcing steel in Figure 5.1 compared to curves for simplified calculation methods in figure 4.2a, and reference curves 2 and 3 compared to curves in Figure 4.3 are presented below:

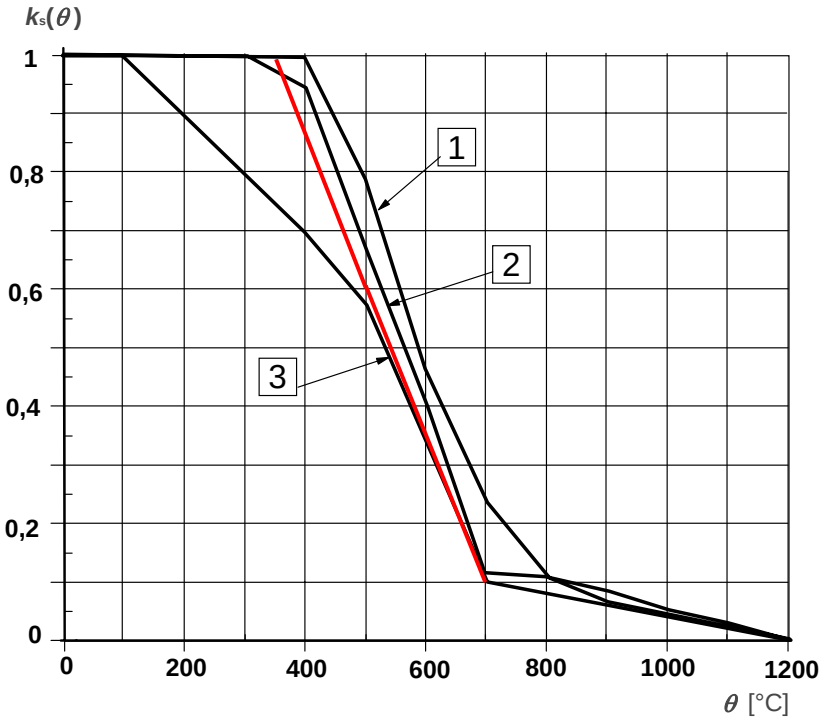

Curve 1 : Tension reinforcement (hot rolled) for strains $\varepsilon_{s,fi} \geq 2\%$

Curve 2 : Tension reinforcement (cold worked) for strains $\varepsilon_{s,fi} \geq 2\%$

Curve 3 : Compression reinforcement and tension reinforcement for strains $\varepsilon_{s,fi} < 2\%$

Figure BD 5.1: Coefficient $k_s(\theta)$ allowing for decrease of characteristic strength (f_{yk}) of tension and compression reinforcement (Class N)

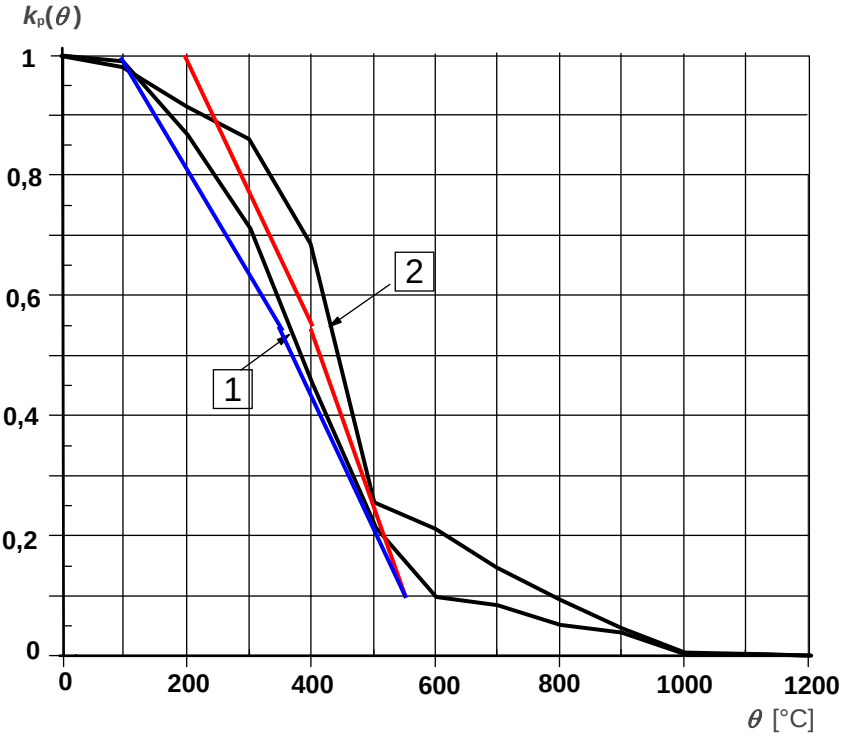

and

steel

Curve (1): Cold worked prestressing steel (wires strands)

Curve (2): Quenched and tempered prestressing (bars)

Figure BD 5.2: Coefficient $k_p(\theta)$ allowing for decrease of characteristic strength ($0.9 \cdot f_{pk}$) of prestressing steel

Adjustment of axis distance for critical temperature deviating from 500°C

Rules for increasing axis distances for prestressing steel in 5.2 (5) and Equation (5.3) in 5.2 (7) are approximations:

(5) For prestressing tendons the critical temperature for bars is assumed to be 400°C and for strands and wires to be 350°C. If no special check according to (6) is made in prestressed tensile members, beams and slabs the required axis distance a should be increased by:
10 mm for prestressing bars, corresponding to θ_{cr} = 400°C
15 mm for prestressing wires and strands, corresponding to θ_{cr} = 350°C

(7)

$$\Delta a = 0{,}1\,(500 - \theta_{cr}) \text{ (mm)} \qquad (5.3)$$

Figure BD 5.3 illustrates the difference between approximation (straight lines) and temperature profiles for slabs in Annex A. At 500°C the straight lines correspond to minimum required axis distance for one way slabs (Table 5.8, column 3).

The straight lines do not give lower temperatures than the temperature profiles (Axis distances below 20°C are disregarded as impossible in practice), except for R 240 with steel temperatures below 400°C, i.e. the approximation is on the safe side in the temperature range $350^oC<\theta_{cr}<700^oC$, and when used for the minimum axis requirements given in tabulated data, as stated in 5.2 (8).

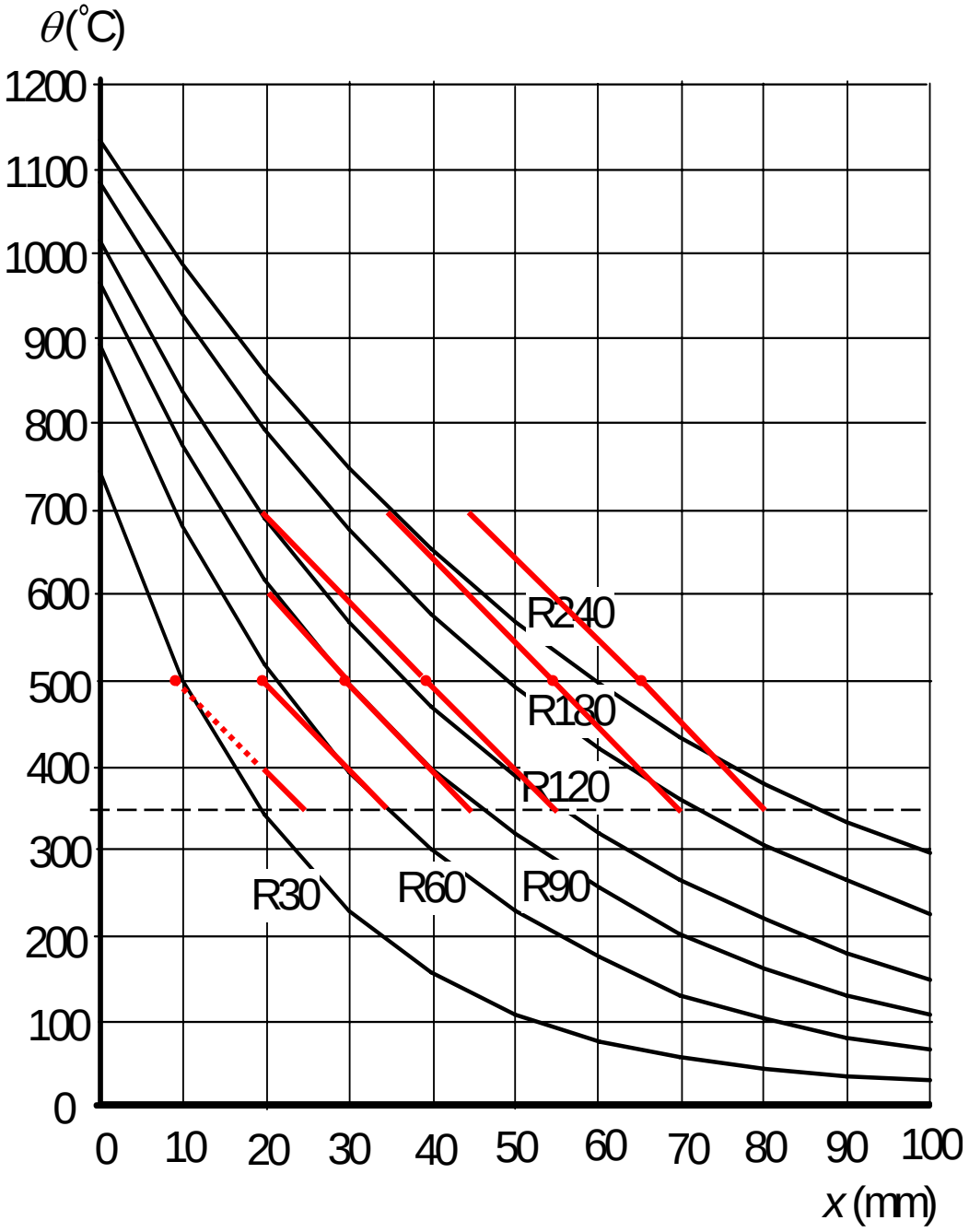

Figure BD 5.3: Adjustment of axis distance of slabs for critical temperature deviating from 500°C

5.3 COLUMNS

Tabulated data for columns in ENV was considered in some national comments to be unsafe, especially for slender columns. Tabulated data in ENV was replaced by two alternative methods.

Method A was developed in Belgium for the National Application Document. It is based on analysis of 76 fire tests from 4 different laboratories. Background is given in PT document N 169.

Method B is based on calculations as described in Annex B.3. More comprehensive Tabulated data in Annex C is based on the same calculation method.

Both methods have been compared to test results in Background documents. Method B is more conservative, and both methods provide sufficient safety.

Both methods in normative part 5.3 have limitations in field of application. Method A is limited to effective lengths and eccentricities which are covered by test results. Method B is simplification of more comprehensive Tabulated data in informative Annex C, covering most columns in multi-storey buildings.

In the background documents mentioned below, "NAD1" refers to Method A, "prEN" refers to Method B, and "NAD2" refers to a calculation method in Belgian NAD, but this method is not included in EN 1992-1-2.

Reference:

BDA 5.1 *Comparison of fire resistance of columns in Tabulated data to test results*
BDA 5.2 *Background for Tabulated data Method A for columns*
BDA 5.3 *Comparison of Belgian simplified calculation methods and ENV 1992-1-2 Tabulated data to circular column test results*

5.4 WALLS

Fire walls

Rules for fire walls have been added, because there is European M – Mechanical action classification in

Commission decision implementing Council Directive 89/106/EEC as regards the classification of the resistance to fire performance of construction products, construction works and parts thereof,

and in

EN 13501-2 fire classification of construction products and building elements – Part 2: Classification using data from fire resistance tests, excluding ventilation services

Test method is given in:

EN 1363-2 Fire resistance tests- Part 2: Alternative and additional procedures

M-class is additional to REI or EI, designation REI-M or EI-M.

It depends on the national fire regulations if M – Mechanical action is required for fire walls.

Reference: Tabulated data for fire walls is taken from DIN 4102 Teil 4.

5.5 TENSILE MEMBERS

Table for tensile members in ENV is identical with table for simply supported beams, but without intermediate values, and with two exceptions: for R 30 200/10 and for R 90 400/45.

When $A_c \geq 2b^2_{min}$, the same axis distances should be valid for tensile members, beams exposed on all sides and flanges of I shaped beams.

Therefore table for tensile members is replaced by reference to table for simply supported beams.

5.6 BEAMS

Axis distance of I shaped beams

Equation (5.7) in in 5.6.1 (6):

Increase of axis distance of I shaped beams where the actual width of the bottom flange b exceeds the limit 1,4 b_w

$$a_{eff} = a\,(1{,}85 - \frac{d_{eff}}{b_{min}}\sqrt{\frac{b_w}{b}}) \geq a \qquad (5.7)$$

The reason for this increase is that the bottom flange is heated also from the top of the flange and due to the small dimensions of the bottom flange heating conditions are more severe than assumed for beam tables. However, in some cases equation (5.7) gives higher axis distances than required for beams exposed on all sides.

This is not reasonable, and therefore the validity of the equation has been limited to:

and $b \times d_{eff} < 2b^2_{min}$ …

With this limitation, the following rule in ENV has been deleted as unnecessary:

(7) For flanges with $b > 3{,}5\ b_w$ (see (6) above for definitions) 4.2.6.4 applies.

Because when $b \times d_{eff} \geq 2b^2_{min}$ and $d_{eff} \geq b_{min}$, requirements for beams exposed on all sides (referred to in ENV) are fulfilled, and axis distances given in tables 5.5 and 5.6 apply.

Minimum width of continuous beams

Minimum width of continuous beam (Table 4.6) have been changed from the ENV values. The reason for increased minimum width in ENV (compared to CEB 208) was found to be risk for shear failure due to moment re-distribution.

Because this risk is covered by rule (6) and table 5.7, minimum width of continuous beams can be the same as for simply supported beams.

Minimum web thickness

Three classes are introduced. Class WA is the same as in ENV, class WB was requested by Sweden and class WC by Spain.

5.7 SLABS

Flat slabs

Minimum thickness of flat slabs in REI 60 has been changed from 200 mm in ENV to 180 mm. Justification with reference to PT Doc N 35 is given below

Reference:
BD 5.4 PT Doc N 35 *Flat slabs under fire, redistribution of the internal forces and punching tests, Prof. Kordina, Abstract 1993*

10 slabs with thickness 200 mm and 4 slabs with thickness 150 mm were tested for punching.

Investigations show redistribution of bending moments and increase of column loads at first inside column. This was taken into account by increasing the load during first 30 minutes in the test, approximately by 50 %.

Short summary on test results (see figures 6 and 7 in N 35):

- Two slabs with thickness 150 mm failed before 30 min during the increase of loads: failure load versus design load 1,31 and 1,37.
- Four slabs with thickness 200 mm failed before 30 min during the increase of loads: failure load versus design load 1,07, 1,23, 1,36 and 1,39.
- fire resistance of all the other slabs was at least 70 min, the best 180 min without failure (150 mm thickness)
- there seems to be correlation between load level and fire resistance (see Figure 7), with two exceptions, one bad (22 min with low load) and one good (120 min with very high load).

The test arrangements were on the safe side, because there was no restraint for longitudinal expansion (in practice it increases shear capacity), neither membrane effect.

SECTION 6 HIGH STRENGTH CONCRETE

Background for the choice of strength reduction classes is given in:

Reference:
BDA 6.1 *Mechanical behaviour of HPC at high temperature, Pirre Pimienta, Izabela Hager*

Test results on influence of different amounts of polypropylene fibres on spalling are given in document:

Reference:
BDA 6.2 *Tunnel fire safety, Kees Both, TNO*

Additional Project Team documents:

N 29		Design handbook for high performance concrete, Section 3.12 Fire design, Yngve Anderberg, Jens Oredsson, Bödvar Thomasson, 11.06.97, Rev A
N 30		Spalling phenomena of HPC and OC, Yngve Anderberg
N 31	p	Extract from NS 3473:1993, Reduction of concrete compressive strength at high temperatures
N 32	p	Mechanical properties of high strength concrete at high temperatures – a strain model, Ulf Göransson, 19.03.96
N 37	p	Extract from Finnish code by 34 High strength concrete, Supplementary rules, Fire design
N 49		Spalling considerations from national comments, Le Duff 1999-08-20
N 50		Spalling, Comments and assessments, Le Duff 1999-08-20
N 67	p	CSTB, Test results on high strength concrete
N 68	p	HITECO, Task 7 Prenormative action, final report
N 69	p	HITECO, Task 7.2 Background for task 7
N 80	p	Articles from Concrete, March 2000: High-strength concrete and fire, High-grade concrete columns in fire

June 1995

12 p. + Annex

BACKGROUND DOCUMENT

ENV 1992-1-2: STRUCTURAL FIRE DESIGN OF CONCRETE STRUCTURES

This document has been prepared by the Project Team Structural Fire Design of CEN/TC 250/SC 2.

The aim of this document is to give background information and references which could be useful in preparing National Application Documents, for use of the standard and in transferring it to an EN.

Project Team started the work autumn 1991 on the basis of 1990 Draft, prepared by an expert group for the Commission of European Communities, and national comments received on it. Drafts August 1992 and May 1993 were prepared for national comments, and voting Draft prENV was completed in October 1993. It was approved as ENV at SC 2 meeting in January 1994 with changes made at the meeting.

Convenor of the Project Team also participated in CEN/TC 250 Horizontal Group of Structural Fire Design.

Following experts have participated in the work of the Project Team:

NOMINATED EXPERTS

Mr. T. Hietanen	Convenor
Finnish Association of Construction Product Industries	
P.O. Box 11	Phone +358 0 1728 4435
FIN-00131 HELSINKI	Fax +358 0 179 588
Prof. J. Dotreppe	
Université de Liége	
Institut du Génie Civil	
Quai Banning, 6	Phone +32 41 669 351
B-4000 LIEGE	Fax +32 41 669 534
Mr. A. Gerritse	
Stichting CUR	
Büchnerweg 3	
P.O. Box 420	Phone +31 1820 396 00
NL-2800 AK GOUDA	Fax +31 1820 300 46
Dr. Ekkehard Richter from 1992	
(Ms Lore Krampf until 1992)	
TU Braunschweig	
IBMB	
Beethovenstraße 52	Phone +49 531 391 5483/31
D-3300 BRAUNSCHWEIG	Fax +49 531 391 4573
Mr. R.T. Whittle	
Ove Arup and Partners	
13 Fitzroy Street	Phone +44 171 465 3229
GB-LONDON W1P 6BQ	Fax +44 171 465 3669
Prof. Ing. S. Tattoni	
Dipart. di Ingegneria Strutt.	
Piazza Leonardo da Vinci 32	Phone +39 2 2399 4385
I-20133 MILANO	Fax +39 2 2399 4399
	2399 4220

PERMANENTLY INVITED EXPERTS

Ass.Prof. Ph.D. K. Hertz	
Techn. University of Denmark	
Building 118	Phone +45 45 93 4431
DK-2800 LYNGBY	Fax +45 45 93 4430
J. Izquierdo	
Intemac	
Monte Esquinza, 30, 5° D	Phone +34 1 410 5158
E-28010 MADRID	Fax +34 1 410 2580

Mr. J. Mathez
BNTEC
9 rue La Perouse
F-75784 PARIS CEDEX 16

Phone +33 1 4069 5259
Fax +33 1 4553 5877

SC 2 CHAIRMAN

Dr. U. Litzner
Deutscher Beton-Verein E.V.
Postfach 2126
Bahnhofstrasse 61
D-65011 WIESBADEN

Phone +49 611 140 3137
Fax +49 611 140 3150

BASIC PRINCIPLES

Chapter 1 Introduction and Chapter 2 Basic principles are based on "Model Clauses" agreed by CEN/TC 250 Horizontal Group Structural Fire Design. Model Clauses have been followed in all Fire Parts of Eurocodes 2 - 6 as far as relevant.

2.1 PERFORMANCE REQUIREMENTS

Deformation criteria

For loadbearing function there is no deformation criteria.

For separating function it may be necessary to limit the deformation of a loadbearing structure supporting a separating member (e.g. beam supporting separating wall), or being situated above a separating member (e.g. beam above a a separating wall, which could be damaged by the deflection of the beam).

No general limits can be given, reference is made to relevant product specifications.

For tests there are deformation limits in test standards, e.g. ISO 834-1 and CEN-standards under preparation. These limitations are generally expressed as follows:

a) For flexural members:

Limiting deflection of $L^2/400\ d$ mm; and

Limiting rate of deflection of $L^2/9000\ d$ mm/min;

where L is the clear span of the specimen (mm)

d is the distance from the extreme fibre of the design compression zone to the extreme fibre of the design tension zone of the structural section (mm)

The limiting rate of deflection shall not apply before a deflection of L/30 is exceeded.

b) For axially loaded members:

Limiting axial contrction of h/100 mm; and

Limiting rate of axial contraction of 3 h/1000 mm/min;

where h is the initial height (mm)

Limiting rate of deflection $L^2/9000d$ is based on experience. It indicates yielding in the reinforcement leading to failure.

Since Tabulated Data are mainly based on tests, they roughly correspond to deflection L/30 and/or rate of deflection $L^2/9000d$.

2.2 ACTIONS

See ENV 1991-2-2

Approximation rules on mechanical actions are given in 2.4.3 (4) and (5). They apply to Analysis of parts of the structure and Member analysis and may also be used in Global Structural analysis.

Equation (2.5) and η_{fi} given in (4) is safe side simplification. In case of more than one variable load, ENV 1991-2-2, F.3.1 General Rule may be used instead if more accurate $E_{fi,d}$ is required.

Safe side simplifications η_{fi} given in (5) may always be applied. Accurate calculation of $E_{fi,d}$ gives more favourable results especially in cases where ratio between variable and permanent actions is high, see Figure 2.1 in ENV 1992-1-2.

2.3 DESIGN VALUES OF MATERIAL PROPERTIES

Values given in Chapter 3 and Appendix 1 are characteristic values based mainly on tests.

Material safety factor for concrete and reinforcement is taken as 1,0, justified by following study made by Horizontal Group, see Evaluation of $\gamma_{M,fi}$ below:

Evaluation of $\gamma_{M,fi} = 1$

1. It is agreed to use the following formulae :

   (see page 1 of annex 10 of EC1)

   at room temperature : $\gamma_M = e^{(3.04 * V_R - 1.645 * V_f)}$
   (part 1.1)

   for fire : $\gamma_{M,fi} = e^{(0.7 * V_R - 1.645 * V_f)}$
   (part 1.2)

   The figure 0.7 is due to the relation with existing results obtained from 2 tests.

   And : $V_R = \sqrt{V_m^2 + V_G^2 + V_f^2}$

   where : V_m : coefficient of variation for model uncertainly

   V_G : coefficient of variation for geometry of element

   V_f : coefficient of variation for material property

2. Values of the various coefficients were assumed to be :

   - unchanged (for room temperature and fire)

     for V_a and V_f

   - $V_{m,fire} = 2 * V_{m,room\ temperature\ (RT)}$

3. The following values were used and results obtained :

   RT = room temperature (part 1.2)

Materials	V_f	V_G	$V_{m,RT}$	$V_{m,fire}$	$V_{R,RT}$	$V_{R,fire}$	$\gamma_{M,RT}$	$\gamma_{M,fi}$
concrete	0.15	0.05	0.05	0.1	0.166	0.187	1.29	0.89
reinforcing steel	0.05	0.05	0.05	0.1	0.087	0.122	1.20	1.00
structural steel	0.03	0.03	0.03	0.06	0.052	0.073	1.11	1.00
regular timber	0.20	0.05	0.05	0.10	0.212	0.229	1.37	0.84
laminated timber	0.15	0.03	0.05	0.10	0.161	0.183	1.27	0.89
laminated timber (*)	0.05	0.03	0.03	0.06	0.066	0.084	1.12	0.98
masonry	0.20	0.05 to 0.1	?	-	-	-	-	-

(*) *These other assumptions were used in order to obtain the value of $\gamma_{M,fi} = 1,1$ currently used in EC5*

4. In order to ensure that values of V_f, V_G and V_m at room temperature are those already taken into account for the existing part 1.1 of the various Eurocode, we would be grateful to the Chairman or the Technical Secretary to check them.

5. If these values are right, the proposal is so to use $\gamma_{M,fi} = 1$ whatever the materials are due to the rough assumptions used so far.

Note for concrete: In room temperature it is assumed that the difference between calculated $\gamma_{M,RT} = 1,29$ and $\gamma_c = 1,5$ in Eurocode 2 Part 1 takes into account the uncertainty that compressive strength of concrete is controlled using test specimens not taken from the structure. Correspondingly, the calculated value $\gamma_{M,fi} = 0,89$ has to be increased to approximately 1,0.

2.4 VERIFICATION METHODS

Axis distances

Following information is also related to 4.2.2 General design rules.

In Tabulated Data the axis distances for tensile and simple supported bending members correspond to steel temperature 500°C.

Using the safe values $E_{fi,d}/E_d = 0,7$ and $A_{s,req} = A_{s,prov}$ and $\gamma_s = 1,15$ Equation 4.2 gives $\sigma_{fi,s}/\sigma_{yk}(20°C) = 0,7/1,15 = 0,609$. This stress level corresponds to reduction factor $k_s(\Theta) = 0,6$ and steel temperature 500°C for curve 1 in Figure 3.2.

For prestressing steels the same stress level and reduction factor $k_p(\Theta) = 0,6$ gives steel temperatures 400°C for bars and 350°C for wires and strands. This is the reason to increased axis distances in 4.2.2 (4).

When modifying axis distances according to 4.2.2 (5), the new critical temperature (step c)) can also be determined using temperature graphs in Appendix 2, other reliable temperature graphs or tests results.

Testing

Test methods relevant for concrete:

ISO 834(EN YYY-1) Fire resistance tests - Elements of building construction: General requirements for fire resistance testing

Under preparation in CEN/TC 127:

prEN 1363-1 Fire resistance tests of building construction - Part 1: Alternative and additional procedures

prEN 1364-1 Fire resistance tests on non-loadbearing elements in buildings - Part 1: Partitions

prEN 1364-2 Fire resistance tests on non-loadbearing elements in buildings - Part 2: External walls

prEN 1364-3 Fire resistance tests on non-loadbearing elements in buildings - Part 3: Ceilings

prEN 1365-1 Fire resistance tests on loadbearing elements in buildings - Part 1: Internal walls

prEN 1365-2 Fire resistance tests on loadbearing elements in buildings - Part 2: External walls

prEN 1365-3 Fire resistance tests on loadbearing elements in buildings - Part 3: Floor construction

prEN 1365-4 Fire resistance tests on loadbearing elements in buildings - Part 4: Roof constructions heated from the underside

prEN 1365-5 Fire resistance tests on loadbearing elements in buildings - Part 5: Beams

prEN 1365-6 Fire resistance tests on loadbearing elements in buildings - Part 6: Columns

prENV YYY5 Contribution to fire resistance of structural members -Part 2 Applied protection to concrete elements

Test methods for material properties of concrete and steel at elevated temperatures are under preparation in CEN/TC 127 and RILEM.

MATERIAL PROPERTIES

Chapter 3 and Appendix 1

Material properties presented in Appendix 1 are unchanged "harmonized properties" agreed by experts who prepared 1990 Drafts for concrete, steel and composite structures. Work is going on in CEN/TC 127 and RILEM to produce test methods for "hot data". When these methods are available, the material properties can be checked.

Material properties which are needed for Tabulated Data and for some simplified calculations, have been included in Chapter 3, in some cases modified to be suitable for practical design.

STRUCTURAL FIRE DESIGN

Chapter 4

4.1 GENERAL

Spalling

A number of Finnish tests on hollow core slabs and German tests on columns show that spalling does not occur when moisture content does not exceed 2 - 2,5 weight-%. According to Finnish investigations the moisture content of concrete is between 1 and 2 % in dry indoor climate.

References

Hietanen, T., Fire tests for Finnish hollow core slabs, November 1992, summary of 40 full scale fire tests made at Technical Research Center of Finland

Walter, R., Brandversuche an Stahlbetonstützen ohne Längsdehnungsbehinderung, Technische Universität Braunschweig, 1977

4.2 TABULATED DATA

4.2.2 GENERAL DESIGN RULES

Tabulated Data is mainly based on CEB recommendations. Some rules have been modified taking into account new test results.

Reference

CEB, Bulletin d'Information N° 208, Fire Design of Concrete Structures, July 1991

This Bulletin is mainly based on tests.

Criteria used in Tabulated Data

Separating function has been taken into account by minimum thicknesses of walls and slabs.

Loadbearing function has been taken into account by considering different possible failure modes and by giving rules for minimum dimensions, axis distances for the reinforcement etc., generally being on the safe side.

Yielding of the reinforcement is taken into account by the critical steel temparature. Yielding of the main reinforcement of beams and slabs leads to rapid increase of the deflection, followed by compression failure of concrete.

The Tables are based on critical temperature 500°C which roughly corresponds to the highest possible steel stress in fire situation. Axis distances in the Tables are given to limit the steel temperature to 500°C. Rules are given to reduce the axis distances when the actual steel stress is calculated.

Compression failure of concrete is taken into account by minimum dimensions of the cross-section. Generally, it is possible to deviate from the minimum dimension only by using simplified and general calculation method, but then also other possible failure modes, and sometimes separating function, have to be considered.

Shear and anchorage failure can occur in seldom cases only. They are covered by minimum dimensions and some additional detailing rules e.g. for continuous beams.

4.2.3 COLUMNS and

4.2.4 WALLS

Table 4.1: Reinforced concrete columns; rectangular and circular section and Table 4.3: Load-bearing reinforced concrete walls have been calculated by the computer program STABA-F [1]. The general validity of the theoretical approach of this program is demonstrated by analysis of tests on columns [2]. Fig. 1 shows the comparison between calculated t_u^n and measured t_u^e failure times of approx. 30 tests on reinforced concrete columns.

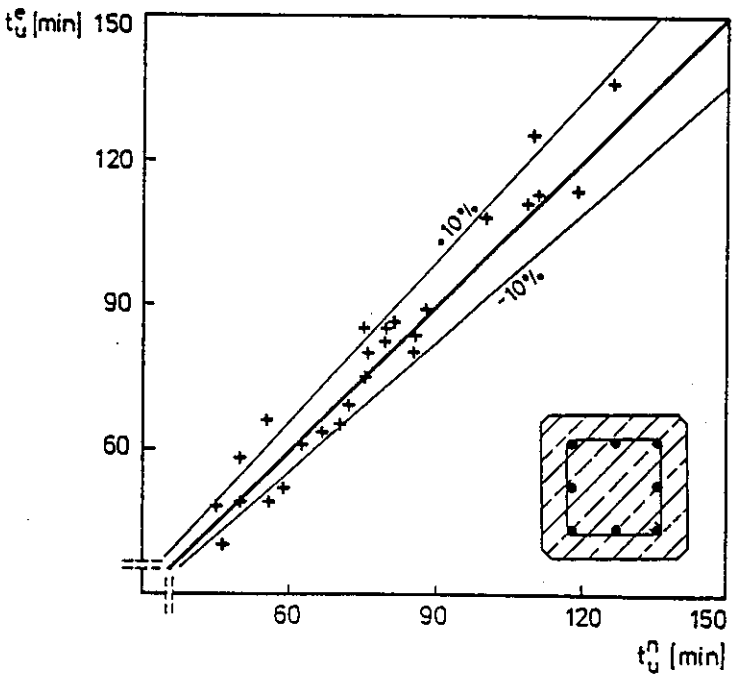

Figure 1: Comparison between calculated t_u^n and measured t_u^e failure times of approx. 30 tests on reinforced concrete columns

[1] Quast, U.; Hass, R.; Rudolph, K.: STABA-F; A Computer Program for the Determination of Loard-Bearing and Deformation Behaviour of Uni-Axial Structural Elements under Fire Action. Institut für Baustoffe, Massivbau und Brandschutz der Technischen Universität Braunschweig. 1984.

[2] Hass, R.: Zur praxisgerechten brandschutztechnischen Beurteilung von Stützen aus Stahl und Beton. Institut für Baustoffe, Massivbau und Brandschutz der Technischen Universität Braunschweig, Heft 69, 1986.

[3] Hass, R.; Klingsch, W.; Walter, R.: Brandversuche an Stahlbetonstützen - Versuchsergebnisse und numerische Analyse. Sonderforschungsbereich 148 "Brandverhalten von Bauteilen". Arbeitsberichte 1975 - 1977 und 1978 - 1980, Technische Universität Braunschweig, 1977 und 1980.

4.2.5 TENSILE MEMBERS

Generally, it is adviced not to use higher critical temperatures than 400°C, if the deformations and their influence have not been calculated. For calculation of deformations, the stress-strain curves in Appendix 1 may be used.

4.2.6 BEAMS

In 4.2.6.1 it is possible to deviate from the rules (5) to (9) if the steel temperatures have been determined and the procedure given in 4.2.2 (5) has been followed.

The rules for continuous beams are based on moment redistribution from the spans to the supports. The main reinforcement at the supports has full or almost full strength due to the lower temperature. Axis distances in spans may be decreased. It is to note, that axis distances in Table 4.6 are not based on critical temperature 500_oC, but higher, and should not be futher reduced.

It also may be necessary to increase the length of the negative reinforcement due to the increased negative moment. A simplified rule in 4.2.6.3 (3) covers this. Several trial calculations show that this is not always needed, because the variable loads are often reduced in fire design. Thus, the most unfavourable load case in design according to Part 1 may require longer negative reinforcement than the increased negative moment in fire design.

On the other hand, the shear forces may change. Therefore the minimum beam widths are larger for continuous beams than for simply supported beams for high fire resistances. For end spans, a special rule is given in 4.2.6.3 (6).

4.2.7 SLABS

It is to note that the axis distances for two way slabs are not based on critical temperature 500°C.

For continuous slabs, the same principles as for continuous beams apply.

4.3 SIMPLIFIED CALCULATION METHOD

See Annex of this Background Document.

5. PROTECTIVE LAYERS

See test methods in 2.4.

APPENDIX 1

See Chapter 3 Material properties.

APPENDIX 2

The temperature graphs for slabs are from CEB Bulletin N° 145, 1982. The graphs for beams are from Dutch code with minor modifications to be in line with CEB.

APPENDIX 3

This is a limited simplified calculation method for practical use.

APPENDIX 4

This is guidance for general calculation method, not excluding other methods.

ANNEX Kristian Hertz: Simplified calculation method

INSTITUTE OF BUILDING DESIGN
Report no. **203**

KRISTIAN HERTZ

SIMPLIFIED CALCULATION METHOD FOR FIRE EXPOSED CONCRETE STRUCTURES

SUPPORTING DOCUMENT FOR CEN PR-ENV 1992-1-2

Den polytekniske Læreanstalt, Danmarks tekniske Højskole
Technical University of Denmark. DK-2800 Lyngby **1993**

CONTENTS

PREFACE

This report is a supporting document for the chapter 4.3 "Simplified Calculation Method" of the proposal CEN prENV 1992-1-2 for Eurocode 2 "Design of concrete structures" Part 1-2 "Structural fire design".

Lyngby, december 1993
Kristian Hertz
M.Sc. Ph.D. Struct.Eng.

ACKNOWLEDGEMENTS

I wish to express my gratitude to the other members of the project team CEN/TC250/SC2/PT10 writing the proposal of the fire design part of the Eurocode on concrete structures for many fruitful discussions leading to the present proposal for the code, and to the staff of the Institute of Building Design for printing the report.

A special thank should be given to Mr.Robin Whittle from Ove Arup and Partners in London for many suggestions which have improved the final code text considerably.

SUMMARY

The distributions of the compressive strength and the E-modulus through a fire exposed cross-section is analysed, and simple methods are developed for the estimation of the ultimate compressive resistance and the stiffness of a cross-section subjected to compression and to bending.

Reduced cross sections are established for the analysis in the ultimate limit state of beams and slabs in positive and negative bending, where negative bending is defined by fire exposure at the more compressed edge of the cross-section. Further, it is shown how the reduced cross sections can be used estimating the shear capacity of beams and walls.

The methods mentioned can be applied analyzing the load-bearing capacity of a structure with or without prestressing at any time of any fire course and especially at a fixed time of a standard fire exposure.

In Appendix A examples are shown of the development of the load- bearing capacity and the deflections of fire exposed concrete columns and beams.

The calculated values are compared with test results on the same structural elements as reported in the literature.

In general it appears that the calculational procedures are on the safe side and quite close to the data observed.

In Appendix B drawings are shown of the distribution of temperature and strength through cross-sections of various thicknesses and exposed to various fire courses.

SYMBOLS

A_c	area of a concrete cross-section
A_s	area of a steel cross-section
A_{sw}	area of shear reinforcement
a	thermal diffusivity
a_z	width of damaged zone
b_w	width of web
C	thickness of cross-section
C_i	constant of number i
d	depth of a cross-section
d_c	depth of the force of the compr. zone
d_s	depth of steel reinforcement
E	E-modulus
E_c	E-modulus of concrete
E_{co}	initial tangent modulus of concrete
E_{co20}	E_{co} at 20°C
E_p	tangent modulus of a prestressed steel
E_s	E-modulus of a steel
E_{s20}	E_s at 20°C
F	force
F_{cE}	Euler force of a concrete column
F_c	force at a concrete cross-section
F_{cr}	critical force
F_{cu}	ult. force of a concr. cross-section
F_s	force of a steel cross-section
$F_{s(0.2\%)}$	force of steel at strain 0.2%
$F_{s(2.0\%)}$	force of steel at srain 2.0%
F_{sE}	Euler force of a steel column
F_{su}	ult. force of a steel cross-section

f	strength
f_{ck}	compressive strength of concrete
$f_{ck,ave}$	average of f_{ck}
f_{ck20}	f_{ck} at 20°C
f_{ct}	tensile strength of concrete
f_{ct20}	f_{ct} at 20°C
f_{yk}	characteristic yield strength of steel
f_{su}	ultimate tensile stress of steel
I	moment of inertia
I_c	I of a reduced concrete cross-section
I_s	I of a steel cross-section
i	number
k	parameter defined as N/F_{cu}
k_c	reduction of concrete strength
k_{cM}	do at mid point of a wall
$k_{c,m}$	average reduction of concrete strength
k_s	reduction of yield stress of steel
$k_{s(0.2\%)}$	reduction of 0.2% stress of steel
$k_{s(2.0\%)}$	reduction of 2.0% stress of steel
$k_{yw(0.2\%)}$	reduction of 0.2% stress of shear reinf.
l	length of a beam or a column
M	moment load
M_u	ultimate moment capacity
N	normal load
n	number of layers
P	prestressing force
t	time

V	shear capacity
V_c	V width resp. to concrete in compres.
V_{ct}	V width resp. to concrete in tension
V_{Rc2}	V defined in ENV 1992-1-1
V_{Rc3}	V defined in ENV 1992-1-1
V_s	V width respect to the steel links
w	half width of two sided exposed wall
x	depth of the neutral axis
y	depth of a compression zone
z	coordinate
ε	strain
ε_{cu}	ult. concrete strain at the stress f_{cc}
ε_{cuM}	do at mid point of wall or section
$\varepsilon_{cu,max}$	maximum of ult. concrete strain
ε_{cu20}	ε_{cu} at 20°C
ε_s	steel strain
ε_{tr}	transient strain of concrete
η	stress distribution factor
θ	temperature
θ_M	temperature at mid point
θ_{yw}	temperature of shear reinforcement
σ	stress
σ_p	prestress of steel
σ_s	stress of steel

IDEALIZED MECHANICAL PROPERTIES

In the code proposal idealized mechanical properties are given in chapter 3 for concrete and steel exposed to a standard fire until the time of maximum temperature. The values given are considered to be on the safe side compared to those expected for ordinary building materials in Europe, and the designer is allowed to use other values, if these are known for the material used in the actual construction.

Since the variation of the compressive strength and the E-modulus of concrete is highly depending on the actual material and on the time of a fire exposure at which the property is wanted, it is obvious that: **calculational procedures for analyzing fire exposed concrete structures should be able to take into account different relationships of the mechanical properties of the concrete and the temperature.**

Furthermore, since the percentile reduction of the compressive strength of a heat exposed concrete within a wide range is not dependent on the water-cement ratio and thus is not dependent on the original compressive strength (Hertz [14]), it is advantageous, that **the original compressive strength is an independent parameter in the calculation.**

These requirements are fulfilled by the procedures presented in the chapter 4.3 on a simplified calculation method.

Comparing a large number of curves (documented in Hertz [14]) on the development of the short time modulus of elasticity to curves on the development of the compressive strength with temperature for the same concretes exposed to the same temperature-time courses and subjected to the same loading, it appears to be a universal truth, that the reduction of the short time modulus of elasticity is the square of the reduction of the compressive strength.

$$E_{co} = k_c^2 E_{co20}$$

The relation, which is discovered by the author, seems to be valid for a large variety of concretes in a hot condition as well as after a cooling phase.

The relation is valid for the short time values of the properties not including creep and transient strain, where the transient strain is the part of the thermal expansion which is hindered by application of compressive stresses.

Analyzing fire exposed columns and walls the load bearing capacity decreases during the fire course due to the increase in temperature, and buckling becomes more likely to occur. At a certain time the capacity meets the load applied and the member buckles, which means that a deflection and additional stresses caused by this quickly increases. In the analysis the flexural stiffness is used for the estimation of the deflections and the distribution of these additional stresses. And because these appears at the time of buckling, short time values not including creep or transient strains should be used for calculating the flexural stiffness.

During investigations on heated concretes a considerable increase of the ultimate strain ε_{cu} with temperature is noticed. (See for example Hertz [14], Schneider [25], Harmathy and Berndt [12], Harada et al. [11] and Fischer [10]).

From the stress-strain curves of these references it can also be seen that the increase in strain follows the decrease in stress, and the simple model is suggested that the product of stress and strain remains a constant for each point of the stress-strain curve while the material is weakened due to the heat.

This means that

$$\sigma\varepsilon = C_i$$

where C_i is a constant for each point of the stress-strain curve.

Thus, the ultimate strain will be increased by the reciprocal reduction of the compressive strength

$$\varepsilon_{cu} = \varepsilon_{cu20} / k_c$$

which is in accordance with the short time test results.

For an idealized elasto-plastic stress-strain curve the point of change in gradient will be transformed from

$$(\varepsilon, \sigma) = \left(\frac{f_{ck20}}{E_{co20}} , f_{ck20} \right) \text{ to } \left(\frac{1}{k_c} \frac{f_{ck20}}{E_{co20}} , k_c f_{ck20} \right)$$

and it is seen that the constant product of σ and ε with $f_{ck} = k_c f_{ck20}$ also leads to a fulfilment of the relation

$$E_{co} = k_c^2 E_{co20}$$

The lack of knowledge about these relationships has been a main obstacle so far to the development of simple and rationale methods for calculations of the stress-strain developments of fire exposed concrete structures.

Applying a certain variation of the single parameter k_c it is now possible to generate the heat induced changes of idealized stress-strain curves whether the idealizations are elasto-plastic or curved line relations are used.

REDUCED CROSS SECTIONS

Consider a cross-section of thickness 2w exposed to fire at two parallel surfaces.

The isotherms will all be parallel to the surfaces at any time of any fire exposure, and the reduction of the compressive strength of the concrete k_c then is a function of the depth from the surface.

The maximum temperature occurring in the middle of the cross-section until the actual time is denoted θ_M, and the corresponding reduction of the compressive strength of the concrete is $k_{cM} = k_c(\theta_M)$.

The average compressive strength of the concrete in a cross-section of the thickness 2w is expressed as

$$f_{ck,ave} = \eta k_{cM} f_{ck20}$$

where f_{ck20} is the compressive strength at 20°C, and η is a factor expressing the distribution of stresses.

The factor is determined by

$$\eta = \frac{1}{w k_{cM}} \int_0^w k_c(\theta(z))\, dz$$

and is the ratio of the average compressive strength of the cross-section to the compressive strength at the centre of the cross-section, which is

$$f_{ckM} = k_{cM} f_{ck20}$$

Furthermore is utilized that if the compressive strength at any point of the cross-section is reduced by the factor k_c to

$$f_{ck} = k_c f_{ck20} ,$$

then the initial modulus of elasticity of the concrete at the same point is

$$E_{co} = k_c^2 E_{co20}$$

and the ultimate strain is

$$\varepsilon_{cu} = \varepsilon_{cu20}/k_c$$

where ε_{cu20} is often considered to be 0.35 pct.

From elasto-plastic stress-strain relations it is then seen that the ultimate stress is reached at the strain ε_{cu20} for most of the temperature levels.

It is therefore a reasonable approximation to assume the cross-section being able to act at its ultimate stresses at every point, when compressed to a uniform strain of ε_{cu20} in a plastic analysis.

If k_{cM} is less than unity the approximation is even more valid when the entire cross-section is compressed to $\varepsilon_{cuM} = \varepsilon_{cu20}/k_{cM} > \varepsilon_{cu20}$.

This means that the cross-section can be loaded to an ultimate resistance equal to the average compressive strength multiplied by the thickness of the section, before the ultimate strain is reached at the centre-line.

For applications, where the strain may vary along the centre-line, but has a constant value across the section, the material could be considered to be uniformly damaged through the section.

The stress-strain curve of the material is assessed to be the one of an impaired concrete with a compressive strength equal to the mean value through the cross-section, but with an ultimate strain not exceeding ε_{cuM}.

The ultimate resistance per unit length of the cross-section thus is

$$\eta k_{cM} f_{ck20} 2w$$

and the initial stiffness per unit length is

$$2\int_o^w k_c^2 \, dz E_{co20}$$

If the cross-section is assumed to consist of an uniform "average" concrete, the initial stiffness per unit length may also be

$$2w(\eta k_{cM})^2 E_{co20}$$

The factor $(\eta k_{cM})^2$ is smaller than the integral, and thus it would be a safe approximation to be used for calculations of instability and deflections of structural members.

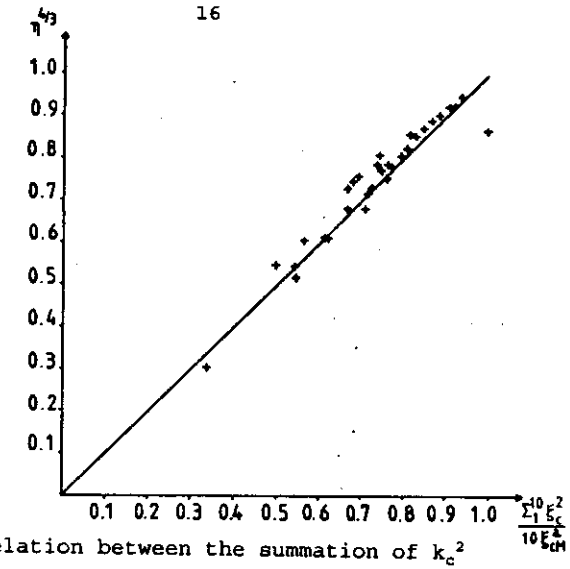

Relation between the summation of k_c^2 and the approximation $\eta^{4/3}$.

However, calculations of the integral for a large number of different fire exposures and thicknesses of the concrete cross-section show that a better approximation would be

$$2\int_o^w k_c^2 \, dz \approx \eta^{\frac{4}{3}} k_{cM}^2 2w$$

The average deviation was less than 5 pct., and no single deviation was above 10 pct.

The distributions of the maximum temperatures and of the corresponding reductions of strength are shown in Appendix B for a hot condition, where the temperature is a maximum at 30 mm from the surface, and in the cold condition after the fire exposure for a number of fully developed fires and cross-section thicknesses.

Thus, the initial stiffness per unit length is

$$\eta^{\frac{4}{3}} k_{cM}^2 E_{co20} 2w.$$

Comparison between the model using a reduced cross-section and the actual distribution of stiffness for a typical fire development.
($2w$ = 0.40 m, granite aggregates, $A\sqrt{h}/A_t$ = 0.04 $m^{1/2}$, q = 400 MJ/m^2, after cooling).

If elastic parts of elasto-plastic stress-strain relations are used, or a more detailed analysis is made based on a curved stress-strain relation, the cross-section could be considered to have a fictive thickness of

$$\eta^{\frac{4}{3}} 2w$$

and to consist of concrete with the mechanical properties of the concrete at the centre-line, i.e.

$$f_{ck} = k_{cM} f_{ck20} \ , \ E_{co} = k_{cM}^2 E_{co20} \ , \ \varepsilon_{cu} = \varepsilon_{cu20} / k_{cM}$$

This means that the cross-section is considered to be reduced by the thickness

$$w\,(1 - \eta^{\frac{4}{3}})$$

from each side.

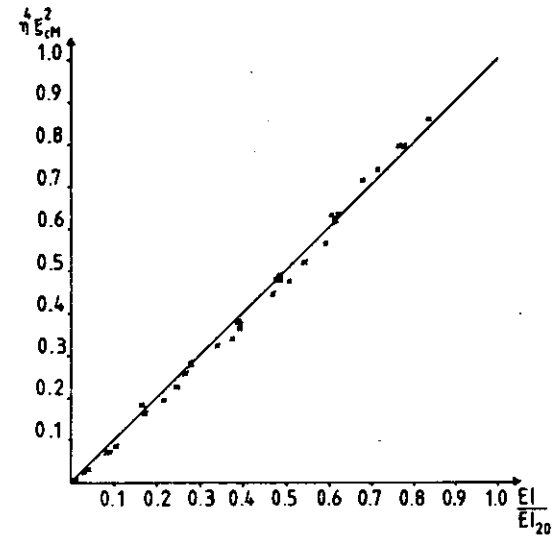

Relation between the relative flexural stiffness and the approximation $\eta^4 k_{cM}^2$.

This rough model, where the E_{co}-modulus is zero at both sides and of full central value over the thickness $\eta^{4/3}C$ at the middle, is actually very close to the distribution of k_c^2 over the cross-section.

The agreement is so close, that even the moment of inertia weighted by the E_{co}-modulus is almost identical for the two models.

This means that

$$2\int_o^w z^2 k_c^2 E_{co20}\, dz \approx \frac{1}{12} \eta^4 (2w)^3 k_{cM}^2 E_{co20}$$

Also the validity of this approximation has been tested by calculation of the integral for the previously mentioned fires and cross-sections.

The average deviation was less than 1 pct. and the maximum deviation less than 4 pct. of the initial value of the moment of inertia times the E_{co}-modulus before the fire exposure.

The model using a reduced cross-section of thickness $\eta^{4/3}2w$ therefore is valuable to the calculation of the load-bearing capacity of a fire exposed wall or column as well as for the elastic- or curved-line analysis of a cross-section.

However, in case a plastic analysis is carried out, all parts of the cross-section will be able to act by their ultimate stresses, when they are compressed at a large uniform strain.

For this analysis the cross-section could be reduced to one of a thickness $\eta 2w$ having the uniform mechanical properties of the concrete at the centre-line

$$f_{ck} = k_{cM} f_{ck20} , \quad \varepsilon_{cu} = \varepsilon_{cu20} / k_{cM}$$

In the early phases of a fire, development of large temperature gradients may occur near the surface of the cross-section.

For practical calculations the cross section may be divided into n parallel zones of equal thickness, where $n \geq 3$. The temperature θ_i is calculated for the middle of each zone, and the corresponding reductions $k_c(\theta_i)$ of the compressive strength of the concrete are determined.

The average reduction is found as

$$k_{c,m} = \frac{(1-0.2/n)}{n} \sum_{i=1}^{n} k_c(\theta_i) .$$

where a factor (1 - 0.2/n) allows for the variation in temperature within each zone.

The factor η is thus equal to

$$\eta = \frac{k_{c,m}}{k_c(\theta_M)} ,$$

and the reduced cross section for compressive strength, i.e. for beams, slabs and members subjected to implane shear becomes the thickness $2w\eta$, which is found by neglecting a damaged zone of thickness

$$a_z = w \left[1 - \frac{k_{c,m}}{k_c(\theta_M)} \right]$$

at each fire exposed surface.

The reduced cross section for axial or flexural stiffness, i.e. for columns, walls and other constructions where second order effects may be calculated the thickness becomes $2w\eta^{4/3}$, which is found by neglecting a damaged zone at each fire exposed surface of thickness

$$a_z = w \left[1 - \left(\frac{k_{c,m}}{k_c(\theta_M)} \right)^{1.3} \right] .$$

CALCULATIONS OF LOAD BEARING CAPACITIES

It is seen from the theory mentioned above that if reduced properties are introduced for the reinforcement, the reduced cross sections have the same ultimate compressive resistances and the same short time flexural stiffnesses as those of corresponding fire exposed members. This means that any cross section based method which is applicable for the calculation of the ultimate capacity of a structural member without a fire exposure may be used for the analysis of the same member exposed to fire. In particular the methods of the application rules of the main part of the Eurocode may be used unchanged to calculate the fire resistance of the members using the properties of the reduced cross sections. This ensures continuity between the two parts of the code and it opens a possibility of reusing computer routines for calculation of structural members.

For a single fire such as the standard fire and a single concrete quality such as a siliceous concrete on standard cement, the reduced cross section can be estimated extremely quick by means of one page of curves like those presented in appendix 2 of pr-ENV 1992-1-2 page 73.

For other fires and concretes similar pages can be made or the reduced cross sections calculated by calculation of the temperature in 3 points of a wall of the same thickness as the smallest dimension of the fire exposed cross section according to the detailed method given in the code text.

This appears to be the simplest possible method by means of which different fire courses and different concrete qualities can be treated.

EXAMPLE ON SIMPLE CALCULATION OF A BEAM.

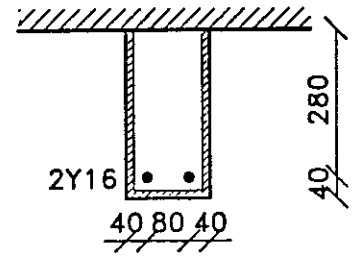

The ultimate moment of a rectangular cross section with siliceous aggregates subjected to a 1 hour standard fire exposure is calculated.

The characteristic material properties are

$f_{yk}(20°C)$ = 560 MPa, $f_{ck}(20°C)$ = 20 MPa.

The ultimate steel force is

$F_s = 402 \bullet 10^{-6} \bullet 560 \bullet 10^3$ = 225 kN.

Temperatures are estimated by means of diagram.

Temperature of a steel θ_s = 480°C.

Temperature in mid-point θ_M = 250°C, $k_c(250°C)$ = 0.90.

The average reduction of the concrete strength is found through the thickness w = 80 mm from the reduction in n = 4 points in depths x_i

x_i	θ_i	$k_c(\theta_i)$
10 mm	580°C	0.51
30 mm	360°C	0.83
50 mm	290°C	0.87
70 mm	260°C	0.89
Sum		= 3.10, $k_{c,m}$ = (1-0.2/4)•3.10/4 = 0.74

Damaged zone

a_z = 80 (1-0.74/0.90) = 80•0.18 = 14.6 mm

With of reduced cross section = 160-2•14.6 = 131 mm.

If 2.0 % strain in steel is assumed.

$k_{s(2.0\%)}(480°C)$ = 0.67.

Ultimate steel force $F_{s(2.0\%)}$ = 0.67•225 kN = 150.8 Kn.

Depth of compression zone

$y = 150.8/(0.131 \cdot 0.9 \cdot 20 \cdot 10^3) = 0.0640$ m.

Ultimate moment capacity

$M_u = 150.8(0.280-0.0640/2) = 37.4$ kNm.

$\varepsilon_{cu,max} = 0.0035/0.9 = 0.00389 = 0.389$ %,

$x = 64/0.8 = 80$ mm.

Obtained steel strain

$\varepsilon_s = 0.389(280 - 80)/80 = 0.97$ % < 2.0 %,

which is not in agreement with the assumption.

Therefore: <u>0.2 % strain</u> in steel is assumed.

$k_{s(0.2\%)}(480°C) = 0.51$.

Ultimate steel force

$F_{s(0.2\%)} = 0.51 \cdot 225$ kN = 114.8 kN.

Depth of compression zone

$y = 114.8/(0.131 \cdot 0.9 \cdot 20 \cdot 10^3) = 0.0487$ m.

Ultimate moment capacity

$M_u = 114.8(0.280-0.0487/2) = 29.4$ kNm.

$x = 48.7/0.8 = 60.9$ mm. Obtained steel strain

$\varepsilon_s = 0.389(280 - 60.9)/60.9 = 1.40$ % > 0.2 %, which is sufficient.

The ultimate load bearing capacity of the cross section is <u>29.4 kNm</u> after 1 hour standard fire exposure.

<u>Shear</u> If the shear capacity is wanted, the temperature is found (diagram) of the stirrups (Y8 per 100 mm in depth 28 mm) to be

$\theta_{yw} = 380°C$, $k_{yw(0.2\%)} = 0.720$. According to Part 1 (4.3.2.4.4) is

$z = 0.9 \cdot 0.280 = 0.252$ m, $\nu = 0.7 - 20/200 = 0.6$, and with $\theta = 45°$ the characteristic capacities are found before the fire as

$V_{Rc2}(20°C) = b_w z \nu \sin\theta \cos\theta f_{ck}$

$= 0.16 \cdot 0.252 \cdot 0.6 \cdot 0.5 \cdot 20 \cdot 10^3 = 242$ kN,

and $V_{Rc3}(20°C) = (A_{sw}/s) z f_{ywc} \cot\theta$

$= (100 \cdot 10^{-6}/0.1) 0.252 \cdot 560 \cdot 10^3 \cdot 1.0 = 142$ kN.

After 1 hour fire exposure these becomes

$V_{Rc2} = (0.131/0.160) \cdot 0.90 \cdot 242 =$ <u>178 kN</u> and

$V_{Rc3} = 0.720 \cdot 142 =$ <u>102 kN</u>.

EXAMPLE ON SIMPLE CALCULATION OF A BEAM.

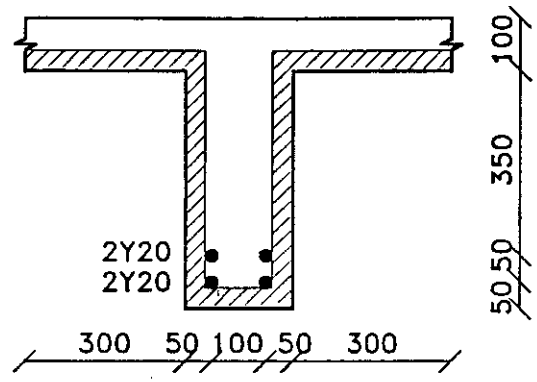

The ultimate moment of a T-shaped cross section with siliceous aggregates subjected to a 2 hour standard fire exposure is calculated.

The characteristic material properties are

$f_{yk}(20°C) = 560$ MPa, $f_{ck}(20°C) = 25$ MPa.

The ultimate steel force is
$F_s = 2 \bullet 628 \bullet 10^{-6} \bullet 560 \bullet 10^3 = 2 \bullet 352 = 704$ kN.
Temperatures are estimated by means of diagram.
Temperature of the steels $\theta_{s1} = 650°C$, $\theta_{s2} = 520°C$.
Temperature at top of slab
$\theta_M = 360°C$, $k_c(360°C) = 0.826$.
The average reduction of the concrete strength is found through the thickness w = 100 mm of the slab from the reduction in n = 3 points in depths x_i

x_i	θ_i	$k_c(\theta_i)$
17 mm	760°C	0.224
50 mm	520°C	0.608
83 mm	380°C	0.813
Sum		= 1.645,

$k_{c,m} = (1 - 0.2/3) \bullet 1.645/3 = 0.512$
Damaged zone $a_z = 100\ (1 - 0.512/0.826) = 38.0$ mm
2.0 % strain in steel is assumed.
$k_{s(2.0\%)}(650°C) = 0.229$. $k_{s(2.0\%)}(520°C) = 0.563$.
Ultimate steel force
$F_{s(2.0\%)} = (0.229 + 0.563) \bullet 352$ kN
$= 80.6 + 198.2 = 279$ kN.
Depth of compression zone
$y = 279/(0.8 \bullet 0.826 \bullet 25 \bullet 10^3) = 0.0169$ m.
It is seen that 16.9 mm < 100 - 38 = 62 mm,
and the entire compression zone is in the slab.
The ultimate moment capacity is
$M_u = 80.6(0.50-0.0169/2) + 198.2(0.45-0.174/2)$
$= 127.1$ kNm.
$\varepsilon_{cu,max} = 0.0035/0.826 = 0.00424 = 0.424$ %,
$x = 16.9/0.8 = 21.1$ mm.
Obtained steel strain $\varepsilon_s = 0.424(450 - 21.1)/21.1$
$= 8.62$ % > 2.0 %,
and the assumption is valid.
The ultimate load bearing capacity of the cross section is 127 kNm after 2 hours standard fire exposure.

EXAMPLE ON SIMPLE CALCULATION OF A COLUMN.

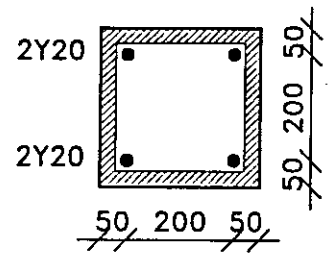

The load bearing capacity is calculated for a centrally loaded column with a quadratic cross section and an effective height of 4 m subjected to a 1 hour standard fire exposure.
The concrete is based on siliceous aggregates.
The characteristic material properties are
$f_{yk}(20°C) = 560$ MPa, $f_{ck}(20°C) = 20$ MPa,
$E_s(20°C) = 210$ GPa, $E_c(20°C) = 31$ GPa
The area of the reinforcement is
$A_s = 2 \bullet 628 \bullet 10^{-6} = 1257 \bullet 10^{-6}$ m^2.
Temperatures are estimated by means of diagram.
Temperature of a steel
$\theta_s = 360°C$. $k_{s(0.2\%)}(360°C) = 0.740$.
A maximum steel strain of 0.2% is assumed to ensure the coherence between the strains of concrete and steel.
Temperature at mid point $\theta_M = 20°C$, $k_c(20°C) = 1.00$.
The average reduction of the concrete strength is found through the thickness W = 150 mm from the reduction in n = 3 points in depths x_i

x_i	θ_i	$k_c(\theta_i)$
25 mm	430°C	0.752
75 mm	150°C	0.967

125 mm 50°C 1.000
Sum = 2.719,
$k_{c,m}$ = (1 - 0.2/3)•2.719/3 = 0.846
Damaged zone a_z = 150 (1 - (0.846/1.0)$^{1.3}$) = 29.3 mm
The with of the reduced cross section is
= 300 - 2•29.3 = 241 mm, and the material properties of this section are
f_y = 0.740•560 = 414 MPa, f_c = 1.0•20 = 20 MPa,
E_s = 0.740•210 = 155.4 GPa, E_c = 1.0^2•31 = 31 GPa.
The flexural stiffness of concrete section is
I_cE_c = (0.241^4/12)31•10^6 = 8715 kNm^2.
The flexural stiffness of steel section in the concrete is
I_sE_s = 2•628•10^{-6}•0.10^2•155.4•10^6 = 1952 kNm^2.
This reduced column may be analyzed by means of any method applicable to concrete columns.

(If for example the ultimate load bearing capacity of the centrally loaded column is estimated by means of the Rankine formula it becomes
1/(1/(0.241^2•20•10^3 + 1257•10^{-6}•414•10^3)
+ 4^2/π^2(8715 + 1952)) = 1340 kN
The ultimate load bearing capacity of the column is 1340 kN after 1 hour standard fire exposure.)

REFERENCES

[1] FISCHER, R.:
Über das Verhalten von Zementmörtel und Beton bei höheren Temperaturen
Deutscher Ausschuss für Stahlbeton,
Heft 214, pp. 61-128
Berlin 1970.

[2] HARADA, T. TAKEDA, J.
YAMANE, S. FUTUMURA, F.:
Strength, Elasticity and Thermal Properties of Concrete Subjected to Elevated Temperatures.
ACI, SP-34, pp. 377-406
Detroit 1972

[3] HARMATHY, T.Z. BERNDT, J.E.:
Hydrated Portland Cement and Light Weight Concrete at Elevated Temperatures.
Journal of the ACI Vol.63,
No.1, pp. 93-112
Research Paper No. 280.
Division of Building Research.
Ottawa 1966.

[4] HERTZ, K.D.:
Analyses of Prestressed Concrete Structures Exposed to Fire.
Report No. 174. 152 p.
Institute of Building Design
Technical University of Denmark
Lyngby, december 1985.

[5] HERTZ, K.D.:
Betonkonstruktioners
brandtekniske egenskaber
(Properties of Fire Exposed Concrete
Structures.
Part 1 and 2 of Ph.D. Thesis)
Report No. 140. 210 p. (In Danish).
Institute of Building Design,
Technical University of Denmark.
Lyngby, July 1980.

[6] SCHNEIDER, U.:
Festigkeits- und Verformungsverhalten
von Beton unter stationär und
instationärer Temperaturbeanspruchung.
Die Bautechnik heft 4. pp. 123-132.
Wilhelm Ernst und Sohn.
Berlin 1977.

APPENDIX A
EXAMPLES

A number of structural elements has been analysed by means of the procedures presented in the main text, and the main data and results are shown in standardized schedules.

In addition each schedule is provided with two illustrations showing the structural element in question and the development in time of the load-bearing capacity and for beams also that of the deflection.

The data of the examples are chosen in accordance with the data of testings reported in the literature, and the test results are for comparison shown with the results of the calculations.

In general the calculations of the load-bearing capacities are slightly on the safe side due to the conservative idealizations made in the theory and estimating the material properties.

Also the calculated deflections appear to be in a reasonable agreement with the observations.

Yet, some differences are seen immediately before collapse of the structural elements, mainly caused by a plastic behaviour of the reinforcement at this stage of the test and the neglect of creep strains.

The calculational procedures could be extended to take these effects into account, but structural elements, having been so close to collapse, would be of almost no use after the fire, and the contributions to the deflections calculated are found to be clearly unacceptable for most purposes.

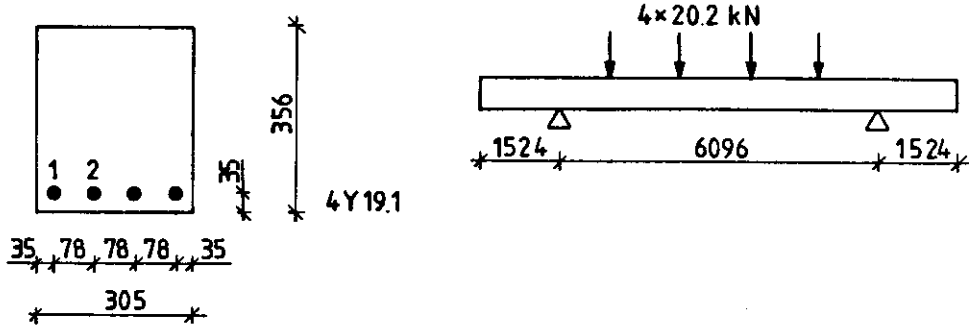

Cross-section and structural system. (All measures in mm).

FIRE DATA: Standard 1.33h

LOAD: M = 70.6 kNm, N = kN, d_N = m

REFERENCE: Note 59 (PCA), CRSI [C 1]

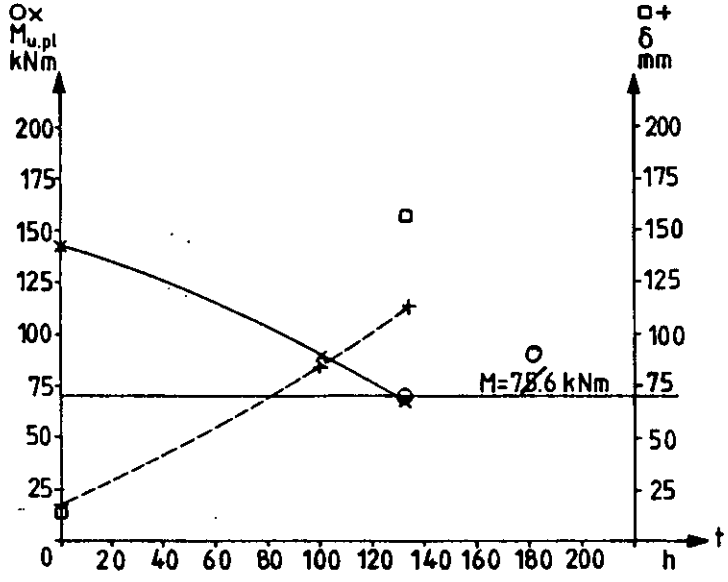

Comparison of test: O and calculation: X.

CROSS SECTION: C = 0.305 m C_{slab} = m A_s = 1146 mm^2

d_{s1} = 0.321 m d_{s2} = m d_{s3} = m

CONCRETE: a = 0.348 mm^2/s aggregate; Elgin gravel

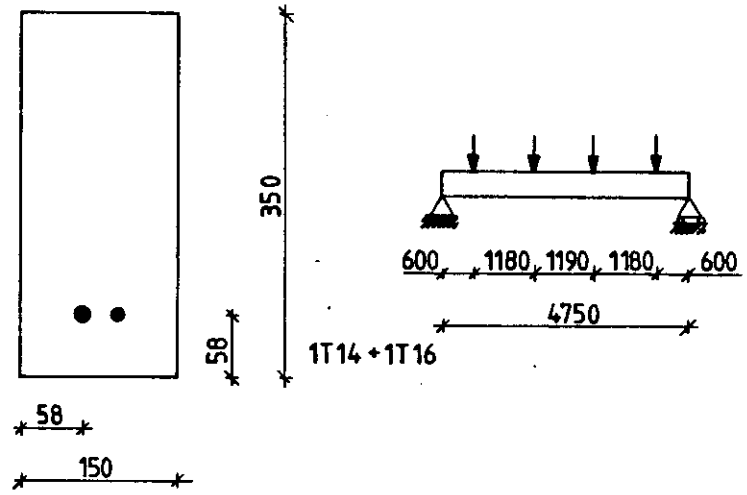

Cross-section and structural system. (All measures in mm).

FIRE DATA: Standard 1.63h

LOAD: M = 21.3 kNm, N = kN, d_N = m

REFERENCE: Beam 2, von Postel [C 2]

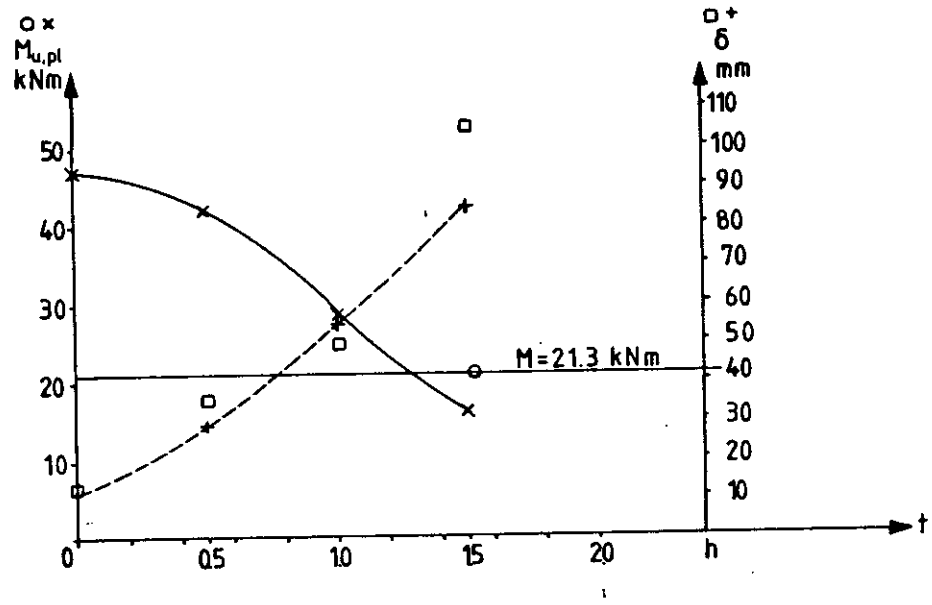

Comparison of test: O and calculation: X.

CROSS SECTION: C = 0.150 m C_{slab} = m A_s = 355 mm^2

d_{s1} = 0.292 m d_{s2} = m d_{s3} = m

CONCRETE: a = 0.520 mm^2/s aggregate: Siliceous age: 89 days

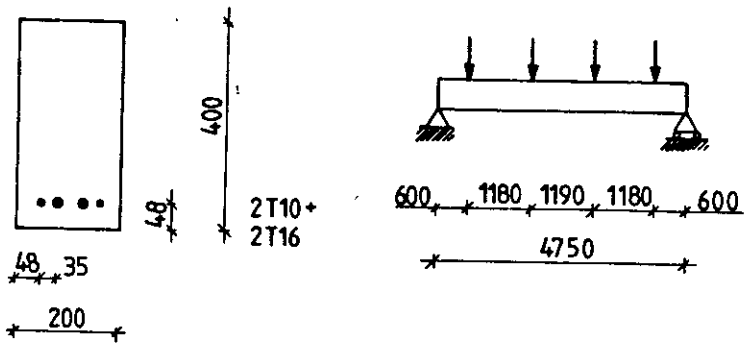

Cross-section and structural system. (All measures in mm).

FIRE DATA: Standard 1.93h

LOAD: M = 41.8 kNm, N = kN, d_N = m

REFERENCE: Beam 3, von Postel [C 2]

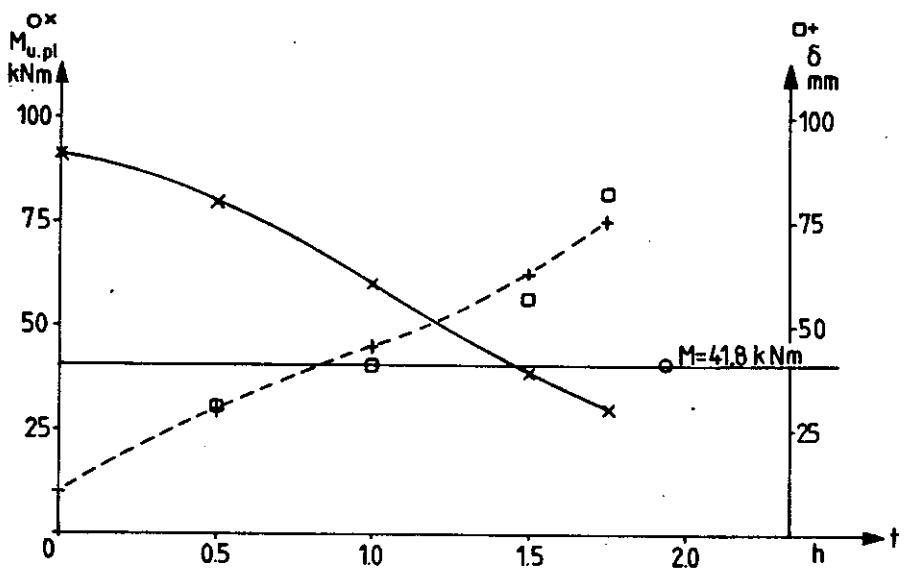

Comparison of test: O and calculation: X.

CROSS SECTION: C = 0.200 m C_{slab} = m A_s = 559 mm^2

d_{s1} = 0.352 m d_{s2} = m d_{s3} = m

CONCRETE: a = 0.520 mm^2/s aggregate: Siliceous age: 160 days

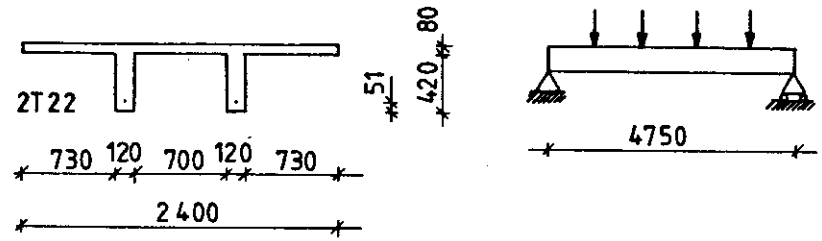

Cross-section and structural system. (All measures in mm).

FIRE DATA: Standard 1.38h

LOAD: M = 76.0 kNm, N = kN, d_N = m

REFERENCE: Beam 6, von Postel [C 2]

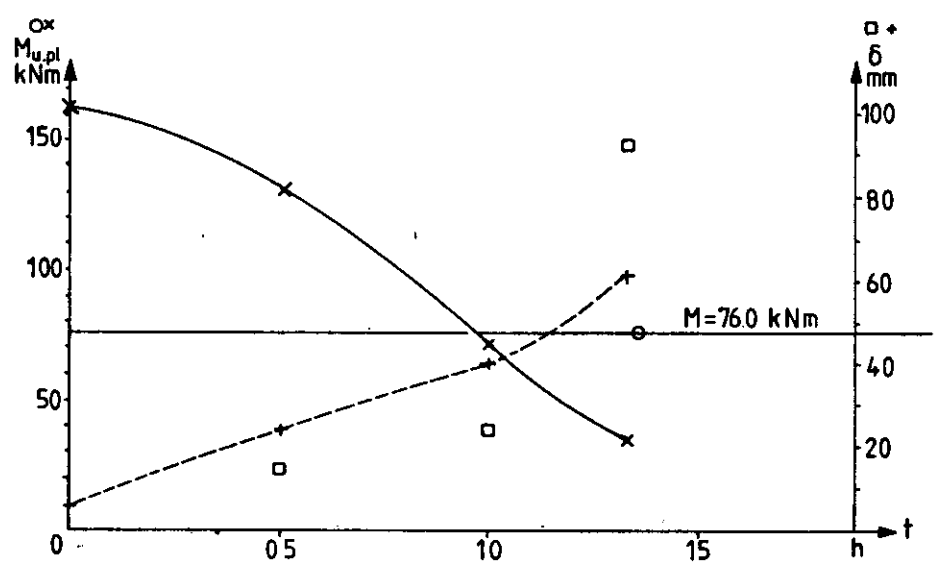

Comparison of test: O and calculation: X.

CROSS SECTION: C = 0.120 m C_{slab} = 0.320 m A_s = 760 mm^2

d_{s1} = 0.449 m d_{s2} = m d_{s3} = m

CONCRETE: a = 0.520 mm^2/s aggregate: Siliceous age: 106 days

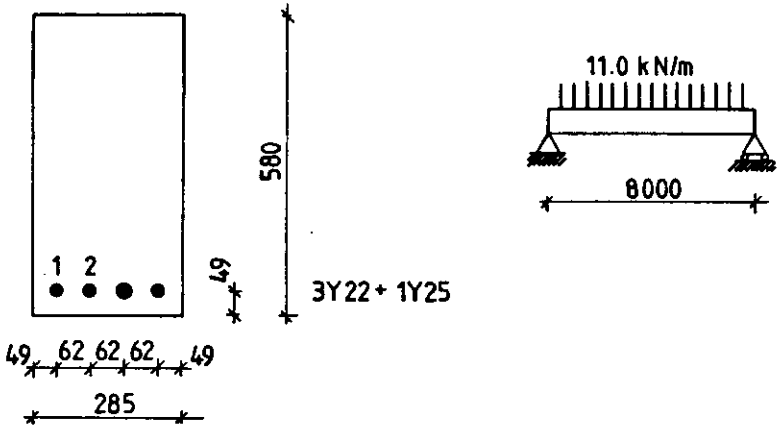

Cross-section and structural system. (All measures in mm).

FIRE DATA: Standard 3.00h

LOAD: M = 88.0 kNm, N = kN, d_N = m

REFERENCE: Beam M.2, Deutschmann [C 3]

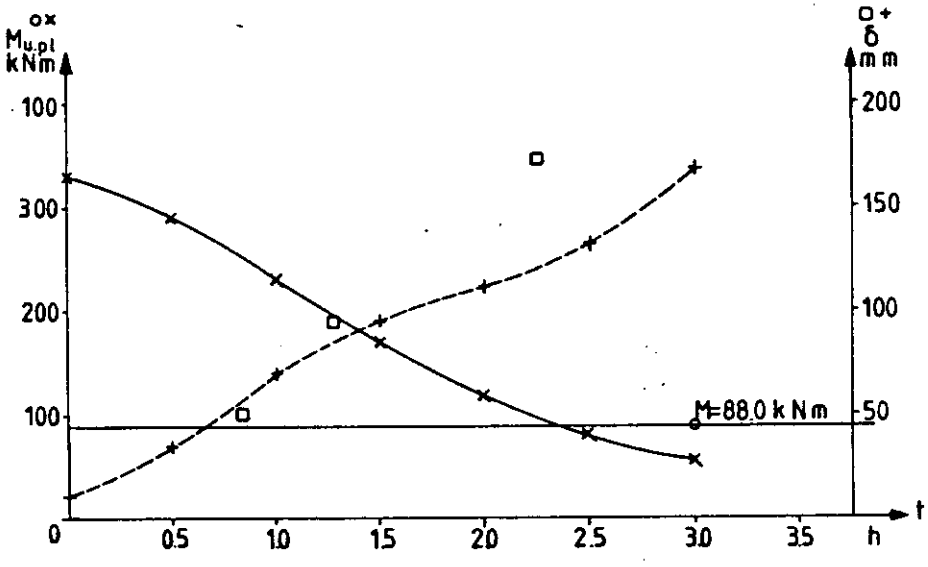

Comparison of test: O and calculation: X.

CROSS SECTION: C = 0.285 m C_{slab} = m A_s = 1631 mm^2

d_{s1} = 0.531 m d_{s2} = m d_{s3} = m

CONCRETE: a = 0.520 mm^2/s aggregate:

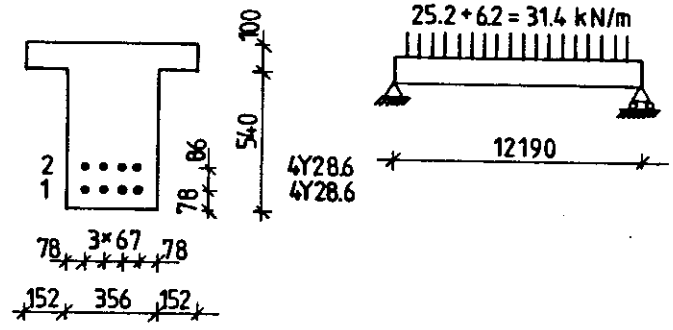

Cross-section and structural system. (All measures in mm).

FIRE DATA: Standard 6.22 h

LOAD: M = 594 kNm, N = kN, d_N = m

REFERENCE: Beam 85, Gustaferro et al, [C 4]

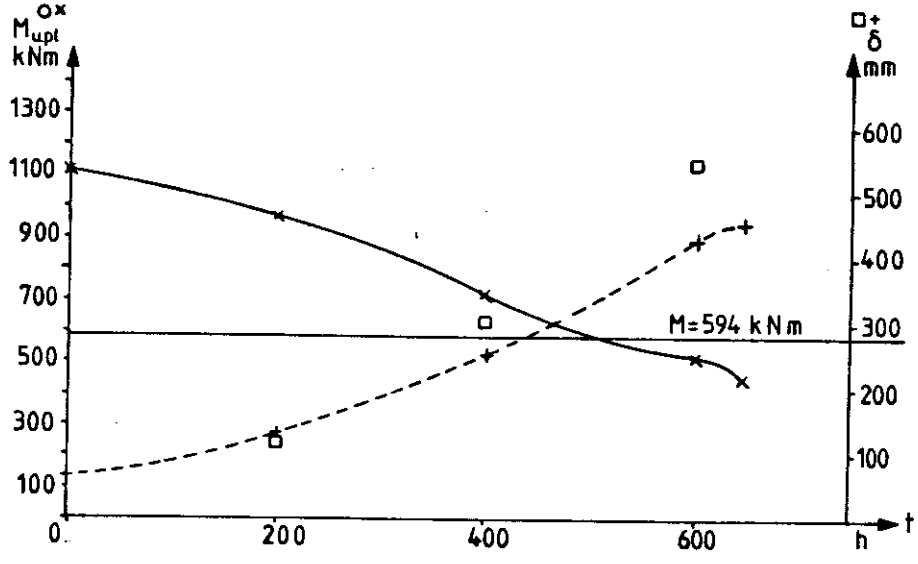

Comparison of test: O and calculation: X.

CROSS SECTION: C = 0.356 m C_{slab} 0.400m A_s = 5130 mm^2

d_{s1} = 0.562 m d_{s2} 0.476m d_{s3} m

CONCRETE: a = 0.348 mm^2/s aggregate: Elgin gravel age: 903 days

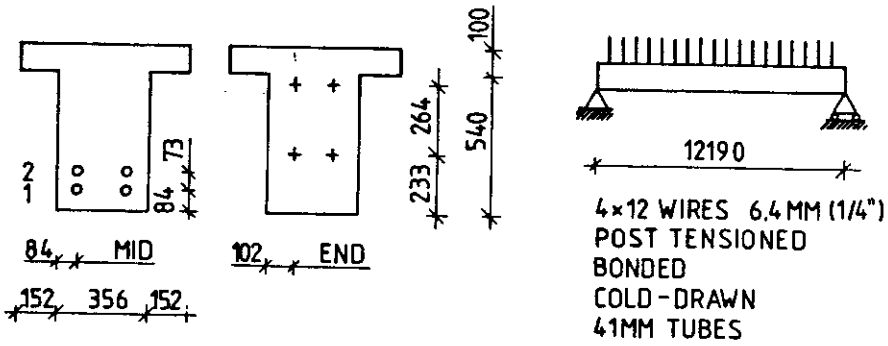

Cross-section and structural system. (All measures in mm).

FIRE DATA: Standard 3.33 m

LOAD: M = 598 kNm, N = kN, d_N = m

REFERENCE: Beam 78, Gustaferro et al, [C 4]

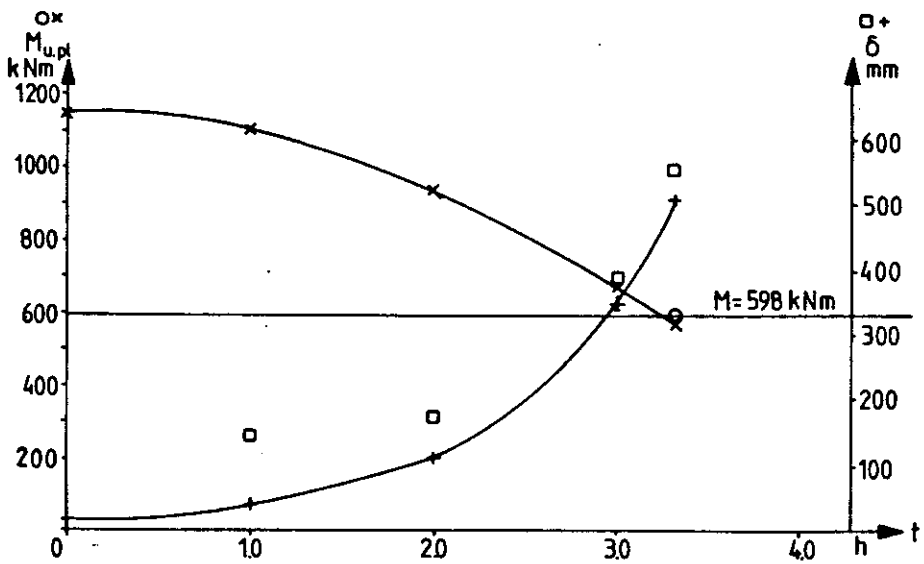

Comparison of test: O and calculation: X.

CROSS SECTION: C = 0.356 m C_{slab} 0.400 m A_s = 1520 mm^2

d_{s1} 0.556 m d_{s2} 0.483 m d_{s3} m

CONCRETE: a = 0.348 mm^2/s aggregate: Elgin gravel age: 910 days

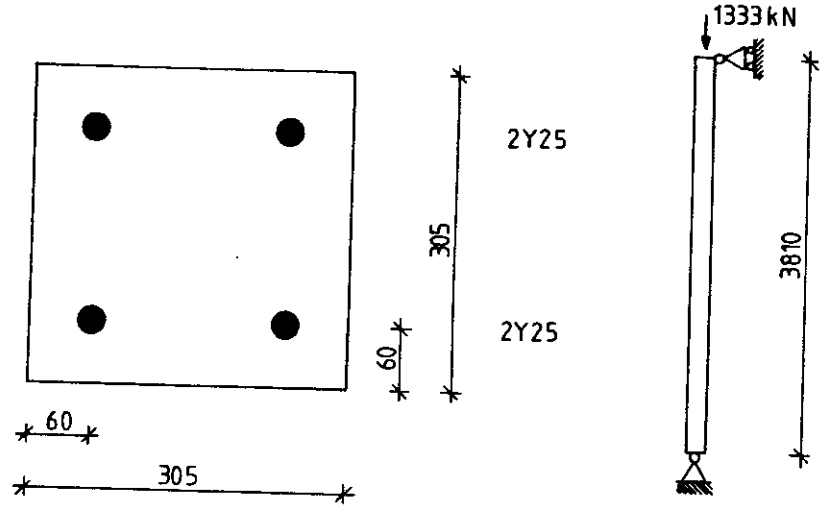

Cross-section and structural system. (All measures in mm).

FIRE DATA: Standard 2.83h

LOAD: M = kNm, N = 1333 kN, d_N = 0.153 m

REFERENCE: Column 2, Lie, Allen and Abrams [C 5]

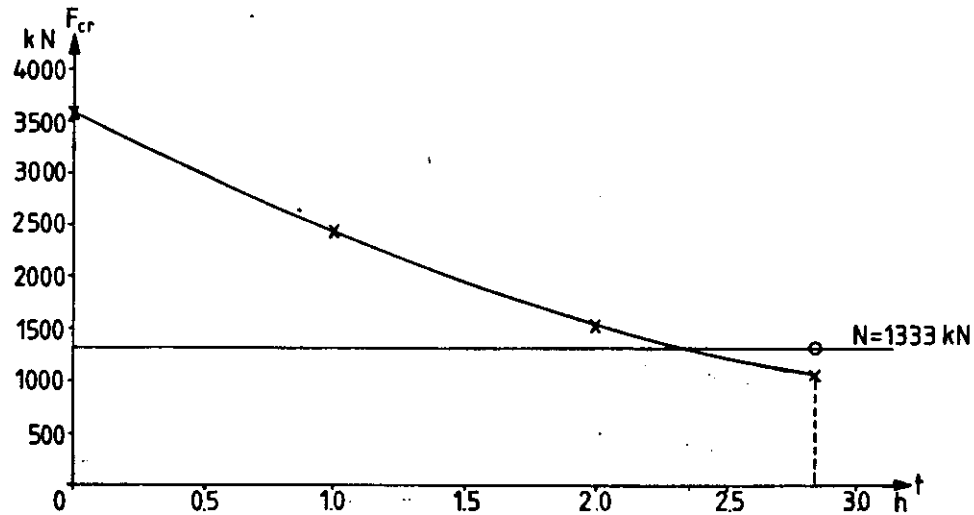

Comparison of test: O and calculation: X.

CROSS SECTION: C = 0.305 m C_{slab} m A_s = 1963 mm^2

d_{s1} 0.245 m d_{s2} m d_{s3} m

CONCRETE: a = 0.520 mm^2/s aggregate: Siliceous

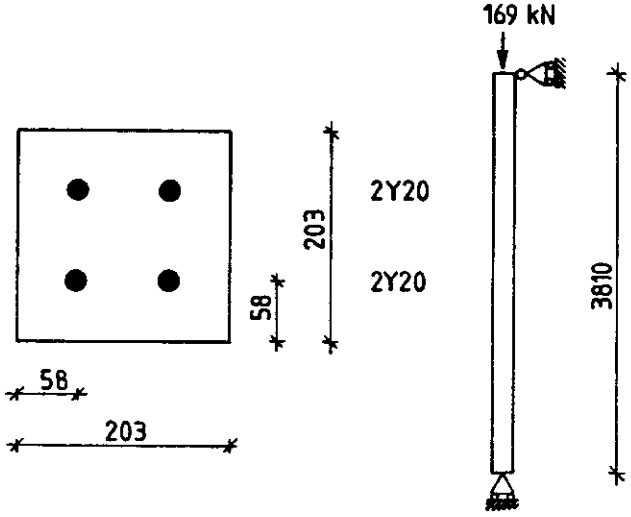

Cross-section and structural system. (All measures in mm).

FIRE DATA: Standard 3.00h

LOAD: M = kNm, N = 169 kN, d_N = 0.102 m

REFERENCE: Colomn 6, Lie, Allen and Abrams [C 5]

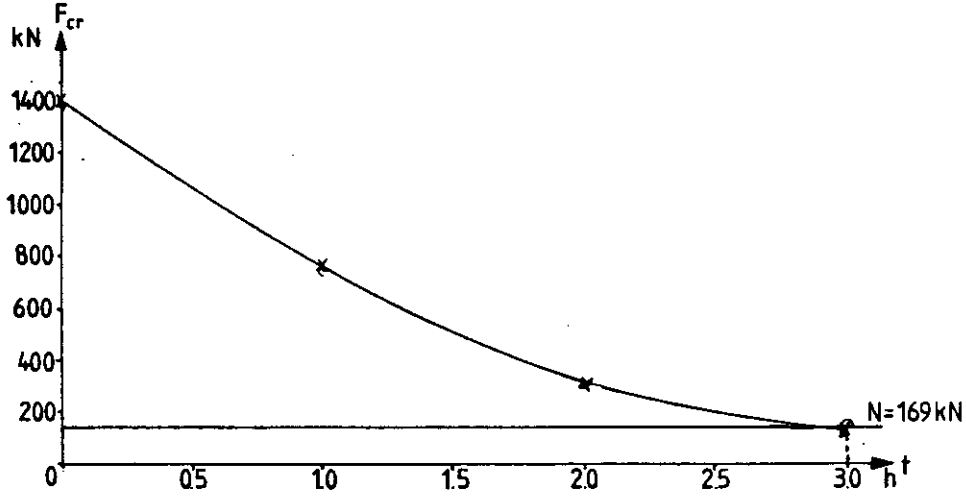

Comparison of test: O and calculation: X.

CROSS SECTION: C = 0.203 m C_{slab} = m A_s = 1257 mm^2

d_{s1} = 0.145 m d_{s2} = m d_{s3} = m

CONCRETE: a = 0.520 mm^2/s aggregate: Siliceous

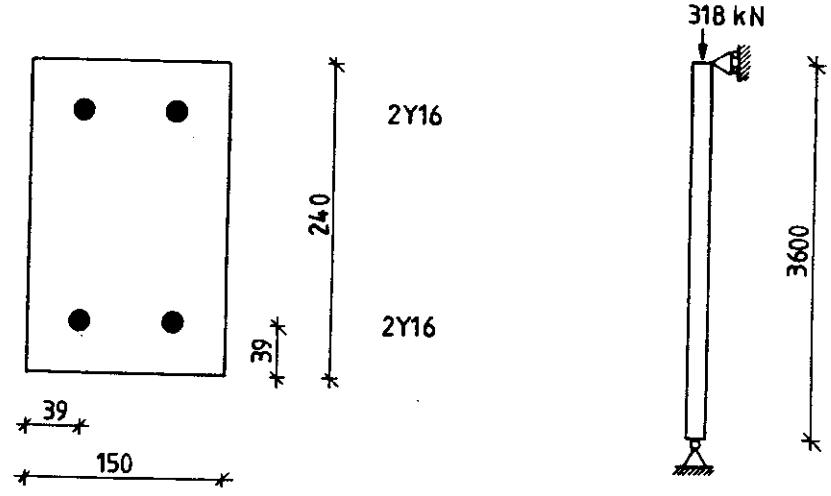

Cross-section and structural system. (All measures in mm).

FIRE DATA: Standard 1.78h

LOAD: M = kNm, N = 318 kN, d_N = m

REFERENCE: Column 5, Seekamp, Becker, Struck [C 6]

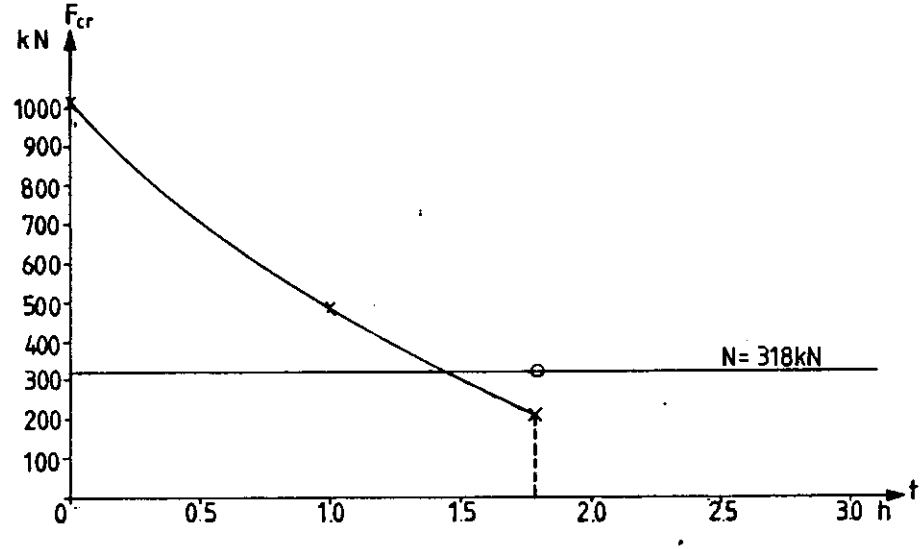

Comparison of test: O and calculation: X.

CROSS SECTION: C = m C_{slab} = m A_s = 804 mm^2

d_{s1} = m d_{s2} = m d_{s3} = m

CONCRETE: a = 0.348 mm^2/s aggregate: Limestone age: 14 months

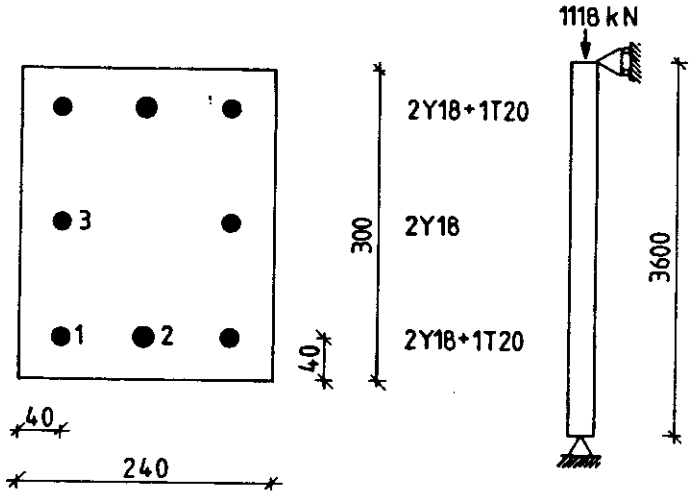

Cross-section and structural system. (All measures in mm).

FIRE DATA: Standard 2.45h

LOAD: M = kNm, N = 1118 kN, d_N = m

REFERENCE: Column 20, Seekamp, Becker, Struck [C 6]

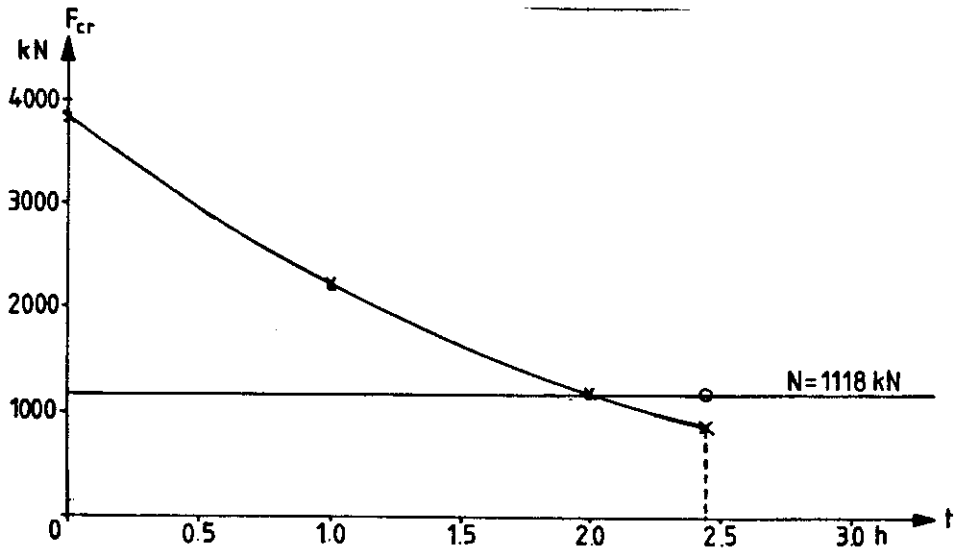

Comparison of test: O and calculation: X.

CROSS SECTION: C = 0.240 m $C_{\overline{slab}}$ m A_s = 2155 mm^2

$d_{s\overline{1}}$ m $d_{s\overline{2}}$ m $d_{s\overline{3}}$ m

CONCRETE: a = 0.520 mm^2/s aggregate: Quartz age: 19 months

REFERENCES TO THE EXAMPLES

[C 1] CONCRETE REINFORCING STEEL INSTITUTE:
Reinforced Concrete Fire Resistance.
CRSI Engineering Practice Committee, 238p.
Chicago, 1980.

[C 2] POSTEL, R. VON:
Brandversuche an statisch bestimmt aufgelagerten Stahlbetonplatten und - balken mit Rechteck- und Plattenbalkenquerschnitt.
Deutscher Ausschuss für Stahlbeton
Heft 230, Teil 3, pp. 95 - 118.
Wilhelm Ernst und Sohn.
Berlin 1975.

[C 3] DEUTSCHMANN, H.:
Brandprüfungen an vorgespannten Betonbauteilen.
Deutscher Ausschuss für Stahlbeton
Heft 162, Teil 4, 18 p.
Wilhelm Ernst und Sohn.
Berlin 1964.

[C 4] GUSTAFERRO, A.H. ABRAMS, M.S.
SALSE, E.A.B.:
Fire Resistance of Prestressed Concrete beams.
Study C: Structural Behaviour During Fire Tests.
Research and Development
Bulletin RD009,01B
Portland Cement Association.
Skokie 1971.

[C 5] LIE, T.T ALLEN, D.E ABRAMS, M.S.:
Fire Resistance of
Reinforced Concrete Columns.
DBR Paper No. 1167. 54 p.
National Research Council Canada.
Ottawa, February 1984.

[C 6] SEEKAMP, H. BECKER, W. STRUCK, W.:
Brandversuche an
Stahlbetonfertigsäulen.
Heft 162, Teil 1. 46 p.
Wilhelm Ernst und Sohn.
Berlin 1964.

APPENDIX B

STRENGTH AND TEMPERATURE DISTRIBUTIONS

Thermal diffusivity 3.48×10^{-7} m²/s. C= 1.2 . D= 180 . E=540 .

q= 200 MJ/m². $A\sqrt{h}/A_c = 0.04$ m$^{-1/2}$. HOT

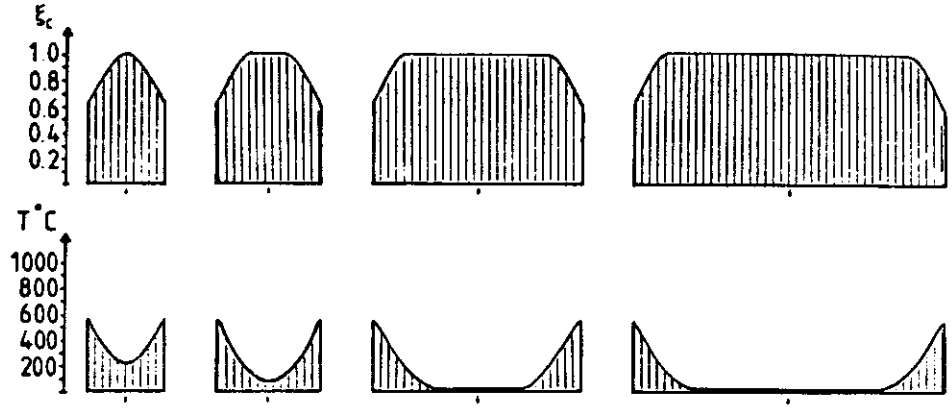

C =	150mm	200mm	400mm	600mm
η =	0.8529	0.8918	0.9448	0.9624
$\frac{1}{10\xi_{cM}^2}\Sigma_{10}\xi_c^2$ =	0.7424	0.8119	0.9048	0.9358
I_c/I_{c20} =	0.5542	0.6225	0.7657	0.8309

COLD

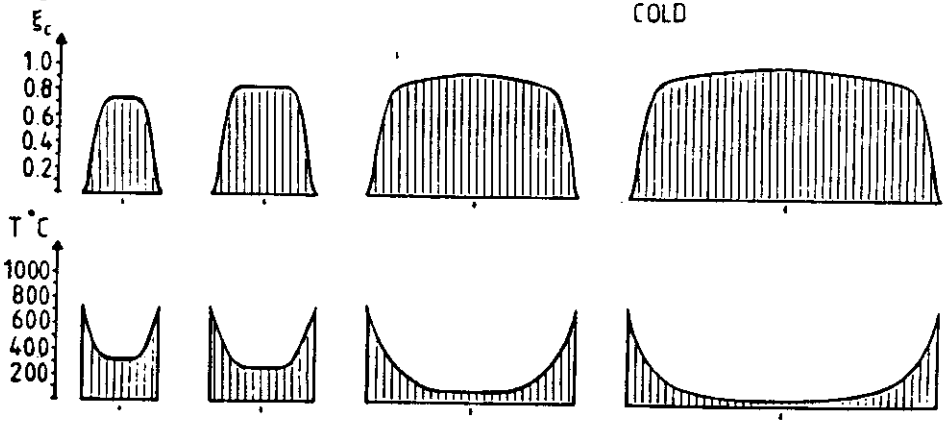

C =	150mm	200mm	400mm	600mm
η =	0.7504	0.8116	0.8533	0.8671
$\frac{1}{10\xi_{cM}^2}\Sigma_{10}\xi_c^2$ =	0.6694	0.7601	0.7911	0.8029
I_c/I_{c20} =	0.1785	0.2784	0.4894	0.5944

Thermal diffusivity 3.48×10^{-7} m²/s. C= 2.8 . D= 240 . E=540 .

q= 400 MJ/m². $A\sqrt{h}/A_c$= 0.04 m$^{-1/2}$. HOT

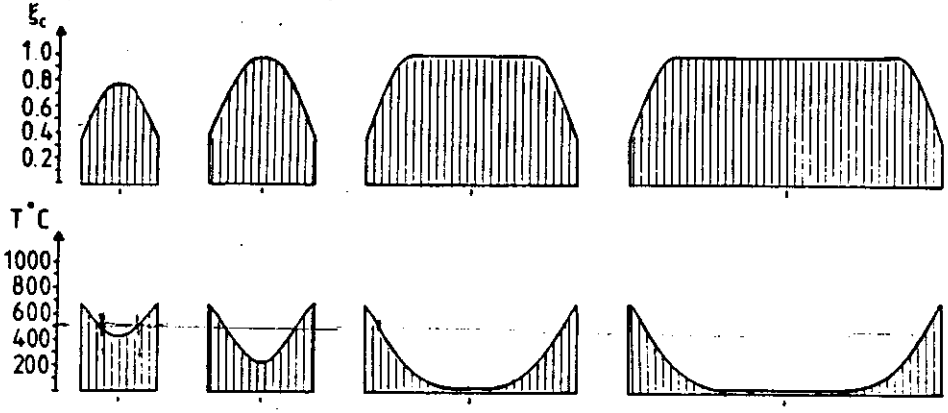

C =	150mm	200mm	400mm	600mm
η =	0.8128	0.7912	0.8916	0.9273
$\frac{1}{10\xi_{cM}^2}\Sigma_{10}\xi_c^2$ =	0.6933	0.6645	0.8294	0.8862
I_c/I_{c20} =	0.2664	0.3899	0.6041	0.7131

COLD

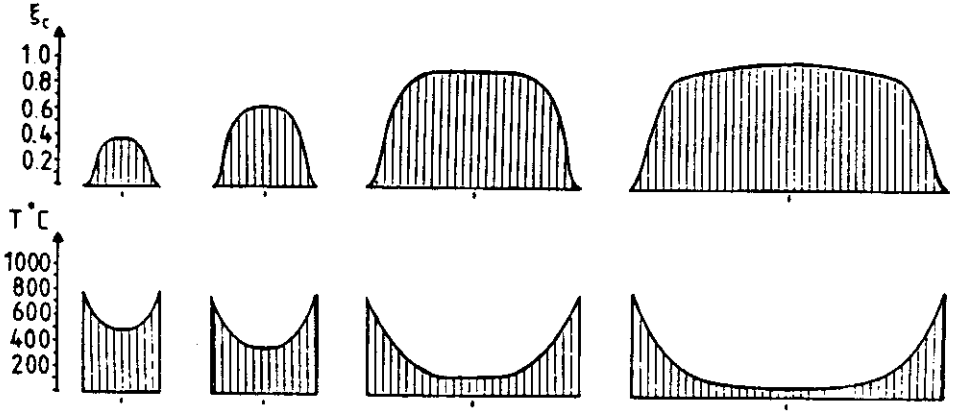

C =	150mm	200mm	400mm	600mm
η =	0.6328	0.6964	0.7938	0.8241
$\frac{1}{10\xi_{cM}^2}\Sigma_{10}\xi_c^2$ =	0.5390	0.6164	0.7258	0.7487
I_c/I_{c20} =	0.0269	0.1009	0.3371	0.4686

Thermal diffusivity 3.48×10^{-7} m²/s. C= 1.2 . D= 180 . E= 650 .

q= 400 MJ/m². $A\sqrt{h}/A_c$= 0.08 m$^{-1/2}$. HOT

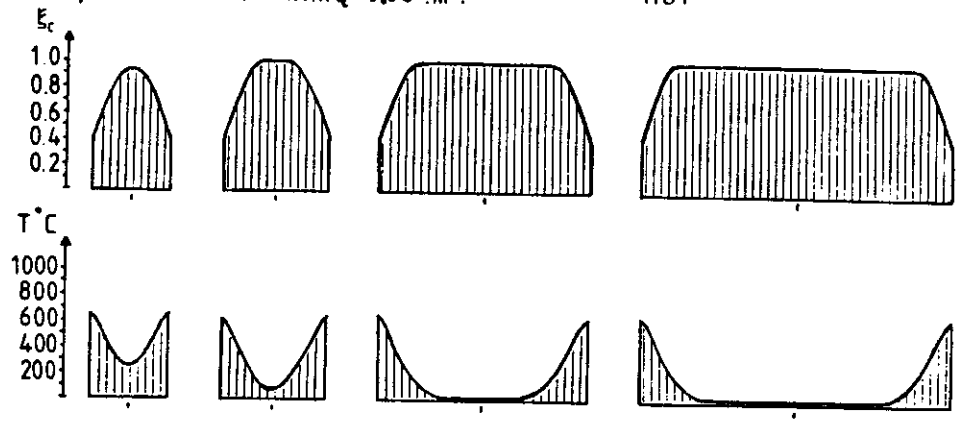

C =	150mm	200mm	400mm	600mm
η =	0.8040	0.8366	0.9181	0.9445
$\frac{1}{10\xi_{cM}^2}\Sigma_{10}\xi_c^2$ =	0.6785	0.7363	0.8687	0.9128
I_c/I_{c20} =	0.3942	0.4818	0.6797	0.7706

COLD

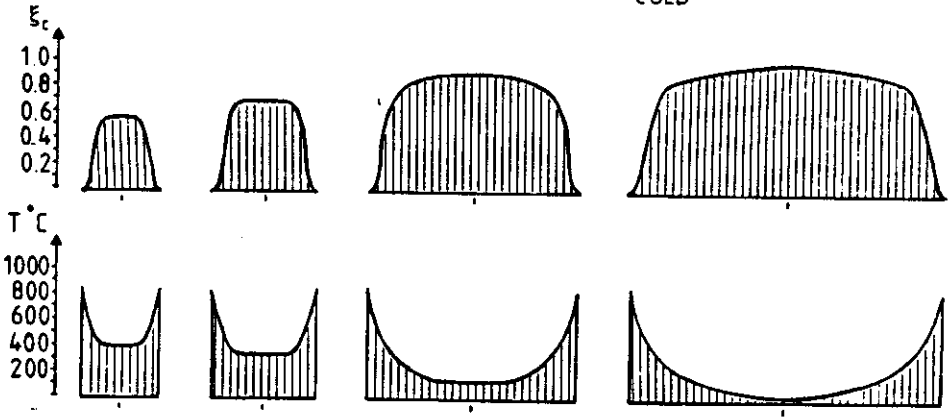

C =	150mm	200mm	400mm	600mm
η =	0.6925	0.8972	0.8312	0.8284
$\frac{1}{10\xi_{cM}^2}\Sigma_{10}\xi_c^2$ =	0.6201	0.9946	0.7725	0.7439
I_c/I_{c20} =	0.0895	0.1624	0.3885	0.5065

Thermal diffusivity 3.48×10^{-7} m²/s. C= 2.4 . D= 245 . E= 720 .

q= 800 .MJ/m². $A\sqrt{h}/A_c = 0.08$ .m⁻¹. HOT

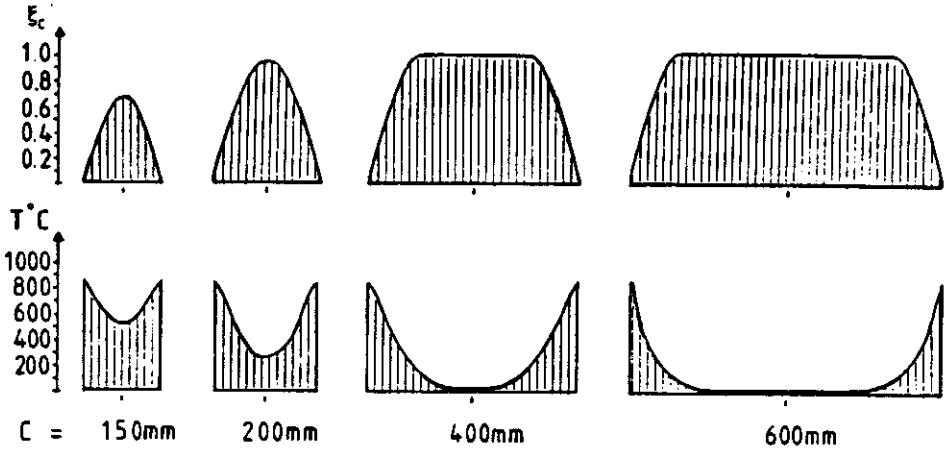

C =	150mm	200mm	400mm	600mm
η =	0.6374.	0.6853 .	0.8322.	0.8855 .
$\frac{1}{10}\xi_{CM}^{-1}\Sigma_{10}\xi_c^2$ =	0.4972.	0.5619 .	0.7694 .	0.8451 .
I_c/I_{c20} =	0.0873.	0.2192 .	0.4814 .	0.6154 .

COLD

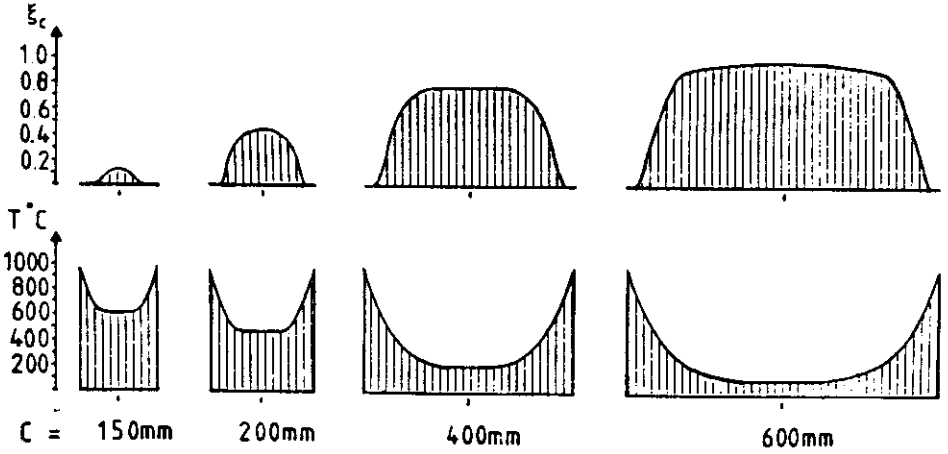

C =	150mm	200mm	400mm	600mm
η =	0.4085.	0.6124 .	0.7521.	0.7859
$\frac{1}{10}\xi_{CM}^{-1}\Sigma_{10}\xi_c^2$ =	0.3366.	0.5445 .	0.7070 .	0.7188
I_c/I_{c20} =	0.0009.	0.0328 .	0.2466 .	0.3743

BDA 1.2 July 2002

Note from CEN TC 250 – Horizontal Group "Fire"

To the Fire Regulator Group

Insulation criteria for "natural" fire development situation

The criteria currently used, as far as fire resistance of separating elements is concerned, for assessing the thermal insulation is an increase of temperature of 140 K in average or of 180 K in maximum.

When dealing with standard fire (ISO fire) these criteria are checked for each rating (30 min, 60 min, … 180 min, …) assuming the fire is put out after the relevant time.

When making calculation of heat transfer with a natural fire development (meaning that a cooling phase will be considered) the maximum increase of temperature of a separating element will be obtained after the fire reached its maximum (in the cooling phase), due to its thermal inertia.

Here after is explained the reason why CEN TC 250/HGF is proposing an increase of the above mentioned insulation criteria for natural fire assessment to, respectively, 200 K and 240 K in the cooling phase.

CEN TC 250/HGF is keen to obtain the support of the FRG on these new criteria, since it is connected to physical phenomena. However if a full consensus could not be obtained within FRG, it should possible to consider these limiting values as Nationally Determined Parameters.

November 2001

TC 250 - H G "Fire"

Background for increasing insulation criteria in natural fire situation

1. INTRODUCTION

In the Model Clauses for the fire parts of Eurocodes (to be used by prEN 1992-1.2 to prEN 1996-1.2 and prEN 1999-1.2), as far as the insulation criterion is concerned, the following proposal is made:

" *The separating function with respect to insulation is ensured when:*
- *the average temperature rise over the whole of the non-exposed surface is limited to 140 K, and the maximum temperature rise of that surface does not exceed 200 K at the time of the maximum gas temperature,*
- *and the average temperature rise over the whole of the non-exposed surface is limited to 180 K, and the maximum temperature rise of that surface does not exceed 240 K during the decay phase of the fire or up to a required period of time."*

Since this proposal is not exactly in line with criteria used with the Standard fire (140 K average and 180 K maximum, for both testing and calculation), it was planned to refer to the Fire Regulator Group (FRG of the CPD Standing Committee) to obtain their agreement.

However, a comment was already made by the Finnish mirror group (see annex 1) and was sent to the CEN TC 127 and FRG. This item was shortly discussed within TC 127 at its last meeting on 23rd October 2001, and I have given some explanations and said that a background document will be provided later by CEN TC 250-HGF.

2. PURPOSE OF THE INSULATION CRITERIA

The main purpose of insulation criterion is to avoid thermal ignition of combustible materials on the unexposed side of separating elements.

The figures mentioned, regarding Standard fire tests, in ISO 834 and EN1363-1 is 140 K average and 180 K maximum at any point of a separating element.

According to these figures, it cannot be considered that the purpose of this reduction of temperature is against skin burning since it is too high. But it is for preventing the spread of fire through a wall or a floor.

3. BACKGROUND OF THE LIMITING VALUES

The 140K average increase of temperature comes from US ASTM E119 standard in which 250°F (139 K) was required in 1933, assuming that:

- the temperature of the unexposed side could rise up to 300°F after the furnace fire was extinguished,
- a 300°F (167K) rise could be a risk for ignition of wood or cotton waste.

In fact further experimentations were carried out in the 80s ("Investigating the unexposed surface temperature criteria of standard ASTM E 119", by K. J. Schwartz and T.T. Lie, Fire technology, vol 21, N0 3, August 1985) and concluded that :

- The self-ignition temperatures of ordinary combustibles, in contact with unexposed surface of separating element are in excess of 520 °F (271°C),
- It is suggested that a 400°F (222 K) average temperature rise and a maximum 450°F (250 K) temperature rise at any point be considered for criteria of the unexposed surface temperatures.

In addition the situation in Sweden was also considered. The functional requirement from the Swedish Building Regulations SBN 1980 (later on they were removed and passed to handbooks) is that the mean temperature on the ambient side was not greater than 200°C and the maximum local temperature was 240°C. (NB: Since this is an ignition criterion, the temperature is given, not the temperature rise)

4. "Natural FIRE" VERSUS "Standard FIRE"

When the criteria I is required by regulation, it is for a specified period of time : I30, I60 … I240, and is never alone, but always associated with the criteria for integrity E (and R for load bearing elements) which means that for ignition there is no risk of piloted ignition by hot gas or flames going through a separating element.

Regarding requirements expressed in terms of Standard fire durations, when testing, or even when calculating, the only parameter for insulation criterion is the temperature reached on the unexposed face at the requested time (30 min, 60min… 240 min) whatever the temperature rise could be after.

For example in figure 1 gives the temperature history on the unexposed face of 2 partitions able to provide either EI30 or EI240. Assuming that just after this period of time, the furnace is shut down, there is still a decay phase in the compartment / furnace. Due to the thermal inertia of the separating element, a maximum increase of temperature of 210 K is obtained after 49 min for the I30 element and of 187 K after 181 min for the I240 element.

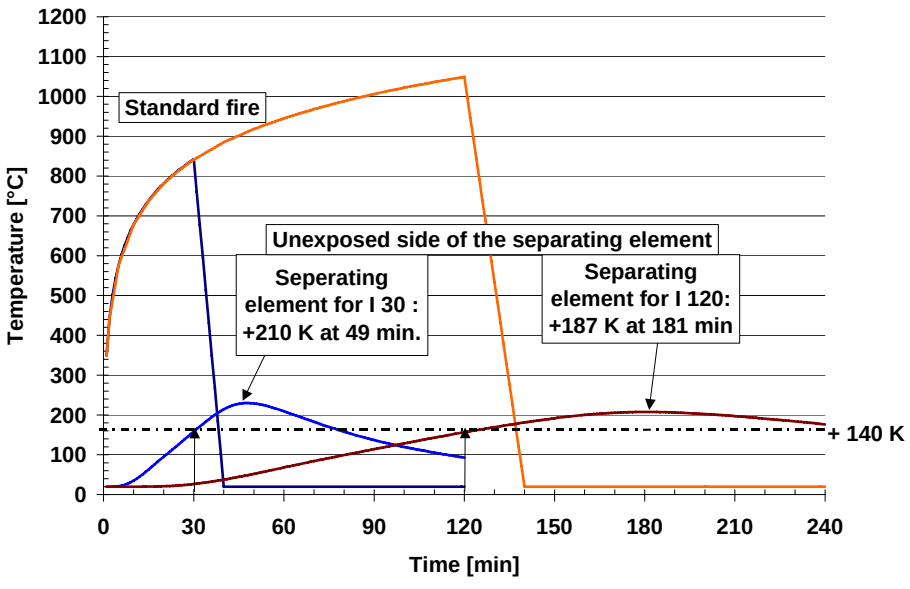

Figure 1 : Temperature of unexposed side of separating elements, having a fire rating of I30 and I120 regarding the insulation criteria of 140K in average.

Of course, this behaviour is never taken into account in the current classification system since it is only requested to have a look to the temperature reached at a given requested period of time.

But when dealing with natural fire, as it is mentioned in ENV 1991-1.2 clause 2.4 (4), the calculation has to be done for the whole fire duration, including cooling phase (unless otherwise specified by national authority).

Consequently it seems adequate to have the same behaviour as it is really happening when considering Standard fire :

- average temperature increase of 140 K in the growing phase of the fire,
- but limiting average temperature of 180 K for the whole duration of the fire (mainly within the decay phase)

And regarding the maximum temperature increase, in any point of a separating element, it is also wise to allow a higher value in the cooling phase, for instance 240 K.

In this respect , the current proposals of Model Clauses can be summarized as given in table 1.

Table 1: Limiting values for $\Delta\Theta_{non\ exposed}$, as proposed in Eurocodes “Fire” (prEN version)

$\Delta\Theta_{non\ exposed}$ [K]	growing phase only	decay phase included	ignition conditions based on Schwartz et al
average	140	180	220
max	200	240	250

5. PROPOSAL for FURTHER IMPROVEMENT

In order to have a more consistent "safety" margin with respect to both the average temperature and the maximum temperature rise, as far as the ignition conditions are concerned; and also to keep the same criteria for the growing phase as used with the Standard fire, the alternative proposal given in table 2 could be followed.

Table 2: Alternative proposal

$\Delta\Theta_{non\ exposed}$ [K]	growing phase only	decay phase included	ignition conditions based on Schwartz et al
average	140	200	220
max	180	240	250

With such figures, there is still a safety margin with the self-ignition temperatures of combustible materials as reported above.

J. Kruppa
On the behalf of TC 250-HG"Fire"

POSTAL ADDRESS
P.O.Box 380, FIN-00131
Helsinki, Finland
Exchang
e +358 9 19911 +358 9
1991 9545
kirjaamo
ym@vyh.fi

MINISTRY OF THE ENVIRONMENT
FI N L A N D

Date

4.9.2001

HGF – N201

CEN/TC 250/ Horizontal Group Fire
prof. J. Kruppa

CEN/TC 127
Mrs Magda DiCarlo

Fire Regulators Group
Ms Helen Sutcliffe

Finnish comments on surface temperature rise limits presented in Fire Design Parts of Eurocodes for parametric fire exposure

Second draft of prEN 1992-1-2 concerning structural fire design of concrete structures has been considered in the Finnish National Mirror Group. In paragraph 2.1.3 (2) of the 2nd draft performance requirements have been given for parametric fire exposure concerning the separating function of a structure with respect to insulation. Following allowed values have been defined in this paragraph:
- at the time of the maximum gas temperature the average temperature rise over the whole of the non-exposed surface (140 ^{o}K) and the maximum temperature rise of that surface (200 ^{o}K)
- during the decay phase of the fire or up to a required period of time the average temperature rise over the whole of the non-exposed surface (180 ^{o}K) and the maximum temperature rise of that surface (240 ^{o}K).

We wonder 1) why these values deviate from those given for nominal fire exposure (which is the basis of resistance to fire classification) and 2) why such values should be given at all. In our opinion, when parametric fire is applied the criteria should be considered case by case, taking into account the risks caused by temperature rise on the unexposed surface, without setting any binding temperature limits beforehand. Moreover, it is up to the competent authorities in the Member States to define the acceptance criteria for parametric fire exposure.

We suggest that the given temperature rise limits be removed. If any limits would be set the criteria should be the same as in nominal fire exposure. The corresponding change should be done in other Fire Design Parts of material-based Eurocodes, too.

On behalf of the Finnish Mirror Group

Jaakko Huuhtanen

BDA 3.1
Background documentation for thermal conductivity of concrete

This report is aimed to validate the use of thermal properties given in the first and second draft of prEN 1992-1-2 for concrete structures. 6 different computer simulations will illustrate the good concordance between measurements and computer simulations by use of the thermal properties given in the first and second draft of prEN 1992-1-2 (see figure 1). The use of the former thermal properties in ENV 1992-1-2 give a very conservative result.

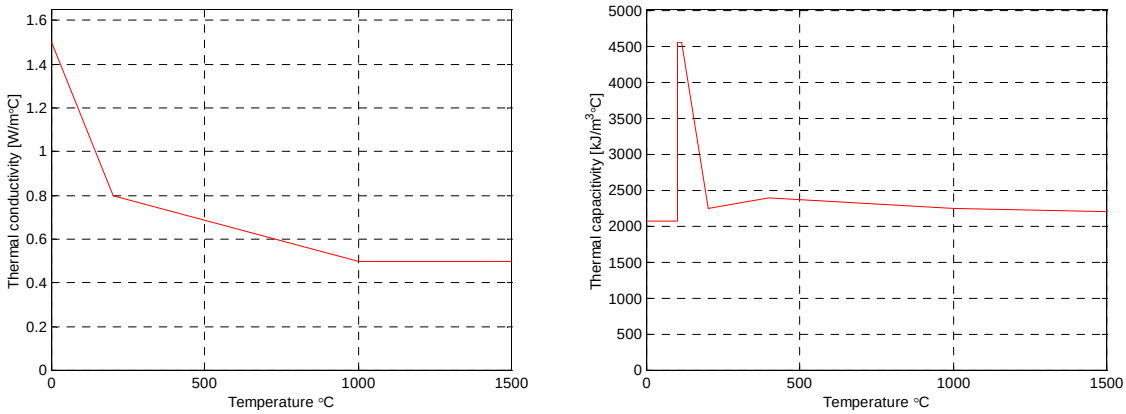

Conductivity Density*Capacitivity

Figure 1 *Temperature-dependent thermal material properties of concrete with a moisture content of 3% and a density of 2300 kg/m^3 according to the first and second draft of prEN 1992-1-2.*

For comparison the former EC-thermal properties shown in figure 2 are used in the two first simulations.

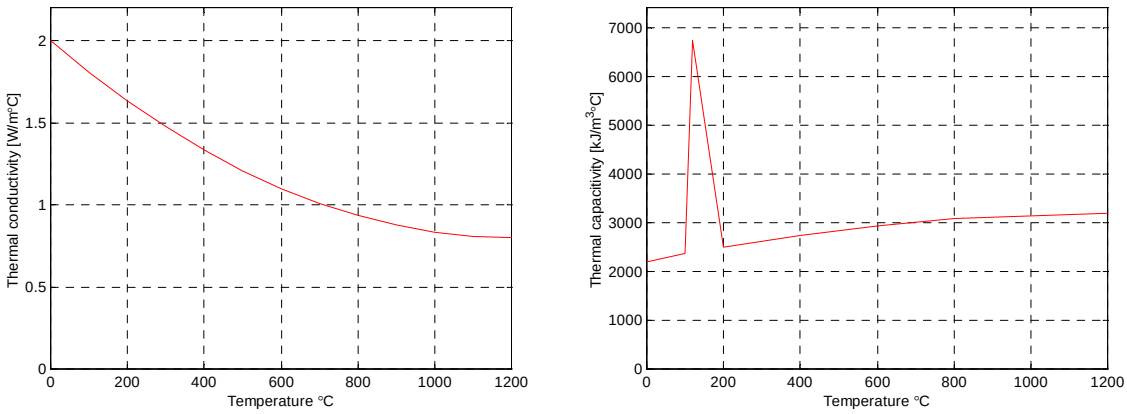

Conductivity Density*Capacitivity

Figure 2 *Temperature-dependent thermal material properties of concrete with a moisture content of 4% and a density of 2450 kg/m^3 according to ENV 1992-1-2.*

Simulation 1

A computer simulation of a fire resistance test on a prestressed TT-roof slab (240-07/40) (Figure 3) (test carried out 1977-07-06 at TNO in Holland).

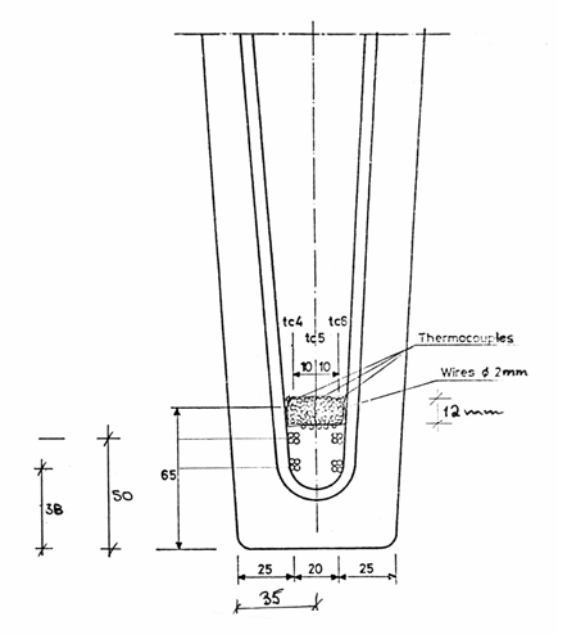

Figure 3 *Cross-section of TTF 240-07/40 slab.*

The measured temperatures shall be compared with the curve representing prEN 1992-1-2 properties. Measured and calculated curves are very close to each other in Figure 4. The curve representing the ENV properties is deviating up to 90 °C which is unacceptable.

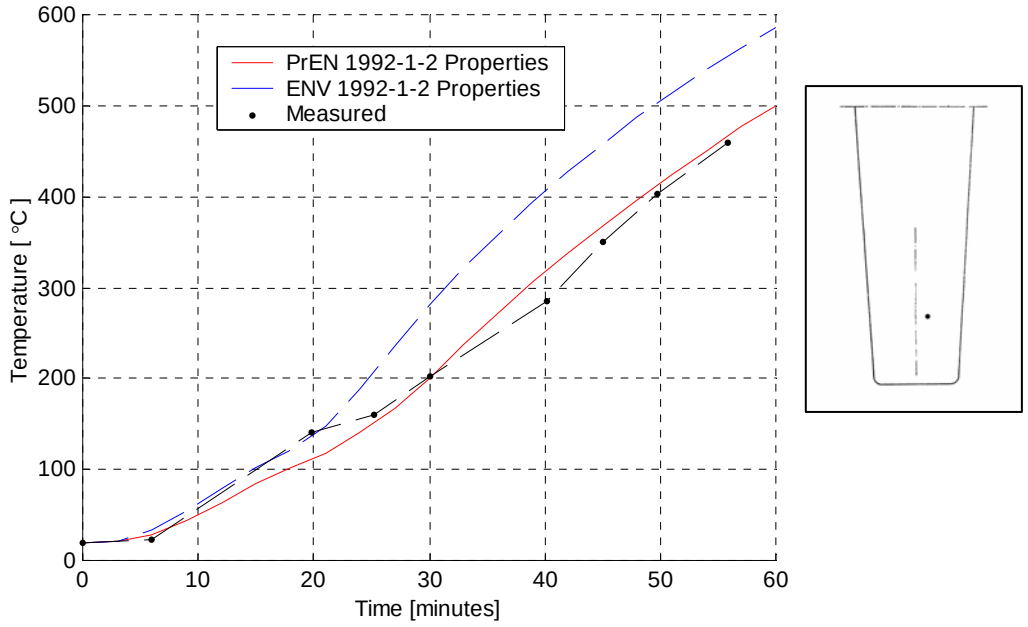

Figure 4 *Comparison between measured and calculated temperature in reinforcement located 10 mm to the left of the centre line and 59 mm from the bottom of the TT slab.*

Simulation 2

The same TT slab (240-07/40) as in simulation 1 was tested at SP in Borås, Sweden 1978-06-09. The slab was exposed to 60 minutes of ISO 834 standard fire. A very good agreement was also attained in this simulation as shown in Figure 5. Also here the ENV-properties gave too high temperatures (90 °C).

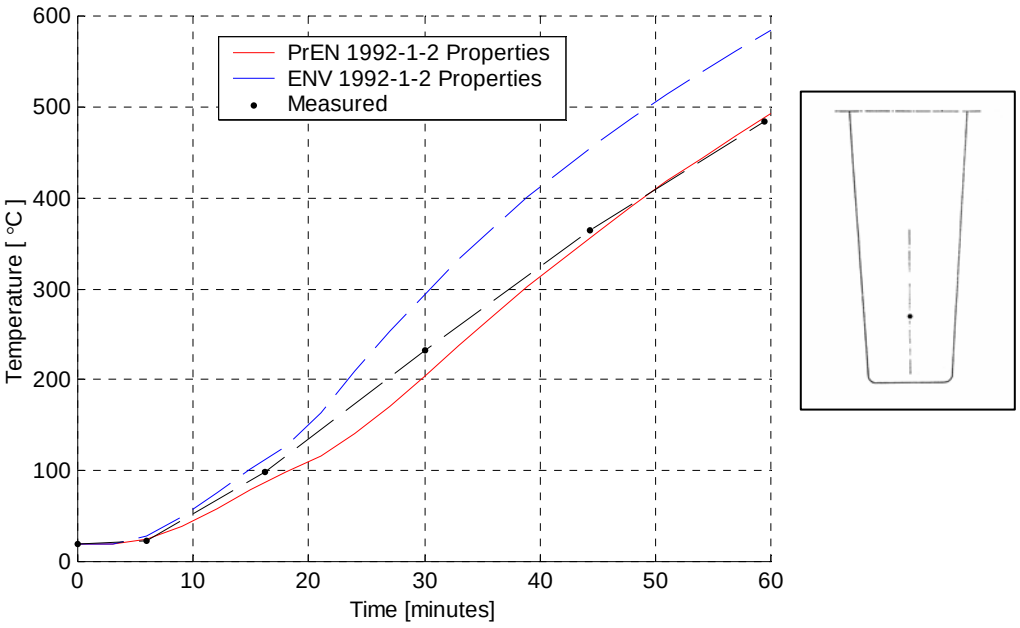

Figure 5 *Comparison between measured and calculated temperature in reinforcement located on the centre line of the web and 59 mm from the bottom of the TT slab.*

Simulation 3

A hollow core slab (see figure 6a) was fire-tested by VTT in Finland in 1991 and the duration of the ISO 834 fire was 157 min with a subsequent cooling phase. In figure 6 b the measured temperature in the prestressing bar 50 mm from the surface is very close to the predicted one both during the heating and cooling phase when based on the prEN 1992-1-2 thermal properties. Based on the ENV-properties the temperatures are up tp 80 °C too high which also is unacceptable.

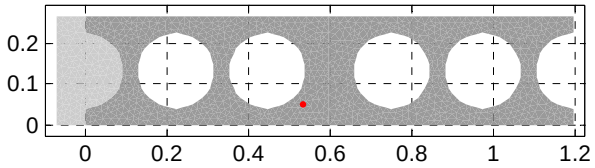

Figure 6 a Cross-section of hollow core slab with a measureing point 50 mm from the bottom

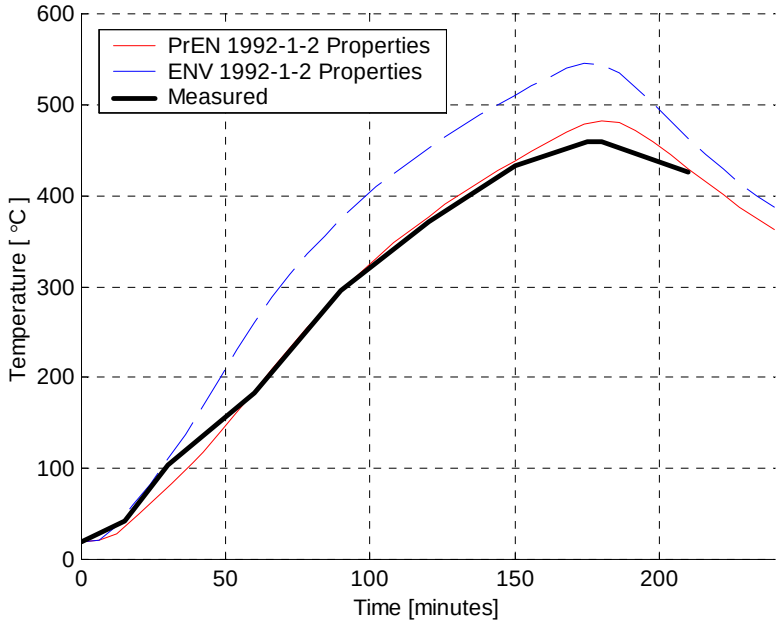

Figure 6 b Temperature development in a point located 50 mm from the bottom as indicated in the figure. Measured temperatures are shown as the thicker line. Temperature history as calculated with prEN 1992-1-2 properties are represented by the solid thin line and the corresponding ENV- properties calculations are represented by the thin, dashed line. (Point 13 in test report, [.535 .05])

Simulation 4

A hollow core slab (Pal 1126/91), see figure 7, was tested in Finland 26 april 1991 and test and simulated results are shown in Fig 8 and 9 respectively. A very good agreement can be found between measurements and predictions based on the prEN 1992-1-2 thermal properties.

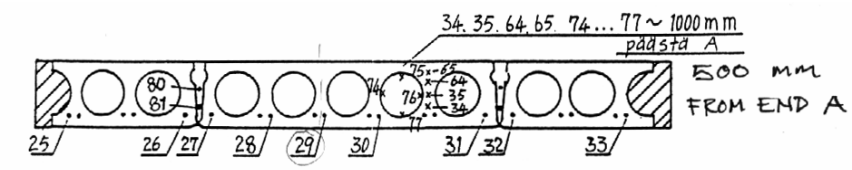

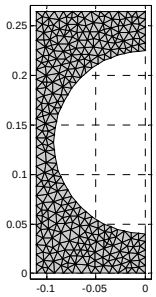

Figure 7 Cross-section and finite element mesh of hollow slab, Pal 1126/91

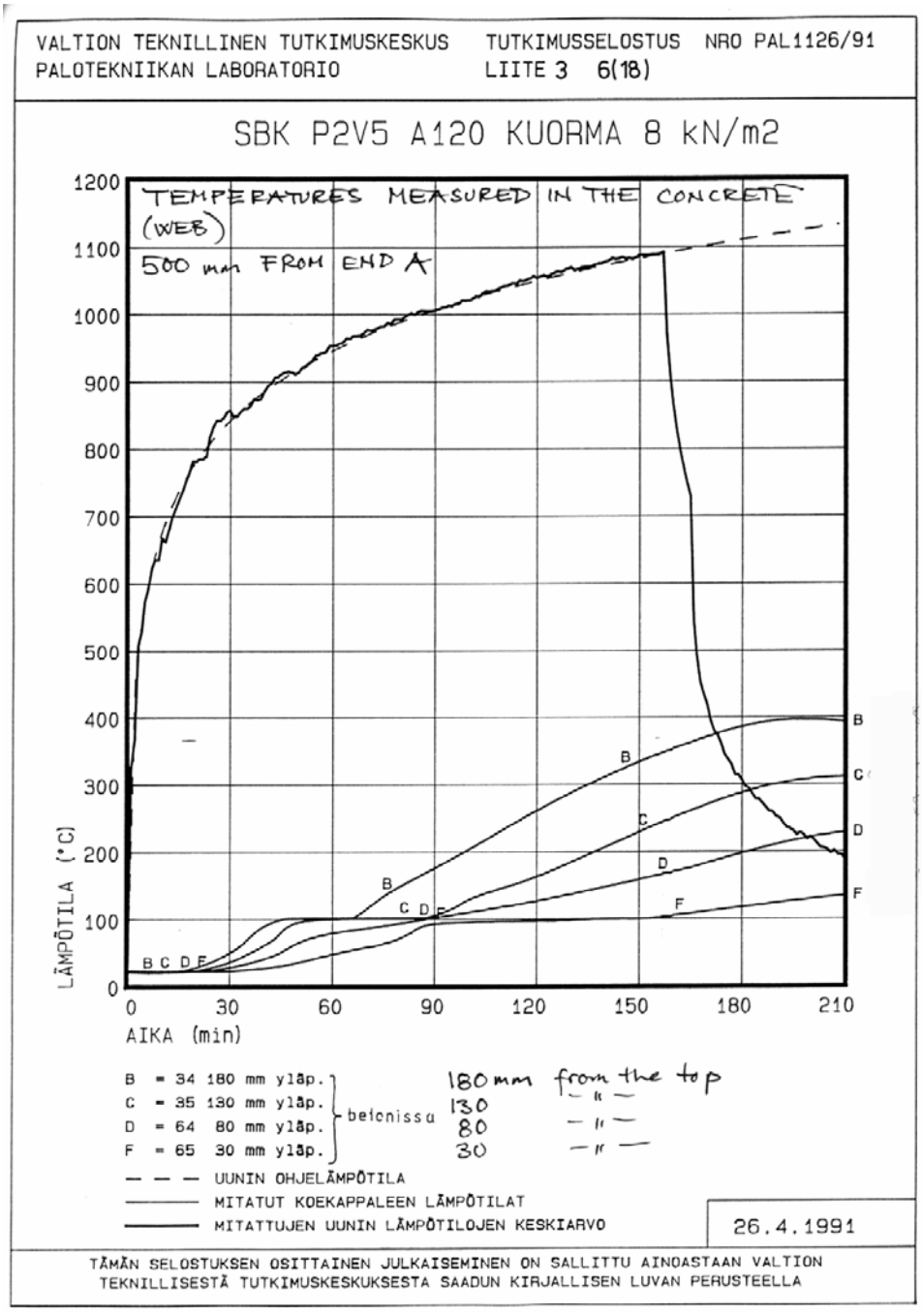

Figure 8 Measured temperature curves at different depths

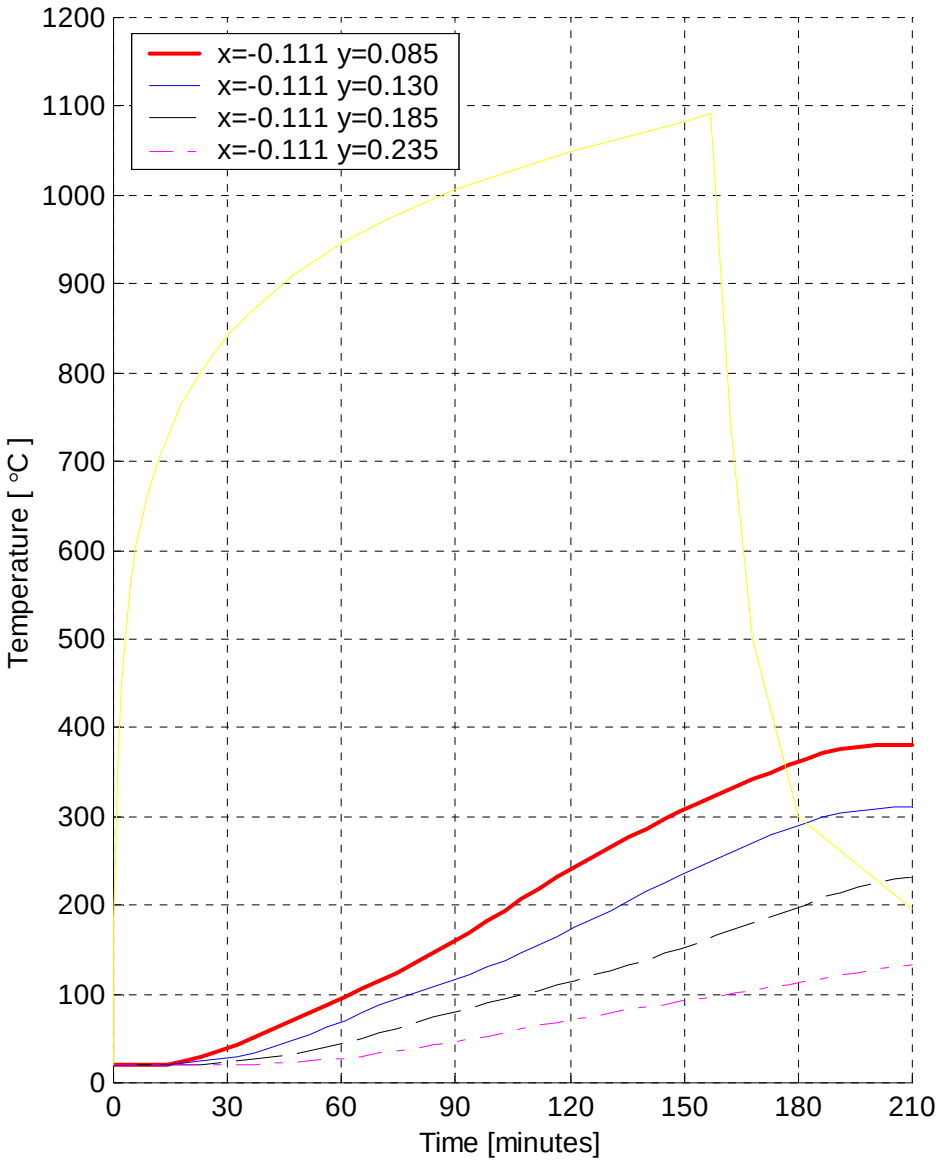

Figure 9 Calculated results for hollow core slab Pal 1126/91 when based on prEN 1992-1-2 thermal properties

Simulation 5

Two concrete walls (Dift Rep x 526 50) of a thickness of 120 mm and 150 mm and fire-exposed on one side was tested in Denmark, November 1999. Test results and predicted results (based on prEN 1992-1-2 thermal properties) are shown in Fig 10 and 11 for the slab of thickness 120 mm and in 12 and 13 respectively. A comparison illustrates a very good agreement.

Group name	Concrete cover	Thermocouples No.	Element: Thermocouples:
T_15mm_DB1200	15 mm	7	DB1200 A2: T1, T2, T3 DB1200 B: T1, T2, T3, T4
t__105mm_DB1200	105 mm	2	DB1200 A2: T4 DB1200 B: T5

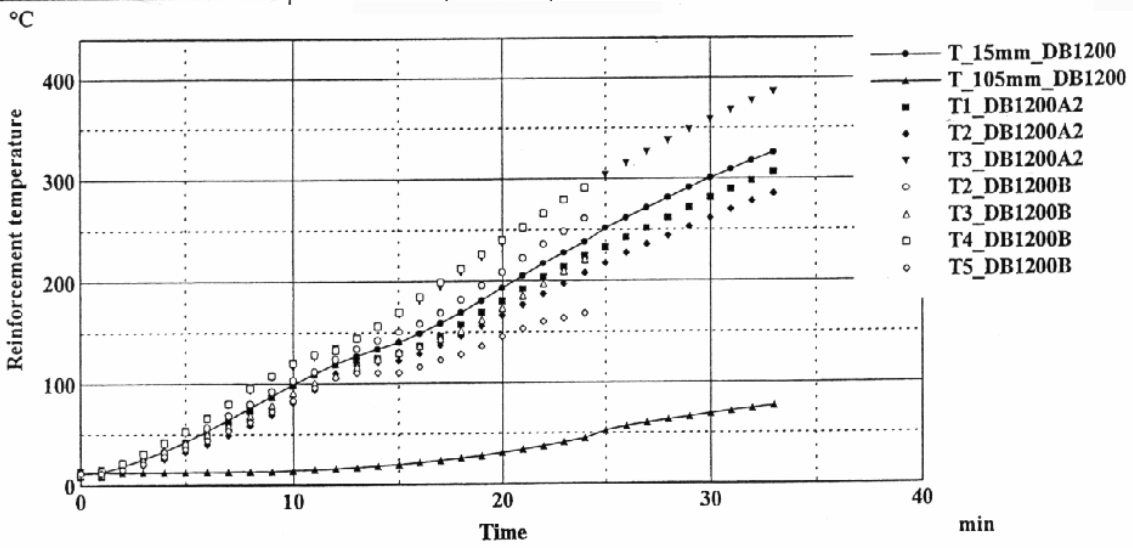

Reinforcement temperature for element No. DB1200 A2 and DB1200 B.

Figure 10 Measured temperatures at different depths of the wall (120 mm).

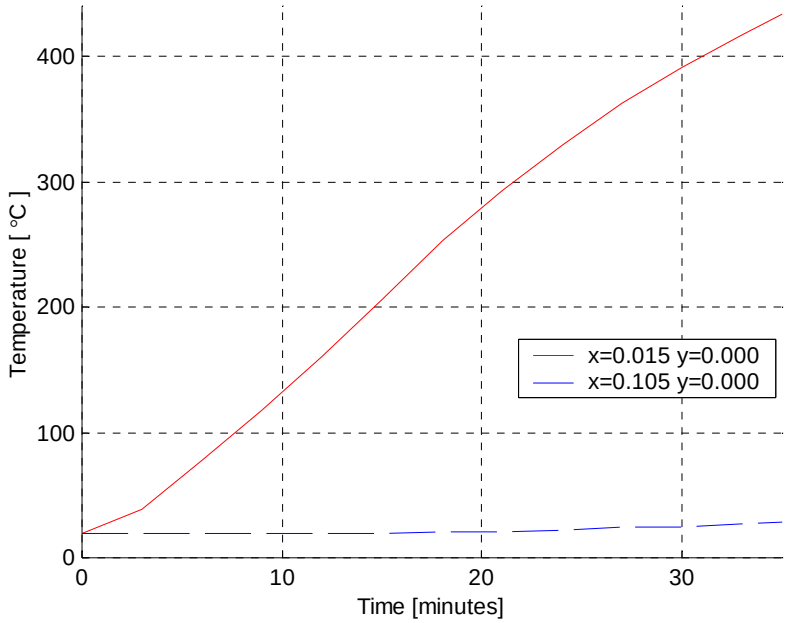

Figure 11 Predicted temperatures for the wall (120 mm)

Group name	Concrete cover	Thermocouples No.	Element:	Thermocouples:
T_15mm_DB1500	15 mm	8	DB1500 A: DB1500 B:	T1, T2, T3, T4 T1, T2, T3, T4
T_135mm_DB1500	135 mm	2	DB1500 A: DB1500 B:	T5 T5
T_75mm_DB1501	75 mm	10	DB1501 A: DB1501 B:	T1, T2, T3, T4, T5 T1, T2, T3, T4, T5

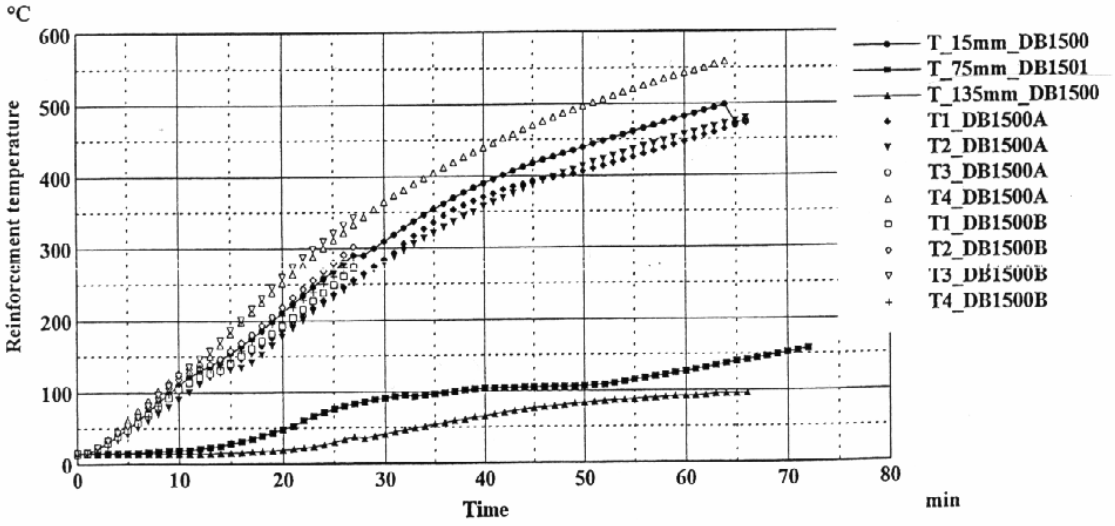

Reinforcement temperature for element No. DB 1500 A and B, DB1501 A and B.

Figure 12 Measured temperatures at different depths of the wall (150 mm).

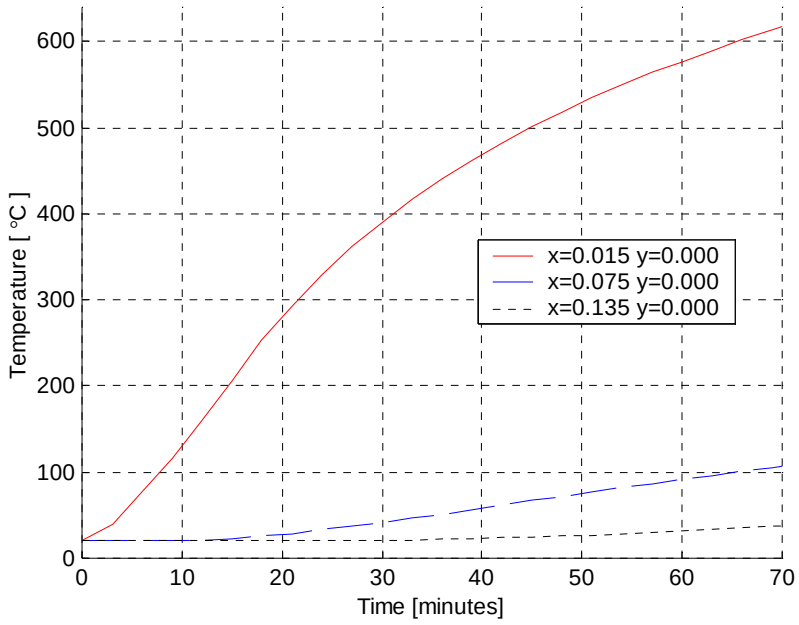

Figure 13 Predicted temperatures for the wall (150 mm)

Simulation 6

A standard fire resistance test was carried out in UK in July 1969 on a floor of prestressed concrete ”Spiroll units, frosi No 4904. The hollow core slab is shown in Figure 14. Measured and predicted results are gathered in Figurs 15 illustrating a very good agreement for the prestressing bar as well as on the unexposed surface.

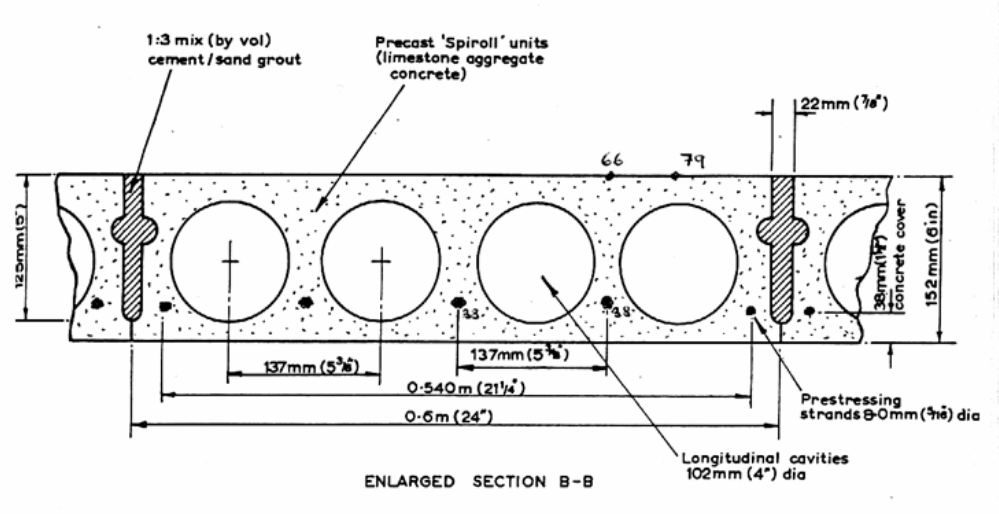

Figure 14 Cross-section of ”Spiroll” units – hollow core slab

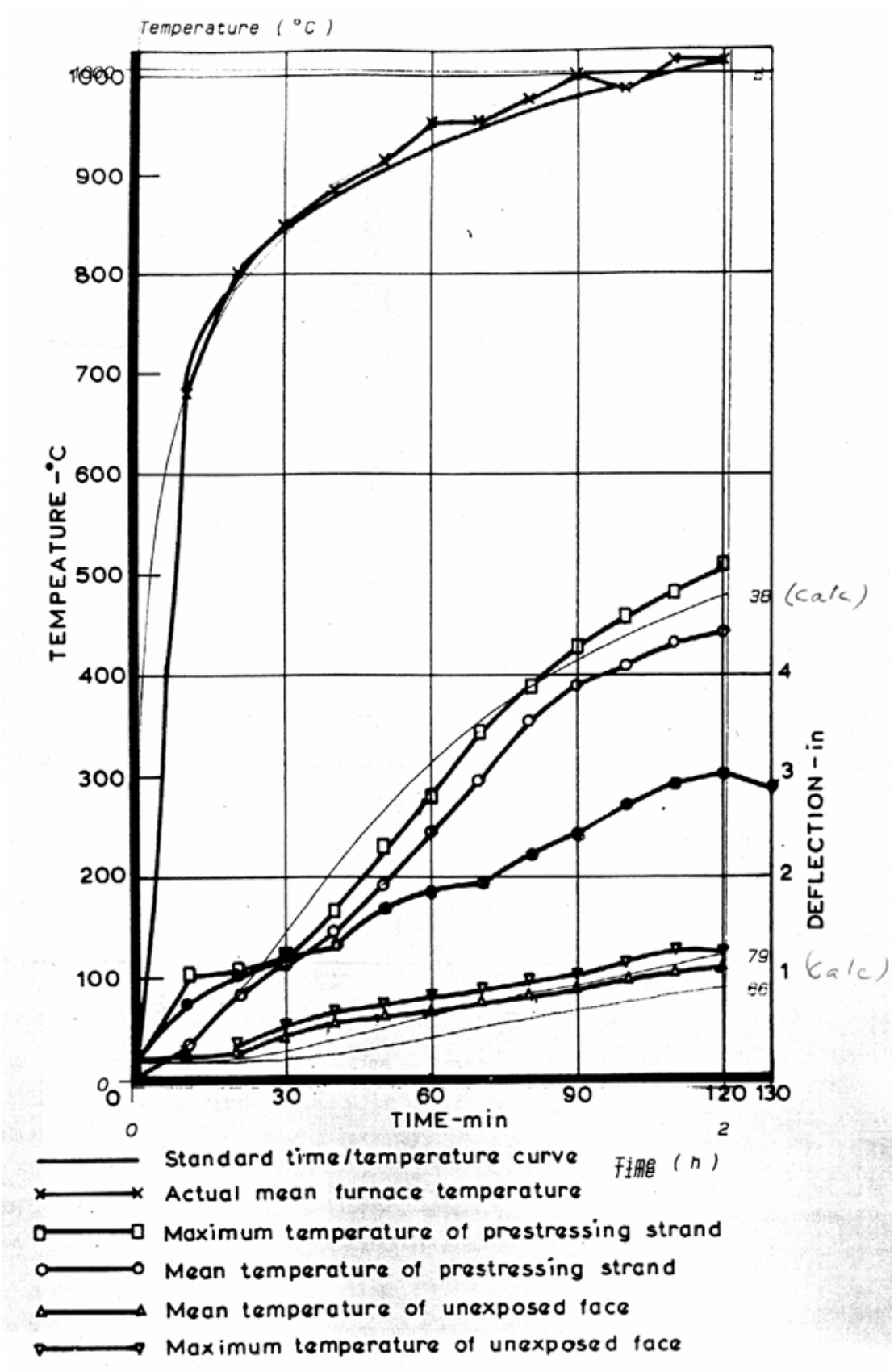

Figure 15 Measured and predicted temperatures of the ”spiroll ” unit.

COMPARISON OF THERMAL PROPERTIES, SLAB 100 mm

Ref: Annex to minutes of Horizontal Group Fire 12 October 2001

HGF convenor Kruppa had calculated temperatures of 100 mm by using thermal properties in prEN 1992-1-2 and thermal properties used in ENV 1992-1-2 and ENV 1994-1-2, attached as Annex to minutes of Horizontal Group Fire 12 October 2001.

This calculation was made without moisture content. He has also made additional calculations with 4 % moisture content, and presented them with his conclusions as follows:

– – –

From Kruppa :

21 Novembre 2001

Effect of thermal properties of concrete

Temperature calculation within a 100mm concrete slab with :

- thermal properties given by ENV 1992-1.2 / ENV 1994 1.2
- thermal properties proposed by prEN 1992-1.2
- assuming furnace control by plate thermometer : "furnace emissivity = 1.0
- concrete emissivity = 0.7
- convection coefficient on exposed side : 25, on unexposed side : 4
- with 4% moisture and without

Conclusion:

- without moisture, new thermal properties lead to +18% for fire stability and + 74% for insulation criterion
- with 4% moisture, new thermal properties lead to + 17% for fire stability and + 61% for insulation criterion

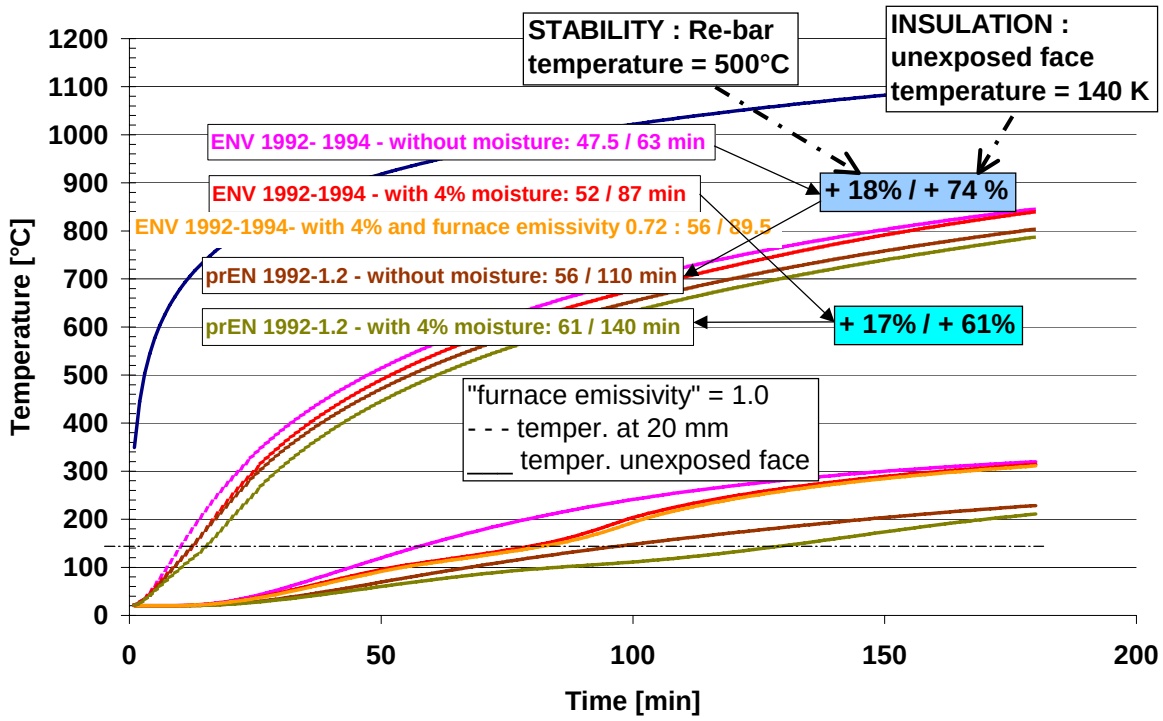

– – –

However, there was no comparison to test results.

In the figure below temperatures given in CEB Bulletin d'Information 145 « Design of concrete structures for fire resistance » have been added. These temperatures are based on tests, used as basis for Tabulated Data in many national fire design codes, and also in ENV 1992-1-2.

The figure is self-explaining: the proposed thermal properties in prEN 1992-1-2 give very similar temperatures as CEB 145, and are in this comparison on the safe side. ENV values give clearly conservative results.

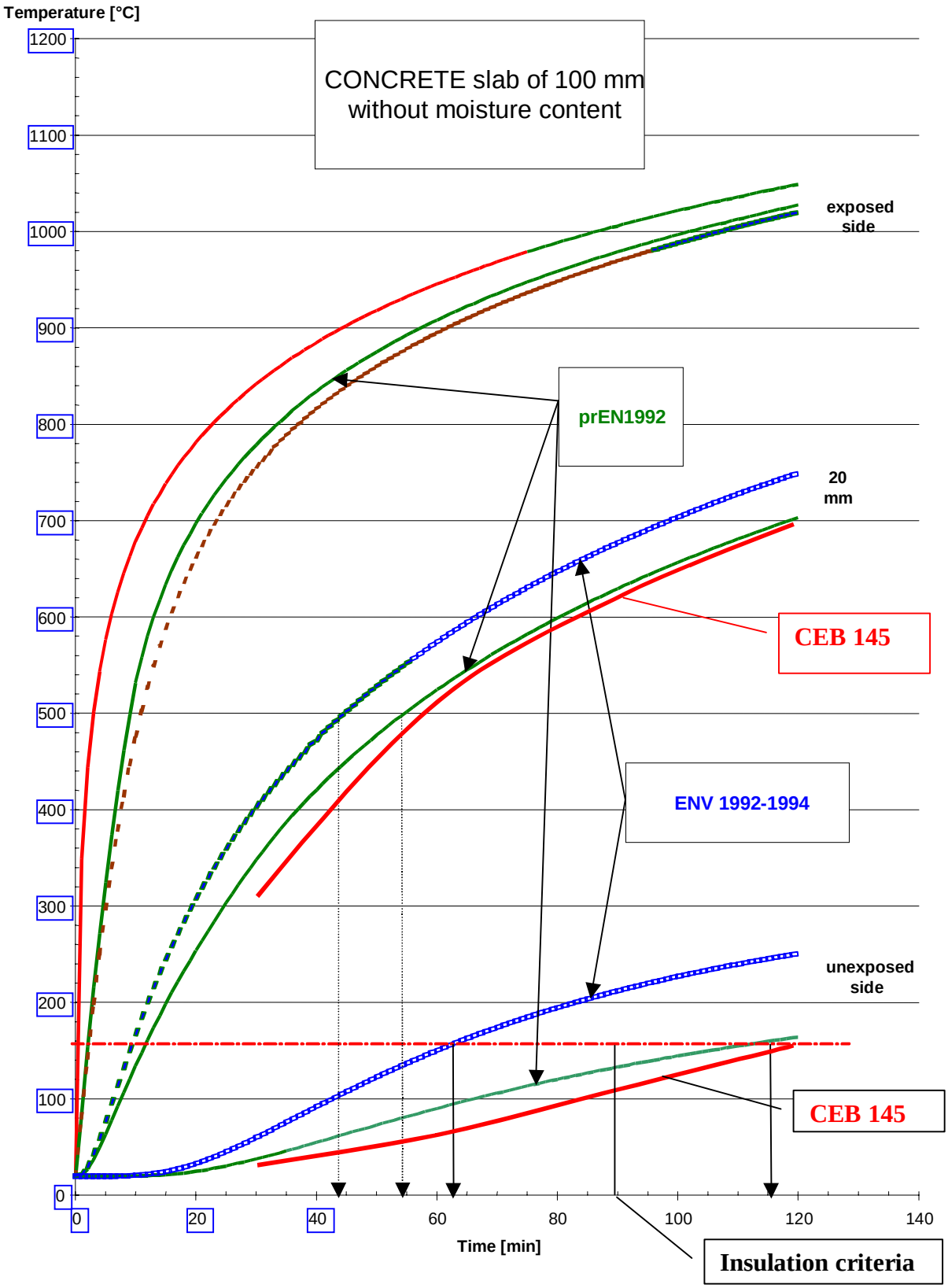
Temperature [°C]
1200
1100
1000
900
800
700
600
500
400
300
200
100
0
CONCRETE slab of 100 mm
without moisture content
exposed
side
prEN1992
20
mm
CEB 145
ENV 1992-1994
unexposed
side
CEB 145
0
20
40
60
80
100
120
140
Time [min]
Insulation criteria

BDA 3.3

THERMAL PROPERTIES OF CONCRETE
- ADDITIONAL COMPARISON AND RESPONSE

Background

SC 4 Fire part Project Team does not accept the change of thermal properties of concrete included in prEN 1992-1-2. There has been an extensive exchange of opinions and e-mails.

Summary of the arguments against justification of the values in prEN 1992-1-2 are presented in document by Jules Mathieu/Profil Arbed 4/02/2002. This document is copied in the first part of this document, with response from SC 2 Fire part Project Team.

Response to arguments concerning insulation criteria is given in the second part.

Third part of this document is comparison to French slab tests.

1. Document by Jules Mathieu/Profil Arbed and EC 2 PT response

Document CEN/TC 250/SC 2/PT 1-2 Doc N 150

Yngve Anderberg 2001-07-03

Background documentation for thermal conductivity of concrete

Critical analysis of the conclusions (summary)

In the report above the new modified thermal laws of concrete (conductivity and specific heat) introduced in prEN 1992-1-2 are justified on the basis of 6 different computer simulations of tests. They concern, in detail:

- simulation 1 : Prestressed TT-roof slab (1977 at TNO) : about **60** minutes
- simulation 2 : Prestressed TT-roof slab (1978 in Sweden) : about **60** minutes
- simulation 3 : Hollow core slab (1991 at VTT) : about **200** minutes
- simulation 4 : Hollow core slab (1991 in Finland): about **200** minutes
- simulation 5 : Concrete wall 120 mm (1999 in Danmark) : about **33** minutes
- simulation 5 bis : Concrete wall 150 mm (1999 in Danmark) : about **65** minutes
- simulation 6 : Hollow core slab (1969 in UK): about **120** minutes

The following remarks can be made about these simulations:

1) **The range of temperatures put in the comparison is limited to 500 °C**. Therefore the validity of the new laws is not established for temperatures over that value.

Response: Temperatures above 500°C are not much of interest for concrete structures because temperatures between exposed surface and reinforcement has practically no influence on the fire resistance of concrete structures.

Comparison to French slab tests show that that prEN 1992-1-2 values are safe near the exposed surface.

2) The simulations 3, 4 and 6 concern **hollow core slabs**. They cannot be accepted as relevant, for **the results don't depend only on the material laws for concrete**, but also depend on the material laws adopted for the enclosed air in the holes, and on the conditions of radiation (and convection?) into the holes.

Response: The holes have been modelled in the simulations as mentioned several times by Dr Anderberg. Critics on the modelling seems to be an assumption only made without knowing the details of the modelling.
It would be a funny coincidence if thermal properties were wrong and the simulation model was wrong but the results fit with temperatures measured in the tests?

3) The simulations **3, 4 and 6 are the only ones going over 60 minutes**. If they are not relevant as observed in 2) above, **the validity of the new laws in prEN is not established for calculations exceeding 60 minutes**.

Response: It follows from response to point 2 above that this point 3 is not correct. Additionally, the French slab tests go to 120 minutes.

Strange comment: Thermal properties depend on temperature, why would they depend on time?

4) The tests used for simulations 1 and 2 are very old, and it seems that some informations are missing to check the validity of the comparison.

Response: Why would tests from late 70'ies not be valid?

5) In the Danish tests 5 and 5bis, the calculated temperatures have been **compared with the <u>average</u> temperatures** of a group of thermocouples including one at the centre of the wall, and 3 or 4 located at the periphery. It can be seen on figures 10 and 12 reproduced in the document that **the peripheral thermocouples have given temperatures <u>well grouped</u> but lower (up to 100°C) than in the centre** of the wall panel. It is obvious that a border effect could not be neglected, and the average temperature is lower up to about 60°C than the maximum one. **The**

conclusion should have been draft on the basis of the maximum temperature in the centre, and not on the basis of the average temperature.

Response: Calculated temperatures at depth 15 mm (Fig 13 in N 150) are approximately 50°C higher than reinforcement temperature in the middle of the wall (T4 DB1500A in Fig 12). Concrete cover is 15 mm, reinforcing bar diameter 6 mm, this makes axis distance 18 mm. 3 mm difference in axis distance corresponds approximately 30°C difference in temperature. This means that calculated temperatures are 20°C higher than the measured ones.

6) **The simulation of the Danish tests with the ENV previous concrete laws give temperature in good concordance with the maximum measured temperature in centre of the wall**. (See enclosed file comparison.xls)

Response: It was not mentioned in the attached excel file at which depth the temperatures were calculated. In comparison to measured reinforcement temperature it should be axis distance (18 mm). Compared to N 150 Fig 13 the prEN 1992-1-2 curve seems to be too low.

7) The need and the experience in simulating tests or in realistic calculations are much smaller in the concrete industry than in the composite and steel industry. Therefore it is not logical to calibrate thermal laws only on pure concrete elements, without consideration for composite elements.

Response: We agree to the statement that the need is smaller for concrete structures. It is very important to have correct temperature for reinforcement. For reinforcing steel this temperature area is around 450°C to 600°C and for prestressing steel around 350°C to 450°C. Concrete temperatures below 300°C are of no interest, because in those temperatures concrete has practically the full strength.

For insulation criteria, see response below and PT document N 176.

EC 2 Project Team has not considered composite elements. Of course, thermal properties of concrete are the same in concrete structures and in composite structures. We do not know how composite elements have been modelled, like thermal transfer to steel and from steel to concrete, different conditions for the moisture to evaporate when concrete in encased in steel, possible buckling of steel sheet etc.

<u>Conclusion</u>: ***the background document is not sufficient in itself to justify a modification of the existing concrete thermal laws in ENV1992-1-2, which seem to be more realistic as well for concrete elements (Danish tests) as for composite elements***.

Response: EC 2 Project Team can not agree to this conclusion.

MATHIEU Jules

Technical Assistance

EUROPROFIL

ProfilARBED

4/02/2002

2. Response to arguments concerning insulation criteria

Reference is made to EC 2 Project Team Document N 176.

Conclusion is clear: Compared to experimental experience and Tabulated Data in prEN 1992-1-2 (the same as in ENV 1992-1-2) prEN 1992-1-2 thermal properties do not give unsafe values. ENV 1992-1-2 thermal properties give very conservative values, or the temperature calculation models are not reliable.

Unfortunately the curves calculated by Horizontal Group Fire convenor Kruppa have been widely distributed, even as annexes to last TC 250 meeting minutes.

3. French slab tests

CSTB fire tests 1975 for 4 slabs 140 mm and 2 columns 200x200 and 300x300 mm.

Slab temperatures were measured each 10 mm from the exposed side at several points on axis, diagonal and on a line between centre and the ¼ of the side.

Aggregates were 70 % siliceous and 30 5 calcareous. Moisture content from 1,7 to 4,3 %.

Measured temperatures (range between minimum and maximum of 4 tests) are presented in the attached figure for 60 and 120 min. Also corresponding temperature profiles given in Annex A of prEN 1992-1-2 and CEB Bulletin 145 are presented.

Observations:

At 500°C maximum of 60 min test results, prEN 1992-1-2 and CEB are the same.

At 500°C average of 120 min test results, prEN 1992-1-2 are the same, CEB curve and maximum of test results are the same. Difference of the depth from exposed surface at 500°C between prEN 1992-1-2 and CEB curves is 3 mm.

At higher temperatures prEN 1992-1-2 and CEB are practically identical and safe compared to test results.

Between 500°C and 100°C prEN 1992-1-2 are within the scatter of test results, except for 120 min blow 270°C they are below minimum of test results. CEB curves are between maximum and average of tests results.

Below 100°C both prEN 1992-1-2 and CEB curves are below test results. These temperatures have no influence on the fire resistance of concrete structures.

HGF – N 219

BDA 3.4

CEN/TC 250 N 528-rev

May 16th, 2002

CEN - TC 250

Special meeting
on
Thermal properties of concrete

Delft - 15 May 2002

Attendants

Dr U. Litzner	chairman TC 250/SC2
Prof. J. Stark	chairman TC 250/SC4
Mr. M. Vallès	chairman TC 229
Dr. Y. Anderberg	member of TC 250/SC2 – PT2
M. L. Twilt	member of TC 250/SC4 – PT2
Prof U. Wikström	expert, member of TC 250 / HGF
Ms F. Robert	expert, NTC of TC 250/SC2- PT2
Mr. F. Biasioli	representing CEPMC
Dr. J. Kruppa	co-ordinator TC 250/HGF

OUTCOMES

After presentation of available information and large amount of discussions among the members, the following conclusions were agreed, as far as concrete with siliceous and calcareous aggregates is concerned.

.

1- The following values for the variation of mass unit (density) versus temperature shall be used in both prEN 1992-1.2 and prEN 1994-1.2

$$\rho(\theta) = \rho(20°C) \quad \text{for } 20°C \le \theta \le 115°C$$
$$\rho(\theta) = \rho(20°C)\cdot(1 - 0{,}02(\theta - 115)/85) \quad \text{for } 115°C < \theta \le 200°C$$
$$\rho(\theta) = \rho(20°C)\cdot(0{,}98 - 0{,}03(\theta - 200)/200) \quad \text{for } 200°C < \theta \le 400°C$$
$$\rho(\theta) = \rho(20°C)\cdot(0{,}95 - 0{,}07(\theta - 400)/800) \quad \text{for } 400°C < \theta \le 1200°C$$

where θ is the concrete temperature (°C)

2- The following values for specific heat of dry concrete shall be used in both prEN 1992-1.2 and prEN 1994-1.2

$$C_c = 900 \text{ (J/kgK)} \quad \text{for } 20°C \le \theta \le 100°C$$
$$C_c = 900 + (\theta - 100) \text{ (J/kgK)} \quad \text{for } 100°C < \theta \le 200°C$$
$$C_c = 1000 + (\theta - 200)/2 \text{ (J/kgK)} \quad \text{for } 200°C < \theta \le 400°C$$

C_c = 1100 (J/kgK) for 400°C < $\theta \leq$ 1200°C

where θ is the concrete temperature (°C)

Where the moisture content is not considered explicitly in the calculation method, the function given for the specific heat of concrete with siliceous or calcareous aggregates may be modelled by a constant ~~peak~~ value ~~situated~~ between 100°C and 115°C such as

$c_{p.peak}$ = 900 J/kgK for moisture content of 0 % of concrete weight
$c_{p.peak}$ = 1470 J/kgK for moisture content of 1,5 % of concrete weight
$c_{p.peak}$ = 2020 J/kgK for moisture content of 3,0 % of concrete weight

and linear relationship between (115, $C_{p,peak}$) and (200, 1000).

For other moisture contents a linear interpolation regarding $C_{p,peak}$ is acceptable.

3- The thermal conductivity shall be a Nationally Determined Parameter with, in both prEN 1992-1.2 and prEN 1994-1.2, the same lower and upper recommended limit values, with the possibility, for member states, to choose values in-between :

   a. The upper limit will be derived from the "ENV" values, taking into account the agreed values for density and specific,
   b. The lower limit will be derived from a new proposal (connected to the "prEN 1992-1.2" proposal) presented by Ms Robert.

4- Final proposals for thermal conductivity have to be ready by end of June 2002 to be presented at the next TC 250/SC2 on 1st and 2nd of July 2002. Proposals will be made by :

   a. Prof. Stark, with the help of L. Twilt and Prof Schleich (convenor of TC 250/SC2 – PT2) as far as the upper limit is concerned
   b. Ms Robert, with the help of Dr Anderberg and T. Hietanen (convenor of TC 250/SC2 – PT2), in consultation with the other members of this special meeting, as far as the lower limit is concerned.

J. Kruppa

Nota : compared to the document TC 250 N 528, distributed at the TC 250 meeting, the modifications made in this final document (highlighted) are due to comments received and discussion with T. Hietanen.

draft TC 250 Resolution N° …

Subject: Thermal properties of concrete

CEN/TC 250 agrees to adopt the compromise specified in document N 528 concerning rules to be implemented in parts 1.2 of prEN 1992 and prEN 1994.

BDA 3.5 Background document for the new proposal of the lower limit for thermal conductivity

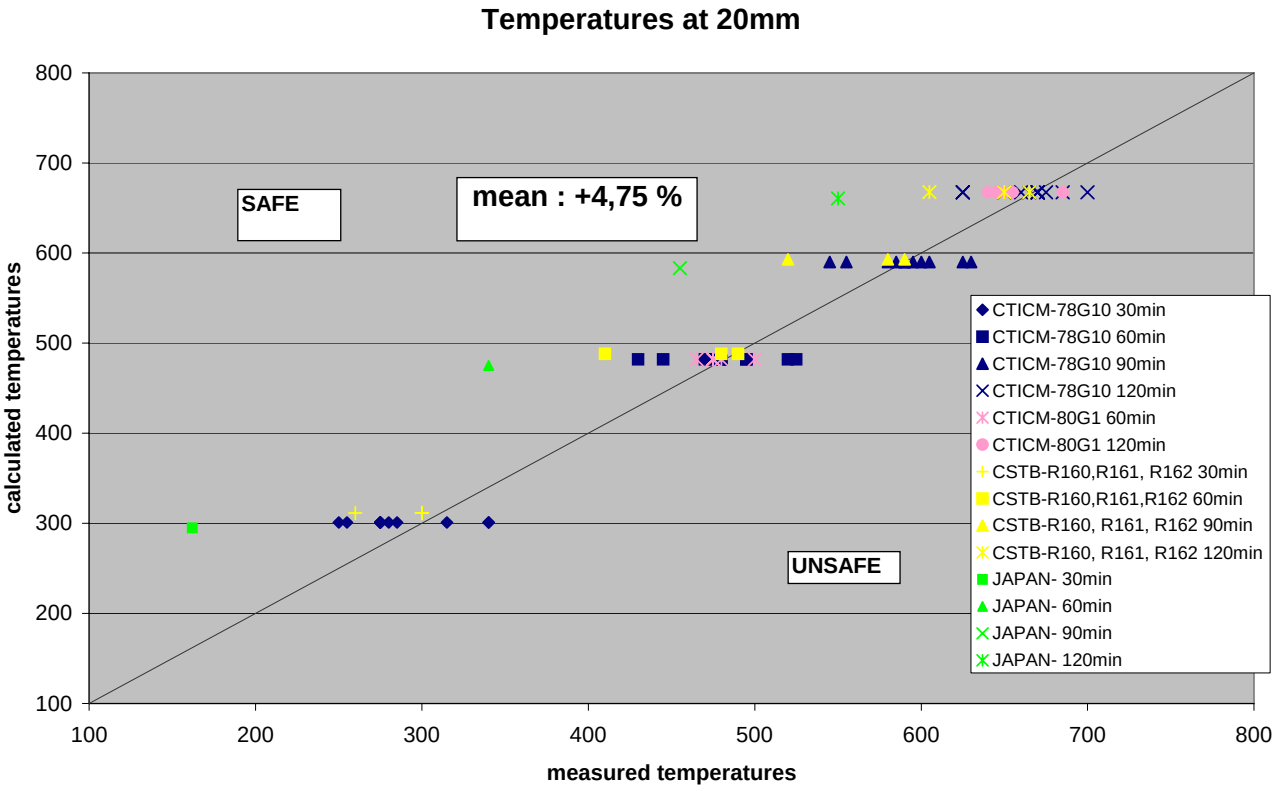

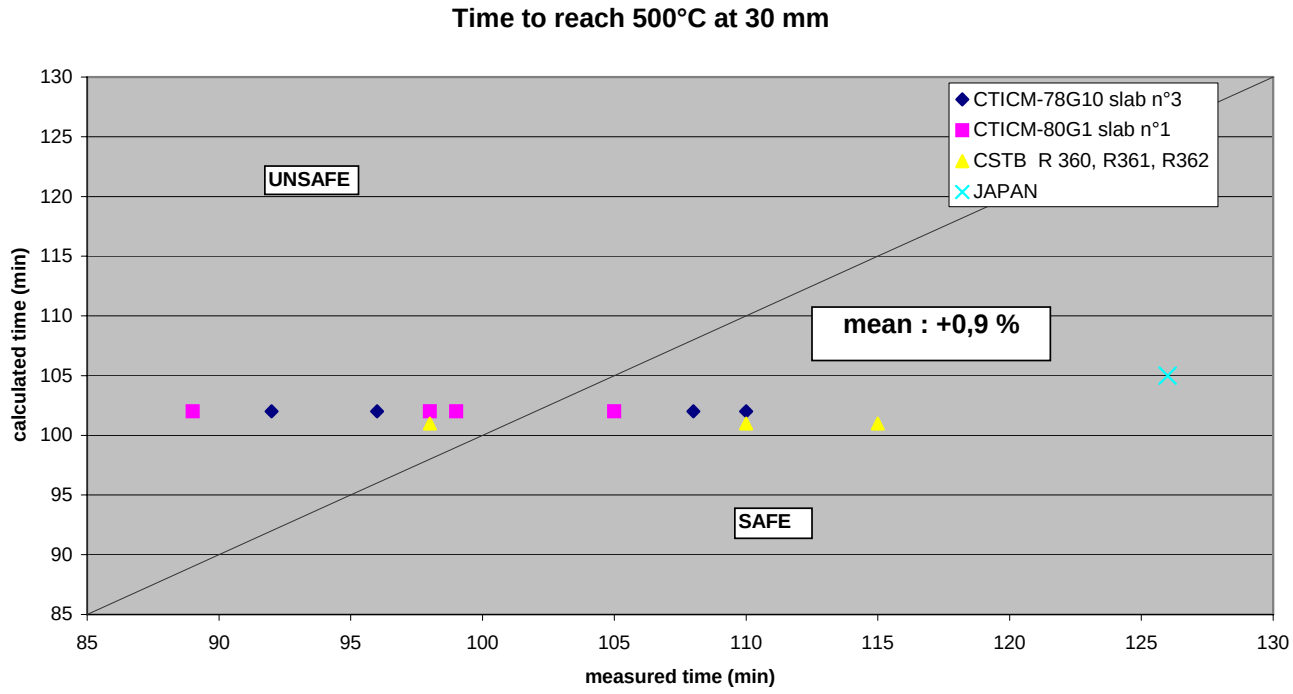

Time for an increase of 140 K on the unexposed side

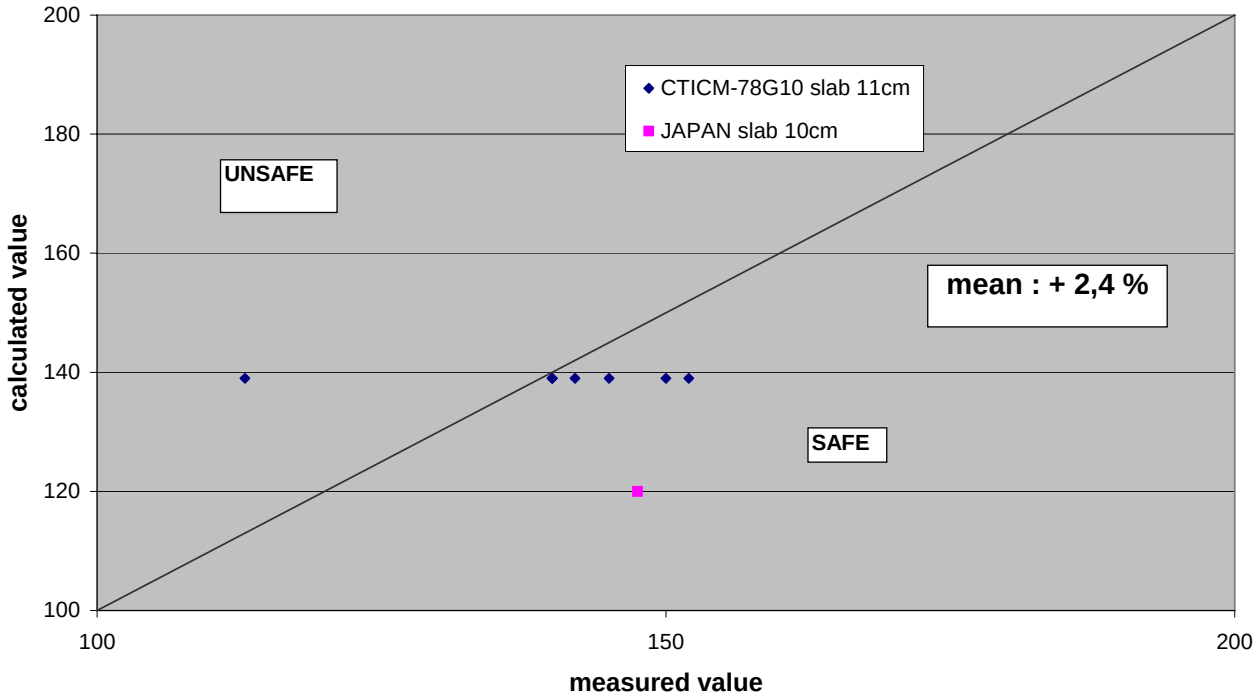

Proposed revision of prEN 1992-1-2 revised Final draft April 2002 :

(2) The upper limit of thermal conductivity λ_c of normal weight concrete may be determined from:

$\lambda_c = 2 - 0{,}24\ (\theta_c / 120) + 0{,}012\ (\theta_c / 120)^2$ W/m K for $20°C \leq \theta_c \leq 1200°C$

where θ_c is the concrete temperature.

The lower limit of thermal conductivity λ_c of normal weight concrete may be determined from:

$\lambda_c = 1{,}36 - 0{,}163\ (\theta_c / 120) + 0{,}0082\ (\theta_c / 120)^2$ W/m K for $20°C \leq \theta_c \leq 1200°C$

where θ_c is the concrete temperature.

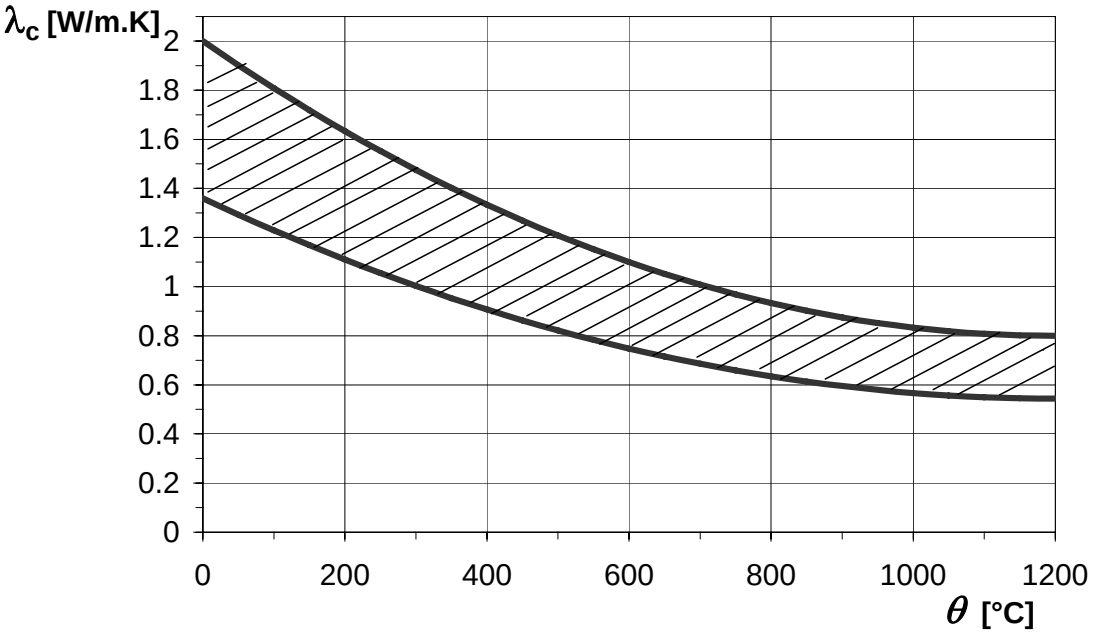

BDA 3.6

Temperature comparisons CERIB/DPO/DCO/FR

Thermal conductivity of concrete
Comparisons of measured and calculated temperatures

Curve 1 “ENV”: ENV curve and upper limit in EN
Curve 2 “EN”: Lower limit in ENV
Curve 3 “prEN”: Curve proposed by PT, used in comparisons in BDA 3.1, BDA 3.2 and BDA 3. 3
Curve 4 “Proposition”: Curve proposed by Fabienne Robert/CERIB/France and used in comparisons in this document

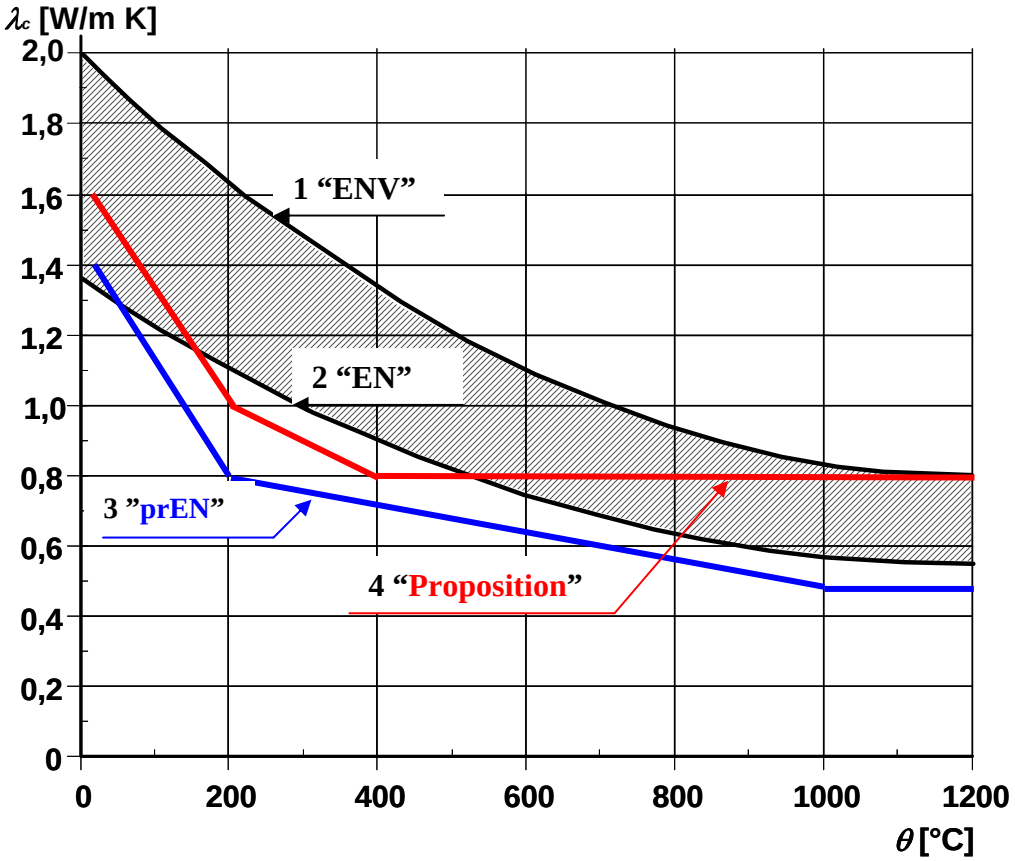

Thermal conductivity curves compared to measured temperatures

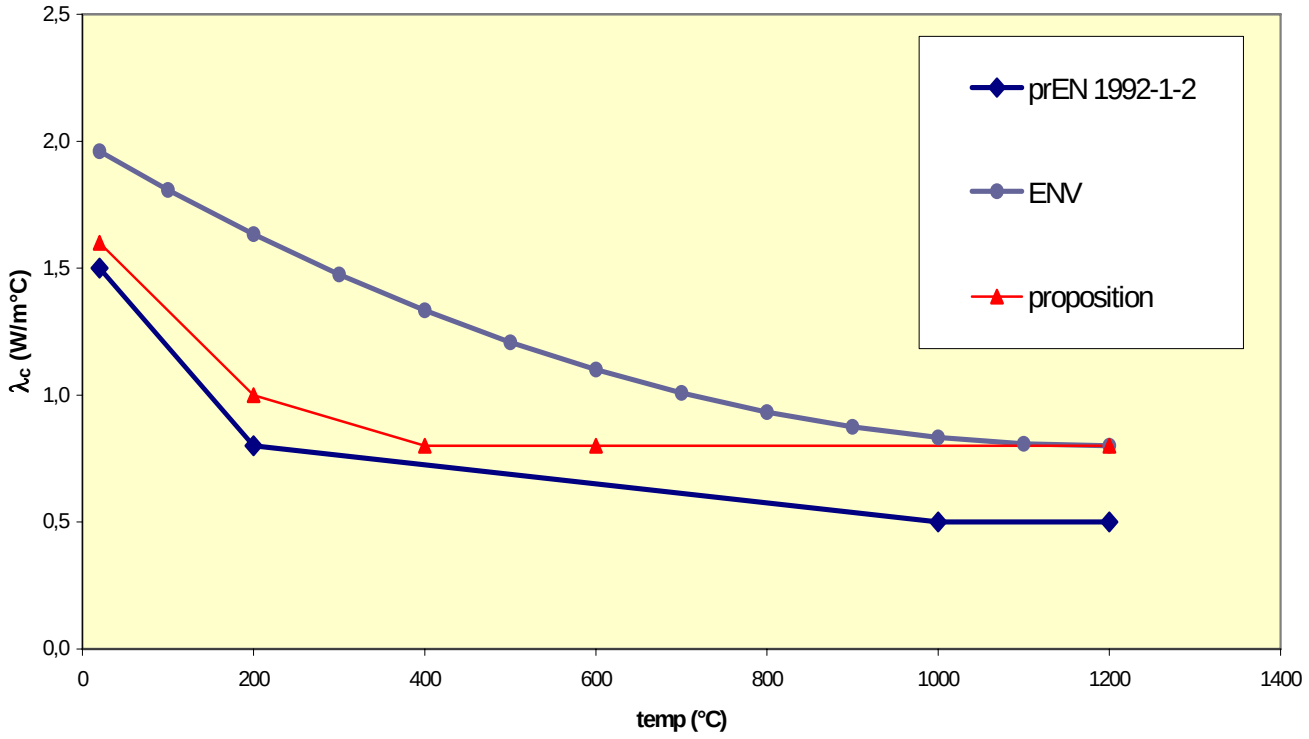

CTICM slab 11 (France)

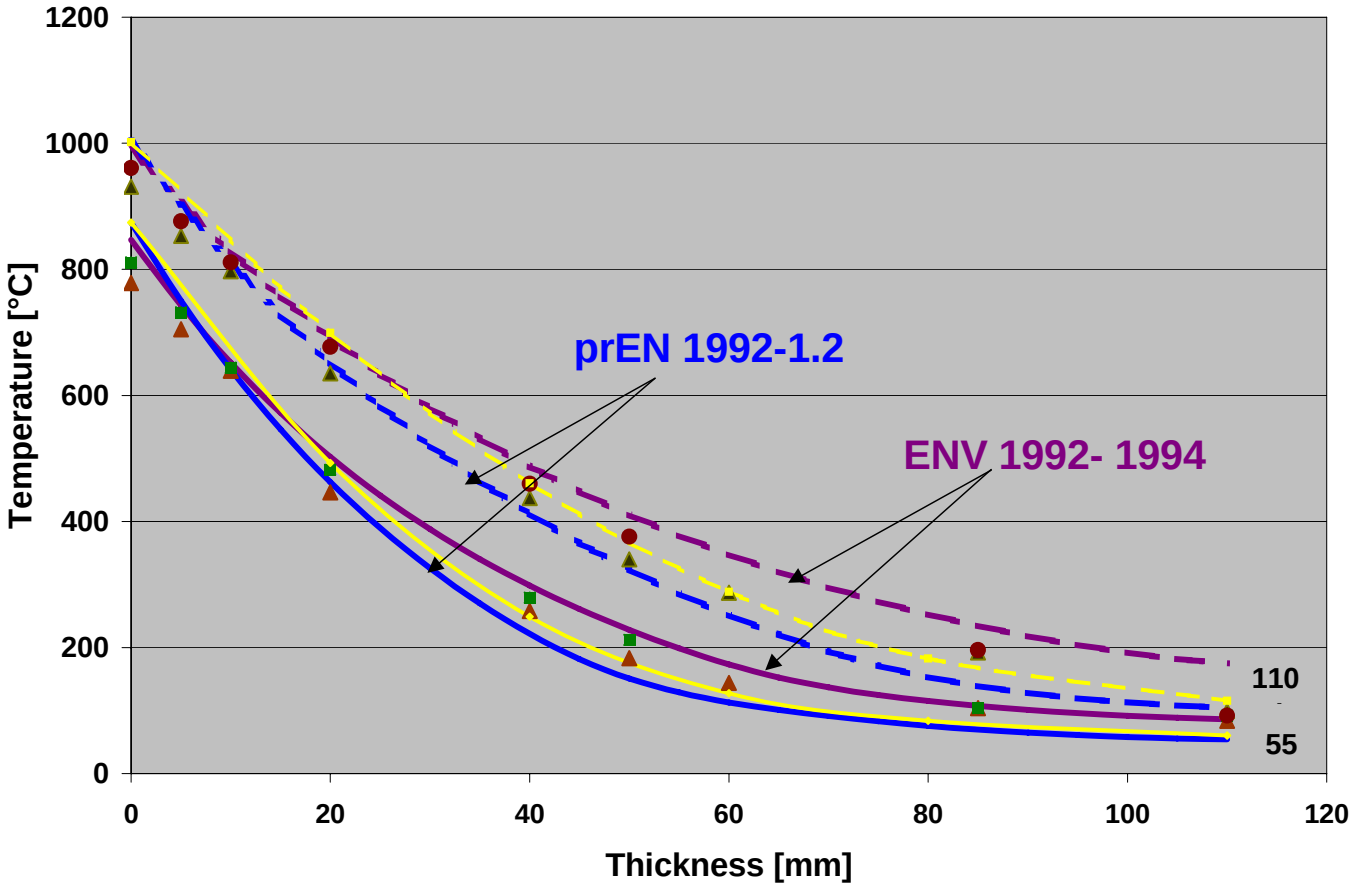

CSTB (France)

Evolution of the temperature in the slab at 60 minutes - slab 14 cm - water content 4 %

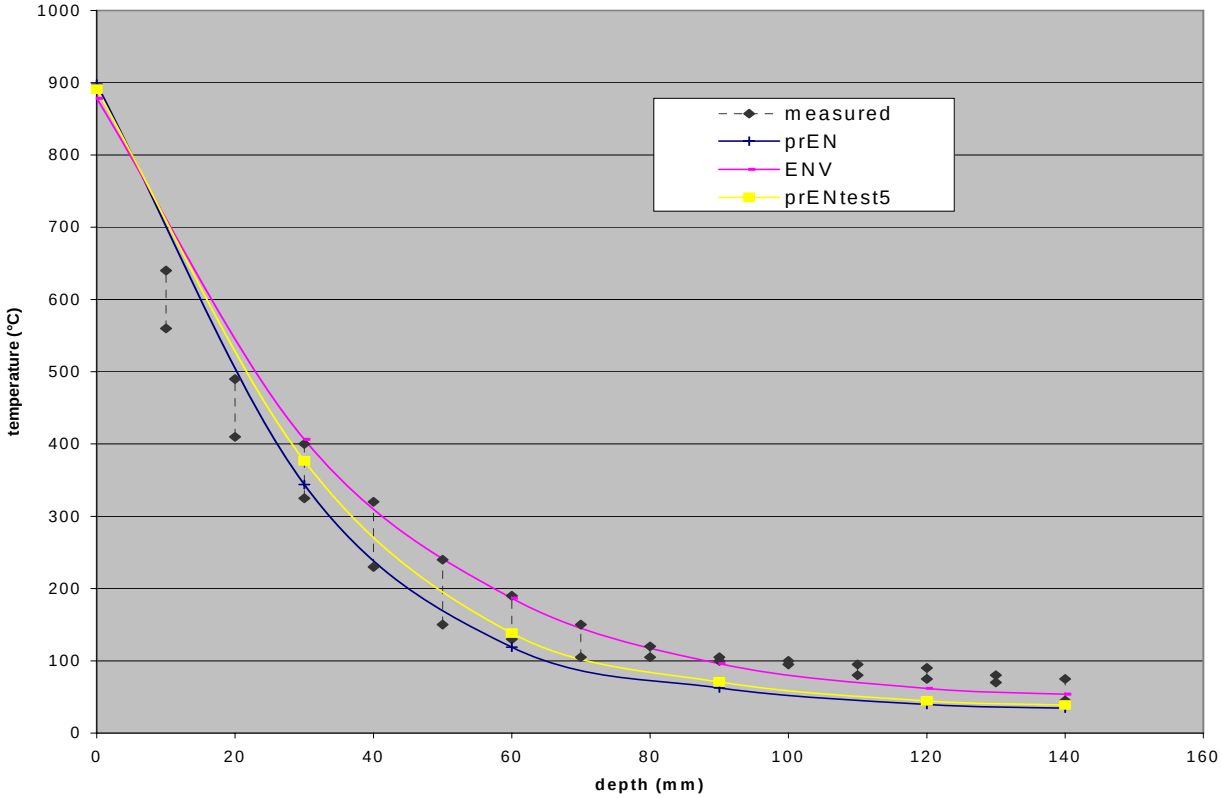

Evolution of the temperature in the slab at 120 minutes - slab 14 cm - water content 4 %

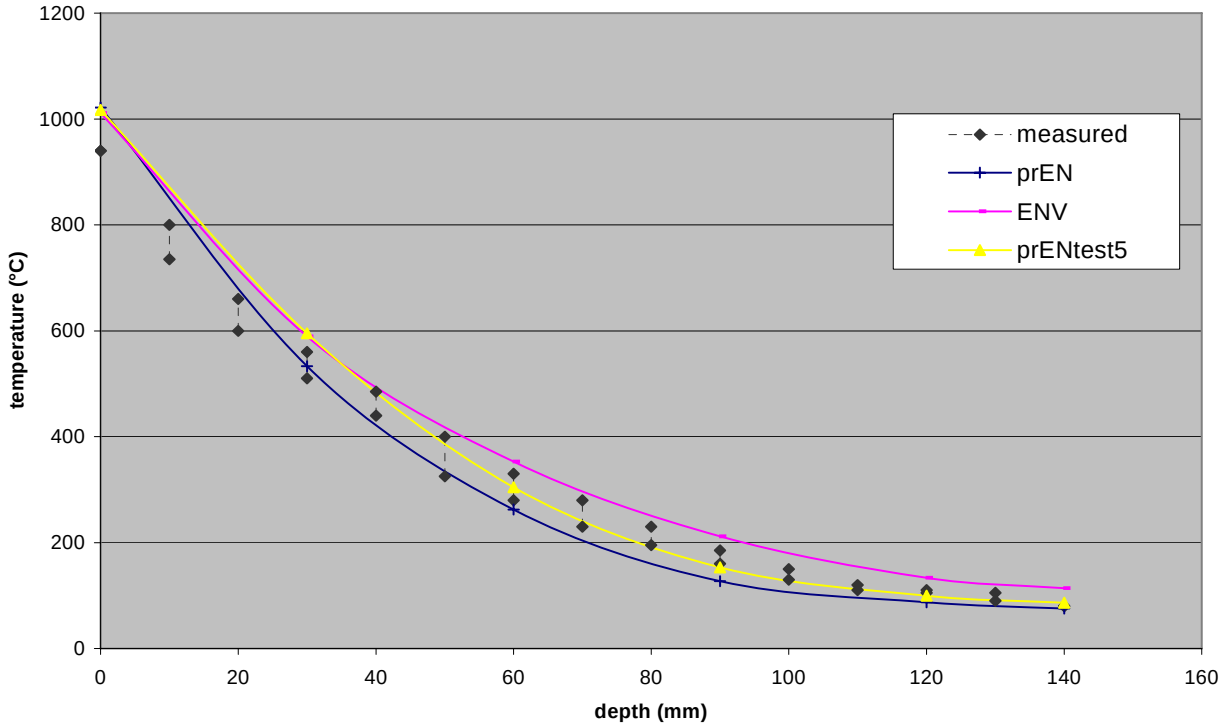

Japanese and Danish (prENtest5) tests

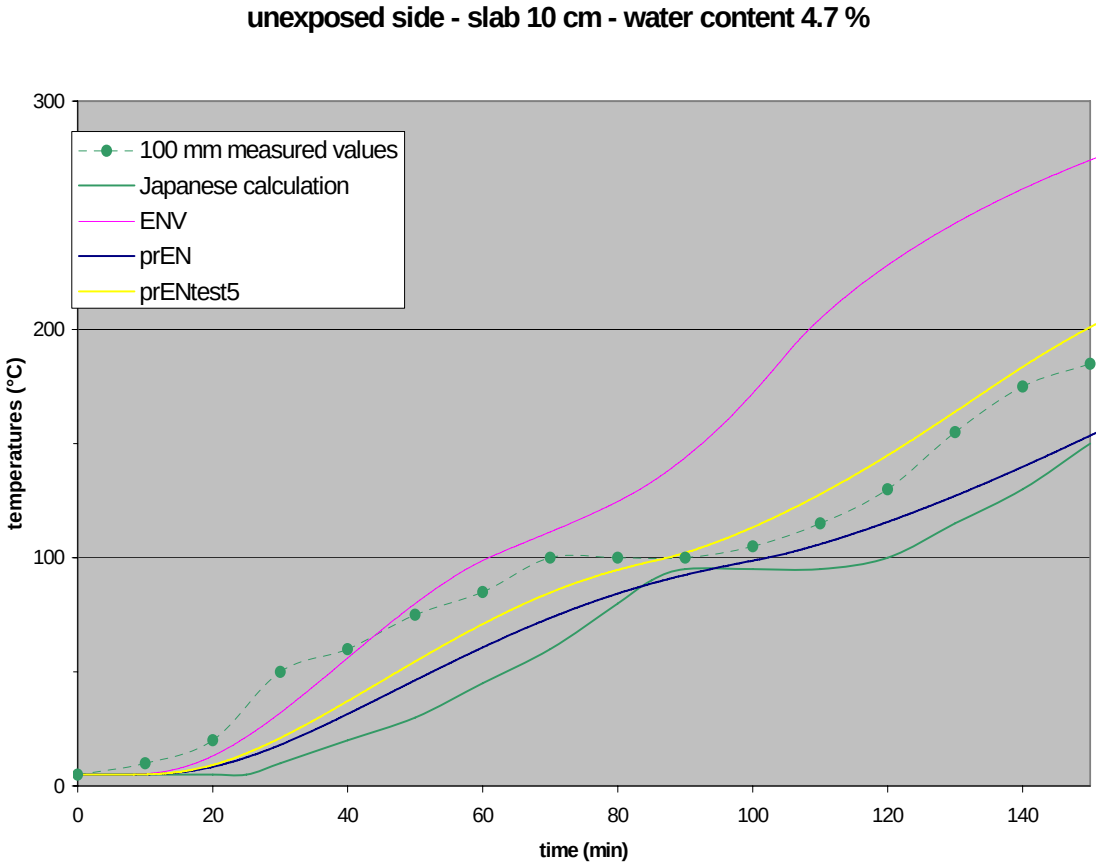

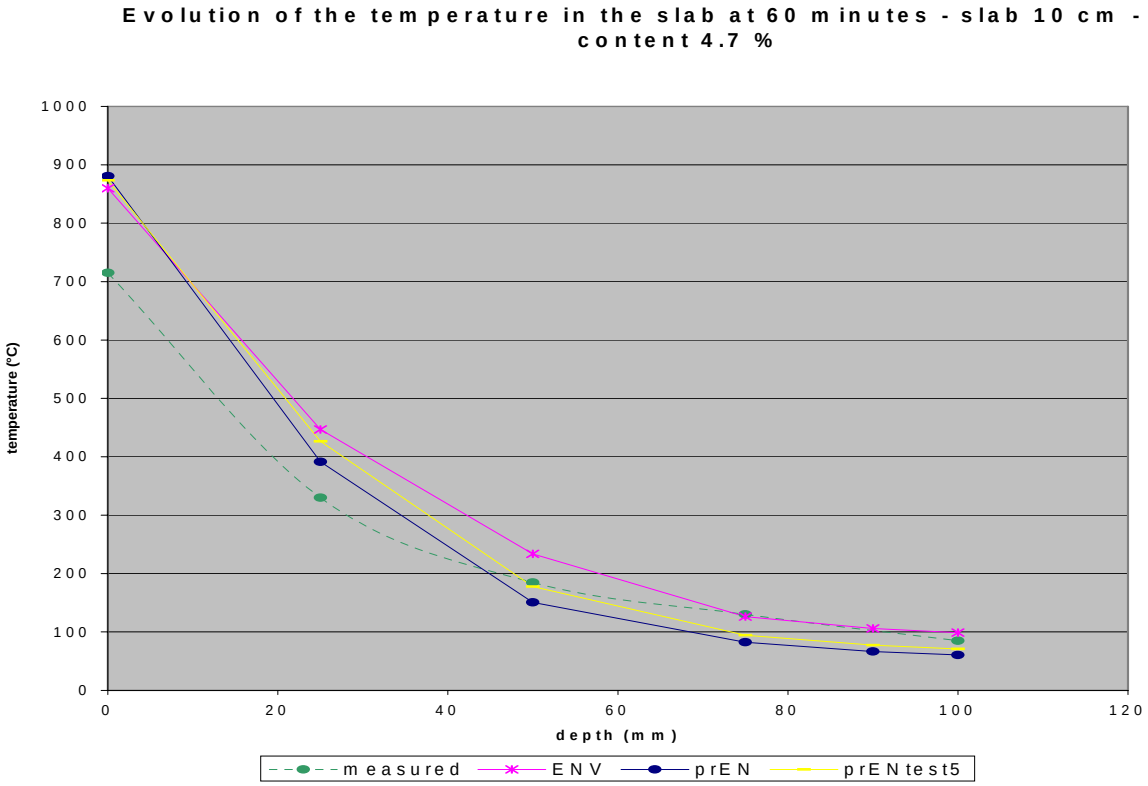

Evolution of the temperature in the slab at 120 minutes - slab 10 cm - water content 4.7 %

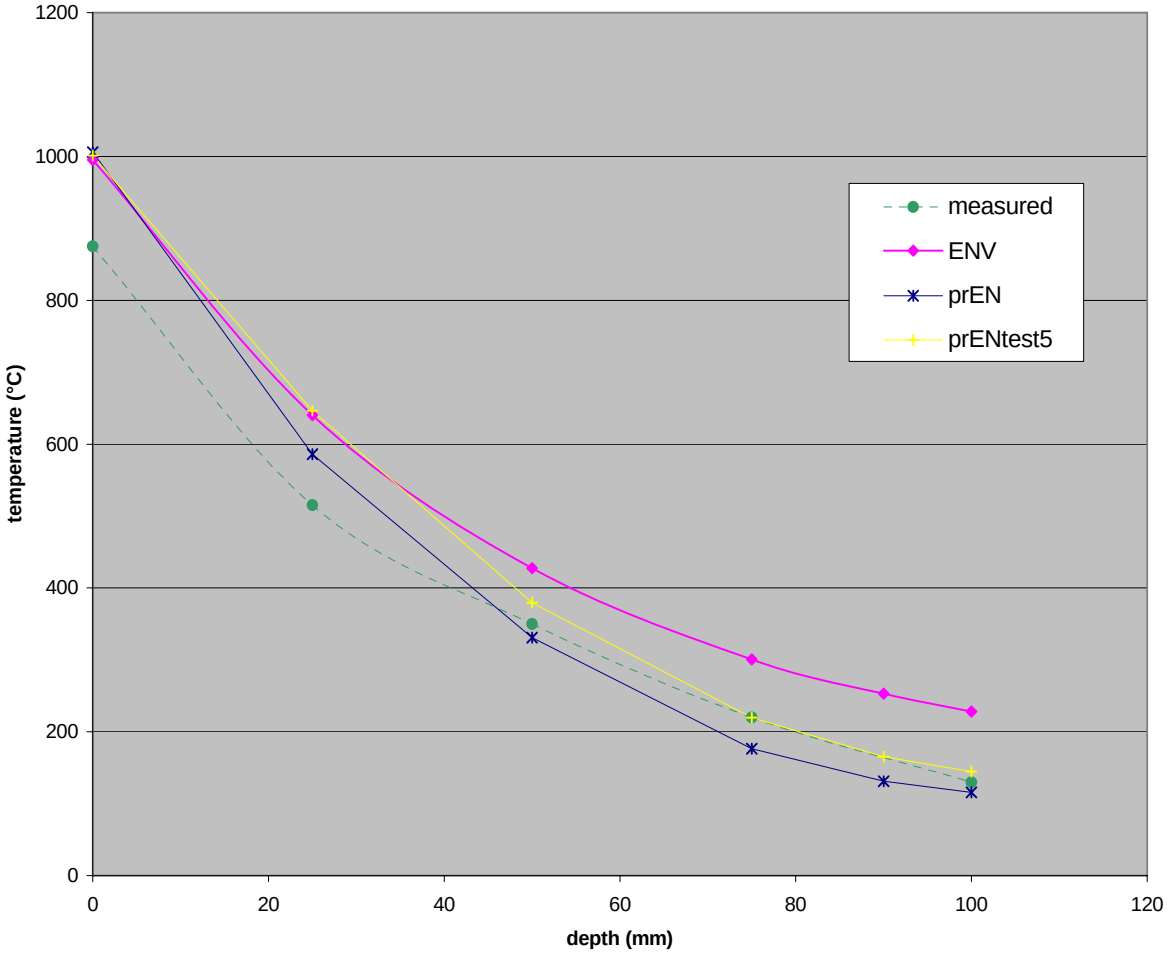

BDA 3.7

EC 4 Background document for thermal laws of concrete EC4-1-2/75

Observations and remarks

Document EC4-1-2/75, 28 December 2001, Profil Arbed, concludes on the basis of 18 fire tests for composite structures and one concrete wall test:

- The old thermal laws (ENV) give a very good evaluation for the temperature of the reinforcement, and
- The new proposed thermal laws according to prEN 1992-1-2 are unsafe, for they under-evaluate the temperature of the re-bars by 50°C from 60 to 120 minutes.

A quick study shows following **observations**:

- In more than half of the reported measurements **the difference** between measured and calculated (ENV thermal properties) **is more than 50°C, even 200°C**
- A general tendency is that near the fire exposed surface the measured temperatures are higher than calculated (e.g. corner reinforcement) and deeper inside the cross section lower (upper flange). This indicates **that thermal conductivity in calculations should be lower.**
- **All the measurements are not included in the document**. Only for one test the lower flange temperatures were given, although there were thermocouples in all tests. In this one test, the measured temperature was clearly higher than calculated.
- Conclusion that prEN 1992-1-2 is unsafe is based on one measurement in one test and compared to EC 2 background document there seems to be **a gross error** (concrete cover/axis distance).

Further **remarks**:

- Composite structures with heavy steel sections are not the best examples for calibration of concrete properties (sensitivity for modelling, emissivity and thermal transfer from one material to another).

Comparisons measured/calculated temperatures

Note: The values presented in the table below are based on readings from a paper copy and they are not very accurate. Deviations less than 50°C are neglected. Also some very large deviations are neglected (possibly errors?)

Tauno Hietanen
P.O. Box 381
FIN - 00131 HELSINKI

Phone +358 917284435
Fax +358 917284444
e-mail tauno.hietanen@rtt.ttliitot.fi

Tests with standard fire exposure

Test type	Page reference	Measured - calculated temperature Δ (°C) "< "means Δ < ± 50°C		
		Reinforcement	Steel web	Upper flange
Column	A19			
	A20		+100	
	A21	-100, +60		
Column	A30		+100	
	A31	± 50		
Column	A39		+100	
	A40		+100	
	A 41	-200, +150		
Beam	A48		+50	
	A49			-50
	A50	-100		
Beam	A61		<	
	A62		±50	
	A64	+50		
	A69		<	
	A70			<
	A72	+100		
Beam + slab	A80		<	
	A81	-100		
	A84	<		
	A85 slab <			
	A87		<	
	A89	-70		
	A91 slab <			
	A92 slab <			
Beam + slab	A87		+50	
	A89	-50		
	A99			<
Column	B4		+70	
	B5	-50		
Column	B12		<	
	B13	-60		
	B15	±50		
Column	B21		<	
	B24	-120		
Column	B30		<	
	B31		<	
	B32		±50	
Frame beam + column	B41		+100	
	B42		±100	
	B43		<	
	B45	±50		
	B48		<	
	B49			-50
	B51 slab <			
	B53 slab <			
Frame beam + column	B66		<	
	B67		<	
	B68		-150	
	B70	+100		
	B73		+70	
	B74			-50
	B76 slab <			
	B78 slab <			

Tauno Hietanen
P.O. Box 381
FIN - 00131 HELSINKI

Phone +358 917284435
Fax +358 917284444
e-mail tauno.hietanen@rtt.ttliitot.fi

Remarks:

Reinforcement: Only in 1 case of 16 the temperature difference is less than ± 50°C. there seems to be a tendency that the bottom corner bars have lower temperatures than calculated.

Steel section web: In 12 cases of 25 the temperature difference is less than ± 50°C.

Steel section upper flange: Only a few measurements, in most cases within ± 50°C.

Steel section lower flange: No information is given, although there has been thermocouples. Why?

Are some pages missing, because there are jumps in the page references?

Tests with parametric fire exposure

Many results with low temperatures (less than 300°C) where the temperature difference is less than ± 50°C.

Interesting results are C.2.2, D.2.2, composite beams where also the lower flange temperature is measures. During the cooling phase the measured temperature exceeds the calculated by 50 to 100°C. In D.2.3, D.2.4 and D.2.5 steel section web and reinforcement temperature are exceeded by around ± 70°C.

Tauno Hietanen
P.O. Box 381
FIN - 00131 HELSINKI

Phone +358 917284435
Fax +358 917284444
e-mail tauno.hietanen@rtt.ttliitot.fi

BDA 3.8 Eurocode 2 Part 1.2 : New proposal for the mechanical properties of prestressing steel (wires and strands) at elevated temperatures

1. Introduction

The translation of the prEN 1992-1.2 brought our attention to the values used for the mechanical properties of prestressing steel. Some comparisons between fire design of prestressed elements following prEN 1992-1.2 [1] rules and our national code DTU-FB [2], which is based on experimental results, were then carried out. They have shown that prEN 1992-1.2 rules were unfavourable due in part to the mechanical properties of prestressing steel. This could lead to the banning of some products which are currently present on the French market.
That's why we present in this document a new proposal (chapter 3) whose values have been chosen to be the nearest to the experimental evidences obtained in several countries (UK, Belgium, France) while keeping the mathematical model for stress-strain relationship of reinforcing steel as the actual prEN 1992-1.2 do.

In spite of the progress of prEN 1992-1.2, we are asking for the adoption of one of the options proposed below :

- **1.** change the Table 3.3 of the prEN 1992-1.2 using the table given in chapter 3 of this document
- **2.** propose a new class in the normative part of the prEN 1992-1.2, based on the table given in the chapter 3 of this document, as it has been done for the reinforcing steel.
- **3.** if neither option 1. nor option 2. can be adopted, the values for the Table 3.3 of the prEN 1992-1.2 may be found in the National Annex.

2. Comparison between the ENV 1992-1.2 [3], the prEN 1992-1.2 [1], the DTU-FB [2] values and the experimental results

2.1 Reduction factor of mechanical properties at elevated temperature

It has to be mentioned that the values currently used in prEN 1992-1.2 were given in an informative annex of the ENV 1992-1.2. They did not fit with the values which were given in the normative part of the ENV 1992-1.2 (see annex A).

The detailed description of the tests conducted by Holmes & Co [4] are given in annex B, the results, presented by Malaval [5], on which DTU-FB is based are given in annex C. Furthermore, some other results obtained at the university of Liège and presented by Dotreppe [6] are given in annex D. In this last study, the tests were conducted up to 400°C. In all these studies, wires and strands with different diameters were tested.

For the comparison presented after, only the lowest results of each study are plotted.

Figure 1 : Normalised ultimate tensile strength

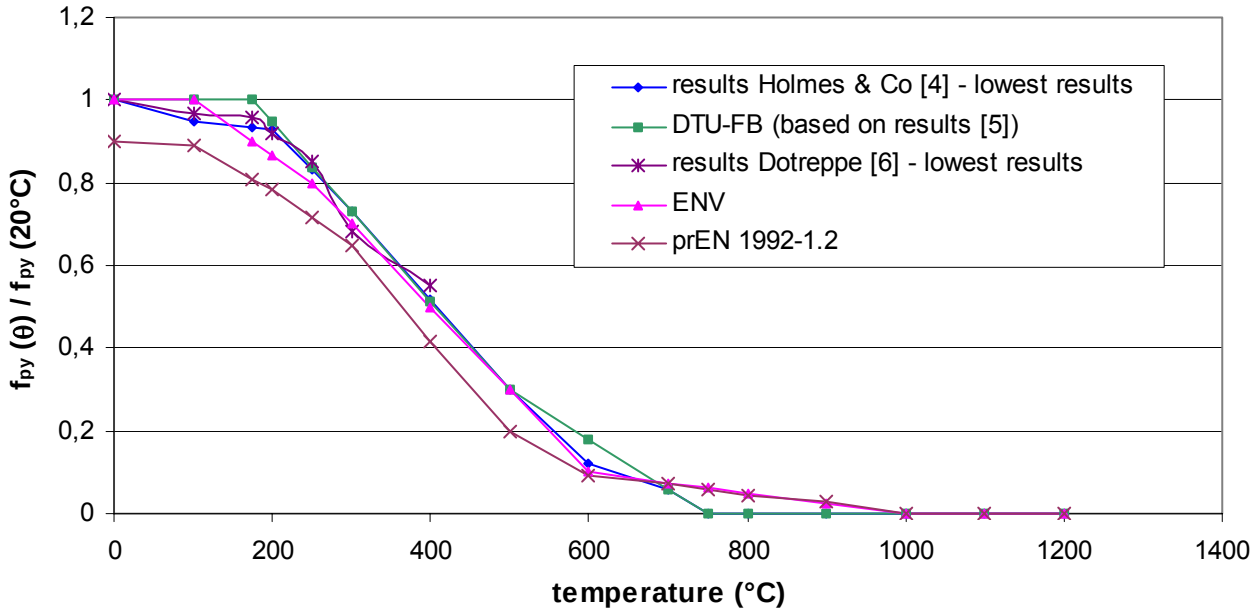

At 500°C, the values given in prEN 1992-1.2 are 34 % lower than the lowest results obtained by Holmes and Co and Malaval.

Figure 2 : Normalised yield strength

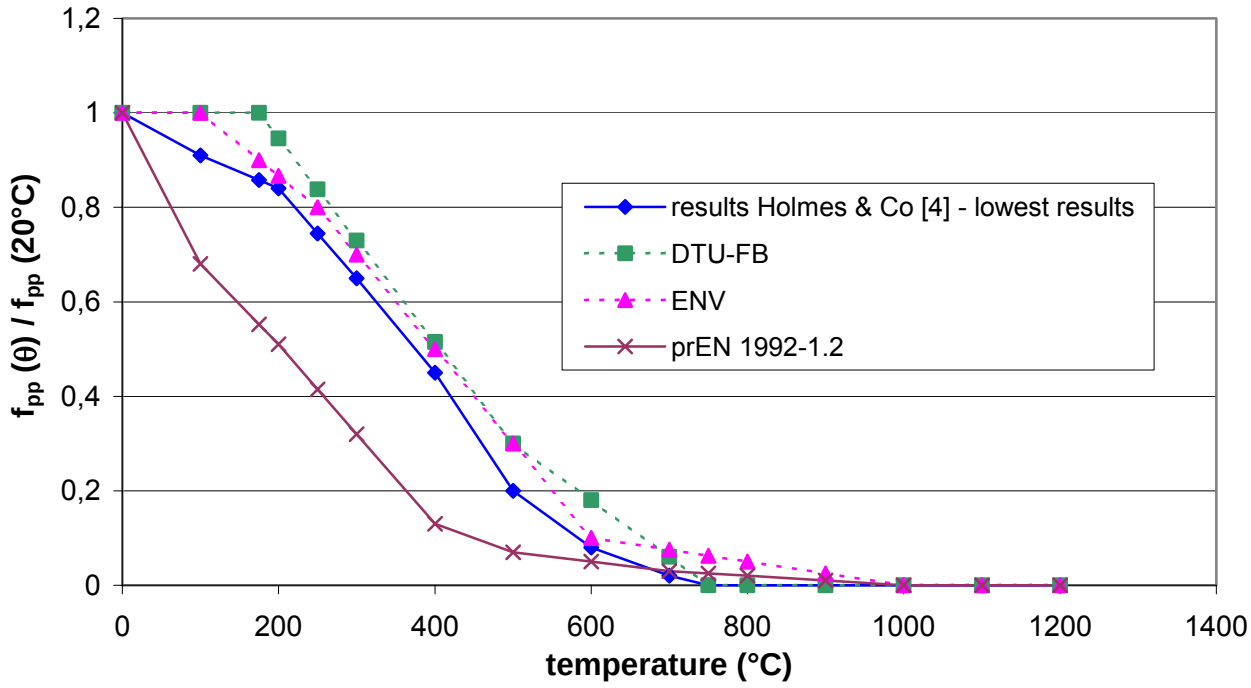

At 400°C, the values given in prEN 1992-1.2 are 71 % lower than the lowest results obtained by Holmes and Co.

Figure 3 : Normalised elastic modulus

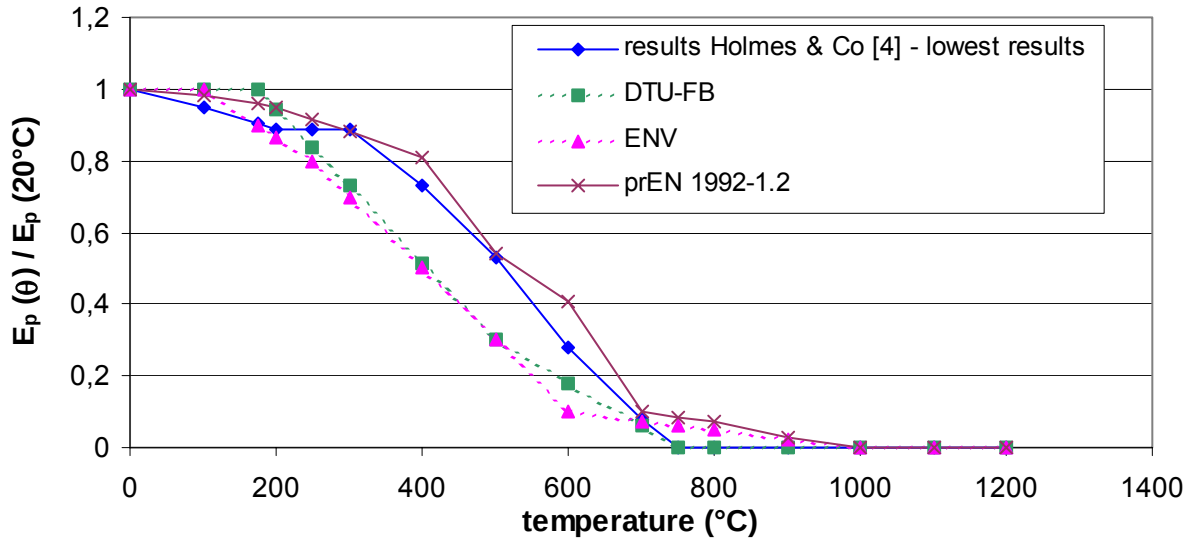

At 600°C, the values given in prEN 1992-1.2 are 46 % higher than the lowest results obtained by Holmes and Co.

2.2 Stress-strain relationships

The figures below show a comparison of stress-strain relationships of prestressing steel at 20°C, 350°C and 500°C. The DTU-FB relationship is based on the BPEL relationship [7] affected of the DTU-FB coefficient of reduction.

Figure 4 : stress-strain relationships of prestressing steel at 20°C

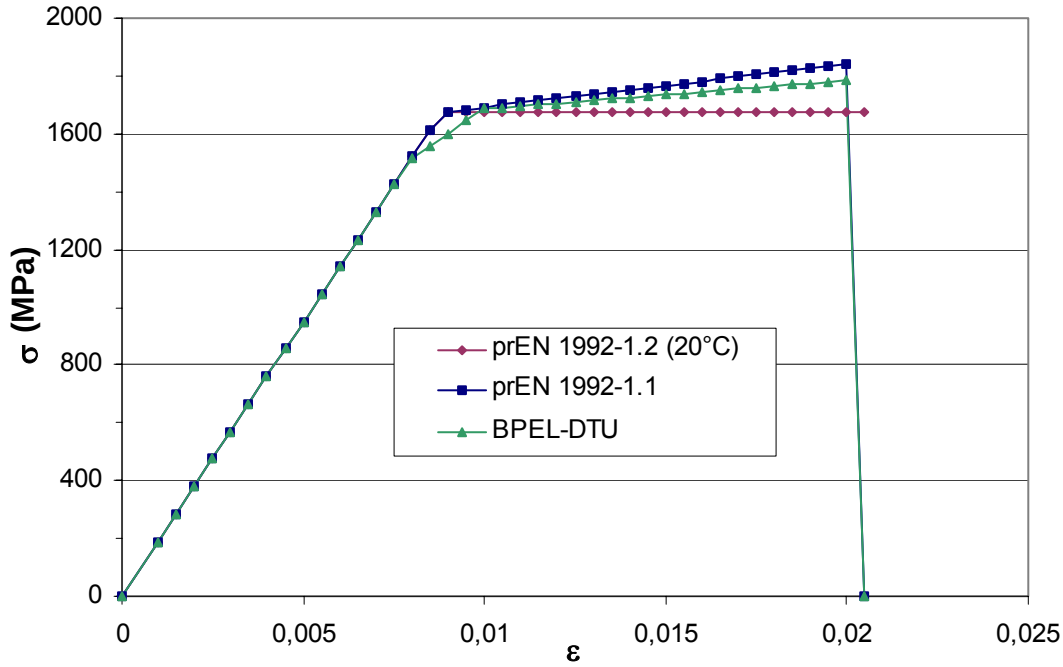

Figure 5 : stress-strain relationships of prestressing steel at 350°C

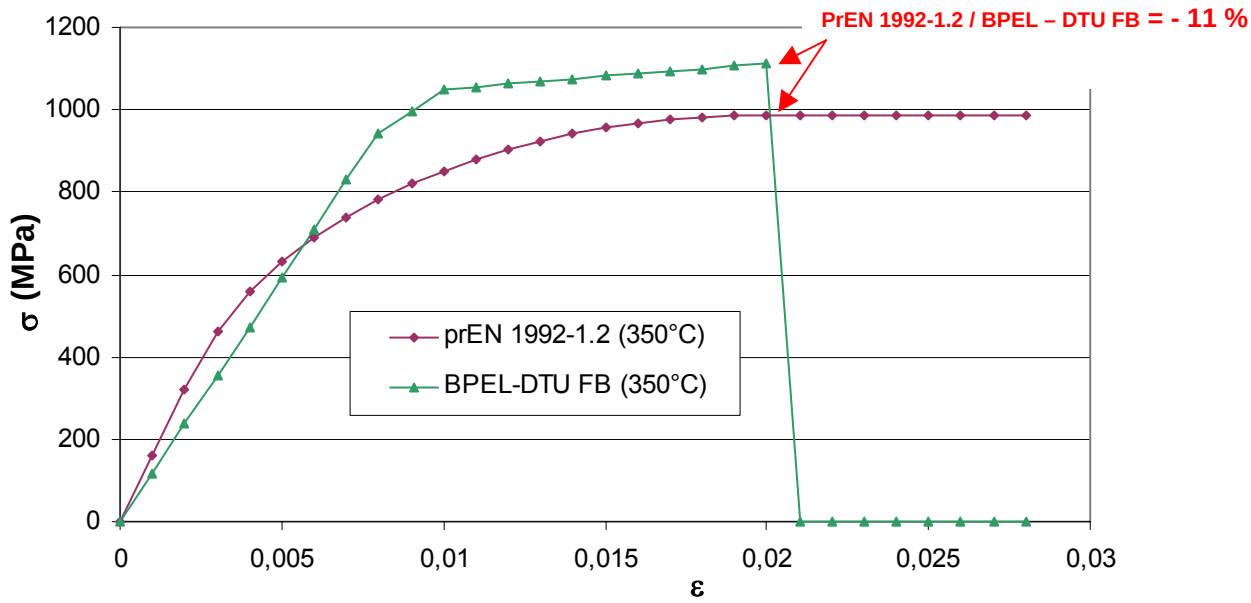

Figure 6 : stress-strain relationships of prestressing steel at 500°C

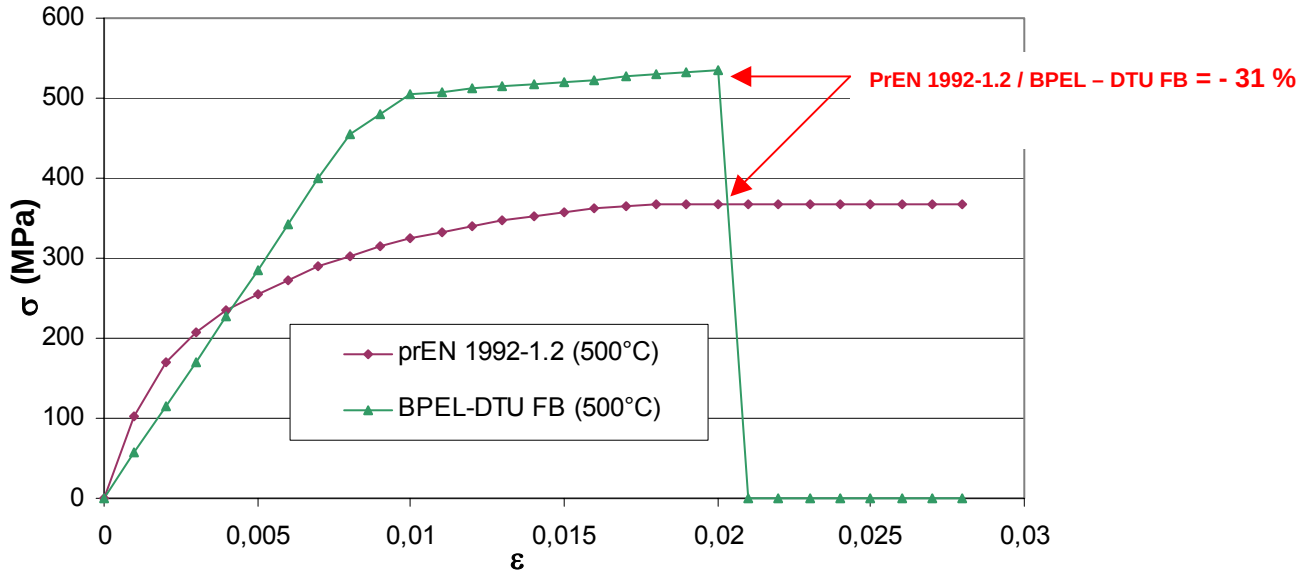

2.3 Application in the case of a floor with shuttering floor slabs elements

Some comparative calculations have been done on a typical case of floor with shuttering prestressed floor slabs (for example, the floor of a car park). The shuttering floor slabs considered were 6 cm depth ; they were prestressed with strands T 5,2 2060. Three scenarios of reinforcement have been studied :

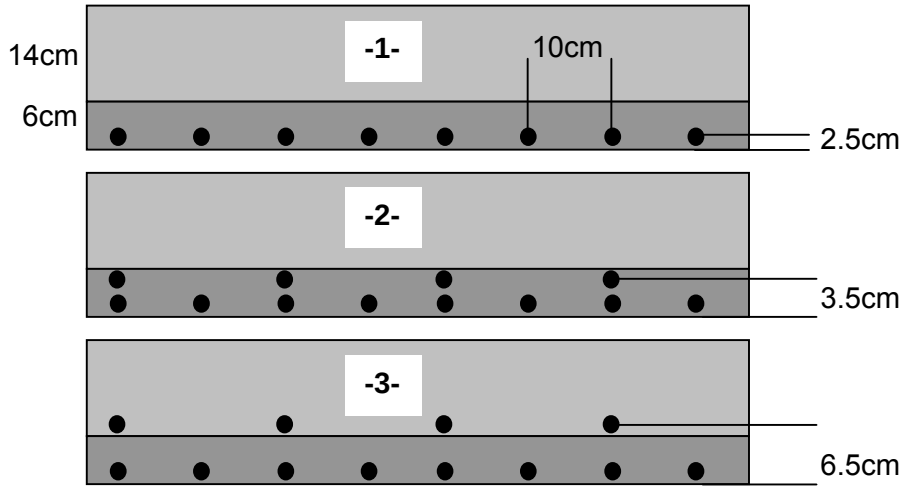

The fire resistance calculations have been made in isostatic situation at 90 minutes. The results are given in the following table.

floor with shuttering floor slabs elements 6 + 14

calcareous aggregates, R90

	span case 1	span case 2	span case 3
ρ (strands)	0,07%	0,07%	0,07%
ρ (ϕ8)	…	0,07%	0,07%
a concrete cover (m)	0,025	0,025	0,025
$M_{u\ EC2}$ (MN m)	0,0372	0,0464	0,0446
$\theta_{steel\ EC2\ (°C)\ -\ steel\ layer\ 1}$	588,7	588,7	588,7
$\theta_{steel\ EC2\ (°C)\ -\ steel\ layer\ 2}$	…	475,4	252,3
$M_{u,\ fi\ EC2}$ (MN m)	0,0044	0,0138	0,0136
$\eta_{fi\ EC2}$	0,1182	0,2981	0,3049
$M_{u\ BAEL}$ (MN m)	0,0351	0,0426	0,0414
$\theta_{steel\ DTU\ (°C)\ -\ steel\ layer\ 1}$	521,1	521,1	521,1
$\theta_{steel\ DTU\ (°C)\ -\ steel\ layer\ 2}$	…	0,0	0,0
$M_{u,\ fi\ DTU}$ (MN m)	0,0113	0,0186	0,0199
$\eta_{fi\ DTU}$	0,3211	0,4368	0,4798
Mu, fi EC2 / Mu, fi DTU	**-61%**	**-26%**	**-32%**

3. New proposal for the mechanical properties of prestressing steel (wires and strands) at elevated temperatures

The values below are given on the basis of the different tests results. They have been chosen to be the nearest of these results while keeping the mathematical model for stress-strain relationship of reinforcing steel as the actual prEN 1992-1.2 do.
The following figures show the stress-strain relationships obtained with this proposal. The example with a floor with shuttering floor slabs elements has been recalculated.

Values for the parameters of the stress-strain relationship of cold worked (cw) (wires and strands) and quenched and tempered (q & t) (bars) prestressing steel at elevated temperatures

Steel temp.	$f_{py,\theta}$ / (0,9 f_{pk})		$f_{pp,\theta}$ / (0,9 f_{pk})		$E_{p,\theta}/E_p$		$\varepsilon_{pt,\theta}$ [-]	$\varepsilon_{pu,\theta}$ [-]
θ [°C]	cw	q & t	cw	q & t	cw	q & t	cw, q&t	cw, q&t
1	2	3	4	5	6	7	8	9
20	1,00	1,00	1,00	1,00	1,00	1,00	0,050	0,100
100	**1,00**	0,98	**0,86**	0,77	0,98	0,76	0,050	0,100
200	**1,00**	0,92	**0,78**	0,62	**0,9**	0,61	0,050	0,100
300	**0,77**	0,86	**0,51**	0,58	**0,82**	0,52	0,055	0,105
400	**0,54**	0,69	**0,33**	0,52	**0,57**	0,41	0,060	0,110
500	**0,32**	0,26	**0,2**	0,14	**0,3**	0,20	0,065	0,115
600	**0,19**	0,21	**0,1**	0,11	**0,2**	0,15	0,070	0,120
700	0,08	0,15	0,03	0,09	0,10	0,10	0,075	0,125
800	0,05	0,09	0,02	0,06	0,07	0,06	0,080	0,130
900	0,03	0,04	0,01	0,03	0,03	0,03	0,085	0,135
1000	0,00	0,00	0,00	0,00	0,00	0,00	0,090	0,140
1100	0,00	0,00	0,00	0,00	0,00	0,00	0,095	0,145
1200	0,00	0,00	0,00	0,00	0,00	0,00	0,100	0,150

Figure 7 : Normalised ultimate tensile strength

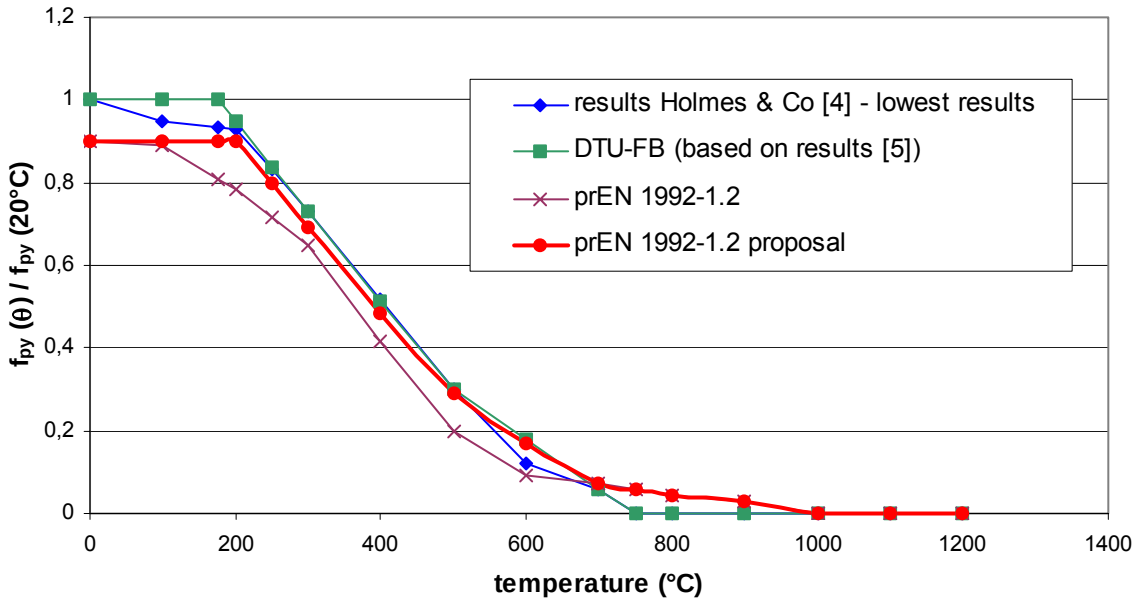

Figure 8 : Normalised yield strength

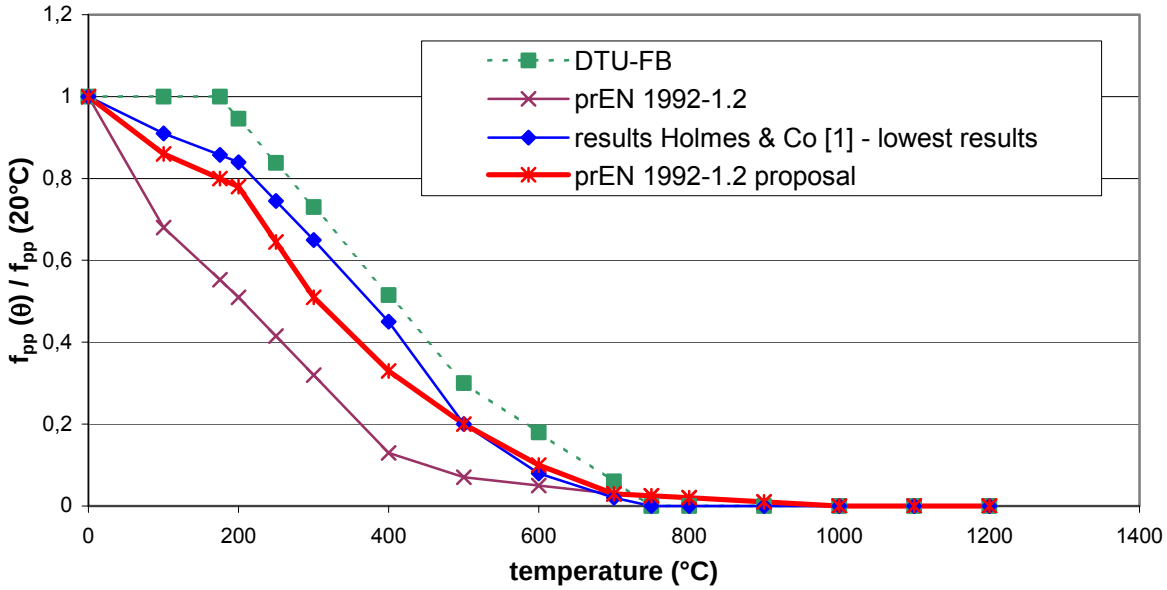

Figure 9 : Normalised elastic modulus

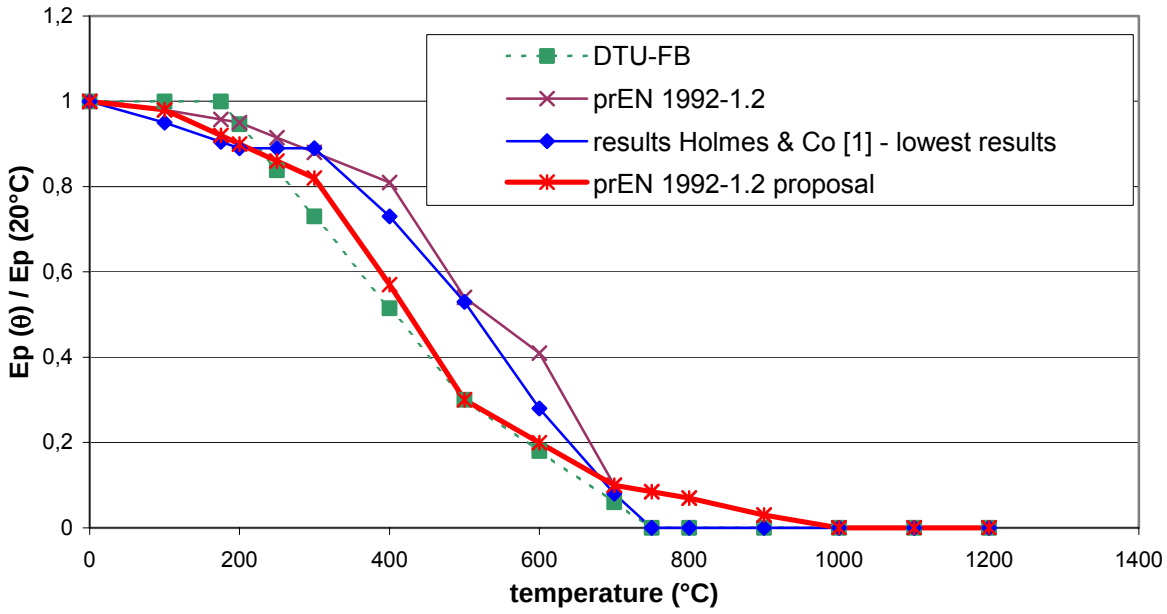

Figure 10 : stress-strain relationships of prestressing steel at different temperatures

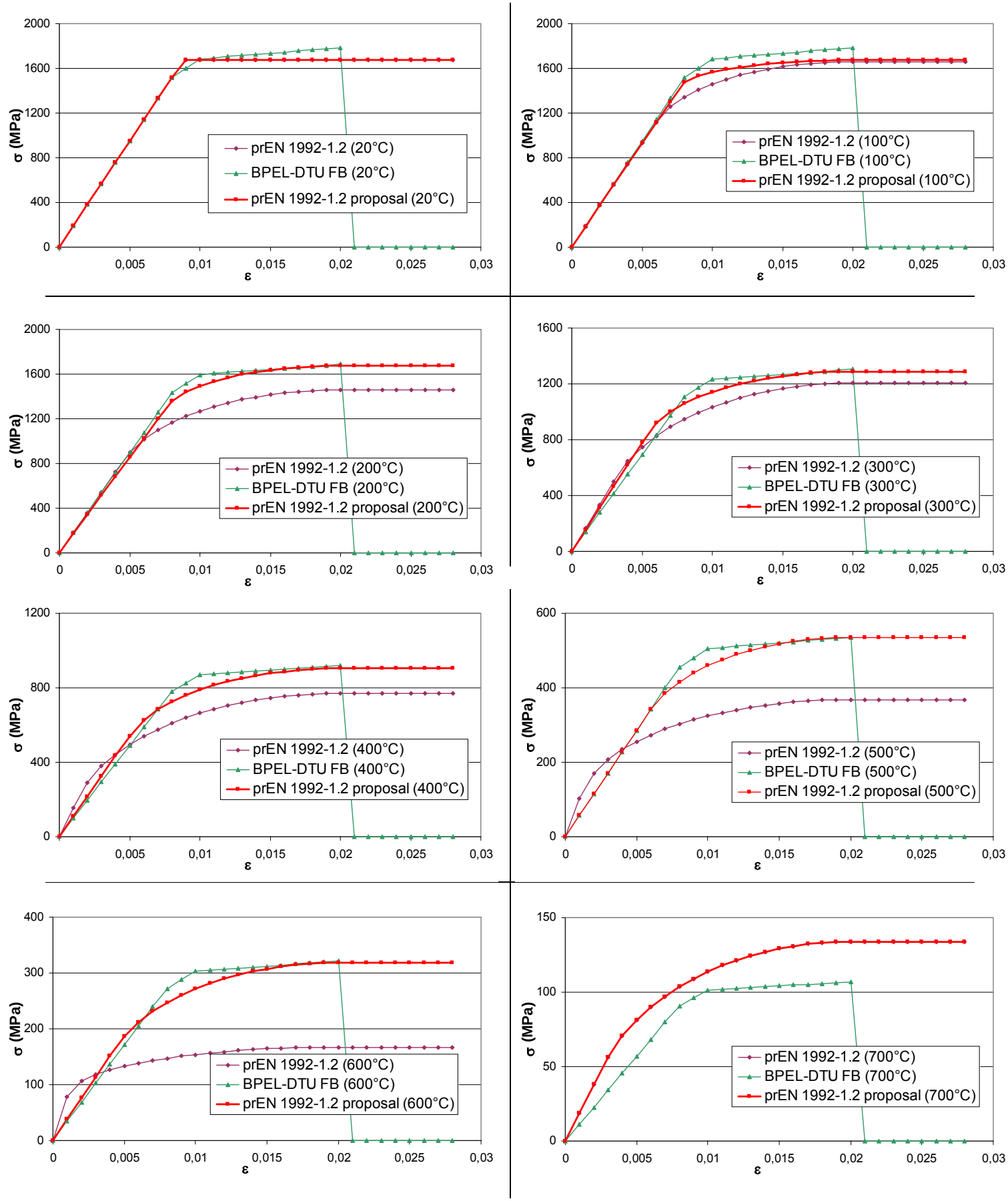

The table below gives the results of the recalculation of the floor with shuttering floor slabs elements.

floor with shuttering floor slabs elements 6 + 14

calcareous aggregates, R90

	span case 1	span case 2	span case 3
ρ (strands)	0,07%	0,07%	0,07%
ρ (ϕ8)	…	0,07%	0,07%
a concrete cover (m)	0,025	0,025	0,025
$M_{u\ EC2}$ (MN m)	0,0372	0,0464	0,0446
$\theta_{steel\ EC2\ (°C)\ -\ steel\ layer\ 1}$	588,7	588,7	588,7
$\theta_{steel\ EC2\ (°C)\ -\ steel\ layer\ 2}$	…	475,4	252,3
$M_{u,\ fi\ EC2}$ (MN m)	0,0079	0,0174	0,0171
$\eta_{fi\ EC2}$	0,2130	0,3740	0,3841
$M_{u\ BPEL}$ (MN m)	0,0351	0,0426	0,0414
$\theta_{steel\ DTU\ (°C)\ -\ steel\ layer\ 1}$	521,1	521,1	521,1
$\theta_{steel\ DTU\ (°C)\ -\ steel\ layer\ 2}$	…	427,8	241,9
$M_{u,\ fi\ DTU}$ (MN m)	0,0113	0,0186	0,0199
$\eta_{fi\ DTU}$	0,3211	0,4368	0,4798
Mu, fi EC2 / Mu, fi DTU	**-30%**	**-7%**	**-14%**

4. References

[1] Eurocode 2 : Design of concrete structures – Part 1.2 : General rules – Structural fire design, October 2002, prEN 1992-1.2

[2] DTU FB – Méthode de prevision par le calcul du comportement au feu des structures en béton – P 92-701, December 1993

[3] Eurocode 2 : Calcul des structures en béton – Partie 1.2 : Règles générales – Calcul du comportement au feu, 1997, ENV 1992-1.2

[4] The effects of elevated temperatures on the strength properties of reinforcing and prestressing steels, M. Holmes, R. D. Anchor, G. M. E. Cook, R. N. Crook, The structural Engineer, Volume 60 B, No. 1, March 1982

[5] Synthèse des essais de comportement à chaud des aciers pour béton armé et pour béton précontraint – Malaval, AITBTP, série matériaux, n°58, Paris, July – August 1981

[6] Méthodes numériques pour la simulation du comportement au feu des structures en acier et en béton armé, J. C. Dotreppe, thèse d'agrégation de l'enseignement supérieur, Université de Liège, 1980

[7] Règles techniques de conception et de calcul des ouvrages et constructions en béton précontraint suivant la méthode des états limites – BPEL 91 révisé 99 – Fascicule n°62 – titre I – Section II, April 1999

ANNEX A – Values given for the determination of the mechanical properties of prestressing steel at elevated temperature in the standards mentioned

1. ENV 1992-1.2

The reduction of the characteristic strength of prestressing steel is defined as a function of the temperature by the factor $k_p(\theta)$ as follow :

$$f_{pk}(\theta) = k_p(\theta)\, f_{pk}(20°C)$$

for wires and strands

$k_p(\theta) = 1{,}0$	for $20°C \le \theta \le 100°C$
$k_p(\theta) = (850 - \theta) / 750$	for $100°C \le \theta \le 250°C$
$k_p(\theta) = (650 - \theta) / 500$	for $250°C \le \theta \le 600°C$
$k_p(\theta) = (1000 - \theta) / 4000$	for $600°C \le \theta \le 1000°C$
$k_p(\theta) = 0$	for $1000°C \le \theta \le 1200°C$

2. prEN 1992-1.2

(1) The strength and deformation properties of prestressing steel at elevated temperatures may be obtained by the same mathematical model as that presented in for reinforcing steel (see below).

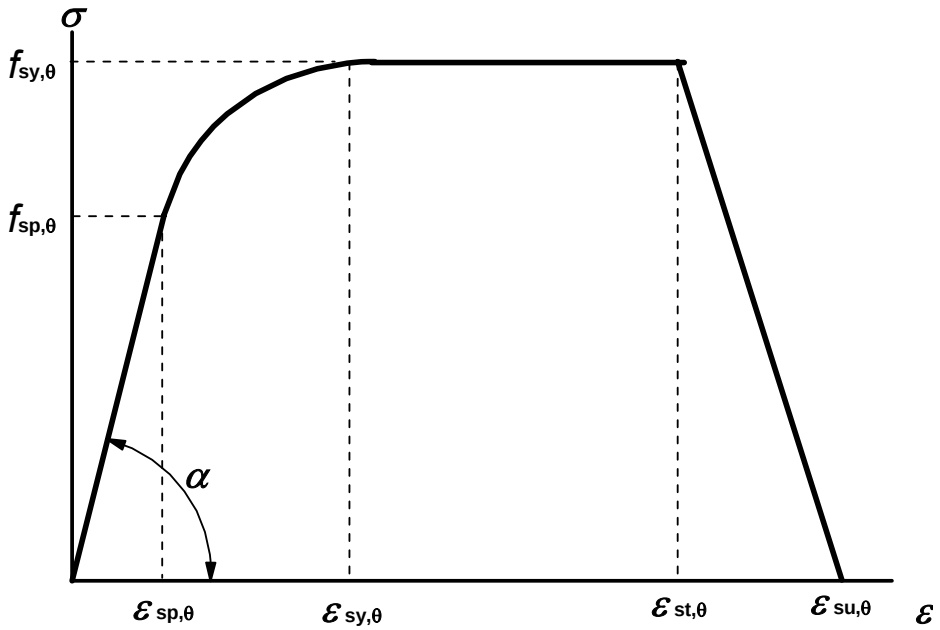

Range	Stress $\sigma(\theta)$	Tangent modulus
$\varepsilon_{sp,\theta}$	$\varepsilon\, E_{s,\theta}$	$E_{s,\theta}$
$\varepsilon_{sp,\theta} \le \varepsilon \le \varepsilon_{sy,\theta}$	$f_{sp,\theta} - c + (b/a)[a^2 - (\varepsilon_{sy,\theta} - \varepsilon)^2]^{0,5}$	$\dfrac{b(\varepsilon_{sy,\theta} - \varepsilon)}{a\left[a^2 - \left(\varepsilon - \varepsilon_{sy,\theta}\right)^2\right]^{0,5}}$
$\varepsilon_{sy,\beta} \le \varepsilon \le \varepsilon_{st,\theta}$	$f_{sy,\theta}$	0
$\varepsilon_{st,\beta} \le \varepsilon \le \varepsilon_{su,\theta}$	$f_{sy,\theta}\,[1-(\varepsilon - \varepsilon_{st,\theta})/(\varepsilon_{su,\theta} - \varepsilon_{st,\theta})]$	-
$\varepsilon = \varepsilon_{su,\theta}$	0,00	-

ANNEX A – Values in different standards

Parameter *)	$\varepsilon_{sp,\theta} = f_{sp,\theta} / E_{s,\theta}$ $\varepsilon_{sy,\theta} = 0,02$ $\varepsilon_{st,\theta} = 0,15$ $\varepsilon_{su,\theta} = 0,20$ lass A reinforcement: $\varepsilon_{st,\theta} = 0,05$ $\varepsilon_{su,\theta} = 0,10$
Functions	$a^2 = (\varepsilon_{sy,\theta} - \varepsilon_{sp,\theta})(\varepsilon_{sy,\theta} - \varepsilon_{sp,\theta} + c/E_{s,\theta})$ $b^2 = c\,(\varepsilon_{sy,\theta} - \varepsilon_{sp,\theta})\,E_{s,\theta} + c^2$ $c = \frac{(f_{sy,\theta} - f_{sp,\theta})^2}{(\varepsilon_{sy,\theta} - \varepsilon_{sp,\theta})E_{s,\theta} - 2(f_{sy,\theta} - f_{sp,\theta})}$

*) Values for the parameters $\varepsilon_{pt,\theta}$ and $\varepsilon_{pu,\theta}$ for prestressing steel may be taken from Table 3.3

Figure 1 : Mathematical model for stress-strain relationships of reinforcing and prestressing steel at elevated temperatures (notations for prestressing steel "p" instead of "s")

(2) Values for the parameters for cold worked (wires and strands) and quenched and tempered (bars) prestressing steel at elevated temperatures are given in Table 1. For intermediate values of the temperature, linear interpolation may be used.

Table 1: Values for the parameters of the stress-strain relationship of cold worked (cw) (wires and strands) and quenched and tempered (q & t) (bars) prestressing steel at elevated temperatures

Steel temp.	$f_{py,\theta} / (0,9\ f_{pk})$		$f_{pp,\theta} / (0,9\ f_{pk})$		$E_{p,\theta} / E_p$		$\varepsilon_{pt,\theta}$ [-]	$\varepsilon_{pu,\theta}$ [-]
θ [°C]	cw	q & t	cw	q & t	cw	q & t	cw, q&t	cw, q&t
1	2	3	4	5	6	7	8	9
20	1,00	1,00	1,00	1,00	1,00	1,00	0,050	0,100
100	0,99	0,98	0,68	0,77	0,98	0,76	0,050	0,100
200	0,87	0,92	0,51	0,62	0,95	0,61	0,050	0,100
300	0,72	0,86	0,32	0,58	0,88	0,52	0,055	0,105
400	0,46	0,69	0,13	0,52	0,81	0,41	0,060	0,110
500	0,22	0,26	0,07	0,14	0,54	0,20	0,065	0,115
600	0,10	0,21	0,05	0,11	0,41	0,15	0,070	0,120
700	0,08	0,15	0,03	0,09	0,10	0,10	0,075	0,125
800	0,05	0,09	0,02	0,06	0,07	0,06	0,080	0,130
900	0,03	0,04	0,01	0,03	0,03	0,03	0,085	0,135
1000	0,00	0,00	0,00	0,00	0,00	0,00	0,090	0,140
1100	0,00	0,00	0,00	0,00	0,00	0,00	0,095	0,145
1200	0,00	0,00	0,00	0,00	0,00	0,00	0,100	0,150

3. DTU-FB P 92-701

The reduction factor φ_s for the mechanical properties of prestressing steel at elevated temperature for fire design is defined as below :

	Temperature (°C)			
	0	**175**	**500**	**750**
Wires and strands	1	1	0,30	0

The effects of elevated temperatures on the strength properties of reinforcing and prestressing steels

M. Holmes, PhD, DSc, CEng, FIStructE, FICE
Department of Civil Engineering, University of Aston

R. D. Anchor, BSc, CEng, FIStructE, FICE
University of Aston and R. D. Anchor Consultants

G. M. E. Cook, BSc, CEng, MIMechE, MICE, FIFireE
Fire Research Station, BRE

R. N. Crook, BSc, PhD
Cement & Concrete Association

Synopsis

The effect of elevated temperatures on the strength and stiffness properties of four reinforcing and three prestressing steels of varying size, manufactured to British Standard specifications, has been investigated. To simulate the temperatures likely to be experienced by the steel during a fire, a temperature range of 20° to 700° was adopted. The steels were tested in their 'as manufactured' condition in a purpose-built, tensile testing machine with tube furnaces and associated recording instrumentation. The test programme was designed to provide data on three major strength parameters—yield (or 0·2 % proof) stress, ultimate strength, and elastic modulus. Using the data it is possible to assess the deterioration in strength of a structure during a fire and its residual strength at ambient temperature after a fire.

Introduction

Estimates of the resistance of structures to fire exposure are currently obtained by exposing structural elements to a standard fire (BS 476[1] ASTME[2] and ISO 834[3]). The fully-loaded structural element under test is exposed to the standard fire and the time measured until collapse takes place. Traditionally, in the UK the structural fire resistance of a member is decided by applying rules concerning concrete cover, minimum member size, and protection offered by surface finishes.

The joint report by The Concrete Society and The Institution of Structural Engineers[4] suggests that a more rational design approach for fire resistance should be adopted using limit state philosophy. Such an approach would involve consideration of the total structure response to fire, rather than consideration of the behaviour of isolated structural elements. The report also makes clear that, before limit state principles can be adopted for fire resistance, much additional information and data needs to be acquired, including the behaviour of steel reinforcement at elevated temperature.

This paper describes an extensive study of the behaviour of reinforcing and prestressing steel at elevated temperatures and various applied stress conditions. The data obtained may be used in formulating the limit state design procedures for fire resistance mentioned above.

Types of steel investigated

For the investigation, four types of reinforcement and three types of prestressing steel were selected to represent the wide range of steels currently available to the construction industry. For the reinforcing steels, three nominal diameters were chosen, i.e. 8 mm, 12 mm, and 25 mm. This would enable a correlation, if any, to be made as to the effect of size on the strength properties. The prestressing wire was chosen in 5 mm diameter form and the strand as 9·3 mm seven-wire strand.

Table 1 gives the type of steel to be used, its trade name, and supplier.

The recent introduction of the Torbar type of cold-worked, high yield steel, with much improved bond characteristics, has led to ceased production of the square twisted type of cold-worked steel. However, since the latter type of steel has been widely used in the construction industry, the tests were still considered necessary so that an assessment of the performance and residual properties of existing concrete structures damaged by fire can be made.

The manufacture of the various types of reinforcement was in accordance with BS 4449[5] and BS 4461[6] with prestressing steels covered by BS 2691[7] and BS 3617[8]. These standards lay down specific requirements for chemical composition, characteristic strength (yield or proof), ultimate tensile strength, etc. Although these standards give values that are acceptable for general usage, it was decided to obtain as many of the properties given in the standards from the actual delivered steel.

Testing equipment

A tensile testing machine with the versatility to accommodate the size and length of specimen and deformation under load and capable of operating at elevated temperature, was not available commercially. Therefore, a special purpose machine, working on the basic concept of two load plattens moving apart, was designed and built. A schematic diagram is shown in Fig 1. The loading mechanism had a maximum extension of 150 mm, but this was extended to 300 mm by the use of a spacer inserted between the ram and top loading platten, while the ram core was retracted.

The steel was to be tested in its 'as rolled' condition and this required the use of serrated mechanical wedges so as to grip the reinforcement and enable the load to be transferred to it. Proprietary prestressing anchorages and smooth wedges were used for loading the prestressing steel specimens.

TABLE 1—Steel types and suppliers

Type of steel	Proprietary name or generic description	Supplier/manufacturer
Mild steel	Mild steel	BRC Engineering Co, Stafford
Hot-rolled high yield	Unisteel	Reinforcement Steel Services, Sheffield
Cold-worked high yield	GK Torbar	GKN (South Wales) Ltd., Cardiff
	Square twisted	BRC Engineering Co Stafford
Prestressing wire	Mill Coil	GKN (Somerset Wire) Ltd., Cardiff
	Stabilised wire	
Prestressing strand	seven wire strand	

To heat the specimens a cylindrical tube furnace having an inner silicon heating tube of 87·5 mm diameter, with a maximum operating temperature of 1000°C, was used. The silicon tube was protected in a large diameter, stainless steel tube with the void filled with insulating material. Because of heat losses through the ends of the furnace, which was reduced by Meckenchnie ceramic wool fibre, and the need to obtain a low temperature gradient over the heated length, the furnace was split into three, 150 mm zones. These zones were controlled independently by Eurotherm thyrister units from a preselected digital temperature display. Temperature measurement was obtained from fibreglass-insulated Chromel-Alumel thermocouples fixed to the specimen. The thermocouples were used to monitor the specimen temperature over the three zones, record the gauge length temperature, and control the thyrister units.

Since the gauge length was confined within the furnace and would be subjected to a temperature up to 700°C the choice of a strain measurement device was limited. Ideally, quartz extensometers, having extremely low thermal expansion properties giving accurate results, should be used. However, the fragile nature of quartz ruled out its use and Nimonic 80A alloy steel, having low creep properties, was chosen instead. The susceptibility of this material to thermal expansion meant that, whenever steady-state temperatures were not present, the results needed to be corrected for the thermal expansion of the strain gauge. Two transducers, with an operating range of ± 12·5 mm and temperature range of −10°C to +50°C, used in conjunction with detachable collets and mounted outside the furnace, allowed for all sizes of specimen with differing gauge lengths to be accommodated on one extensometer. Calibration of the transducers was obtained using metric micrometers placed under the transducers.

Load measurement was obtained from two pressure transducers attached to the loading ram. For accuracy, one measured up to 200 kN and the other above 200 kN. Outputs from the pressure tranducers, extensometer transducers and thermocouples were amplified and input into a Bryans X-Yt 29000 series recorder. A continuous plot of two of the inputs was obtained and the scales were adjusted to give the maximum range of values required.

Objectives of the test programme

The test programme outlined below was designed to provide the essential experimental data on the effects of high temperature on the strength and stiffness properties of reinforcing and prestressing steel. In designing the programme, attention was paid to the deterioration in strength of a structure during a fire and its residual strength at ambient temperature after a fire. The three test procedures subsequently derived were common to both types of steel (reinforcing and prestressing).

Test procedures

At least two room-temperature tensile tests were performed on all the different types and sizes of steel before the elevated temperature tests commenced. Separate specimens were used for each test and two nominally identical tests were performed at each temperature increment of 100°C.

The cross-sectional area of each specimen was determined by the method given in BS 4449[8] and BS 4461[9] and for each size of specimen a convenient gauge length based on $5{\cdot}65\sqrt{S_0}$ (where S_0 is the cross-sectional area) was used. Tests, wherever possible, were performed in accordance with BS 18[9] and BS 3688[10]. However, it was not practical, with the positioning of the equipment, to perform the tests under 'strain rate control'. As an alternative, an equivalent loading rate based on the recommended strain rate of between 0·001 and 0·003/min up to yield or proof stress and the physical characteristics of the specimens, was used.

To ensure that the whole cross-section of the specimen had reached the specified temperature, a standard soaking time of ½ h was used. This was based on the minimum fire resistance time given in CP 110[11] and would also allow the extensometers and other gauges to reach a steady state before the test commenced.

The following test procedures (series 1 to 3) are shown diagrammatically in Fig 2.

Series 1

A specimen with extensometers and thermocouples attached was placed through the furnace and suspended from the top loading platten of the test rig. The furnace position was adjusted until the extensometer had an equal clearance both internally and externally from the furnace's silicon tube. The inputs to the *X-Y* plotter were set and the furnace was switched on. With the aid of the digital thermometer the furnace control was adjusted until all three zones on the specimen were within ±5°C of the specified temperature (700°C maximum) and the half-hour soaking period was commenced. At the end of this period the strain due to the expansion of the specimen and extensometers was recorded. After adjusting the *X* axis to allow for the initial movement of the loading platens a tensile test to failure was performed at the specified temperatures.

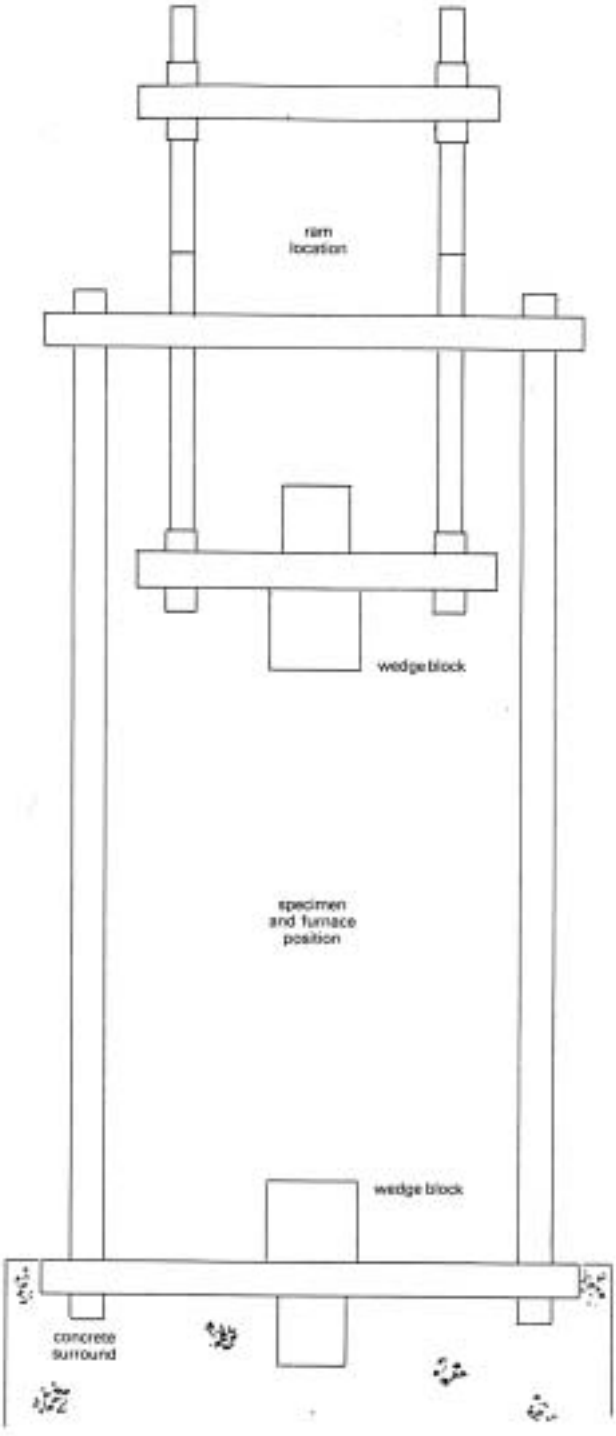

Fig 1. Test frame arrangement

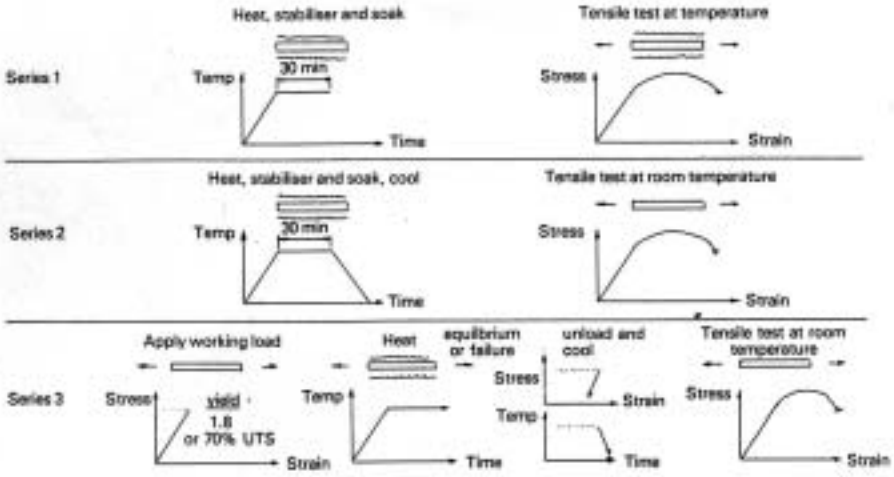

Fig 2. Test procedures

The results from this type of test are applicable to the analysis of the performance of the steels, in terms of the strength parameters at different temperatures over the range for which a fire would be expected.

Series 2

This procedure is concerned with the residual properties of the steel after being subjected to an elevated temperature, and simulates the behaviour of a structure after a fire incident.

Specimens, usually four, one of each type for a specific size with the thermo-couples attached, were placed inside the furnace and the ends lightly packed with ceramic fibre after their position had been adjusted to give the required heated length. After reaching the required temperature (700°C maximum) to within ±5°C and left to soak for half-an-hour, the specimens were allowed to cool naturally to room temperature. An extensometer was fitted to each specimen in turn, the instrumentation adjusted as described above, and a tensile test performed at room temperature to failure.

Series 3

The procedure for arranging the specimen and gauges in the furnace and test rig was identical with that described for series 1. However, instead of raising the temperature of an unloaded specimen, a load was applied equivalent to the working stress for the steel. This was equivalent to yield or 0·2 % proof stress divided by 1·8 for the reinforcing and to 70 % ultimate tensile strength for the prestressing steels. These strength parameters were obtained from the room-temperature control tests on samples of similar size and type. This part of series 3 is referred to as series 3A.

For each specified temperature the strain, temperature, and time were recorded, and the test was terminated either when the strain rate became very small (usually taken as 0·0004/min) or if the test had been running for over 3 h and the strain was non-uniform, or the specimen had failed. If failure had not occurred, the specimen was unloaded, cooled to room temperature and a tensile test performed on it in the test rig. This part of series 3 is referred to as series 3B.

This procedure gives the information necessary to determine the performance of the steels when they had been subjected simultaneously to a stress and an elevated temperature and it would simulate the effect on the steel in a structure loaded to its full design capacity being subjected to a fire.

Test results

Room temperature results

The room-temperature control test results were obtained from the tests performed in an Avery Denison testing machine and the specially-built test rig. To complete all the tests on the reinforcing steels two batches were required, with batch 1 steels being used for series 3 and batch 2 for series 1 and 2. Enough 8 mm unisteel was available to complete the tests from batch 1. Whenever possible, samples for use in both machines were cut from the same length.

Tables 2, 3, 4, and 5 show the 95 % confidence limits and the coefficient of variance for the tests performed. Each of the values recorded in these tables is based on a minimum of five test results.

These two parameters show the spread of results obtained from the tests. The strength parameters of yield (or 0·2% proof) stress, ultimate strength, and elastic modulus obtained from the room-temperature tests would be used to normalise the corresponding values obtained from the specimens tested at, or after being cooled from, an elevated temperature.

TABLE 2—8 mm room-temperature results

Type of steel	Batch no.	Yield or 0·2% proof stress		Ultimate tensile strength		Elastic modulus	
		95% confidence limits (N/mm²)	Coefficient of variance (%)	95% confidence limits (N/mm²)	c/v (%)	95% confidence limits (kN/mm²)	c/v (%)
Mild steel	1	337·7 ± 43·6	6·5	467·3 ± 65·5	7·1	211·56 ± 18·31	4·4
	2	369·0 ± 15·4	2·1	487·0 ± 39·1	4·1	203·13 ± 11·17	2·8
Unisteel	1	491·5 ± 3·0	0·3	711·1 ± 13·4	1·0	208·66 ± 28·79	7·0
Torbar	1	485·1 ± 25·9	2·7	586·7 ± 36·8	3·2	205·32 ± 8·56	2·1
	2	499·1 ± 27·8	2·8	596·4 ± 30·8	2·6	210·64 ± 13·30	3·2
Square twisted	1	471·0 ± 34·9	3·8	569·8 ± 54·9	4·9	206·76 ± 5·17	1·3
	2 (10 mm)	448·9 ± 8·6	1·0	511·1 ± 27·1	2·7	208·57 ± 5·37	1·3

Paper: Holmes/Anchor/Cook/Crook

TABLE 3—12 mm room-temperature results

Type of steel	Batch no.	Yield or 0·2% proof stress		Ultimate tensile strength		Elastic modulus	
		95% confidence limits (N/mm²)	Coefficient of variance (%)	95% confidence limits (N/mm²)	c/v (%)	95% confidence limits (kN/mm²)	c/v (%)
Mild steel	1	326·0 ± 37·5	5·8	443·6 ± 28·2	3·2	208·88 ± 24·91	6·0
	2	293·0 ± 13·2	2·3	452·3 ± 22·1	2·5	212·72 ± 20·55	4·9
Unisteel	1	473·8 ± 20·6	2·2	639·0 ± 10·5	0·8	209·87 ± 29·52	7·1
	2	502·7 ± 4·5	0·5	608·9 ± 10·5	0·9	214·26 ± 39·28	9·4
Torbar	1	492·8 ± 34·3	3·5	587·4 ± 52·1	4·5	204·64 ± 20·24	5·0
	2	519·9 ± 12·8	1·3	593·3 ± 15·4	1·3	222·37 ± 15·09	3·5
Square twisted	1	550·7 ± 21·1	2·0	660·1 ± 25·9	2·0	205·03 ± 20·10	5·0
	2	503·7 ± 21·0	2·1	593·7 ± 6·9	0·6	217·05 ± 12·62	3·0

TABLE 4—25 mm room-temperature results

Type of steel	Batch no.	Yield or 0·2% proof stress		Ultimate tensile strength		Elastic modulus	
		95% confidence limits (N/mm²)	Coefficient of variance (%)	95% confidence limits (N/mm²)	c/v (%)	95% confidence limits (kN/mm²)	c/v (%)
Mild steel	1	319·1 ± 6·8	1·1	464·5 ± 1·4	0·2	204·05 ± 21·42	5·3
	2	313·3 ± 2·7	0·4	485·3 ± 9·5	1·0	198·23 ± 34·21	8·8
Unisteel	1	557·5 ± 24·4	2·2	715·6 ± 9·4	0·6	195·65 ± 34·57	9·0
	2	492·9 ± 9·0	0·9	677·9 ± 7·5	0·6	194·09 ± 26·83	7·0
Torbar	1	450·3 ± 46·0	5·2	558·0 ± 73·3	6·7	244·24 ± 27·03	5·6
	2	460·2 ± 4·8	0·5	551·1 ± 18·8	1·7	222·91 ± 33·15	7·6
Square twisted	1	459·0 ± 17·9	2·0	587·6 ± 2·3	0·2	226·50 ± 18·18	4·1
	2	441·7 ± 1·9	0·2	554·7 ± 8·8	0·8	221·19 ± 24·85	8·0

TABLE 5—Prestressing steel room-temperature results

Type of steel	Yield or 0·2% proof stress		Tensile strength		Elastic modulus	
	95% confidence limits (N/mm²)	Coefficient of variance (%)	95% confidence limits (kN/mm²)	c/v (%)	95% confidence limits (kN/mm²)	c/v (%)
5 mm mill coil	1606·2 ± 43·8	1·4	36·9 ± 1·3	1·8	203·27 ± 8·07	2·0
5 mm stablised wire	1464·8 ± 23·4	0·8	33·5 ± 1·2	1·8	204·12 ± 33·36	8·3
9·3 mm seven wire strand	1864·5 ± 38·0	1·0	104·0 ± 0·4	0·2	199·54 ± 6·04	1·5

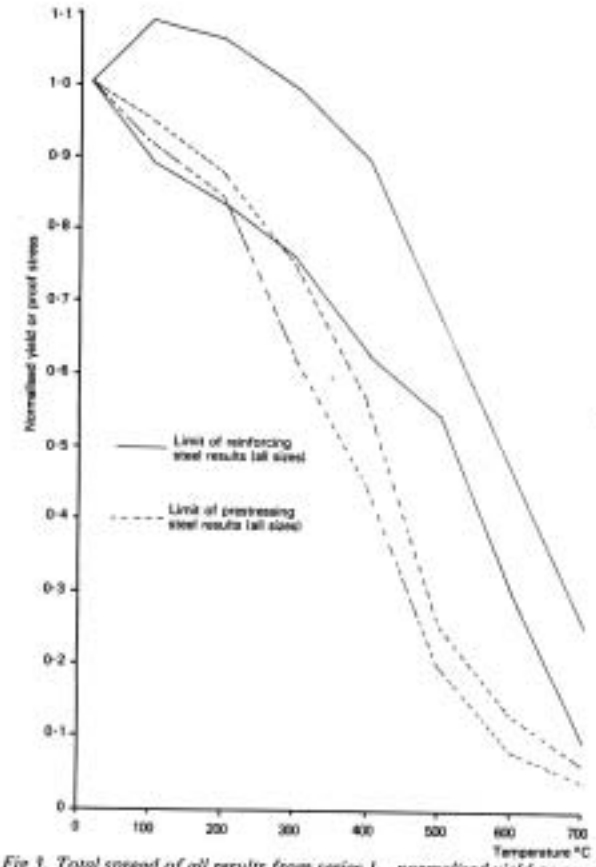

Fig 3. Total spread of all results from series 1—normalised yield or proof stress results

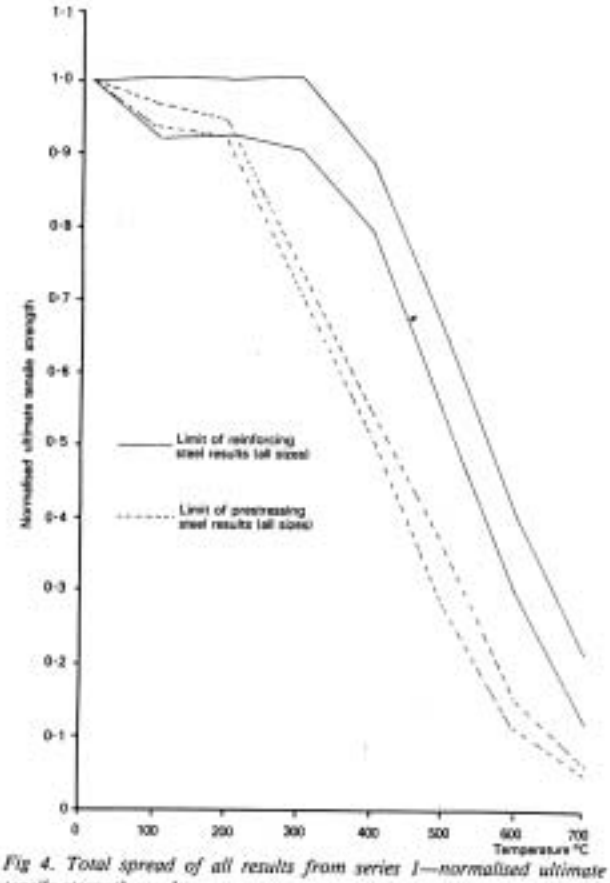

Fig 4. Total spread of all results from series 1—normalised ultimate tensile strength results

From all the mean values given in Tables 2 to 5 the only one to fall below the characteristic strength was for 10 mm square twisted steel, which had a mean 0·2 % proof stress of 448·9 N/mm². The individual results from this batch of steel did not comply with section 20 of BS 4461[6]: all the 0·2 % proof stress values fell below the characteristic strength.

The largest coefficients of variation obtained from the results (over 5·0 %) were those from the 8 and 12 mm mild steel specimens of batch 1, the 25 mm Torbar specimens, also of batch 1, and the majority of the elastic modulus values, which was as large as 9·4 % for the 12 mm unisteel. It was the variation of the strength properties within the material itself that caused the scatter of results, rather than any error in testing or analysis. If the yield stress of the mild steel is considered, the lower points of the 95 % confidence limit, even with the large coefficient of variation, are still greater than the characteristic strength of 250 N/mm². Also, all the mean tensile strengths given are greater than the mean yield stress by a value greater than the 10 % required by the appropriate British Standards[5, 6].

The elastic modulus was obtained from the slope of the linear portion of the stress/strain plot. However, some of the plots, usually from the cold worked steels, had little or no linear portion as they became non-linear either as soon as the load was applied or at low load values. In these cases the initial tangent modulus was measured from the experimental stress/strain plot.

The factor that was consistent throughout the results from series 1, 2 and 3 was that size of section had little influence on the property measured. With reference to the type of steel tested, the hot rolled steels (including one high yield) performed equally as well as each other, the two cold worked steels could not be distinguished, and the three prestressing steels gave identical results, once they were all normalised.

Series 1 results

Although the individual stress/strain plots of the tensile tests have not been included, it was noticeable that, for each of the three series, there was a change in the shape of the plots for certain types of reinforcing steel but not from the prestressing steels[12].

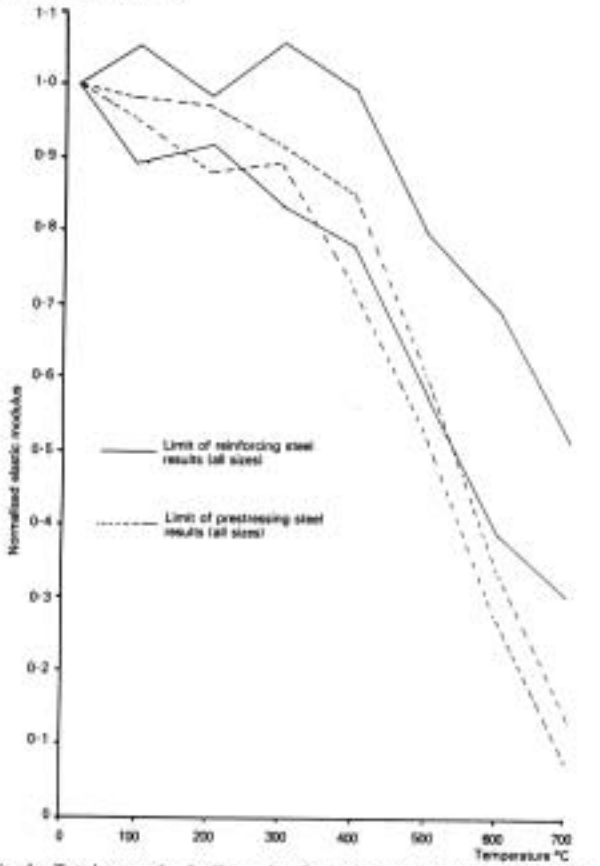

Fig 5. Total spread of all results from series 1—normalised elastic modulus results

The three sizes of Torbar and square twisted type steels, and also the 8 and 12 mm unisteel type, retained the typical 'cold worked' shape of a linear section, followed by a non-linear portion with no distinctive yield point and continued to work harden over the whole range of temperatures. All the mild steels and 25 mm unisteel had the characteristic 'hot rolled' shape plot of an elastic zone up to a yield point, followed by a long plastic zone for temperatures up to 200°C. However, at 300°C the shape changed to a plot that had no distinctive yield point and instead of a plastic zone showed a work hardening region without a distinctive yield point. It was therefore necessary to adopt the offset method usually used for the 'cold worked' steels to obtain the 0·2 % proof stress for temperatures of 300°C and above. The normalised results for the yield stress, ultimate strength and elastic modulus for all sizes and types (including the prestressing steels) are shown in Figs 3, 4, and 5.

These figures show that, for the reinforcing bars, there was no significant change in the normalised values below 300°C, but as soon as the temperature of the prestressing steels was raised to 100°C there was a noticeable reduction in these values.

A 50 % reduction in both the yield stress (Fig 3) and ultimate strength (Fig 4) was obtained between 520°C and 580°C and between 540°C and 700°C for the elastic modulus (Fig 5) for the reinforcing steels. A similar reduction was found from the prestressing steels when the temperature was between 370°C and 420°C for the proof stress (Fig 3) and ultimate strength (Fig 4) and between 510°C and 530°C for the elastic modulus (Fig 5). For the prestressing steels the temperature at which the ultimate tensile strength reduced to 70 % of its original value was between 305°C and 325°C (Fig 4).

A representative value taken as the midpoint of the scatter of results shown in Figs 3, 4 and 5 is given in Fig 6 for both reinforcing and prestressing steels. The curves from the most recent design chart[13] are included in Fig 6, and it can be seen that in the midrange of temperatures good agreement is obtained, but at the upper and lower temperatures the design curves do not form the lower bound limit.

Series 2 results

From the series 2 tests the recorded plots obtained again showed a change in shape for some of the reinforcing steels[12], although this was completely opposite to that obtained from series 1 tests. Here, those steels exhibiting a ductile behaviour (all mild steel plus 25 mm unisteel) retained it over the whole temperature range, but those steels producing the typical 'cold worked' stress/strain characteristic (all Torbar and square twisted plus 8 and 12 mm unisteel) changed the shape of their plot between 200°C and 300°C.

Fig 7 shows the variation in ultimate strength, 0·2 % proof, stress and elastic modulus with temperature for 12 mm square twisted steel illustrating a decrease in strength with increasing temperature. The variation between nominally identical tests (Fig 7) was small for the proof stress and tensile strength, but was larger for the elastic modulus, while still being within the extremes of the values obtained from the room-temperature tests.

When normalised the strength parameters again showed that the size of steel had little effect on the general shape of the graphs[12]. However, the manufacturing process for the reinforcing steel does have an effect on the yield and tensile strength, with the 'cold worked' steels having a greatly reduced strength with increasing temperature compared with the 'hot rolled' steels. As observed with series 1, the type of prestressing steel had no effect on the normalised values.

The decrease in the normalised proof stress and tensile strength for the prestressing steels was not significant, until the temperature exceeded 300°C. Below this temperature a constant strength was obtained for both parameters, except for the mill coil where a 9 % increase in proof stress was observed at 200°C[12]. The decrease in strength was not as drastic as the series 1 results, but a 50 % reduction in proof stress was obtained between 610°C and 650°C. For the two stressing levels of 70 % and 55 % ultimate tensile strength a temperature range of 490°C to 520°C and 570°C to 575°C, respectively, was observed[12]. The elastic modulus for both reinforcing and prestressing steels remained unaltered over the

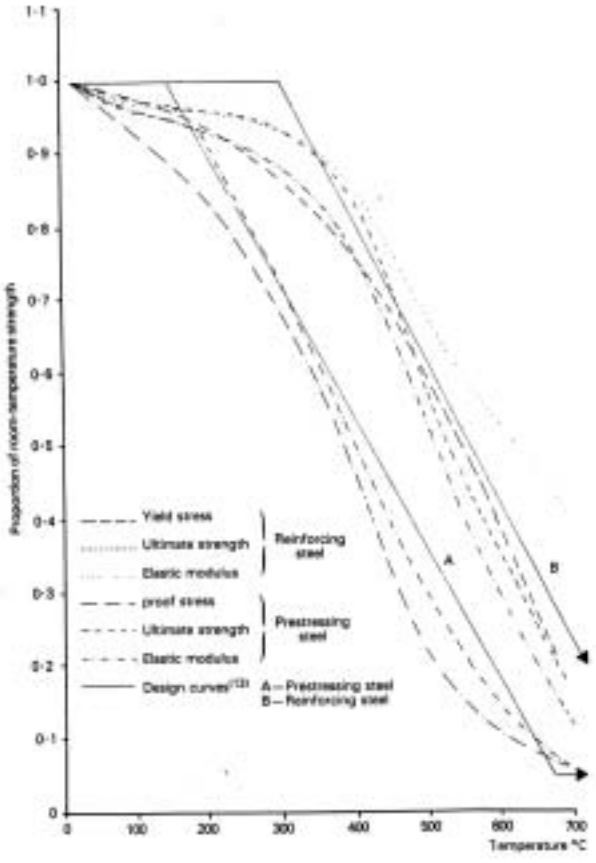

Fig 6. Typical strength properties of reinforcing and prestressing steels tested at elevated temperatures (series 1)

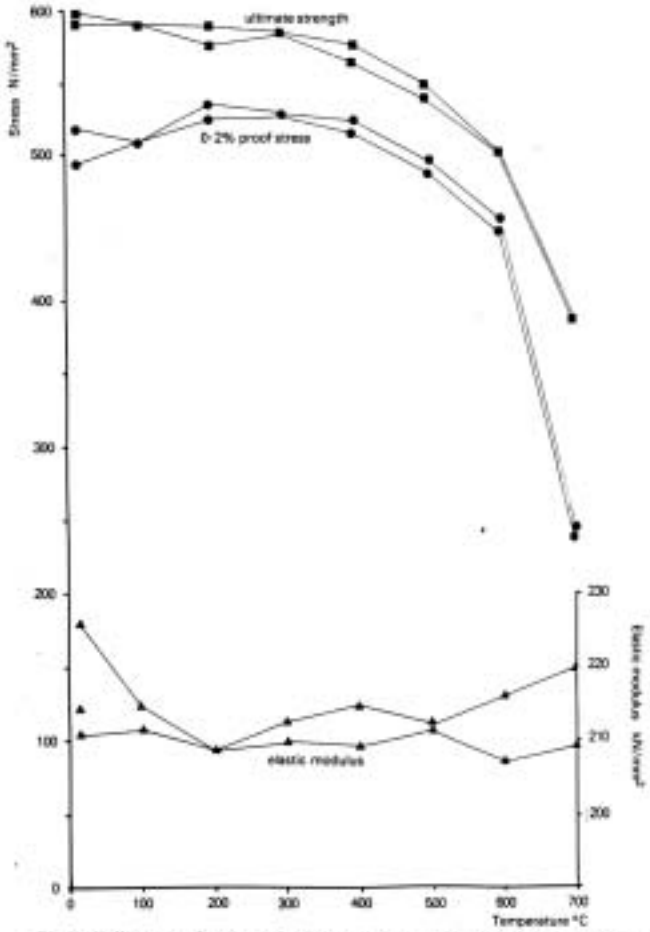

Fig 7. Full range of test results for 12 mm square twisted steel (series 2)

whole temperature range.

Differences between the two types of reinforcing bar were observed. The hot rolled yield stress increased by as much as 12·5 % at 400°C before reducing to 95 % of the original at 700°C. The cold worked steels also exhibited an increase (6 % at 300°C) but at 700°C the loss was 37 %. The ultimate strength values for the two steels were similar up to 500°C, but at 700°C the hot rolled steels had a 12 % reduction compared with a 26 % reduction for the cold worked steels[12]. Fig 8, a representative plot of all the results obtained from this series, shows the difference between the performance of the 'hot rolled' and 'cold worked' reinforcing steels and the prestressing steels after being subjected to an elevated temperature.

Series 3 results

All the prestressing steels failed at 300°C when subjected to 70 % ultimate load being maintained[12]. In retrospect it was felt that this loading was too high and possibly a value of between 50 and 60 % ultimate would have been more representative of the true prestressing force in the steel after the member had been in service for some time.

None of the reinforcing steels failed at 400°C with the working load (yield stress/1·8) applied, but at 600°C they all failed. At 500°C they either obtained equilibrium, failed, or after 3 h of testing continued to creep. There was no clear pattern at this temperature for any of the steels[12].

On cooling and subsequent retesting to failure, there was no reduction in any of the three strength parameters from the available samples for the reinforcing steels, although a slight decrease was obtained for the ultimate tensile strength of the prestressing steels (Fig 9).

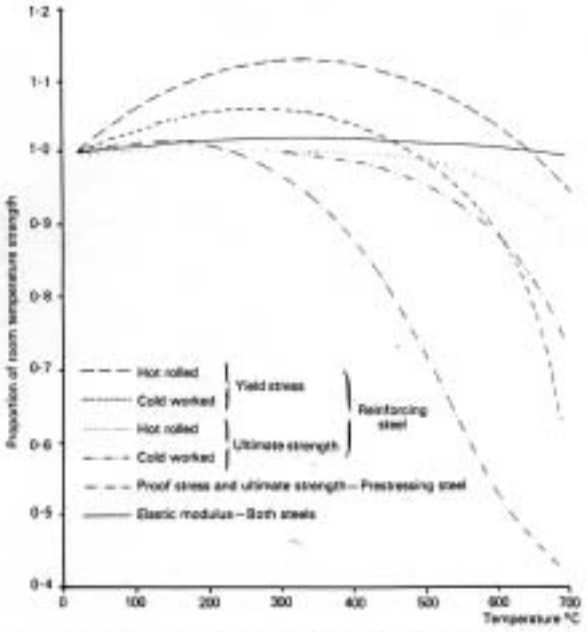

Fig 8. Typical strength properties of reinforcing and prestressing steels tested at room temperature after heating to an elevated temperature (series 2)

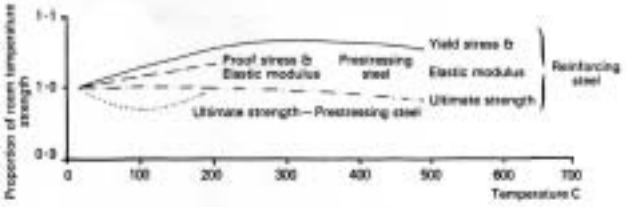

Fig 9. Typical strength properties of reinforcing and prestressing steels tested at room temperature after having a working load applied during heating (series 3)

Conclusions

The paper provides, for the first time, comprehensive data on the performance of reinforcing and prestressing steels in their 'as rolled' condition before, during and after exposure to elevated temperatures likely to be reached in a fire. It is expected that the data will be of use in Codes of Practice and other guidance documents which encourage the design of fire resisting structures using basic material properties.

In a fuller description[12] of the work reported in this paper a more detailed comparison is made between the comprehensive study described here and previous *ad hoc* work on elevated temperature properties of steel.

Acknowledgement

The work described in this paper was financed by the Fire Research Station as part of an extramural research contract awarded to the Department of Civil Engineering, University of Aston.

References

1. BS 476 *Fire tests on building materials and structures: Part 8: Test methods and criteria for the fire resistance of elements of building construction*, London, British Standards Institution, 1972
2. ASTM E119 *Fire tests on building and construction materials*, American Society for Testing and Materials, 1961
3. ISO 834 *Fire resistance test of structures*, International Organization for Standardization, 1968
4. *Fire resistance of concrete structures*, joint report, IStructE and The Concrete Society, August 1975
5. BS 4449 *Specification for hot rolled steel bars for the reinforcement of concrete*, London, British Standards Institution, 1978
6. BS 4461 *Specification for cold worked steel bars for the reinforcement of concrete*, London, British Standards Institution, 1978
7. BS 2691 *Steel wire for prestressed concrete*, London, British Standards Institution, 1969
8. BS 3617 *Seven-wire steel strand for prestressed concrete*, London, British Standards Institution, 1971
9. BS 18 *Methods for tensile testing of metals: Part 2: Steel (general)*, London, British Standards Institution, 1971
10. BS 3688 *Methods for mechanical testing of metals at elevated temperatures: Part 1: Tensile testing*, London, British Standards Institution, 1963
11. CP 110 *The structural use of concrete: Part 1: Design, materials and workmanship*, London, British Standards Institution, 1972
12. Crook, R. N.: 'The elevated temperature properties of reinforced concrete', PhD thesis, University of Aston, 1980
13. *Design and detailing of concrete structures for fire resistance*, IStructE and The Concrete Society, April 1978

ANNALES DE L'INSTITUT TECHNIQUE DU BATIMENT ET DES TRAVAUX PUBLICS

N° 396 JUILLET-AOUT 1981

SERIE : **MATERIAUX**

ISSN 0020-2568 **N° 58**

Synthèse des essais de comportement à chaud des aciers pour béton armé et pour béton précontraint

faite par la Commission d'Etude des Règles de Calcul DTU

« Méthode de prévision par le calcul du comportement au feu des structures en béton »

présentation par

Bernard **MALAVAL**

Secrétaire de la Commission
Chef du Service Réglementation au CATED

SYNDICAT NATIONAL DU BETON ARME ET DES TECHNIQUES INDUSTRIALISEES
INSTITUT TECHNIQUE DU BATIMENT ET DES TRAVAUX PUBLICS

SYNTHESE DES ESSAIS DE COMPORTEMENT A CHAUD DES ACIERS POUR BETON ARME ET POUR BETON PRECONTRAINT

Le DTU de 1974 sur le calcul de la résistance au feu des éléments en béton armé, donnait des courbes et un tableau montrant la diminution de la résistance de l'acier en fonction de la température.

Depuis la parution de ce DTU, des études ont été menées en vue de préciser les valeurs de cet affaiblissement, en fonction de la température, des performances des différents types d'aciers, tant en ce qui concerne les aciers pour béton armé que ceux utilisés dans les structures précontraintes.

C'est une synthèse des résultats de ces récentes études qui est présentée ici.

SYNTHESIS OF HEAT BEHAVIOUR TESTS OF STEELS FOR REINFORCED CONCRETE AND FOR PRESTRESSED CONCRETE

The DTU of 1974 on the calculation of the fire-resistance of reinforced concrete elements gave curves and a table showing the decrease in the strength of steel as a function of temperature.

Since this DTU appeared studies have been made with a view to establishing the precise values of this weakening, as a function of temperature, of the performances of the different types of steel, both steels for reinforced concrete and those used in prestressed structures.

It is a synthesis of the results of these recent studies that is presented here.

VERHALTEN VON BEWEHRUNGSSTAHL UNTER HOHEN TEMPERATUREN

Die DTU-Vorschriften von 1974 zur Berechnung der Tragfähigkeit von Stahlbetonbauteilen unter Feuerbeanspruchung enthalten Diagramme und Tabellen zur Bestimmung der Festigkeitsminderung von Bewehrungsstählen in Abhängigkeit von der Temperatur.

Seit dem Erscheinen dieser DTU-Vorschrift wurden Untersuchungen mit dem Ziel durchgeführt, diese Festigkeitsminderung in Abhängigkeit von der Temperatur für schlaffe Bewehrungsstäbe und Vorspannbewehrung genauer zu bestimmen.

Eine Synthese der dabei erzielten Ergebnisse wird in diesem Artikel mitgeteilt.

SINTESIS DE LOS ENSAYOS DE COMPORTAMIENTO EN CALIENTE DE LOS ACEROS PARA HORMIGON ARMADO Y PARA HORMIGON PRETENSADO

El DTU de 1974 relativo al cálculo de la resistencia al fuego de los elemenyos de hormigón armado, indicaba diversas curvas y una tabla con objeto de precisar la disminución de la resistencia del acero en función de la temperatura.

Desde el momento en que este DTU ha sido publicado, han sido emprendidos diversos estudios con objeto de precisar los valores de este debilitamiento, en función de la temperatura, y asi mismo de las caracteristicas de los distintos tipos de aceros, tanto por lo que respecta a los aceros para hormigón armado como aquéllos que se utilizan en las estructuras pretensadas.

En el presente articulo se presenta una síntesis de los resultados de estos recientes estudios.

Les thèses et la méthode d'exposition adoptées par les auteurs peuvent parfois heurter certains points de vue habituellement admis. Mais il doit être compris que ces thèses, à l'égard desquelles l'Institut Technique ne saurait prendre parti, ne visent en rien les personnes ni le principe des Institutions.

Synthèse des essais de comportement à chaud des aciers pour béton armé et béton précontraint

Les essais en laboratoire agréé ont été pendant longtemps le seul moyen réglementaire de justifier la résistance au feu des ouvrages demandée par les textes relatifs à la sécurité incendie.

Des « Recommandations pour la prévision par le calcul du comportement au feu des structures en béton » ont été publiées en mai 1972. Elles ont été transformées en « Règles de calcul DTU » en octobre 1974 et il a fallu attendre l'arrêté du 19 décembre 1975 (modifiant l'arrêté du 5 janvier 1959 relatif aux essais de résistance au feu) pour qu'elles deviennent officiellement une méthode réglementaire de justification.

Le DTU d'Octobre 1974 et son additif d'avril 1975 ont été annulés et remplacés par un nouveau document paru en avril 1980.

L'évolution des caractéristiques du béton et des armatures en acier en fonction de la température constitue l'un des paramètres principaux de cette méthode. En ce qui concerne l'acier, les courbes figurant dans les Recommandations de 1972, reprises sans modifications dans le DTU de 1974, reposaient sur des essais, pour la plupart étrangers, relativement anciens, et dont l'homogénéité des méthodologies n'avait pu être vérifiée. Toutefois, on ne disposait pas d'autres informations à l'époque.

Nous présentons dans cet article une synthèse des connaissances acquises depuis, qui ont abouti à l'indication de nouvelles valeurs dans le DTU d'avril 1980, autant pour les aciers de précontrainte que pour ceux de béton armé.

1. Aciers pour béton précontraint

C'est pour ce type d'acier que la motivation d'expérimentations plus précises et plus fiables est apparue la première. En effet, les courbes de la figure 8 et les valeurs du tableau de l'article 3.221 du DTU de 1974 (reproduit sur la figure 1 ci-dessous) semblaient pessimistes à certains préfabricants de planchers à poutrelles précontraintes, à la lumière des essais dans les fours agréés qu'ils avaient réalisés.

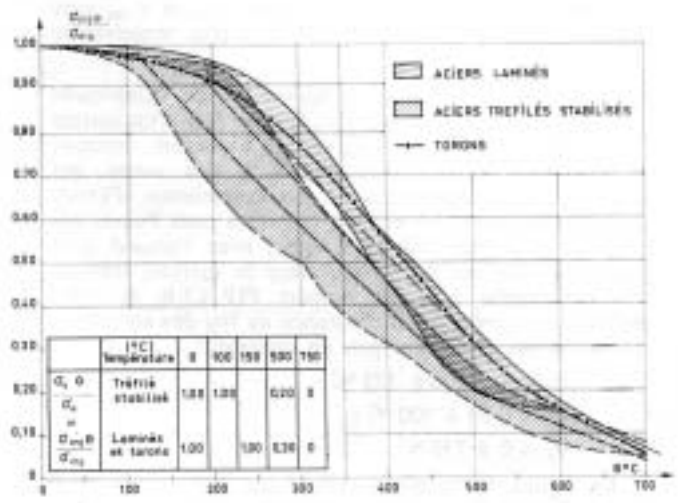

Fig. 1. — **Courbes et tableau du DTU de 1974 donnant la diminution de la résistance en fonction de la température.**

Il était indiqué en tête du chapitre correspondant du DTU :

...« *A défaut d'utiliser ces données, on pourra leur substituer les résultats expérimentaux obtenus dans les laboratoires agréés à cet effet, sur les matériaux effectivement mis en œuvre. Il sera alors nécessaire, dans cette éventualité, de solliciter et d'obtenir l'accord de la Commission d'Etude sur les nouveaux chiffres proposés...* ».

Des essais d'aciers de précontrainte effectués au laboratoire de l'Université de Liège (Belgique) par M. Brenneisen, puis Mme Brenneisen, dont les résultats étaient plus optimistes que les valeurs ci-dessus, ont été proposés début 1976 à la Commission d'Etude.

Après consultation de ce laboratoire, cette Commission établit, lors de sa réunion du 24 juin 1976, une méthodologie d'essais qui devait servir de base d'accord pour tous les résultats expérimentaux qui lui seraient proposés.

Les essais de tension à température constante et les essais d'échauffement à tension constante donnant pratiquement les mêmes résultats, l'essai retenu est l'essai isotherme. Les contraintes retenues sont les contraintes à 0.2 % d'allongement ; toutefois, dans le cas des aciers de précontrainte, dans la mesure où elles sont très voisines des contraintes à rupture qui facilitent la réalisation des essais, on retient ces dernières.

- Les températures retenues, autres que la température ambiante sont 300 °C et 500 °C.
- L'essai est conduit selon le schéma de la figure 2.
- La vitesse de montée en température doit rester inférieure à 100 °C par minute. (Une rectification

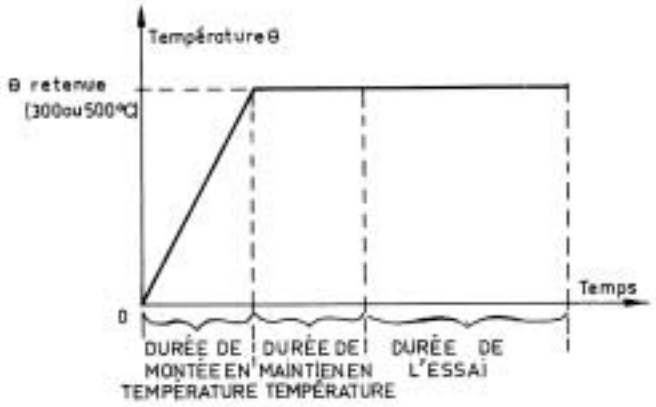

Fig. 2. — **Conduite de l'essai.**

fut apportée par la suite, sur ce point, en imposant une vitesse inférieure à 10 °C par minute, avec tolérance de plus ou moins 5 °C).

- La mise en tension pendant la durée de l'essai est effectuée selon les prescriptions de la norme ISO concernée pour les essais à température ambiante.
- La mise en tension peut être précédée d'une opération de préchargement à une tension au plus égale au dixième de celle escomptée à la rupture.
- La température est maintenue constante pendant la durée de maintien et la durée d'essai, à plus ou moins 5 °C près, la mesure étant effectuée sur l'acier.
- Les mesures sont effectuées uniquement sur la partie d'éprouvette répondant aux critères précédents de température.
- Le critère de rupture retenu est celui de la tension maximale enregistrée.

Les essais ont pour objet de définir la courbe d'affaiblissement des caractéristiques de rupture d'un acier en fonction de l'élévation de la température suivant le tracé d'un polygone déterminé conventionnellement par le schéma de la figure 3, à partir de :

- l'horizontale : $\varphi_s = 1$;
- les valeurs : $\varphi_{s\,300}$;
  $\varphi_{s\,500}$;
  et $\varphi_s = 0$ à 750 °C.

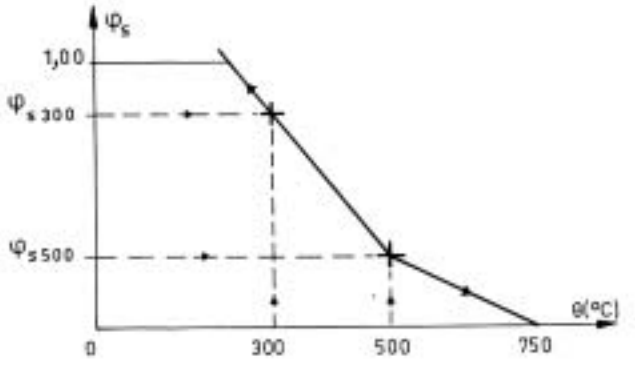

Fig. 3. — **Tracé conventionnel de la diminution de la résistance en fonction de la température.**

Le fabricant doit garantir, avec la même probabilité que les caractéristiques d'agrément de l'acier à température ambiante, l'affaiblissement maximal de ces caractéristiques à 300 °C et 500 °C ($\varphi_{s\,300}$ et $\varphi_{s\,500}$). Il est admis que cette garantie est obtenue par interpolation pour toutes les températures, si elle l'est à 300 °C et à 500 °C. Les documents à fournir par le fabricant à la Commission d'Etude sont :

1) Les compte rendus d'essais effectués par un laboratoire indépendant suivant le processus décrit ci-dessus et faisant apparaître :
   - les courbes contrainte/allongement à température ambiante, à 300 °C et à 500 °C, ces courbes pouvant être arrêtées juste avant la rupture ;
   - les contraintes de rupture à ces mêmes températures.
2) Les valeurs $\varphi_{s\,300}$ et $\varphi_{s\,500}$.
3) L'engagement de respecter une procédure d'autocontrôle.
4) L'identification de l'acier, son mode de fabrication et son numéro d'agrément.

Le producteur d'acier hollandais NDI fut le premier à utiliser cette méthodologie pour proposer à la Commission d'Etude des valeurs garanties de $\varphi_{s\,300}$ et $\varphi_{s\,500}$ pour ses aciers de précontrainte ; celle-ci les entérina en octobre 1977.

Parallèlement, les aciéries de Chiers-Châtillon-Gorcy entamèrent également des essais à chaud de leurs aciers dès 1976. La Commission confirmant son refus d'extrapoler aux autres aciers les résultats de NDI tant que le nombre d'essais ne serait pas suffisant et que les producteurs ne s'engageraient pas par écrit sur des valeurs garanties, les essais furent poursuivis jusqu'en 1978 au nom de l'ensemble des fournisseurs d'armatures tréfilées sur le marché français.

Les résultats expérimentaux sont reportés sur la figure 4 **(charges de rupture réelles).**

La ligne polygonale simplifiée des valeurs garanties correspondantes fut définie dans un premier temps par :

$\varphi_s = 0.70$ à 300 °C ;

$\varphi_s = 0.25$ à 500 °C ;

$\varphi_s = 0$ à 750 °C.

L'intersection de la droite joignant $\varphi_{s\,300}$ et $\varphi_{s\,500}$ avec l'horizontale $\varphi_s = 1$ correspondait à une température de 170 °C.

Une concertation avec le laboratoire de l'Université de Liège eut lieu alors, celui-ci faisant état d'un certain nombre de résultats différents. Toutefois, ceux-ci correspondaient pour la plupart à des aciers qui n'étaient plus commercialisés. La Commission d'Etude adopta finalement les valeurs suivantes pour l'ensemble des aciers tréfilés (fils et torons), avec l'accord écrit de l'ensemble des fournisseurs sur le marché français (le paragraphe 3.22 du rapport FIP/CEB de 1978 relatif au contrôle de la résistance au feu des structures en béton fut également pris en compte) :

$\varphi_s = 1$ jusqu'à 175 °C ;

$\varphi_s = 0.30$ à 500 °C ;

$\varphi_s = 0$ à 750 °C.

La figure 5 reproduit cette ligne polygonale ainsi que le fuseau des valeurs expérimentales de la figure 4, celles-ci étant cette fois rapportées à la **charge de rupture garantie** à la température ambiante.

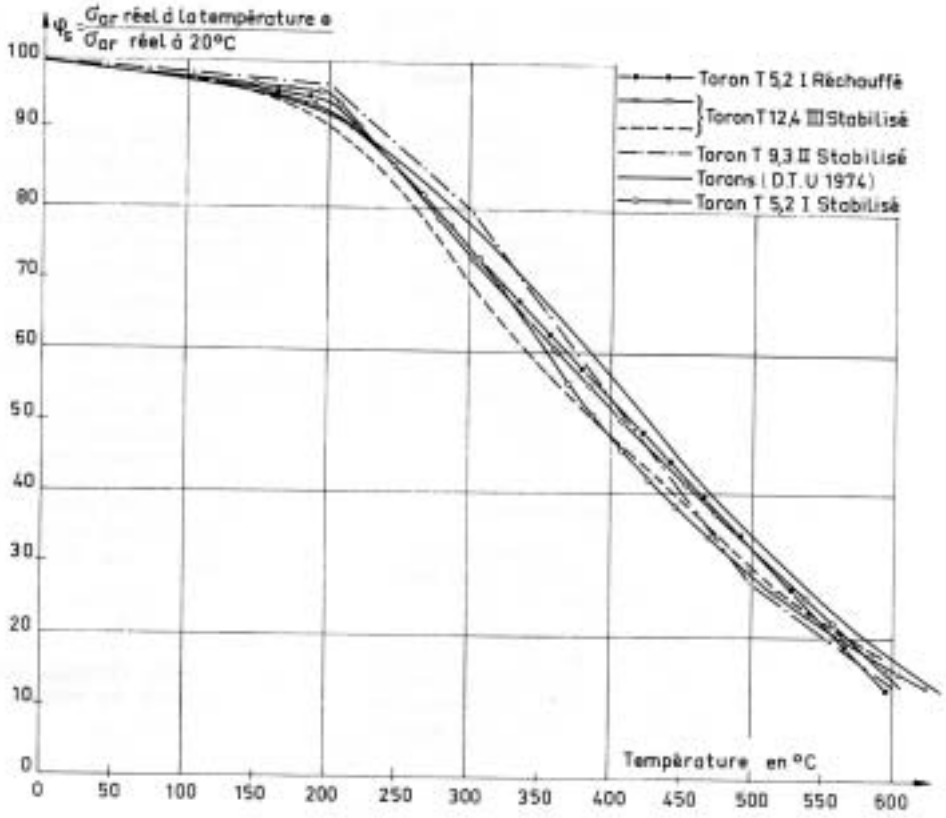

Fig. 4. — **Affaiblissement des aciers de précontrainte en fonction de la température (rapporté aux charges de rupture réelles) : résultats expérimentaux.**

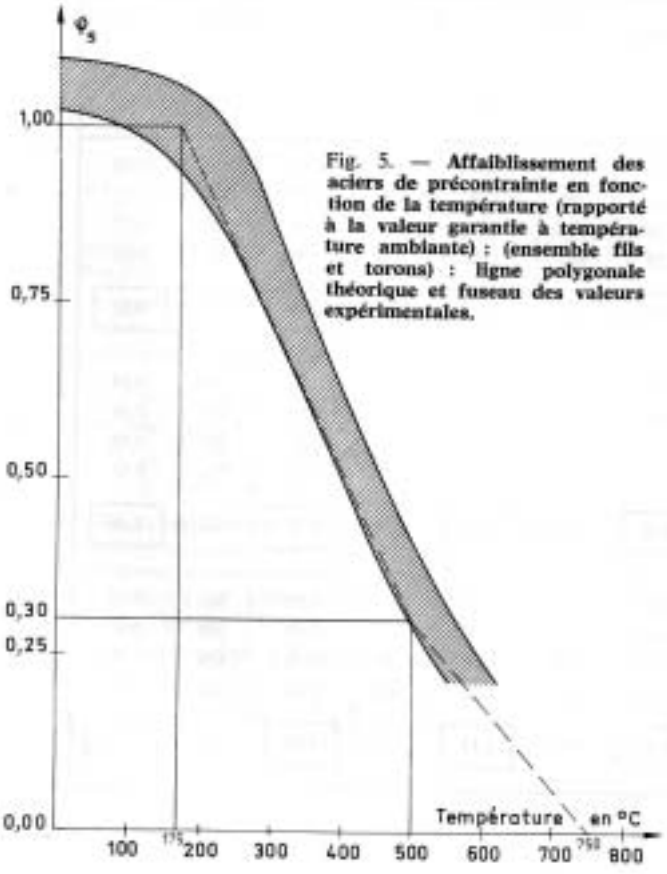

Fig. 5. — **Affaiblissement des aciers de précontrainte en fonction de la température (rapporté à la valeur garantie à température ambiante) : (ensemble fils et torons) : ligne polygonale théorique et fuseau des valeurs expérimentales.**

La partie du fuseau située légèrement en dessous de la ligne polygonale entre 400 °C et 500 °C ne correspond qu'à un très faible pourcentage (3 à 4 %) des divers types d'aciers de précontrainte commercialisés en 1979.

On accepta de conserver ces mêmes valeurs, à défaut de justifications particulières, pour les aciers laminés, moins courants sur le marché, pour lesquels aucun résultat d'essai nouveau n'avait été présenté à la Commission d'Etude depuis 1972.

2. Aciers pour béton armé

Les valeurs d'affaiblissement de la résistance en traction des aciers pour béton armé en fonction de la température, indiqués dans les DTU de mai 1972 et d'octobre 1974, n'avaient pas été remises en cause par les divers essais d'ouvrages en béton effectués depuis.

Toutefois, dès qu'une méthodologie d'essai fut établie et que les valeurs pour les aciers de précontrainte furent actualisées, la Commission d'Etude demanda aux sidérurgistes de proposer un programme d'essais pour actualiser celles des aciers pour béton armé.

La Société SACILOR, représentant l'Association Technique de la Sidérurgie, confia à l'IRSID (*) la réalisation d'un programme d'essais, en 1979, portant sur les aciers des types 1 et 2 selon la méthodologie adoptée pour les aciers de précontrainte en 1976.

(*) IRSID : Institut de Recherche de la Sidérurgie Française, 78105 Saint-Germain-en-Laye Cédex, tél. 451.24.01.

Rappel des définitions de la norme NF A 35-016 relative aux aciers à haute adhérence pour béton armé.

Type 1 : Armatures à haute adhérence obtenues par laminage à chaud d'un acier naturellement dur (ou trempe et autorevenu d'un acier doux).

Type 2 : Armatures à haute adhérence obtenues par laminage à chaud suivi d'un écrouissage sans réduction de section (par exemple, torsion ou traction).

Type 3 : Armatures à haute adhérence obtenues par laminage à chaud suivi d'un tréfilage et (ou) laminage à froid entraînant une forte réduction de section.

Type 4 : Treillis soudés.

Les premiers résultats furent communiqués à la Commission d'Etude fin 1979. Ils permirent de mettre en évidence, pour **les aciers des types 1 et 2 :**

- à température ambiante, un écart moins grand qu'on aurait pu le craindre entre les résultats sur ronds et ceux sur les éprouvettes usinées, ce qui permet de supposer une bonne représentativité des essais à chaud sur les éprouvettes usinées utilisées ;
- à 300 °C, un léger durcissement.
- à 500 °C, une chute de la résistance aux environs des deux tiers de la résistance à température ambiante.

La synthèse des essais fut communiquée à la Commission d'Etude lors de sa réunion du 25 mars 1980. Des essais complémentaires à 650 °C avaient été effectués.

La tableau I et les diagrammes de la figure 6 résument les résultats pour trois catégories d'aciers :

- type 1 (naturellement dur) : acier « Alpa » ;
- type 1 (trempé-revenu) : acier « Torsid » ;
- type 2 (écroui par torsion) : acier « Tor ».

De l'ensemble de ces résultats, on a pu dégager les observations suivantes :

- à 300 °C, le raffermissement des valeurs de rupture est un peu plus important pour les aciers non écrouis, ceux-ci ayant par contre une meilleure tenue de la limite d'élasticité. Une appréciation plus précise du phénomène nécessiterait une exploration plus fine de la plage 20 °C - 300 °C ;
- à 500 °C, tous les aciers testés présentent des rapports $\frac{\sigma_{e\,500}}{\sigma_{e\,20}}$ et $\frac{\sigma_{sr\,500}}{\sigma_{sr\,20}}$ très groupés, entre 0.60 et 0.67 ;
- les valeurs obtenues sont dans l'ensemble cohérentes avec les valeurs du DTU d'octobre 1974 (art. 3.211).

TABLEAU I

Aciers Fe E40 ; Récapitulation des résultats

Type de rond	Ø (mm)	Essais à 20 °C		Essai à 300 °C				Essai à 500 °C			
		R_e	R_m	R_e	r_e	R_m	r_m	R_e	r_e	R_m	r_m
Naturellement dur (acier ALPA)	20	435	690	350	0.80	765	1.11	280	0.64	470	0.68
	16	445	710	365	0.82	770	1.08	320	0.72	475	0.67
	12	465	705	365	0.78	785	1.11	320	0.69	500	0.71
	8	520	775	400	0.77	845	1.09	315	0.60	490	0.63
Moyenne		465	720	370	**0.79**	791	**1.10**	309	**0.66**	484	**0.67**
TOR (écroui par torsion)	20	420	500	375	0.89	500	1.00	295	0.70	338	0.68
	16	445	520	405	0.91	530	1.02	265	0.59	305	0.59
	12	420	520	405	0.96	550	1.06	275	0.65	300	0.58
	8	505	560	465	0.92	555	0.99	265	0.52	310	0.55
Moyenne		448	525	412	**0.92**	534	**1.02**	275	**0.61**	318	**0.60**
TORSID (trempé-revenu)	20	450	570	385	0.85	650	1.14	265	0.59	365	0.64
	16	500	580	425	0.85	635	1.09	305	0.61	360	0.62
	12	490	560	380	0.77	610	1.09	285	0.58	325	0.58
	10	495	560	415	0.84	650	1.16	305	0.62	345	0.62
Moyenne		484	567	401	**0.83**	636	**1.12**	290	**0.60**	349	**0.61**

R_e = limite d'élasticité à 0.2 % (en N/mm²).
$r_e = R_e(\theta)/R_e$ (20 °C)
R_m = résistance (en N/mm²), valeur arrondie.
$r_m = R_m(\theta)/R_m$ (20 °C)

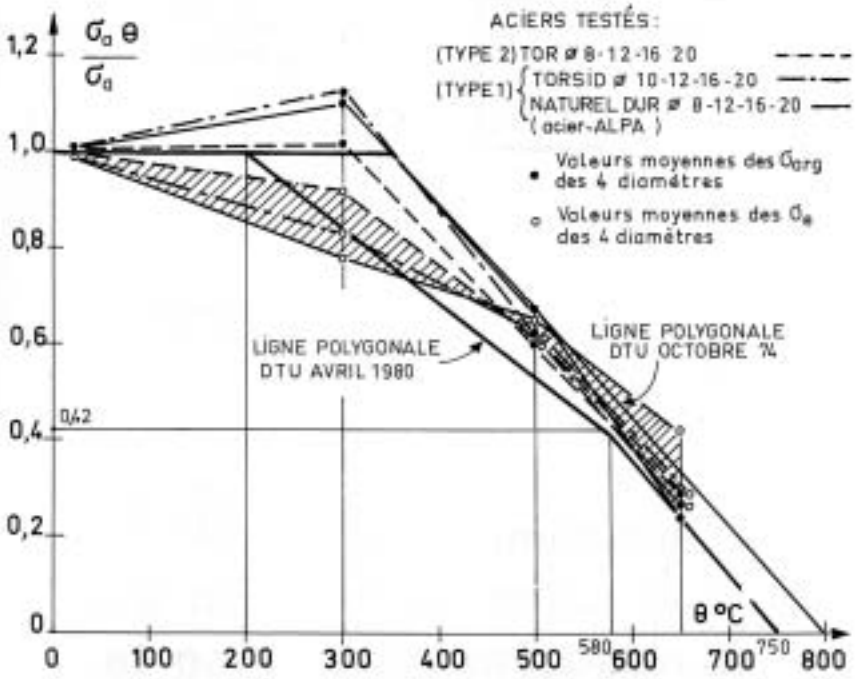

Fig. 6. — **Diagrammes pour aciers de type 1 et 2.**

Pour les aciers doux (Fe E22 et Fe E24) et les aciers Fe E40 des types 1 et 2, la Commission d'Etude adopta ainsi les valeurs suivantes, dans sa réunion du 25 mars 1980 :

$\varphi_s = 1$ jusqu'à 200 °C ;
$\varphi_s = 0.42$ à 580 °C ;
$\varphi_s = 0$ à 750 °C,

le coefficient d'affaiblissement φ_s étant rapporté aux limites élastiques (contrainte à 0.2 % d'allongement).

On a reproduit sur les diagrammes de la figure 6 les modifications par rapport au DTU de 1974 qui indiquait :

- Pour les ronds lisses (Fe E22 et Fe E24) :
  - $\varphi_s = 1$ jusqu'à 350 °C ;
  - $\varphi_s = 0.5$ à 500 °C ;
  - $\varphi_s = 0$ à 800 °C.
- Pour les aciers Fe E40 à haute adhérence :
  - $\varphi_s = 1$ jusqu'à 350 °C ;
  - $\varphi_s = 0$ à 800 °C.

En ce qui concerne les aciers de type 3, Fe TE 50 (tréfilés) **et les aciers de type 4** (treillis soudé), les résultats d'essais communiqués à la Commission d'Etude par les Aciéries de Chiers-Châtillon-Gorcy, sont présentés sur les figures 7, 8 et 9.

Ils ont conduit à l'adoption d'une ligne polygonale définie par :

$\varphi_s = 1$ jusqu'à 400 °C ;
$\varphi_s = 0.15$ à 580 °C ;
$\varphi_s = 0$ à 750 °C.

(Rappel du DTU de 1974 :
$\varphi_s = 1$ jusqu'à 250 °C ;
$\varphi_s = 0$ à 800 °C).

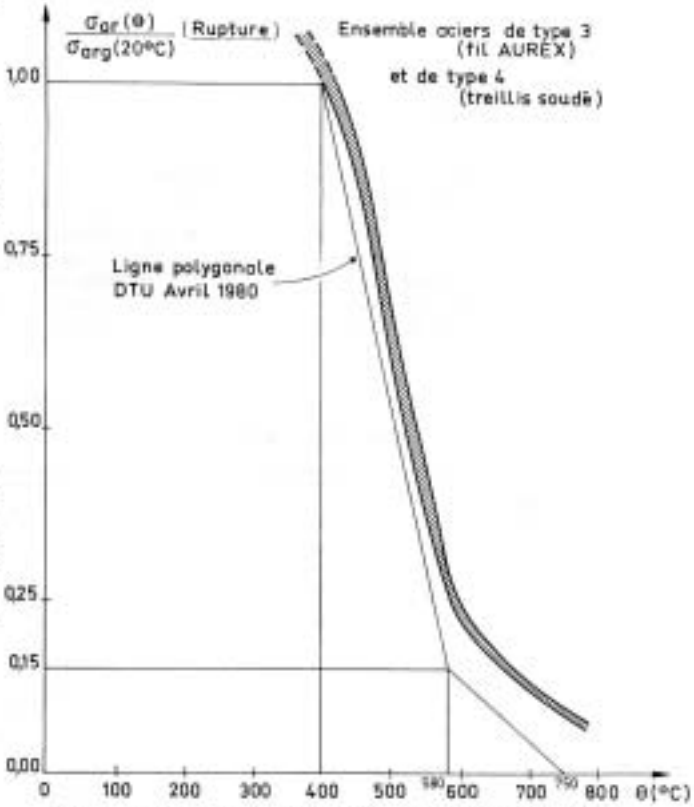

Fig. 7. — **Diagramme pour aciers de type 3 et 4 (rupture).**

63

N° 396 JUILLET-AOUT 1981

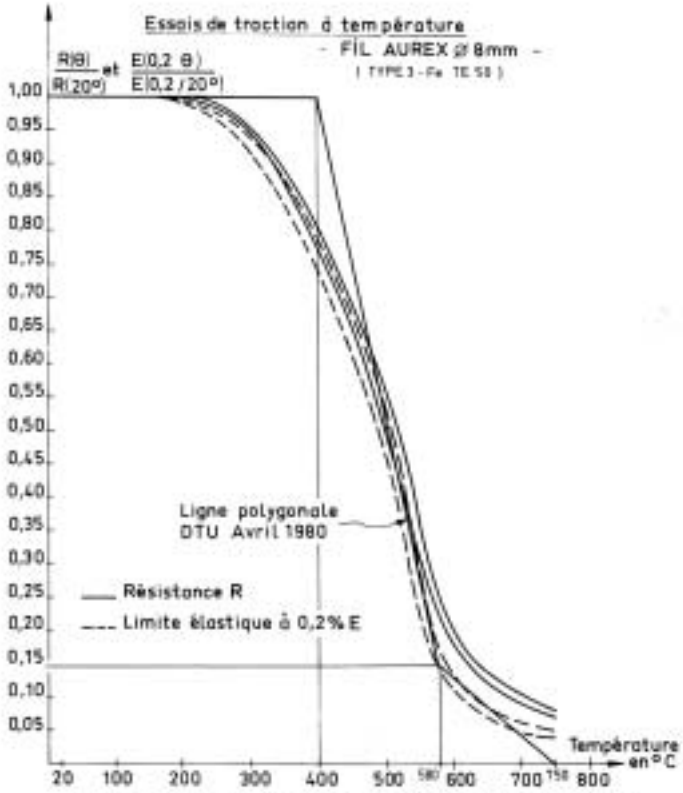

Fig. 8. — **Diagramme pour aciers de type 3 et 4 (limite élastique).**

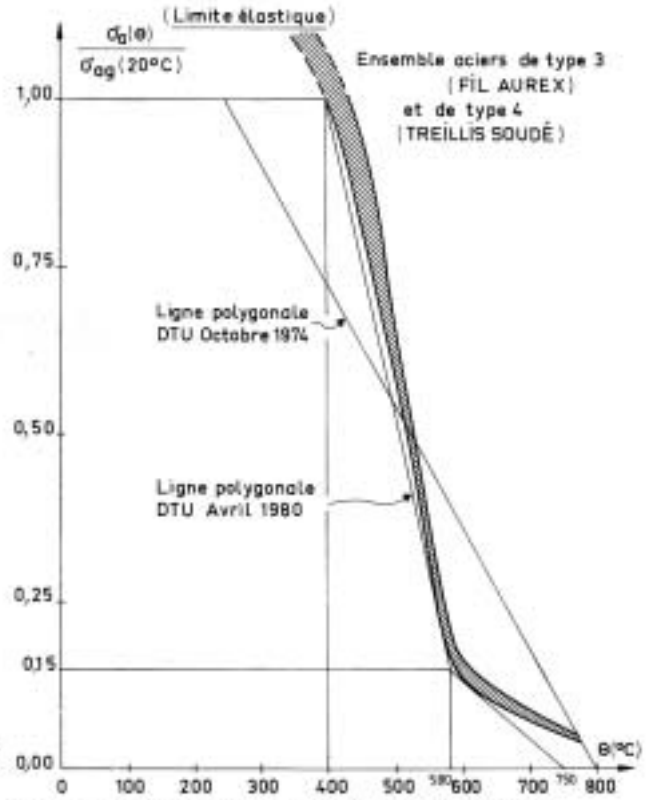

Fig. 9. — **Diagrammes pour un acier de type 3 rapportés l'un à la limite élastique, l'autre à la rupture.**

Les courbes permettent de constater :

- une différence non négligeable entre les φ_e rapportés à la limite élastique et les φ_r rapportés à la rupture ;
- un abaissement des contraintes admissibles à partir de 500 °C par rapport au DTU de 1974.

Rappelons, sur ce dernier point, que cela a conduit, dans un premier temps, la Commission à limiter au degré SF une heure l'application des règles simples pour l'enrobage des armatures en travée des dalles (art. 7 421 du DTU d'avril 1980), le calcul restant possible au-delà.

En tant que fournisseur important de treillis soudés, l'ADETS (1) a pris la décision, au vu de ces valeurs pénalisantes, d'effectuer une campagne d'essais en 1981, selon la méthodologie employée pour les autres aciers. Les résultats qui viennent de nous être communiqués en juin 1981 sont reportés sur le tableau II.

On constate que ces valeurs sont peu différentes de celles du tableau I relatif aux aciers des types 1 et 2 et ne recoupent pas les valeurs adoptées dans le DTU d'avril 1980 pour les aciers des types 3 et 4. Leur prise en compte dans une modification de ce DTU sera soumise à l'examen de la Commision d'Etude lors de sa prochaine réunion.

TABLEAU II

Treillis soudés ADETS (acier Fe TLE 500) (type 4) essais effectués en 1981

⌀	Essai à 20 °C		Essai à 300 °C				Essai à 500 °C			
	R_e	R_m	R_e	r_e	R_m	r_m	R_e	r_e	R_m	r_m
6	632	713	550	0.87	678	0.95	340	0.54	412	0.58
8	592	667	558	0.94	625	0.94	290	0.49	353	0.53
10	512	595	445	0.87	595	1.00	310	0.61	372	0.63
12	604	645	530	0.88	637	0.99	341	0.56	384	0.60
Moyenne	585	655	521	0.89	634	0.97	320	0.55	380	0.58

R_e = limite d'élasticité à 0.2 % (en N/mm²) ; $r_e = \frac{R_e(\theta)}{R_e(20\,°C)}$; R_m = résistance (en N/mm²) ; $r_m = \frac{R_m(\theta)}{R_m(20\,°C)}$.

(1) ADETS : Association Technique pour le Développement de l'Emploi du Treillis Soudé, 2, rue Paul-Cézanne, 75008 Paris. Tél. 562.54.80.

Edité par la S.A.R.L. LE BATIMENT, 6, rue Paul-Valéry, 75116 Paris
NOUVELLES PRESSES DU CENTRE, 87 - LIMOGES — Dépôt légal : 3e trimestre 1981 — Commission Paritaire n° 59.460
Ann. I.T.B.T.P. Le Directeur : J.-C. MALDAGUE

UNIVERSITE DE LIEGE
FACULTE DES SCIENCES APPLIQUEES

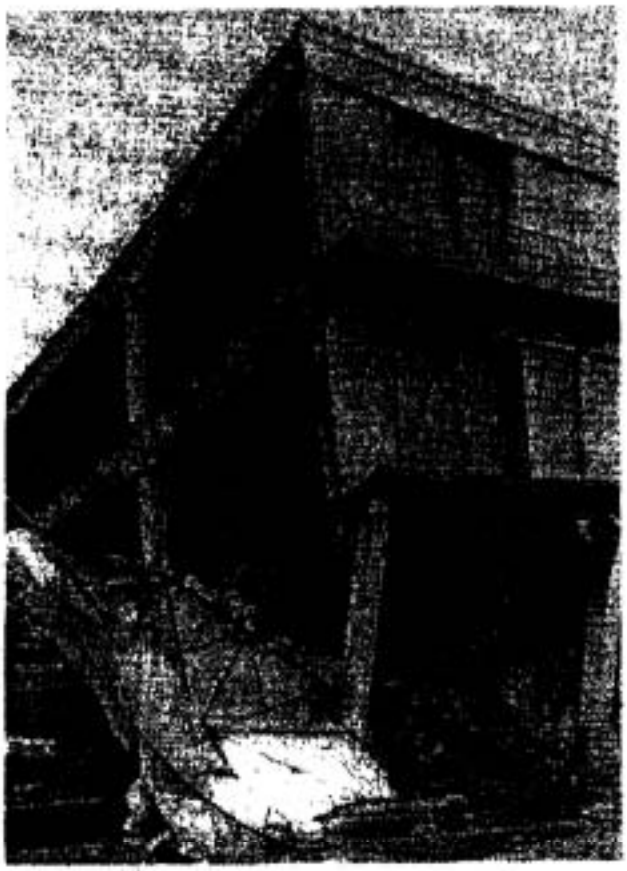

Méthodes numériques pour la simulation du comportement au feu des structures en acier et en béton armé

par
J.-C. DOTREPPE

Chercheur qualifié du F.N.R.S.
Maître de conférences

Thèse présentée en vue de l'obtention
du grade d'Agrégé
de l'Enseignement Supérieur

1980

Il y a une certaine similitude entre ces résultats et ceux obtenus par Magnusson pour des aciers de construction, puisqu'il s'agit dans les deux cas d'aciers à palier. On constate ici aussi qu'entre 300°C et 600°C, le diagramme perd son caractère élastique-parfaitement plastique et devient essentiellement non linéaire. Au-delà de 600°C, on retrouve un palier quasi horizontal.

Les modèles théoriques utilisés ont été définis en supposant que le diagramme (σ, ε) conserve une forme invariable. On admet que la déformation ε_e limitant la zone élastique linéaire ne varie pas en fonction de la température. Elle correspond à $\sigma = R_e$ pour un acier naturel et à $\sigma = 0{,}7\ R_{0.2}$ pour un acier écroui. On admet que la variation de R_e et $R_{0.2}$ en fonction de la température est donnée par le diagramme de la figure 2.34. Comme on peut le voir aux figures 2.37 et 2.38, on a limité les ductilités aux valeurs couramment adoptées, c'est-à-dire 15 % pour les aciers naturels et 10 % pour les aciers écrouis. On suppose que ces limites ne dépendent pas de la température.

Le problème du déchargement se pose dans les mêmes conditions que pour le béton comprimé, et le phénomène à la même allure en traction et en compression. Il faut aussi tenir compte du fait que le module d'élasticité à prendre en compte varie avec la température (cf.figures 2.37 et 2.38).

2.4.3. Aciers de précontrainte.

Bien qu'on n'aborde pas dans ce travail le comportement au feu des éléments en béton précontraint, nous ne pouvons passer sous silence les recherches à caractère fondamental qui ont été exécutées au Laboratoire des Ponts et Charpentes de l'Université de Liège sous la direction de A. (+)[B.13] et K. [B.21] [B.24] Brenneisen.

Les résultats présentés ici ont été obtenus au cours de plusieurs recherches réalisées entre 1973 et 1977. Les essais effectués en 1973 et 1974 ont porté sur un fil de 5 mm. de diamètre, un toron 3 fils de 12,4 mm. de diamètre et un toron de 12,7 mm. de diamètre.

Le programme de recherche prévoyait 3 types d'essais :

1. détermination des caractéristiques mécaniques à température élevée (figure 2.39) ;
2. détermination de la température critique (figure 2.40) ;
3. détermination de la résistance résiduelle d'une armature pour une température et une contrainte initiale données (figure 2.41).

Les essais ont été faits entre 200°C et 500°C ; pour le toron de 3 fils, des températures inférieures à 200°C ont également été envisagées. On présente ici les résultats concernant la contrainte de rupture R_r.

La figure 2.42 donne les résultats relatifs au fil de 5 mm de diamètre. On peut noter :

- la position favorable des points expérimentaux par rapport aux courbes proposées dans les Recommandations FIP-CEB [12] [14] ;
- les valeurs du rapport $\frac{R_r(\theta)}{R_r(20)}$ qui, pour une même température θ, sont plus faibles que dans le cas des aciers de béton armé.

La figure 2.43 donne les résultats d'essais du toron 3 fils. On peut noter ici l'augmentation légère de la résistance pour les températures comprises entre 100°C et 200°C. Il faut d'ailleurs remarquer que cette légère augmentation de résistance n'est pas le seul fait des aciers de précontrainte : elle a aussi été observée pour les aciers de construction et les aciers écrouis de béton armé (cf. figures 2.22 et 2.29.)

Enfin la figure 2.44 reprend les résultats relatifs au toron 12,7 mm. de diamètre.

L'augmentation de résistance qui a été observée pour le toron 3 fils aux températures peu élevées a conduit à un complément d'étude expérimentale au cours de l'année 1976. En effet, dans un élément précontraint, les armatures sont réparties à différents endroits de la section et, par conséquent, l'élévation de température varie d'un fil à l'autre. L'examen de la répartition de la température sur la section droite montre que certaines armatures peuvent atteindre leur température critique, alors que d'autres sont encore à des températures peu élevées. Dans ces conditions, un gain de résistance mécanique à de telles températures peut avoir un effet favorable sur la résistance au feu de la poutre.

I. TRACTION A CHAUD

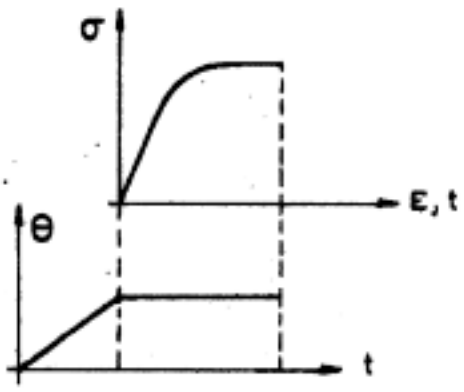

Figure 2.39 : Détermination des caractéristiques mécaniques à température élevée.

II. TEMPERATURE CRITIQUE

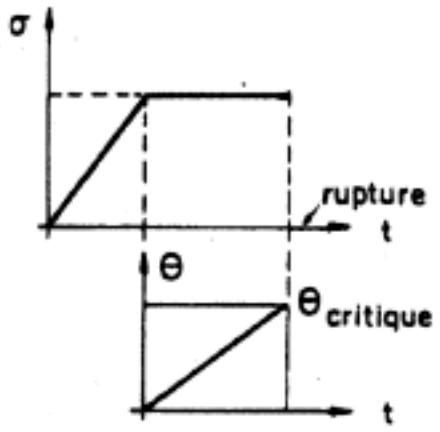

Figure 2.40 : Détermination de la température critique.

III. RESISTANCE RESIDUELLE

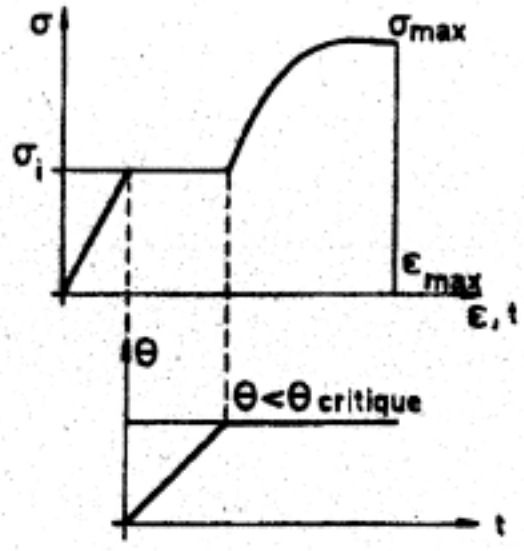

Figure 2.41 : Détermination de la résistance résiduelle d'une armature

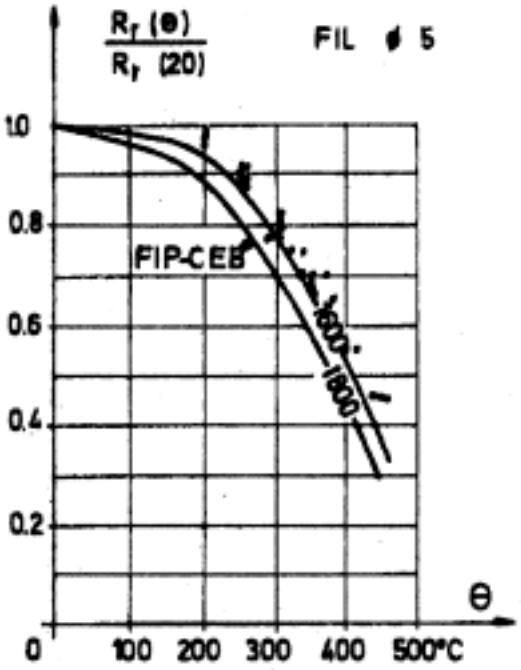

Figure 2.42 : Variation avec la température de la contrainte de rupture d'un fil de précontrainte

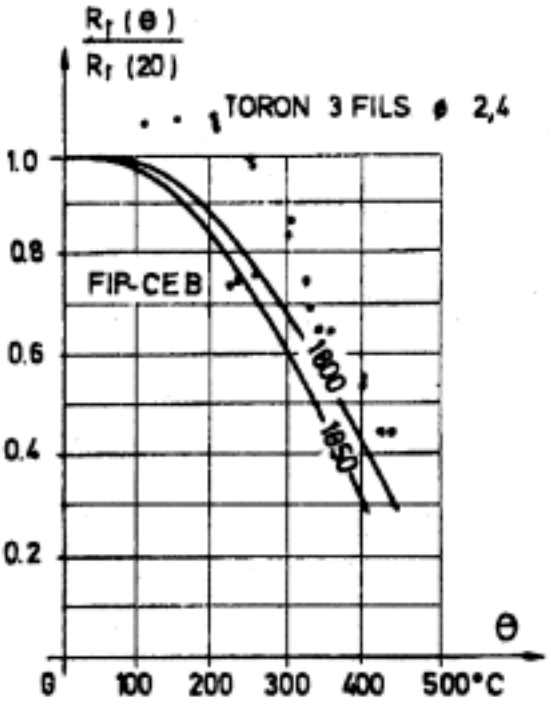

Figure 2.43 : Variation avec la température de la contrainte de rupture d'un toron 3 fils de précontrainte

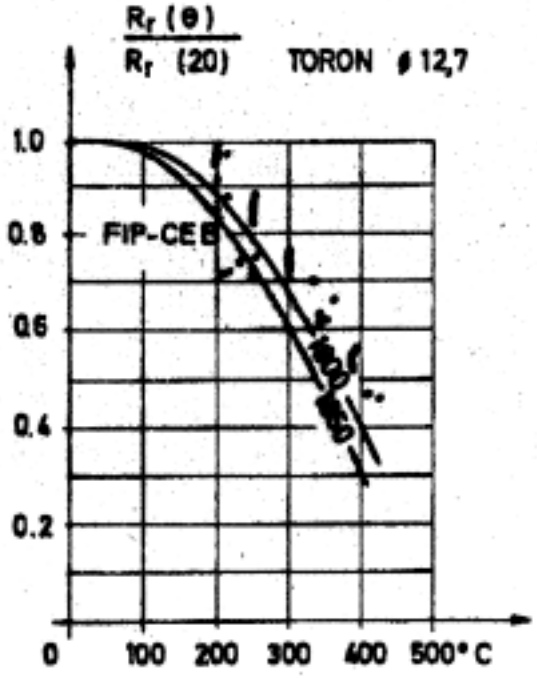

Figure 2.44 : Variation avec la température de la contrainte de rupture

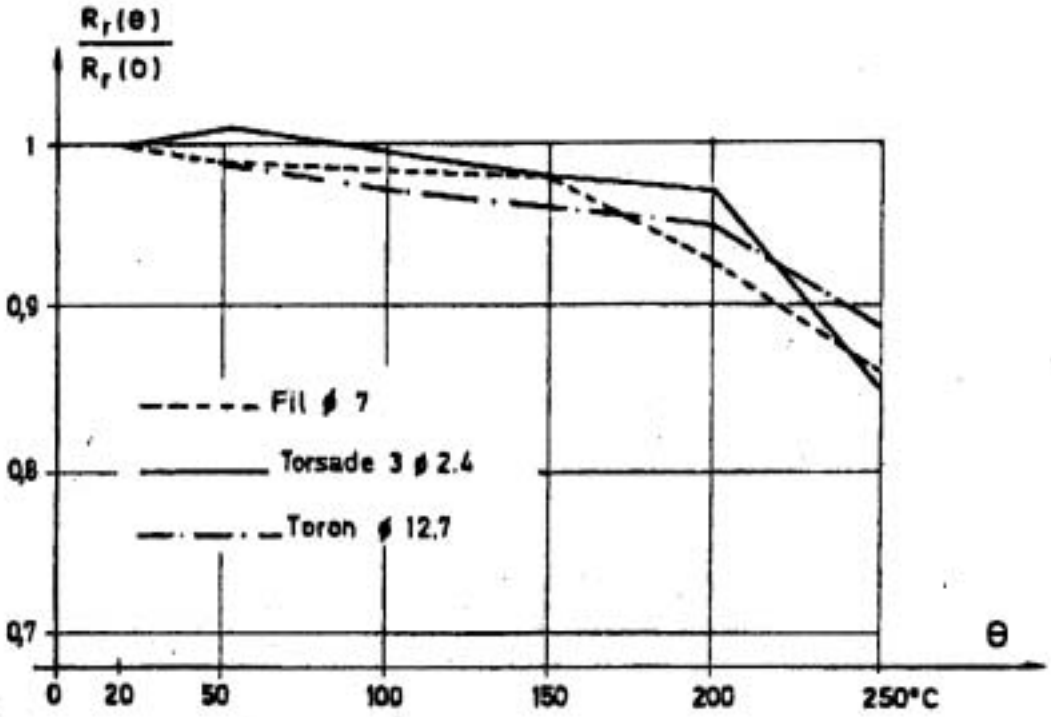

Figure 2.45 : Variation avec la température de la contrainte de rupture des aciers de précontrainte pour des températures modérées.

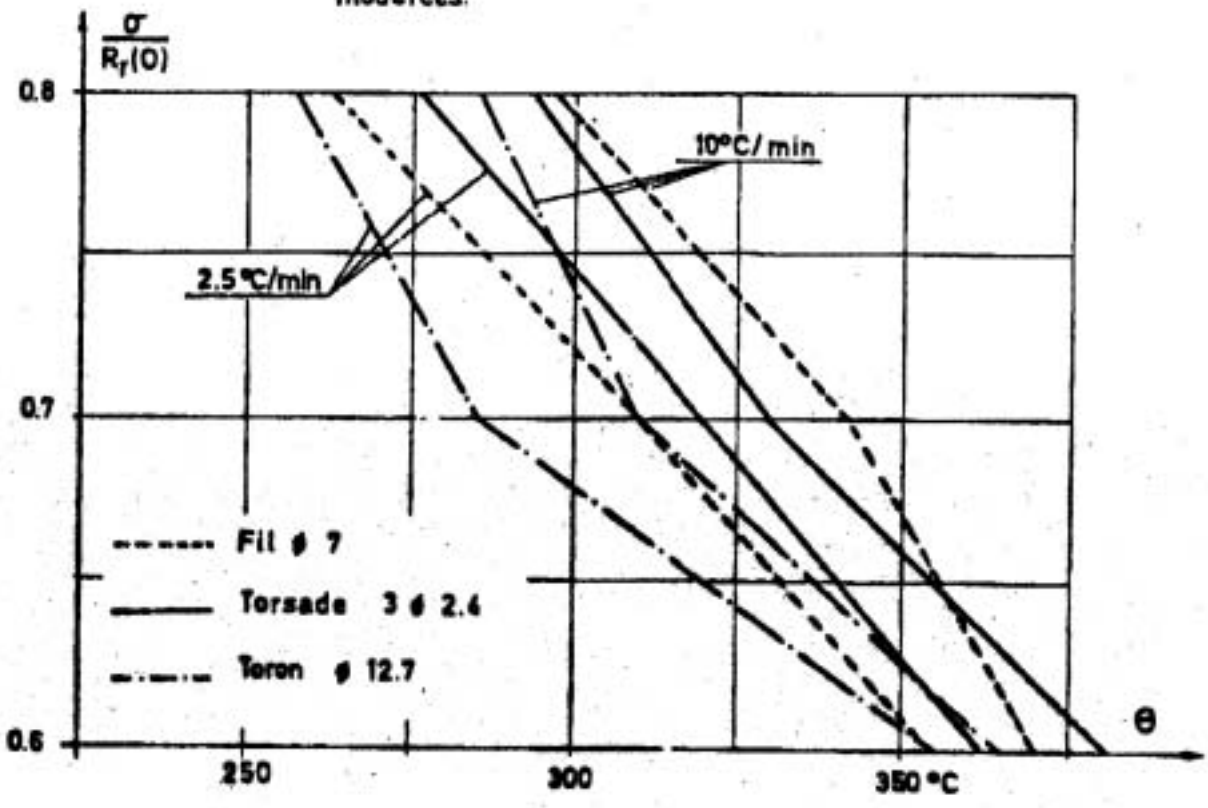

Figure 2.46 : Variation de la température critique des aciers de précontrainte en fonction de la vitesse de chauffage.

Les résultats de cette recherche complémentaire sont représentés à la figure 2.45 Ils montrent qu'il n'y a pas de gain de résistance entre 0 et 200°C. La réduction de résistance est de 5 % environ à 200°C., tandis qu'elle est déjà de 20 % à 300° C.

Un certain nombre de conclusions intéressantes ont aussi pu être dégagées à la lumière de ces travaux.

1. Le fluage est beaucoup plus important aux hautes températures qu'à la température ordinaire.

2. Les allongements de rupture sont sensiblement inférieurs à haute température. Une vérification à la ruine montre qu'ils doivent toutefois garder une certaine valeur si on veut éviter des ruptures prématurées. Les valeurs expérimentales trouvées, soit 3 % au minimum, semblent acceptables.

3. Des essais ont aussi été réalisés en 1976 pour étudier l'influence de la vitesse de chauffage sur la température critique. Deux vitesses différentes ont été adoptées : 2,5 et 10°C/min.On constate(figure 2.46) que l'augmentation de la vitesse de chauffage de 2,5°C/min à 10°C/min. provoque une augmentation de la température critique de 20°C environ pour le fil et le toron, tandis que cette influence est moins nette dans le cas de la torsade. Cette augmentation est sans doute due à une moins bonne uniformisation de la température dans les armatures pour des vitesses de chauffage plus élevées.

4. Il est à souligner également que l'on a observé une parfaite concordance entre les résultats des essais du type 1 (détermination de la contrainte de rupture aux températures élevées) et ceux des essais du type 2 (détermination de la température critique).

On peut ainsi envisager d'adopter un seul essai type pour déterminer l'évolution de la contrainte de rupture. L'essai du type 2 (détermination de la température critique) s'y prête par sa simplicité d'exécution, tandis que l'essai du type 1 (traction à chaud) fournit plus d'informations concernant l'évolution des diverses caractéristiques mécaniques.

BDA 3.9 EN1992-1-2 September 12th 2003

COMMON NEW PROPOSAL FROM THE UNIVERSITY OF LIEGE AND CERIB FOR THE GENERAL AND SIMPLIFIED MODELS OF prEN1992-1-2 FOR THE MECHANICAL PROPERTIES OF PRESTRESSING STEELS (WIRES AND STRANDS) AT ELEVATED TEMPERATURES

For the University of Liège

Ir. Sylvie Majkut
Prof. Jean-Claude Dotreppe

For CERIB

Ir. Fabienne Robert
Ir. André de Chefdebien

1. INTRODUCTION

Some recent comparisons between fire design of prestressed elements according to prEN1992-1-2 and previous ENV1992-1-2 have shown that important changes have been made from previous ENV1992-1-2 to prEN1992-1-2 concerning the mechanical properties of prestressing steel, as the prEN model presents values that are too much on the safe side.

CERIB realised a first draft pointing out the discrepancies existing between the two standards and presenting different test results obtained in Belgium, UK and France. This draft was examined by the University of Liège (ULg), on the request of Tauno Hietanen, Chairman of the Project Team of prEN1992-1-2.

On the 4th of September, a meeting was organised between the representatives of CERIB and ULg and an agreement was found on a common proposal. The two main points on which this new proposal is based are :

- to restore coherence between cold design and hot design (introduction of coefficient β; see hereafter);
- to propose a model based on the ENV1992-1-2 model, slightly modified to present values that are in better agreement with the experimental results.

The aim of this document is to present this common proposal. In section 2 short considerations on the ULS design under normal conditions are given. Section 3 is devoted to a comparison between ENV and prEN simplified models, and experimental results leading to a new model presented in figure A.1 of Annex 1. In section 4 the new common proposal for table 3.3 and figure 4.3 is presented.

The modifications presented here are very important for the designers, whereas they imply minor additional changes. Therefore it is strongly desired to introduce them in the prEN document. If any technical change could no longer be considered, it should become part of the Background Document, and designers should be asked to use it. It should be clearly stated in the document that if one particular country wants to use its own model, this one should be in agreement with experimental results.

2. SHORT CONSIDERATIONS ON THE ULS DESIGN UNDER NORMAL CONDITIONS

For building, the design in bending of prestressed elements is sometimes governed by ULS when tension in concrete or cracking are allowed under service loading. This is the case, for instance, of flooring precast elements like prestressed hollow cores or floor plates.

In prEN1992-1-1, the stress-strain diagram for typical prestressing steel is given in figure 3.9, reproduced here under.

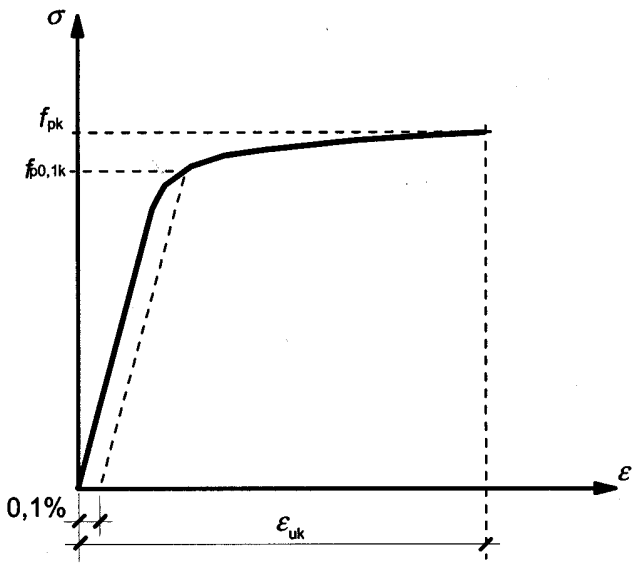

Figure 3.9: Stress-strain diagram for typical prestressing steel (absolute values are shown for tensile stress and strain)

Two models for prestressing steel can be used for the design of cross section (see figure 3.10 of prEN1992-1-1 reproduced below) :

- a "physical" model based on an elastic part followed by an inclined branch reproducing the strain hardening, up to a limited ultimate elongation;
- an "idealised" elasto-plastic model with an horizontal branch without strain limitation.

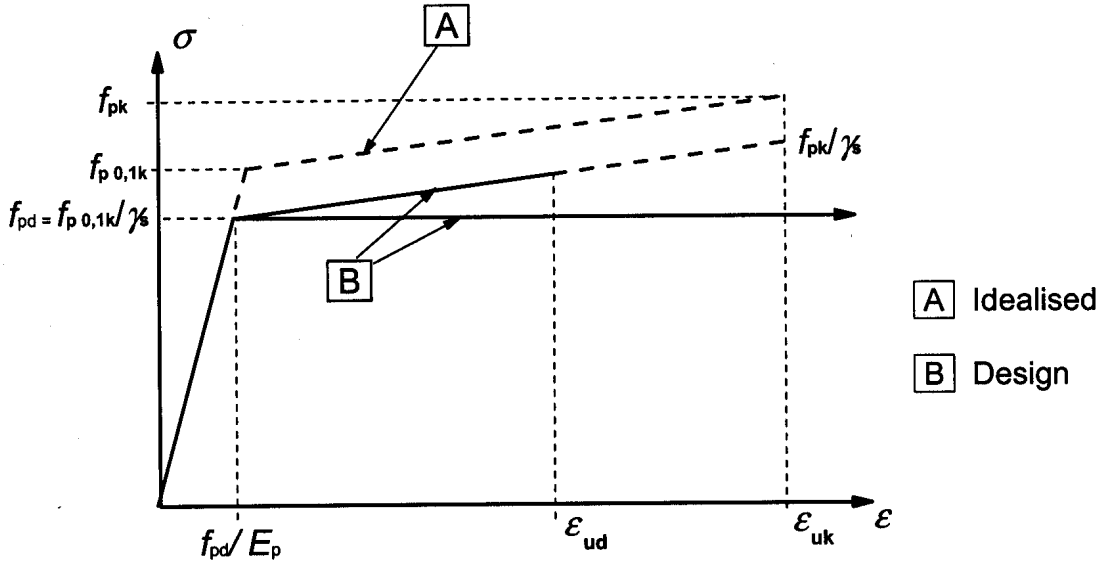

Figure 3.10: Idealised and design stress-strain diagrams for prestressing steel (absolute values are shown for tensile stress and strain)

The first model (with strain hardening, see figure 3.10) was the basic model for prestressing steel in ENV 1992-1-1. It is used preferably in some European countries because it leads to higher cross section performances, with a realistic behaviour model.

The actual stress-strain relationship for prestressing wires and strands (figure 3.9) is obviously more complex than the bilinear curve: around the yielding point the curve is rounded and situated above the simplified inclined branch, while oppositely the maximum strength is reached when the curve becomes very flat for high strain values in the range of 3 to 5 %. In prEN1992-1-1, the design ultimate strain (ε_{ud}, cf. fig 3.10-prEN) - and the associated stress value - shall be defined in a National Annex, with an upper allowable value corresponding to the characteristic strength of the steel f_{pk} (ε_{uk}, cf. fig 3.10-prEN).

In order to maintain consistency between prEN1992-1-1 and prEN1992-1-2 the following model for mechanical properties of prestressing steel at high temperatures has been adopted. It consists in considering the temperature dependent strength reduction factor $k_p(\theta)$ referring to an ultimate strength value used for calculation, chosen at national level between 0,9 f_{pk} and f_{pk} with a mean recommended value 0,95 f_{pk} situated on the safe side (coefficient β in the proposal).

3. COMPARISON BETWEEN MODELS OF ENV1992-1-2 AND prEN1992-1-2, AND EXPERIMENTAL RESULTS

In prEN 1992-1-2, there exist three models allowing the evaluation of the decrease of the mechanical properties of reinforcing and prestressing steels in function of the temperature :

- a sophisticated model (general model) giving the evolution of the stress-strain relationship (figure 3.3-prEN) ;
- a simplified model giving the evolution of the characteristic strength to be used with simplified calculation methods (figure 4.3-prEN) ;
- a simplified model giving the evolution of the critical temperature in function of the stress level to be used for tabulated data (figure 5.1-prEN).

In this document, reference will be made to prestressing steels only.

Since the evolution with temperature of the characteristic strength is not measured by the same experimental procedure as the evolution of the critical temperature in function of the stress level, no additional reference will be made to the critical temperature and attention will only be paid to the models of sections 3 and 4 of prEN.

The simplified model of figure 4.3-prEN for cold worked steels and for quenched and tempered steels has obviously been derived from the general model of figure 3.3-prEN.

Attention was paid to the evolution of the coefficient $k_p(\theta)$ allowing for the decrease of characteristic strength of prestressing steels. Considering the experimental results that were available, a diagram comparing ENV and prEN models with experimental results was built and is presented in Annex 1 (fig. A.1).

Analysing this diagram leads to the following conclusions :

1. the prEN model is in good agreement with experimental results for temperatures in the range of 300-350°C. Between 350°C and 650°C, the prEN model presents values that can be considered too safe ;
2. the ENV model is in better agreement with experimental results for all temperatures, except around 600°C, where the proposed values are too safe.

On the basis of these observations, it is suggested to modify the values given in table 3.3 of prEN for the parameters of the stress-strain relationship of prestressing steels at elevated temperatures. The simplified model of figure 4.3-prEN has of course to be modified in the same way.

CERIB and ULg have agreed to determine the new model in the following way. As the ENV is in better agreement with the test results than the prEN, the proposed values are based on the ENV model. Around 600°C, it is however necessary to modify the ENV curve to come closer to the experimental results. The value at 600°C has been determined on the basis of experimental results published by the French DTU; the proposed value is in fact the mean value of the experimental results at 600°C.

The new curve is presented in Annex 1 (fig A.1.) and is therefore the basis of the new common proposal.

4. NEW COMMON PROPOSAL FROM CERIB AND ULg FOR TABLE 3.3 AND FIGURE 4.3 OF prEN1992-1-2

Below are the two paragraphs that should be changed in prEN1992-1-2 in order to take into account the joint proposal from ULG and CERIB.

"[…]

3.2.4 Prestressing steel

(1) The strength and deformation properties of prestressing steel at elevated temperatures may be obtained by the same mathematical model as that presented in 3.2.3 for reinforcing steel.

(2) Values for the parameters $f_{py,\theta} / (\beta f_{pk})$, $f_{pp,\theta} / (\beta f_{pk})$, $E_{p,\theta}/E_{p,}$ $\varepsilon_{pt,\theta}$ [-],$\varepsilon_{pu,\theta}$ [-] for cold worked (wires and strands) and quenched and tempered (bars) prestressing steel at elevated temperatures are given in Table 3.3. Linear interpolation may be used for intermediate values of the temperature.

Note: The value for the parameter β for use in a particular country may be found in its National Annex, with $0,90 \leq \beta \leq 1,00$. The recommended value is 0,95.

Table 3.3: Values for the parameters of the stress-strain relationship of cold worked (cw) (wires and strands) and quenched and tempered (q & t) (bars) prestressing steel at elevated temperatures

Steel temp.	$f_{py,\theta} / (\beta f_{pk})$		$f_{pp,\theta} / (\beta f_{pk})$		$E_{p,\theta}/E_p$		$\varepsilon_{pt,\theta}$ [-]	$\varepsilon_{pu,\theta}$ [-]
θ [°C]	cw	q & t	cw	q & t	cw	q & t	cw, q&t	cw, q&t
1	2	3	4	5	6	7	8	9
20	1,00	1,00	1,00	1,00	1,00	1,00	0,050	0,100
100	1,00	0,98	0,68	0,77	0,98	0,76	0,050	0,100
200	0,87	0,92	0,51	0,62	0,95	0,61	0,050	0,100
300	0,70	0,86	0,32	0,58	0,88	0,52	0,055	0,105
400	0,50	0,69	0,13	0,52	0,81	0,41	0,060	0,110
500	0,30	0,26	0,07	0,14	0,54	0,20	0,065	0,115
600	0,14	0,21	0,05	0,11	0,41	0,15	0,070	0,120
700	0,06	0,15	0,03	0,09	0,10	0,10	0,075	0,125
800	0,04	0,09	0,02	0,06	0,07	0,06	0,080	0,130
900	0,02	0,04	0,01	0,03	0,03	0,03	0,085	0,135
1000	0,00	0,00	0,00	0,00	0,00	0,00	0,090	0,140
1100	0,00	0,00	0,00	0,00	0,00	0,00	0,095	0,145
1200	0,00	0,00	0,00	0,00	0,00	0,00	0,100	0,150

(3) When considering thermal actions according to EN 1991-1-2 Section 3 (natural fire simulation), particularly when considering the decreasing temperature branch, the values for the stress-strain relationships of prestressing steel specified in (2) may be used as a sufficiently precise approximation.

[...]

4.2.4.3 Steel

[...]

(2) The reduction of the characteristic strength ($\beta\ f_{pk}$) of a prestressing steel as a function of the temperature θ may be taken from Table 3.3, Column 2 for cold worked and Column 3 for quenched and tempered prestressing steel (see Figure 4.3).

Note : See section 3.2.4 for the value of β.

[…]

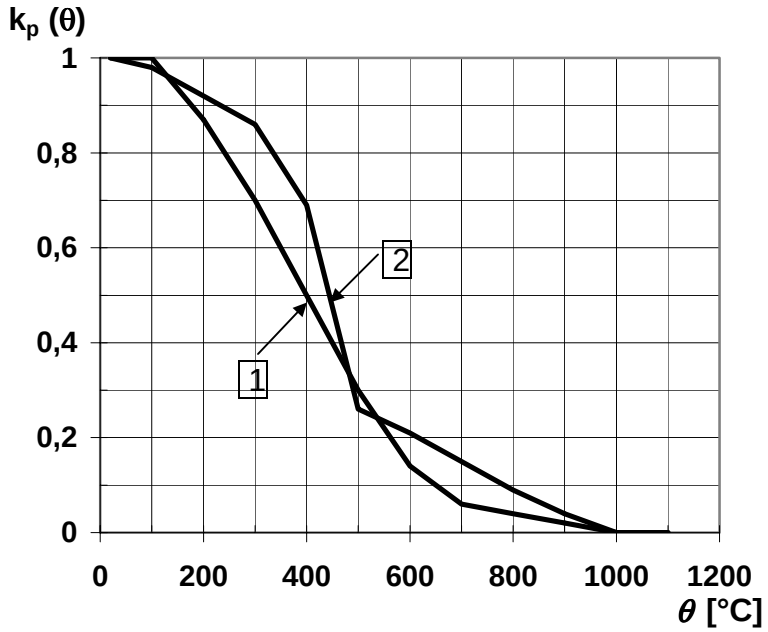

Curve 1 : Cold worked prestressing steel (wires and strands)

Curve 2 : Quenched and tempered prestressing steel (bars)

Figure 4.3 : Coefficient $k_p(\theta)$ allowing for decrease of characteristic strength ($\beta \cdot f_{pk}$) of prestressing steel

[…]

ANNEX 1

Figure A.1 : Coefficient $k_p(\theta)$ allowing for decrease of characteristic strength (βf_{pk}) of prestressing steel

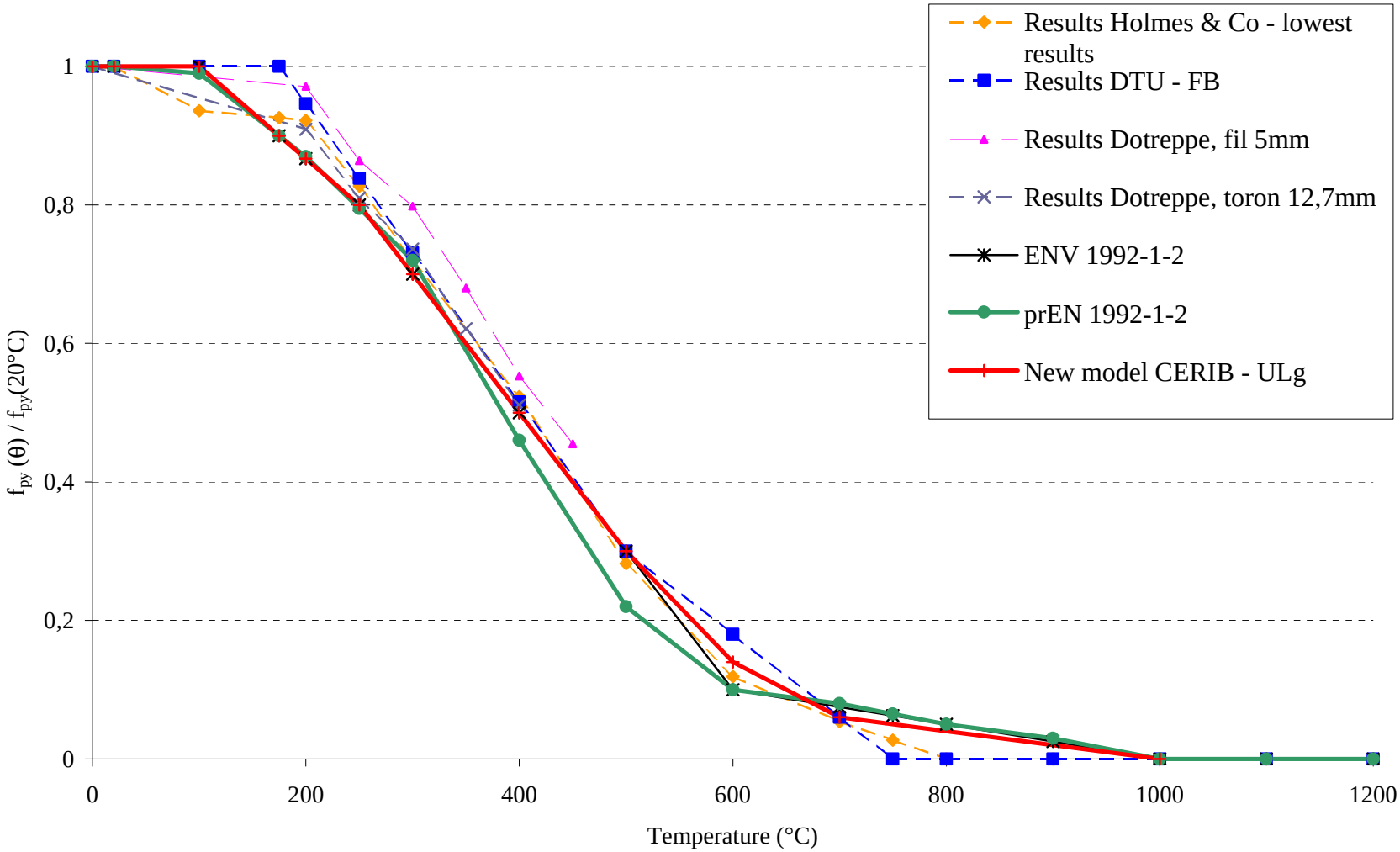

Comparison of fire resistance of columns in Tabulated data to test results

This document consists of updated PT document N 182. Excel sheets are copied as annexes.

In this comparison:

- **prEN method** is **Method B** in EN 1992-1-2
- **NAD1 method** refers to **Belgian NAD** on ENV 1992-1-2. **Method A** in EN 1992-1-2 has been derived from Belgian NAD with introduction of corrective factor $(1+\omega)/(0,85/\alpha_{cc}+\omega)$, see also BDA 5.2
- **NAD2** method is more general calculation method in Belgian NAD on ENV 1992-1-2. It was not included in EN 1992-1-2, as it gives more conservative results than methods A and B.

Comparison of fire resistance of columns according prEN, NAD1, NAD2 versus tests.

You will find below a comprehensive study about the calculation of columns submitted to fire.
It compares the calculated fire resistance of columns (Rf) according to prEN, NAD1, NAD2 with the measured fire resistance of 80 columns tested in fire laboratories. NAD1 refers to the first method according to Belgian NAD, and NAD2 refers to the second method according to Belgian NAD. Here-under, we give the results and conclusions within each focus.

Excel sheets and charts

All the Excel sheets and charts attached are ready for printing. Please do so.

Average values of (Rf calculated / Rf tested)

The ratio (Rf calculated / Rf tested) should approach 1.
Average values:
For application field (74 columns) of the NAD1, the ratio for this method is 0.96.
For application field (51 columns) of the prEN, the ratio for this method is 0.79.
For application field (80 columns) of the NAD2, the ratio for this method is 0.60.
For common application field (51 columns) of the 3 methods, the ratios are
0.94, 0.79, 0.65 respectively for NAD1, prEN, NAD2
The three methods are on the safe side on average (See summary of results on graph below). Additional safety is described below.
The NAD1 method offers a ratio more than 0.15 above the prEN method.
The NAD2 method is the most conservative.

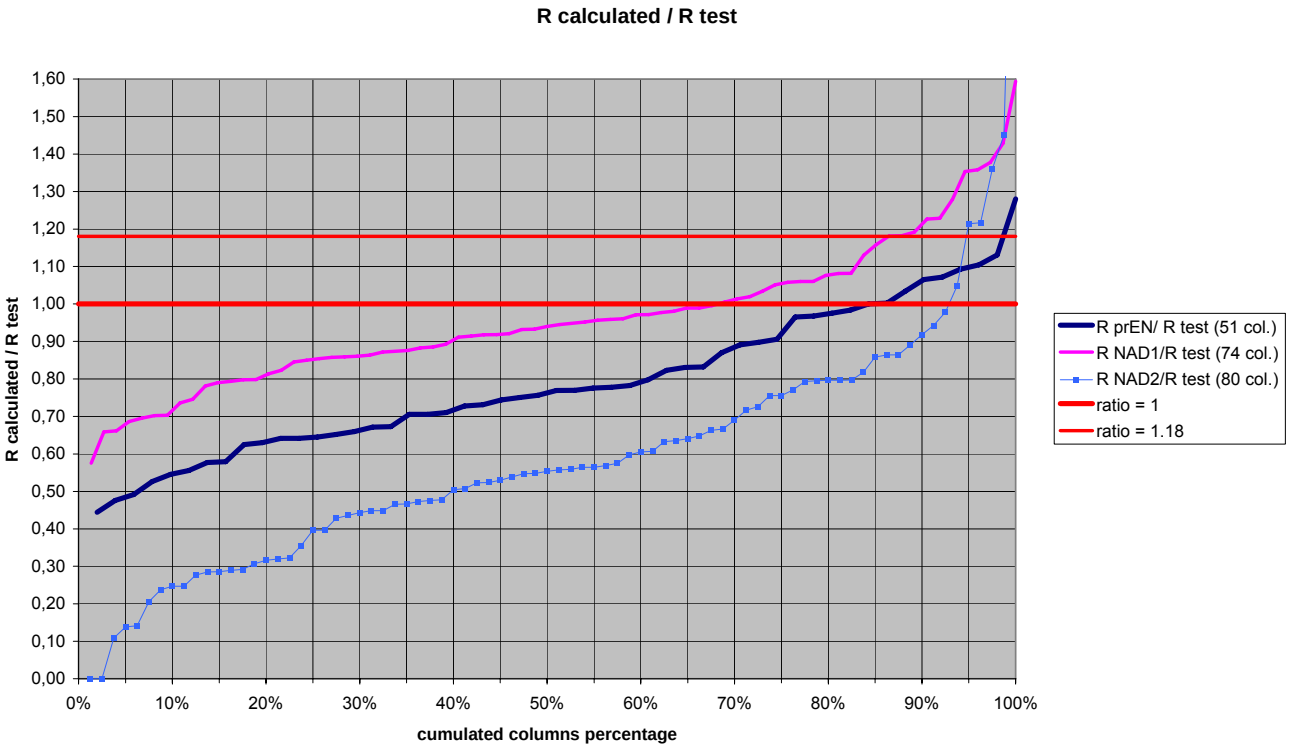

A very important thing to keep in mind follows: The fire resistance has been calculated with the real value of concrete and steel strength for reasons of formula calibration and not with characteristic values for steel and concrete. Let's fix the ideas, and let's assume a 'normal' ratio of 0.75 between fck

(characteristic value) and fcm (mean value) (It means a deviation=0.15). The ratio RNAD1/Rtest has been recalculated using fck = fc,measured/0.75 for the 80 columns. The mean ratio is equal to 0.85. It means that the calculation methods are on the safe side for all the columns with a ratio under 1/0.85=1.18. (For NAD1 88%, for prEN 98% and for NAD2 95% of the columns are on the safe side). This is quite good result considering the large variability of tests.
An additional safety is obtained considering the real resistance reached after, let's say, 3 months:

$f_{ck,90days} = \beta_{cc}(90\ days)*f_{ck,28days} = \pm 1.1*f_{ck,28days}$.

Standard deviations of ratio

Standard deviations for the common application field (51 columns) in comparison with their mean value = STDEV = sqrt($(\Sigma x^2-(\Sigma x)^2) / (n(n-1))$) are respectively 0.178, 0.191, 0.412 for NAD1, prEN and NAD2. These may be regarded as large values, but one must consider that the experimental process has an inherent variability (compare for example the results of tests 11 and 12 in <column tests NAD1.xls!data>).

Slight standard deviations for NAD1 and prEN methods.

Methods application field

For NAD1: 74 columns are in the application field.
The application field of this method has been updated following recent discussions occurring in Belgium. The background is as follows:

The calibration of NAD1 has been carried out successfully on the 80 columns series including 19 tests with reinforcement diam>=25 and 10 tests with e/b>0.25.

For 19 columns with reinforcement diam>=25, 18 results are between 0.74 and 0.99 (this is less than 1,0) and one has a ratio equal to 1.43 with a mean value of 0.92. In fact, 4 tests have already been excluded because they show weak fire resistance due to an increase of spalling. They are not included in the series of the 80 tests.
3 of the 4 tested columns have a large concrete section (300*300 or 400*400) and a weak concrete cover c=25 mm on longitudinal bars. The last one was a 300*300 with c=40 mm.

The following practical recommendation has to appear clearly in the standard text: "Small concrete cover doesn't prevent efficiently from the buckling of large diameter bars (>=25 mm). That is why large bars with small concrete covers are not recommended. Increase rather the number of bars using smaller diameters (<25 mm).

For the 10 columns with a ratio e/b>0.25, 4 columns have a ratio e/b<0.4 results. The 4 tests with e/b=0.32…0.36 give results between 0.92 and 1.05 and a mean value of 0.96. Despite ratios e/b>0.5 (max=0.571), the 6 columns have been considered only for the method calibration (5 results are between 0.81 and 1.36, 1 result is 1.94 and a mean value of 1.23. **The application field of this method has to be mentioned in the standard text: "e/b<=0.4".**
Additional checks (comparison with prEN tables is one possibility) have to be carried out in order to enlarge the application field up to e/b<=0.5.

For prEN : 51 columns lie in the application field. The 29 excluded columns are distributed as follows 11 with lambda>80, 7 with b=/h, 5 with e/b>0.5, 6 with n>0.7.
Among these 51 columns, 23 columns present a limitation of Rf due to interpolation with width greater than 60 cm (see (1) in prEN tables). When including the columns for which the calculated fire resistance is limited by interpolation with column width greater than 60 cm, the ratio (Rf calculated / Rf tested) reaches an average value of 79% as already stated. At the opposite where excluding them, the ratio reaches a average value of 84%.
If we take only the columns where interpolation with width greater than 60 cm, ratio becomes 74%.
For prEN, the 'lambda' and 'n' limitation is not a big problem since it is not a usual situation.
On the contrary, the fact not to be able to calculate **rectangular columns is a strong limitation** be-

cause this type of column is frequent.
Is it possible to give a value of width and cover for the cells in the tables C where notation (1) appears in order to obtain higher calculated Rf?

For NAD2: all the columns lie in the application field.

Limitations and/or calibrations of NAD2 method have to be developed.

Method complexity

For NAD1: The calculation of formulas is very simple.

The greatest difficulty is the assessment of the NRd value. If the slenderness is greater than the critical slenderness 25*(2-e01/e02), the column-model procedure can be applied using either simplified formula (manual calculation) or exact calculation (by program). The problem can also be solved manually using for example tables built for rectangular and circular sections in the bulletin nr123 (1977) of CEB (CEB/FIP Manual of Buckling and Instability). In case of weak slenderness, the problem can be solved manually using for example the diagrams found in design Aids for EC2 handbook (1992). The problem can thus be solved either manually either with a short calculation program (under Excel: see attached <column tests NAD1.xls> for example).

NAD1 has the great advantage that under normal conditions (L<=3m) a simple table can give directly 1 solution without further interpolation . The application of one formula gives directly more accurate results.

For prEN: The accurate prediction of fire resistance implies the extensive use of interpolations, interpolating between up to 128 values to be read among the tables C of prEN comprising a little bit less than 5184 values (9 tables, 6 R, 6 lambda, 4 n different, and 4 values/cell (bmin/a:b/amin)). The parameters between which interpolation has to be carried out are the following ones: lambda, e/b, R, w, n for 2 different values of ‘b’ and 2 different values of ‘a’ associated. Thus interpolation between 2^5*(2+2) = 128 values.
Clearly in the current practice, the problem is clearly not the prediction but the check of a given width and a given cover of a column for a given fire resistance time. Conservative assumptions which also means conservative results!) about parameters can be done in order to accelerate the check, refining the interpolations if necessary. Nevertheless, we can not deny that manual interpolations are fastidious. Again the problem can be solved very efficiently with a short calculation program (under Excel: see attached <column tests prEN.xls>for example).

For NAD2: The manual calculation of formulas is simple requiring no additional tables of diagrams. Again the problem can be solved very efficiently with a short calculation program (under Excel: see attached <column tests NAD2.xls> for example).

Conclusions:
The fire resistance assessment can be solved very efficiently with the help of user-friendly calculation programs for the 3 methods that have to be put at the disposal of designers. The complex manual calculation is a source of mistakes and a loss of time.

Ratio in function of different parameters

All the above analysis has been extracted from the tables and the graphs included in the Excel sheet attached <column comparison prEN, NAD1, NAD2 vs tests.xls>.
The ratios (R calculated / R tested) for the 3 methods are given in charts (named graph xxx) in function of column number, R test, b, a, etafi, L, e/b, lambda, w and n.
The basis of data for graphs is given in the sheet called ‘basis for graph’. The set of columns can be chosen by Autofilter tool namely on Excel sheet columns headed ‘remarks prEN’ and ‘remarks NAD1’ giving the limitations of calculation methods.

Important remarks for NAD1 method application

The ‘etafi’ parameter has to be calculated according to ENV. It means that for NRd estimation the parameter alphacc has to be taken as 0.85 and not 1.00 as in the prEN1992-1-1 otherwise the calculated fire resistance is overestimated approximately of about 10%. This is not acceptable since the safety factor on the ratio is 1.00. NAD1 has been calibrated using ENV and not prEN.

Details about construction of results in Excel sheets.

ULG Excel file > ‘data’ sheet > ‘basis for graph’ sheet > ‘data cumul’ sheet > ‘Graph cumul’ chart
‘interpol’ sheet (for prEN) > ‘data’ sheet
column tests NAD1.xls (for NAD1) > ‘data’ sheet
column tests NAD2.xls (for NAD2) > ‘data’ sheet
‘basis for graph’ > ‘graph xxx’ chart
prEN 1992-1-2 (Final Draft - Dec 2001).pdf > tables C1 to C9.xls > tables C1 to C9 splitted.xls

column comparison prEN, NAD1, NAD2 vs tests.xls with tables C1 to C9 splitted.xls (this last file contains the data for the calculations with ‘column tests prEN.xls!interpol’ sheet).

Note about results with NAD1 method

The calculation of the NRd values with the procedure according to <column tests NAD1.xls!calcul> shows slight differences with the calculation of ULG (See R NAD1 rev / R NAD1 headed column (column AN). A good agreement reached: mean value=0.98, deviation=0.032. In the background document previously distributed under number N169, please note that the label of Y-axis of the figures has to be read as (Rfmeth/Rfexp) and not the contrary. In figure 1, the labels of the X and Y-axis have to be permutated.

Revisions to be done on various documents (prEN, mails, …)

We will send you shortly our comments about revisions to be done on various documents (prEN, mails, …).

Column tests prEN

no	Lab.	N	As	a	b	h	bp	i	L	Ed,fi	R test	circular	w	n	ee+ea	R prEN/ R test	R interpol	b- bmin	a- amin	remarks prEN
1	2	3	4	7	8	9	10	11	12	19	20	27	37	39	41	42	47	48	49	50
			cm²	mm			cm			kN	min.									
1	RUG	31B	8,04	33	30	30	30	8,66	390	950	61	no	0,198	0,556	9,9	0,98	60	58	16	over
2	RUG	31C	8,04	33	30	30	30	8,66	390	622	120	no	0,189	0,351	9,9	1,00	120	8	5	over
3	RUG	31D	8,04	33	30	30	30	8,66	390	220	125	no	0,184	0,121	29,9	1,10	138	15	0	
4	RUG	31E	8,04	33	30	30	30	8,66	390	664	128	no	0,201	0,394	17,9	0,80	102	3	0	
5	RUG	32A	8,04	48	30	30	30	8,66	390	349	123	no	0,183	0,192	29,9	1,07	131	0	12	
6	RUG	34A	16,08	33	30	30	30	8,66	390	370	126	no	0,374	0,178	29,9	1,13	142	23	0	
7	RUG	31F	8,04	33	30	30	30	8,66	390	422	116	no	0,229	0,279	9,9	1,28	148	5	0	
8	RUG	41A	16,08	33	40	40	40	11,55	390	1650	93	no	0,255	0,595	29,9	0,97	90	102	18	over
9	RUG	21A	6,78	31	30	20	24	5,77	390	300	60	no	0,234	0,279	29,9	1,52	91	38	0	b=/h
10	RUG	21B	6,78	31	30	20	24	5,77	390	178	120	no	0,245	0,172	29,9	1,05	126	25	0	b=/h
11	RUG	22A	6,78	41	30	20	24	5,77	390	283	60	no	0,224	0,254	29,9	1,91	114	0	6	b=/h
12	RUG	22B	6,78	41	30	20	24	5,77	390	334	120	no	0,224	0,301	29,9	0,86	104	0	4	b=/h
13	Ulg	31BC	8,04	33	30	30	30	8,66	210	1270	63	no	0,229	0,840	7,2	0,00				n=0,84
14	Ulg	31CC	8,04	33	30	30	30	8,66	210	803	123	no	0,235	0,541	7,2	0,98	120	27	6	over
15	Ulg	21BC	6,78	31	30	20	24	5,77	210	611	107	no	0,237	0,576	7,2	1,08	115	24	0	b=/h
16	Ulg	22BC	6,78	41	30	20	24	5,77	210	620	97	no	0,266	0,641	7,2	1,19	116	1	0	b=/h
17	TUBr	1	18,85	38	30	30	30	8,66	376	710	86	no	0,553	0,452	39,7	0,97	83	20	0	
18	TUBr	2	18,85	38	30	30	30	8,66	376	930	84	no	0,553	0,592	9,7	1,07	90	12	1	over
19	TUBr	3	18,85	38	30	30	30	8,66	376	930	138	no	0,553	0,592	9,7	0,65	90	12	1	over
20	TUBr	4	18,85	38	30	30	30	8,66	476	650	63	no	0,553	0,414	41,9	1,09	69	24	0	
21	TUBr	5	18,85	38	30	30	30	8,66	476	880	108	no	0,553	0,561	11,9	0,56	60	49	8	over
22	TUBr	6	18,85	38	30	30	30	8,66	576	600	61	no	0,553	0,382	44,4	1,00	61	5	0	
23	TUBr	7	18,85	38	30	30	30	8,66	576	800	58	no	0,553	0,510	14,4	1,03	60	24	3	over
24	TUBr	8	12,57	38	20	20	20	5,77	376	420	58	no	0,828	0,511	9,7	0,66	38	0	8	
25	TUBr	9	12,57	38	20	20	20	5,77	376	420	66	no	0,828	0,511	9,7	0,58	38	0	8	
26	TUBr	10	12,57	38	20	20	20	5,77	476	340	48	no	0,828	0,413	11,9	0,00				lambda=82
27	TUBr	11	18,85	38	30	30	30	8,66	476	650	80	no	0,411	0,357	41,9	0,75	60	51	6	over
28	TUBr	12	18,85	38	30	30	30	8,66	476	650	69	no	0,411	0,357	41,9	0,87	60	51	6	over
29	TUBr	13	18,85	38	30	30	30	8,66	476	740	85	no	0,411	0,407	26,9	0,71	60	56	9	over
30	TUBr	14	12,57	38	20	20	20	5,77	476	280	49	no	0,617	0,302	21,9	0,00				lambda=82
31	TUBr	15	12,57	38	20	20	20	5,77	476	240	36	no	0,617	0,259	31,9	0,00				lambda=82
32	TUBr	16	18,85	38	30	30	30	8,66	476	460	75	no	0,411	0,253	101,9	0,78	58	29	0	
33	TUBr	17	18,85	38	30	30	30	8,66	476	362	65	no	0,411	0,199	161,9	0,00				e/b=0,54
34	TUBr	18	12,57	38	20	20	20	5,77	476	170	49	no	0,617	0,183	71,9	0,00				lambda=82
35	TUBr	19	12,57	38	20	20	20	5,77	476	130	53	no	0,617	0,140	111,9	0,00				lambda=82
36	TUBr	20	18,85	38	30	30	30	8,66	266	845	111	no	0,377	0,440	38,2	0,90	100	22	0	
37	TUBr	21	18,85	38	30	30	30	8,66	266	780	125	no	0,344	0,416	58,2	0,67	84	25	0	
38	TUBr	25	12,57	38	20	20	20	5,77	576	208	40	no	0,560	0,220	24,4	0,00				lambda=100
39	TUBr	26	18,85	38	30	30	30	8,66	333,2	735	160	no	0,385	0,411	24,1	0,71	114	0	1	
40	TUBr	27	18,85	38	30	30	30	8,66	333,2	355	89	no	0,344	0,146	159,1	0,00				e/b=0,53
41	TUBr	28	18,85	38	30	30	30	8,66	476	735	93	no	0,433	0,388	16,9	0,65	60	84	15	over
42	TUBr	29	18,85	38	30	30	30	8,66	476	645	135	no	0,321	0,304	22,9	0,44	60	86	15	over
43	TUBr	30	18,85	38	30	30	30	8,66	476	1224	48	no	0,289	0,592	16,9	0,63	30	82	20	over
44	TUBr	31	18,85	38	30	30	30	8,66	376	1695	57	no	0,292	0,738	14,7	0,00				n=0,738
45	TUBr	37	18,85	38	30	30	30	8,66	470	1548	38	no	0,395	0,757	16,8	0,00				n=0,757
46	TUBr	38	18,85	38	30	30	30	8,66	470	970	55	no	0,436	0,510	21,8	0,55	30	121	24	over
47	TUBr	39	18,85	38	30	30	30	8,66	470	1308	57	no	0,456	0,679	21,8	0,53	30	58	16	over
48	TUBr	40	18,85	38	30	30	30	8,66	470	280	49	no	0,436	0,147	161,8	0,00				e/b=0,539
49	TUBr	41	18,85	38	30	30	30	8,66	470	465	50	no	0,456	0,241	161,8	0,00				e/b=0,539
50	TUBr	42	9,24	30	20	20	20	5,77	571	140	31	no	0,348	0,134	114,3	0,00				e/b=0,571
51	TUBr	43	9,24	30	20	20	20	5,77	571	245	40	no	0,346	0,235	24,3	0,00				lambda=99
52	TUBr	44	9,24	30	20	20	20	5,77	571	172	35	no	0,348	0,165	64,3	0,00				lambda=99
53	TUBr	45	9,24	30	20	20	20	5,77	571	175	49	no	0,350	0,167	24,3	0,00				lambda=99
54	TUBr	46	9,24	30	20	20	20	5,77	571	122	52	no	0,352	0,116	64,3	0,00				lambda=99
55	TUBr	47	9,24	30	20	20	20	5,77	571	128	72	no	0,347	0,123	24,3	0,00				lambda=99
56	NRC	I2	20,40	60,75	30,5	30,5	30,5	8,80	190,5	1333	170	no	0,344	0,619	6,9	0,71	120	0	19	over
57	NRC	I3	20,40	60,75	30,5	30,5	30,5	8,80	190,5	800	218	no	0,371	0,393	6,9	0,83	181	0	25	
58	NRC	I4	20,40	60,75	30,5	30,5	30,5	8,80	190,5	711	220	no	0,362	0,343	6,9	0,89	196	0	28	
59	NRC	I6	12,56	58	20,3	20,3	20,3	5,86	190,5	169	180	no	0,415	0,147	6,9	0,82	148	0	23	
60	NRC	I7	20,40	60,75	30,5	30,5	30,5	8,80	190,5	1067	208	no	0,352	0,504	6,9	0,58	120	45	39	over
61	NRC	I8	20,40	60,75	30,5	30,5	30,5	8,80	190,5	1778	146	no	0,365	0,862	6,9	0,00				n=0,862
62	NRC	I9	20,40	60,75	30,5	30,5	30,5	8,80	190,5	1333	187	no	0,332	0,602	6,9	0,64	120	7	21	over
63	NRC	II2	20,40	60,75	30,5	30,5	30,5	8,80	190,5	1044	201	no	0,291	0,427	6,9	0,83	167	0	27	
64	NRC	II3	20,40	60,75	30,5	30,5	30,5	8,80	190,5	916	210	no	0,359	0,439	6,9	0,78	164	0	24	
65	NRC	II4	20,40	60,75	30,5	30,5	30,5	8,80	190,5	1178	227	no	0,240	0,414	6,9	0,76	172	0	29	
66	NRC	II5	20,40	60,75	30,5	30,5	30,5	8,80	190,5	1067	234	no	0,257	0,395	6,9	0,77	180	0	29	
67	NRC	II8	40,90	60,75	30,5	30,5	30,5	8,80	190,5	978	252	no	0,598	0,331	6,9	0,78	196	0	26	
68	NRC	II9	40,90	60,75	30,5	30,5	30,5	8,80	190,5	1333	225	no	0,686	0,491	6,9	0,67	151	0	17	
69	NRC	II10	40,90	60,75	40,6	40,6	40,6	11,72	190,5	2418	262	no	0,370	0,591	6,9	0,73	191	0	18	
70	NRC	II11	65,50	64,15	40,6	40,6	40,6	11,72	190,5	2795	285	no	0,559	0,607	6,9	0,63	180	0	19	
71	NRC	II12	65,50	80,15	40,6	40,6	40,6	11,72	190,5	2978	213	no	0,464	0,572	6,9	0,91	193	0	35	
72	NRC	III1	20,40	60,75	30,5	30,5	30,5	8,80	267	800	242	no	0,321	0,352	8,2	0,74	180	20	33	over
73	NRC	III2	20,40	60,75	30,5	30,5	30,5	8,80	267	1000	220	no	0,324	0,444	8,2	0,73	161	0	25	
74	NRC	III3	20,40	60,75	30,5	30,5	30,5	8,80	381	1000	181	no	0,318	0,438	34,8	0,48	86	0	25	
75	NRC	III5	31,00	59,1	30,5	45,7	36,6	13,19	190,5	1413	356	no	0,283	0,399	6,9	0,50	179	0	26	b=/h
76	NRC	III14	20,40	60,75	30,5	30,5	30,5	8,80	267	1178	183	no	0,335	0,536	18,2	0,49	90	64	35	over
77	Ulg	C1	6,79	44	30	30	30	7,50	210	1260	156	yes	0,104	0,576	7,2	0,77	120	20	19	over
78	Ulg	C2	6,79	44	30	30	30	7,50	210	1770	131	yes	0,104	0,810	7,2	0,00				n=0,810
79	Ulg	C3	18,85	48	30	30	30	7,50	210	1450	187	yes	0,290	0,568	7,2	0,64	120	16	14	over
80	Ulg	C4	18,85	48	30	30	30	7,50	210	1900	163	yes	0,290	0,744	7	0,00				n=0,744

NAD 1

solated columns, assessment of eccentricities ea et e2 according to ENV 1992-1-1: 1991							
Calculation of Nrd and Rf for rectangular section							
données			**result summary**		1/r = 0,007269 M-1	rap =	100 %
no =	1				Nrd = 1763,0 KN	eacier =	-0,076%
dénomi-nation =	RUG31B				Mrd-Msd = 4,976E-08 KNm	eb =	-0,270%
L =	3,9	m	= column buckling length			Rf = 59 min	
L0 =	3,9	m	= column buckling length				
b =	0,3	m	= column width				
h =	0,3	m	= column height (h and lambda values are used to determine L , h is considered as height for reinforced concrete calculation)				
e.01 =	0,000	m	= first order eccentricity at the first extremity				
e.02 =	0,000	m	= first order eccentricity at the second extremity abs(e.02)>=abs(e.01)				
a =	0,033	m	= axis distance				
fc =	33947	KN/M2	= concrete strength				
fy =	576000	KN/M2	= steel yield strength				
As =	0,000804	M2	= reinforcement section				
nbars =	4		= total number of bars				
A.s1 =	4,02E-04	M2	=IF(nbars=6;As/2;(nbars/4+1)/nbars*As)				
A.s2 =	0,00E+00	M2	=As-2*A.s1				
A.s3 =	4,02E-04	M2					
Es =	2,00E+08	KN/M2	= steel elasticity modulus				
gammac =	1,5		= safety factor on concrete				
gammas =	1,15		= safety factor on steel				
alpha =	0,85		= alphacc				
eayes	yes		= yes if ea=additional eccentricity taken into account otherwise no				
correction =	1		= 1 if the concrete is deduced at steel location				
pivot3.7 =	no		= yes if use of pivot at 3/7h otherwise no				
K2simpl =	no		= yes or no				
epsilonb =	0,270%		= maximun strain of concrete allowable				
epsilona =	0,250%		= fyd/Es				
calculs							
Nsd =	1763	KN	= normal force (si >0 then compression)				
ee =	0,000	m	=MAX(0,6*e.02+0,4*e.01;0,4*e.02) = first order equivalent eccentricity				
lambda =	45,0		= L0/(0,289*h)				
lambda-Crit =	25		=if(e.02=0;25;25*(2-e.01/e.02)				
nuMin =	0,00500		=if(lambda<lambdaCrit;1/400;1/200)				
nu =	0,00506		=if(1/(100*SQRT(L))<nuMin;nuMin;1/(100*SQRT(L)))				
ea =	0,0099	m	=if(eayes="yes";nu*L0/2;0) = additionnal eccentricity				
colon-neMod =	conserva-tive		=if(and(lambda<140;or(ee>0,1*h;ee=0,1*h));'yes';'conservative')				
d =	0,267	m	=h-a				
Ac =	0,0900	m2	=b*h				
fyd =	500 870	KN/M2	= fy/gammas				
fcd =	22 631	KN/M2	=fc/gammac				
K.1 =	1		=if(lambda>35;1;if(lambda>15;lambda/20-0,75;0))				
e.2 =	0,011056283	m	=if(lambda<lambdaCrit;0;K.1*(L0*L0/10)*courb				
etot =	0,021	m	= ee+ea+e.2				
Msd =	36,900	KNm	=IF(lambda<lambdaCrit;MAX(Nsd*h/20;Nsd*etot);Nsd*etot)				
etot used =	0,021	m	=Msd/Nsd				
Nrd =	1763	KN					

Mrd =	36,900	KNm	
Mrd-Msd	4,97591E-08	KNm	must be zero to have correct Nrd
Nud =	2134	KN	= alpha*fcd*Ac+fyd*As
Nbal =	815	KN	=0,4f*fcd*Ac
K.2 =	0,281		=if(K2simpl="yes";1;(Nud-Nsd)/(Nud-Nbal))
epsilonyd =	0,002504348		=fyd/Es
1/r selon ENV=	0,005861865	m-1	=2*K.2*epsilonyd/(0,9*d)=courbure
a/h =	0,110		=a/h
w =	0,233		=As*fyd/(Ac*alpha*fc/gammac)
etot/h =	0,070		=Msd/Nsd/h
Diag Value =	0,12		=NRd/(b*h*alpha*fc/gammac) read on interaction diagrams
NRd =	208	KN	= the ultimate normal strength =(DiagValue*b*h*alpha*fc/gammac)
epsilon0 =	-0,16 %		
ndiv =	30		
fb =	19237	KN/M2	= alpha*fcd

Acier	Ai	Yi	ε	σ	Ni	Mi
As1	4,02E-04	0,117	-0,0025	-492024,02	-198	23
As2	0,00	0	-0,0016	-321927,35	0	0
As3	4,02E-04	-0,117	-0,0008	-151830,68	-61	-7
Section de béton						
couche	Ai	Yi	ε	σ		
As1	4,02E-04	0,117	-0,0025	-19236,63	8	-1
As2	0,00	0	-0,0016	-18503,80	0	0
As3	4,02E-04	-0,117	-0,0008	-11831,97	5	1
1	3,00E-03	0,145	-0,0027	-19236,63	-58	8
2	3,00E-03	0,135	-0,0026	-19236,63	-58	8
3	3,00E-03	0,125	-0,0025	-19236,63	-58	7
4	3,00E-03	0,115	-0,0024	-19236,63	-58	7
5	3,00E-03	0,105	-0,0024	-19236,63	-58	6
6	3,00E-03	0,095	-0,0023	-19236,63	-58	5
7	3,00E-03	0,085	-0,0022	-19236,63	-58	5
8	3,00E-03	0,075	-0,0022	-19236,63	-58	4
9	3,00E-03	0,065	-0,0021	-19236,63	-58	4
10	3,00E-03	0,055	-0,0020	-19236,63	-58	3
11	3,00E-03	0,045	-0,0019	-19217,39	-58	3
12	3,00E-03	0,035	-0,0019	-19147,75	-57	2
13	3,00E-03	0,025	-0,0018	-19027,30	-57	1
14	3,00E-03	0,015	-0,0017	-18856,01	-57	1
15	3,00E-03	0,005	-0,0016	-18633,91	-56	0
16	3,00E-03	-0,005	-0,0016	-18360,98	-55	0
17	3,00E-03	-0,015	-0,0015	-18037,23	-54	-1
18	3,00E-03	-0,025	-0,0014	-17662,66	-53	-1
19	3,00E-03	-0,035	-0,0014	-17237,26	-52	-2
20	3,00E-03	-0,045	-0,0013	-16761,04	-50	-2
21	3,00E-03	-0,055	-0,0012	-16234,00	-49	-3
22	3,00E-03	-0,065	-0,0011	-15656,13	-47	-3
23	3,00E-03	-0,075	-0,0011	-15027,45	-45	-3
24	3,00E-03	-0,085	-0,0010	-14347,93	-43	-4
25	3,00E-03	-0,095	-0,0009	-13617,60	-41	-4
26	3,00E-03	-0,105	-0,0008	-12836,44	-39	-4
27	3,00E-03	-0,115	-0,0008	-12004,47	-36	-4
28	3,00E-03	-0,125	-0,0007	-11121,66	-33	-4
29	3,00E-03	-0,135	-0,0006	-10188,04	-31	-4
30	3,00E-03	-0,145	-0,0006	-9203,59	-28	-4
somme =					-1763	37

BDA 5.2 2004-06-02

Background for Tabulated data Method A for columns

This document consist of

- Updated comparison of Method A (Belgian NAD1 method) to test results
- Comments on Background document for Method A (NAD1) in PT N 169
- Background document for Method A (NAD1) = PT document N 169

Comparison between NAD1 rev (based on ENV) , NAD1 new (based on prEN) and R test

Definitions

"R NAD1 rev" notation designates the fire resistance of columns calculated according to the Belgian method based on ENV.

"R NAD1 new" notation designates the fire resistance of columns calculated according to the prEN method A based on prEN1992-1-1(July 2002) for the design in cold situation.

"R test" notation designates the fire resistance of the 74 columns experimentally tested. (Canada, Ghent, Liège, Braunschweig)

Conclusions

The figure shows the excellent concordance between the two methods. The "NAD1 new" uses the prEN1992-1-1 for alphacc, additional eccentricity, procedure for model column and the coefficient

$$\frac{(1.00+\omega)}{(0.85/\alpha_{cc}+\omega)}$$

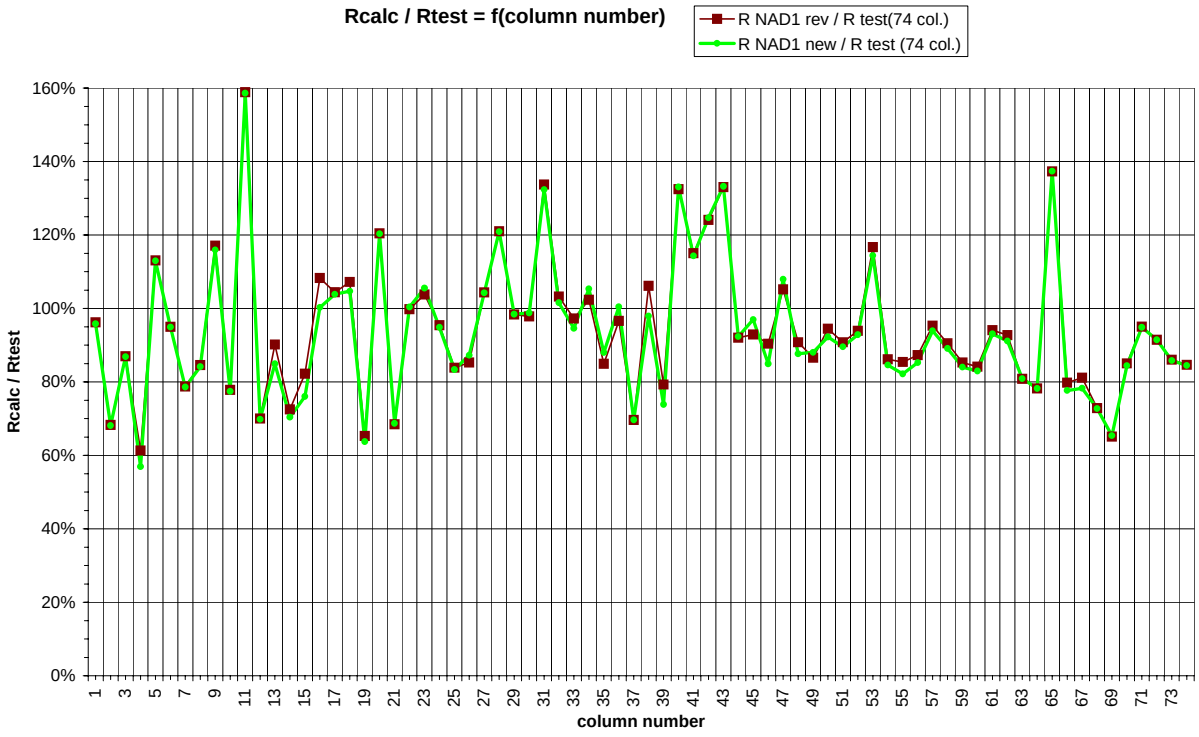

JDF 11-02-2003

COMMENTS

1. Recommendations concerning bars of large diameters.

   1.1. A few (4) unsatisfactory results have only been noticed in tests made in Belgium, and not in other laboratories.

   1.2. We have examined the recommendations proposed in Berlin against the detailing rules of Part 1.1 (see attached document).
   For ϕ = 25 mm, the axis distance for a column in a building will currently be taken as follows :

$$a = c + \Delta c + \phi/2$$
$$= 25 + 10 \text{ (min 5)} + 12.5$$
$$= 47.5 \text{ mm (min 42.5)}$$

Among the 4 Belgian tests, 3 had a = 38 mm and thus were not complying with the recommendations of Part 1.1.

Therefore the recommendations proposed in Berlin appear no longer relevant, and they have been deleted.

2. Jean-François DENOEL and one of my coworkers Pierre STREEL have examined carefully the influence of the value of N_{Rd} calculated according to pr EN1992-1.2 and that calculated according to ENV1992-1.2.

One of the most important differences between the two N_{Rd}'s is related to the fact that the coefficient 0.85 for long term loading has now become 1. We have first examined the problem of a short column centrically loaded which is rather simple. It can be shown easily that in this case a correction coefficient
$(1 + \omega)/(0.85/\alpha_{cc} + \omega)$ has to be introduced.

For a slender column, the problem is more complicated, but the preceding coefficient can be considered as the maximum value of the correction that has to be considered. Therefore we have made the new proposals on the basis of this correction coefficient.

You will see that in formula 5.5, the contribution $R_{\eta fi}$ has been modified consequently.

Table 5.2.1 had also to be modified. There were several ways of doing it. As we had in any case to change some values in the table, we have decided to reconsider all the values proposed. In this way we have been able to keep the same definition for

η^*_{fi} and to keep the same reference values 0.2, 0.5 and 0.7.

On the basis of the preceding considerations, Mr DENOEL and Mr STREEL have analysed 68 columns and have considered the ratio

$$r = R_f (N_{Rd} ; prEN) / R_f (N_{Rd} ; ENV)$$

introducing the coefficient $\frac{(1.00+\omega)}{(0.85/\alpha_{cc}+\omega)}$ in the assessment of $R_{\eta fi}$ for $R_f (N_{Rd} ; prEN)$ calculation.

They have found :
mean value = 99 %
standard deviation = 2.4 %
minimum value = 92 %
maximum value = 104 %

From the attached document, it can be seen that the differences are very small
not only for the whole set of results, but also considering the influence of the various
parameters (width b, axis distance a …..).

Therefore the Belgian method and recommendations remain valid when
N_{Rd} is evaluated according to the recommendations of prEN1992-1.1, provided the correction indicated in formula (5.5) for $R_{\eta fi}$ and the modifications in Table 5.2.1 are made.

3. The two attached documents sent on 29th March, the first one giving an abstract of prEN1992-1.1, and the second one showing various comparisons remain unchanged. The modified values indicated in the second document correspond to R NAD1new.

Faculté des Sciences Appliquées
Génie Civil et Géologie
Mécanique des Matériaux et Structures
J.-M. Franssen, Professeur adjoint, Maître de Recherches F.N.R.S.
16 November 2001

Fire resistance of reinforced concrete columns
Belgian method N°1 (tabulated data)

Background document

$$R_f = 120\left(\frac{R_{f,\eta}+R_{f,a}+R_{f,L}+R_{f,b}+R_{f,n}}{120}\right)^{1.8} \quad (1)$$

where

$$R_{f,\eta} = 83\left(1.00-\eta_{fi}\right) \quad , \qquad \eta_{fi} = N_{d,fi}/R_d \quad (2)$$

$$R_{f,a} = 1.60\left(a-30\right) \quad , \qquad a = \text{axis distance in mm}, \in [25,80] \quad (3)$$

$$R_{f,L} = 9.60\left(5-L\right) \quad , \qquad L = \text{buckling length in m}, \in [2,6] \quad (4)$$

$$R_{f,b} = 0.09\,b' \quad , \qquad b' = \frac{4\times\text{section}}{\text{perimeter}} = \text{Dimension of the section in mm}, \in [200,450] \quad (5)$$

$$R_{f,n} = 12 \quad \text{if more than 4 long. bars are present, 0 otherwise} \quad (6)$$

$h \le 1.5\,b$ in rectangular sections and bar diameter < 25 mm

The procedure for establishing the method has been:

1. Utilisation of a non linear finite element software specifically written for the analysis of structures submitted to the fire (SAFIR) in order to identify the parameters which play a role on the fire resistance. They were found as: length, cover, dimension of the section, number of longitudinal bars, load level.
2. Decision for the analytical function that could represent the influence of each parameter. Linear relationships were chosen for all the parameters, see equation 2 to 6.
3. Creation of a data base of 76 experimental fire test results coming from 4 different laboratories: Liege, Ghent, Ottawa and Braunschweig
4. Verification that the conclusion from steps 1 and 2 were confirmed by the results of the data base.
5. Calibration of the coefficients that are present in the analytical functions based on the results of the data base.

More tests were added later in the data base. For example, four tests on circular columns of H.S.C. were made more recently. They are included in the tables and figures given hereafter, but the method was not recalibrated and modified because the method as it had been established proved to work quite satisfactorily also for these 4 columns.

Table 1 bellow gives all the values of these 76 + 4 = 80 tests.

Table 1

Lab.	N	As	n	a	b1	h	L	fcm	fym	e_{sup}	e_{inf}	e_1	$E_{d,fi}$	Rf exp
		cm²		mm				kN/cm²			cm		kN	min.
RUG	31B	8.04	4	33.00	30	30	390	3.39	57.6	0.0	0.0	0.0	950	61
RUG	31C	8.04	4	33.00	30	30	390	3.54	57.6	0.0	0.0	0.0	622	120
RUG	31D	8.04	4	33.00	30	30	390	3.65	57.6	2.0	2.0	2.0	220	125
RUG	31E	8.04	4	33.00	30	30	390	3.34	57.6	-2.0	2.0	0.8	664	128
RUG	32A	8.04	4	48.00	30	30	390	3.66	57.6	2.0	2.0	2.0	349	123
RUG	34A	16.08	8	33.00	30	30	390	3.59	57.6	2.0	2.0	2.0	370	126
RUG	31F	8.04	4	33.00	30	30	390	2.93	57.6	0.0	0.0	0.0	422	116
RUG	41A	16.08	8	33.00	40	40	390	2.96	57.6	2.0	2.0	2.0	1650	93
RUG	21A	6.78	6	31.00	30	20	390	3.11	49.3	2.0	2.0	2.0	300	60
RUG	21B	6.78	6	31.00	30	20	390	2.96	49.3	2.0	2.0	2.0	178	120
RUG	22A	6.78	6	41.00	30	20	390	3.25	49.3	2.0	2.0	2.0	283	60
RUG	22B	6.78	6	41.00	30	20	390	3.24	49.3	2.0	2.0	2.0	334	120
Ulg	31BC	8.04	4	33.00	30	30	210	2.93	57.6	0.0	0.0	0.0	1270	63
Ulg	31CC	8.04	4	33.00	30	30	210	2.86	57.6	0.0	0.0	0.0	803	123
Ulg	21BC	6.78	6	31.00	30	20	210	3.06	49.3	0.0	0.0	0.0	611	107
Ulg	22BC	6.78	6	41.00	30	20	210	2.73	49.3	0.0	0.0	0.0	620	97
TUBr	1	18.85	6	38.00	30	30	376	2.41	48.7	3.0	3.0	3.0	710	86
TUBr	2	18.85	6	38.00	30	30	376	2.41	48.7	0.0	0.0	0.0	930	84
TUBr	3	18.85	6	38.00	30	30	376	2.41	48.7	0.0	0.0	0.0	930	138
TUBr	4	18.85	6	38.00	30	30	476	2.41	48.7	3.0	3.0	3.0	650	63
TUBr	5	18.85	6	38.00	30	30	476	2.41	48.7	0.0	0.0	0.0	880	108
TUBr	6	18.85	6	38.00	30	30	576	2.41	48.7	3.0	3.0	3.0	600	61
TUBr	7	18.85	6	38.00	30	30	576	2.41	48.7	0.0	0.0	0.0	800	58
TUBr	8	12.57	4	38.00	20	20	376	2.41	48.7	0.0	0.0	0.0	420	58
TUBr	9	12.57	4	38.00	20	20	376	2.41	48.7	0.0	0.0	0.0	420	66
TUBr	10	12.57	4	38.00	20	20	476	2.41	48.7	0.0	0.0	0.0	340	48
TUBr	11	18.85	6	38.00	30	30	476	3.07	46.2	3.0	3.0	3.0	650	80
TUBr	12	18.85	6	38.00	30	30	476	3.07	46.2	3.0	3.0	3.0	650	69
TUBr	13	18.85	6	38.00	30	30	476	3.07	46.2	1.5	1.5	1.5	740	85
TUBr	14	12.57	4	38.00	20	20	476	3.07	46.2	1.0	1.0	1.0	280	49
TUBr	15	12.57	4	38.00	20	20	476	3.07	46.2	2.0	2.0	2.0	240	36
TUBr	16	18.85	6	38.00	30	30	476	3.07	46.2	9.0	9.0	9.0	460	75
TUBr	17	18.85	6	38.00	30	30	476	3.07	46.2	15.0	15.0	15.0	362	65
TUBr	18	12.57	4	38.00	20	20	476	3.07	46.2	6.0	6.0	6.0	170	49
TUBr	19	12.57	4	38.00	20	20	476	3.07	46.2	10.0	10.0	10.0	130	53
TUBr	20	18.85	6	38.00	30	30	266	3.32	45.8	3.0	3.0	3.0	845	111
TUBr	21	18.85	6	38.00	30	30	266	3.32	41.8	5.0	5.0	5.0	780	125
TUBr	25	12.57	4	38.00	20	20	576	3.24	44.3	1.0	1.0	1.0	208	40
TUBr	26	18.85	6	38.00	30	30	333.2	3.07	43.3	1.5	1.5	1.5	735	160
TUBr	27	18.85	6	38.00	30	30	333.2	4.32	54.4	15.0	15.0	15.0	355	89
TUBr	28	18.85	6	38.00	30	30	476	3.15	49.9	-1.5	1.5	0.60	735	93
TUBr	29	18.85	6	38.00	30	30	476	3.82	44.9	-3.0	3.0	1.20	645	135
TUBr	30	18.85	6	38.00	30	30	476	3.82	40.4	0.5	0.5	0.50	1224	48
TUBr	31	18.85	6	38.00	30	30	376	4.23	45.2	0.5	0.5	0.50	1695	57
TUBr	37	18.85	6	38.00	30	30	470	3.49	50.5	0.5	0.5	0.50	1548	38
TUBr	38	18.85	6	38.00	30	30	470	3.15	50.3	1.0	1.0	1.00	970	55
TUBr	39	18.85	6	38.00	30	30	470	3.15	52.6	1.0	1.0	1.00	1308	57
TUBr	40	18.85	6	38.00	30	30	470	3.15	50.3	15.0	15.0	15.00	280	49
TUBr	41	18.85	6	38.00	30	30	470	3.15	52.6	15.0	15.0	15.00	465	50
TUBr	42	9.24	6	30.00	20	20	571	4.15	48.0	10.0	10.0	10.00	140	31
TUBr	43	9.24	6	30.00	20	20	571	4.15	47.7	1.0	1.0	1.00	245	40
TUBr	44	9.24	6	30.00	20	20	571	4.15	48.0	5.0	5.0	5.00	172	35
TUBr	45	9.24	6	30.00	20	20	571	4.15	48.2	1.0	1.0	1.00	175	49
TUBr	46	9.24	6	30.00	20	20	571	4.15	48.5	5.0	5.0	5.00	122	52
TUBr	47	9.24	6	30.00	20	20	571	4.15	47.8	1.0	1.0	1.00	128	72

Lab.	N	As	n	a	b1	h	L	fcm	fym	e_{sup}	e_{inf}	e_1	$E_{d,fi}$	Rf exp
		cm²		mm				kN/cm²			cm		kN	min.
NRC	I2	20.4	4	60.75	30.5	30.5	190.5	3.69	44.4	0.0	0.0	0.00	1333	170
NRC	I3	20.4	4	60.75	30.5	30.5	190.5	3.42	44.4	0.0	0.0	0.00	800	218
NRC	I4	20.4	4	60.75	30.5	30.5	190.5	3.51	44.4	0.0	0.0	0.00	711	220
NRC	I6	12.56	4	58.00	20.3	20.3	190.5	4.23	44.2	0.0	0.0	0.00	169	180
NRC	I7	20.4	4	60.75	30.5	30.5	190.5	3.61	44.4	0.0	0.0	0.00	1067	208
NRC	I8	20.4	4	60.75	30.5	30.5	190.5	3.48	44.4	0.0	0.0	0.00	1778	146
NRC	I9	20.4	4	60.75	30.5	30.5	190.5	3.83	44.4	0.0	0.0	0.00	1333	187
NRC	II2	20.4	4	60.75	30.5	30.5	190.5	4.36	44.4	0.0	0.0	0.00	1044	201
NRC	II3	20.4	4	60.75	30.5	30.5	190.5	3.54	44.4	0.0	0.0	0.00	916	210
NRC	II4	20.4	4	60.75	30.5	30.5	190.5	5.29	44.4	0.0	0.0	0.00	1178	227
NRC	II5	20.4	4	60.75	30.5	30.5	190.5	4.95	44.4	0.0	0.0	0.00	1067	234
NRC	II8	40.9	8	60.75	30.5	30.5	190.5	4.26	44.4	0.0	0.0	0.00	978	252
NRC	II9	40.9	8	60.75	30.5	30.5	190.5	3.71	44.4	0.0	0.0	0.00	1333	225
NRC	II10	40.9	8	60.75	40.6	40.6	190.5	3.88	44.4	0.0	0.0	0.00	2418	262
NRC	II11	65.5	8	64.15	40.6	40.6	190.5	3.84	41.4	0.0	0.0	0.00	2795	285
NRC	II12	65.5	8	80.15	40.6	40.6	190.5	4.62	41.4	0.0	0.0	0.00	2978	213
NRC	III1	20.4	4	60.75	30.5	30.5	267	3.96	44.4	0.0	0.0	0.00	800	242
NRC	III2	20.4	4	60.75	30.5	30.5	267	3.92	44.4	0.0	0.0	0.00	1000	220
NRC	III3	20.4	4	60.75	30.5	30.5	381	3.99	44.4	2.5	2.5	2.50	1000	181
NRC	III5	31	8	59.10	30.5	45.7	190.5	4.25	41.4	0.0	0.0	0.00	1413	356
NRC	III14	20.4	4	60.75	30.5	30.5	267	3.79	44.4	2.5	0.0	1.00	1178	183
Ulg	C1	6.79	6	44.00	30	30	210	6.00	50.0	0.0	0.0	0.0	1260	156
Ulg	C2	6.79	6	44.00	30	30	210	6.00	50.0	0.0	0.0	0.0	1770	131
Ulg	C3	18.85	6	48.00	30	30	210	6.00	50.0	0.0	0.0	0.0	1450	187
Ulg	C4	18.85	6	48.00	30	30	210	6.00	50.0	0.0	0.0	0.0	1900	163

During the calibration process based on the experimental tests:

- Most of the columns were simply supported. If a column had the rotation restricted at one side (as was the case for some of the tests from Braunschweig), then a length of 0.70 L was considered, in the term accounting for the length as well as in the evaluation of R_d which is needed for calculating the load level.
- If an eccentricity e_o was present in the test, R_d was calculated by taking into account this first order eccentricity e_o as well as the accidental eccentricity $e_a = \nu L_0 / 2$ as prescribed by the Eurocode for concrete structures at room temperatures.
- The method of the model column was applied for calculating R_d.
- The load level is based on design strength at room temperature and this one is based on the design strength of materials, $\alpha \frac{f_{c,k}}{\gamma_c}$ for concrete. This is what has to be applied when the model is used in a real design. ***For calibration*** of the model, the measured material properties have of course been used, i.e. $\alpha \frac{f_{c,m}}{\gamma_c}$ for concrete. This means that, when the model is used in a design, an additional safety margin is added in the 95% of the cases where $f_{c,m} > f_{c,k}$.

Table 2 gives the values as calculated by the model after calibration.

Table 2

			η	b	a	L	e	n	
Nrd	η	120	83	0.9	1.6	9.6	0		
kN		1.8	1	0	30	5	0		Rfmeth/Rfexp
1768	0.537	59	38.4	27.0	4.8	10.6	0.0	0.0	0.97
1830	0.340	82	54.8	27.0	4.8	10.6	0.0	0.0	0.69
1562	0.141	109	71.3	27.0	4.8	10.6	0.0	0.0	0.87
1614	0.411	74	48.9	27.0	4.8	10.6	0.0	0.0	0.58
1520	0.230	139	63.9	27.0	28.8	10.6	0.0	0.0	1.13
1768	0.209	120	65.6	27.0	4.8	10.6	0.0	12.0	0.95
1578	0.267	92	60.8	27.0	4.8	10.6	0.0	0.0	0.79
2677	0.616	79	31.8	36.0	4.8	10.6	0.0	12.0	0.85
631	0.476	71	43.5	21.6	1.6	10.6	0.0	12.0	1.18
608	0.293	94	58.7	21.6	1.6	10.6	0.0	12.0	0.78
601	0.471	96	43.9	21.6	17.6	10.6	0.0	12.0	1.59
598	0.558	84	36.6	21.6	17.6	10.6	0.0	12.0	0.70
1898	0.669	68	27.5	27.0	4.8	27.8	0.0	0.0	1.08
1882	0.427	98	47.6	27.0	4.8	27.8	0.0	0.0	0.80
1215	0.503	94	41.3	21.6	1.6	27.8	0.0	12.0	0.87
1156	0.536	116	38.5	21.6	17.6	27.8	0.0	12.0	1.19
1340	0.530	91	39.0	27.0	12.8	11.9	0.0	12.0	1.06
1753	0.530	91	39.0	27.0	12.8	11.9	0.0	12.0	1.08
1753	0.530	91	39.0	27.0	12.8	11.9	0.0	12.0	0.66
1244	0.523	77	39.6	27.0	12.8	2.3	0.0	12.0	1.23
1629	0.540	75	38.2	27.0	12.8	2.3	0.0	12.0	0.70
1118	0.537	62	38.5	27.0	12.8	-7.3	0.0	12.0	1.02
1474	0.543	61	37.9	27.0	12.8	-7.3	0.0	12.0	1.06
743	0.565	57	36.1	18.0	12.8	11.9	0.0	0.0	0.98
743	0.565	57	36.1	18.0	12.8	11.9	0.0	0.0	0.86
575	0.592	43	33.9	18.0	12.8	2.3	0.0	0.0	0.89
1406	0.462	85	44.6	27.0	12.8	2.3	0.0	12.0	1.06
1406	0.462	85	44.6	27.0	12.8	2.3	0.0	12.0	1.23
1597	0.463	85	44.5	27.0	12.8	2.3	0.0	12.0	1.00
541	0.518	50	40.0	18.0	12.8	2.3	0.0	0.0	1.01
463	0.518	50	40.0	18.0	12.8	2.3	0.0	0.0	1.38
902	0.510	79	40.7	27.0	12.8	2.3	0.0	12.0	1.05
679	0.534	76	38.7	27.0	12.8	2.3	0.0	12.0	1.17
307	0.554	46	37.0	18.0	12.8	2.3	0.0	0.0	0.94
227	0.573	44	35.5	18.0	12.8	2.3	0.0	0.0	0.84
1743	0.485	115	42.8	27.0	12.8	22.5	0.0	12.0	1.03
1458	0.535	108	38.6	27.0	12.8	22.5	0.0	12.0	0.86
415	0.501	40	41.4	18.0	12.8	-7.3	0.0	0.0	1.00
1737	0.423	112	47.9	27.0	12.8	16.0	0.0	12.0	0.70
968	0.367	121	52.6	27.0	12.8	16.0	0.0	12.0	1.36
1809	0.406	92	49.3	27.0	12.8	2.3	0.0	12.0	0.99
1886	0.342	101	54.6	27.0	12.8	2.3	0.0	12.0	0.75
1957	0.625	65	31.1	27.0	12.8	2.3	0.0	12.0	1.36
2348	0.722	67	23.1	27.0	12.8	11.9	0.0	12.0	1.18
1963	0.789	49	17.5	27.0	12.8	2.9	0.0	12.0	1.28
1755	0.553	74	37.1	27.0	12.8	2.9	0.0	12.0	1.35
1776	0.736	54	21.9	27.0	12.8	2.9	0.0	12.0	0.95
715	0.391	95	50.5	27.0	12.8	2.9	0.0	12.0	1.94
727	0.639	64	29.9	27.0	12.8	2.9	0.0	12.0	1.29
206	0.680	25	26.6	18.0	0.0	-6.8	0.0	12.0	0.81
479	0.512	39	40.5	18.0	0.0	-6.8	0.0	12.0	0.97
292	0.588	32	34.2	18.0	0.0	-6.8	0.0	12.0	0.92
479	0.366	53	52.7	18.0	0.0	-6.8	0.0	12.0	1.08
292	0.417	48	48.4	18.0	0.0	-6.8	0.0	12.0	0.92
479	0.267	64	60.8	18.0	0.0	-6.8	0.0	12.0	0.88

			η	b	a	L	e	n	
Nrd	η	120	83	0.9	1.6	9.6	0		
kN		1.8	1	0	30	5	0		Rfmeth/Rfexp
2496	0.534	168	38.7	27.5	49.2	29.7	0.0	0.0	0.99
2364	0.338	203	54.9	27.5	49.2	29.7	0.0	0.0	0.93
2408	0.295	211	58.5	27.5	49.2	29.7	0.0	0.0	0.96
1157	0.146	209	70.9	18.3	44.8	29.7	0.0	0.0	1.16
2456	0.434	186	46.9	27.5	49.2	29.7	0.0	0.0	0.89
2392	0.743	134	21.3	27.5	49.2	29.7	0.0	0.0	0.92
2559	0.521	170	39.8	27.5	49.2	29.7	0.0	0.0	0.91
2813	0.371	197	52.2	27.5	49.2	29.7	0.0	0.0	0.98
2424	0.378	196	51.6	27.5	49.2	29.7	0.0	0.0	0.93
3258	0.362	199	53.0	27.5	49.2	29.7	0.0	0.0	0.88
3095	0.345	202	54.4	27.5	49.2	29.7	0.0	0.0	0.86
3443	0.284	242	59.4	27.5	49.2	29.7	0.0	12.0	0.96
3183	0.419	215	48.2	27.5	49.2	29.7	0.0	12.0	0.96
4933	0.490	223	42.3	36.5	49.2	29.7	0.0	12.0	0.85
5641	0.495	234	41.9	36.5	54.6	29.7	0.0	12.0	0.82
6308	0.472	304	43.8	36.5	80.2	29.7	0.0	12.0	1.43
2623	0.305	193	57.7	27.5	49.2	22.4	0.0	0.0	0.80
2607	0.384	179	51.2	27.5	49.2	22.4	0.0	0.0	0.81
1893	0.528	133	39.1	27.5	49.2	11.4	0.0	0.0	0.74
4053	0.349	236	54.1	32.9	46.6	29.7	0.0	12.0	0.66
2019	0.584	145	34.6	27.5	49.2	22.4	0.0	0.0	0.79
2806	0.449	148	45.7	27.0	22.4	27.8	0.0	12.0	0.95
2806	0.631	120	30.6	27.0	22.4	27.8	0.0	12.0	0.91
3219	0.450	160	45.6	27.0	28.8	27.8	0.0	12.0	0.86
3219	0.590	138	34.0	27.0	28.8	27.8	0.0	12.0	0.84

The average of all the values Rf(model)/Rf(test) is 0.983 (slightly less than 1.00 because of the new 4 tests) and the standard deviation is 0.22. This may be regarded as an important value, but it has to be considered that the experimental process has an inherent variability (compare for example the results of tests 22A and 22B in Table 1).

Figure 1 shows the comparison between the fire resistances calculated by the model and those observed in the tests.

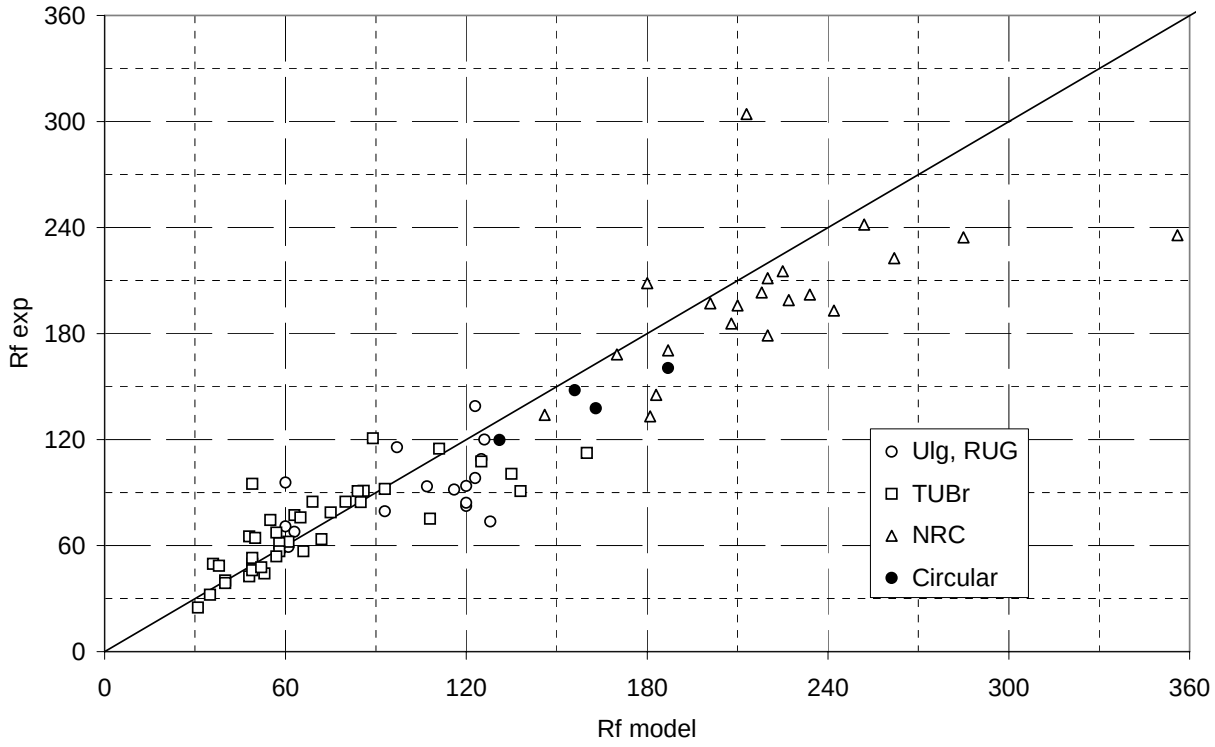

Figure 1

Figure 2 shows the evolution of the ratio Rf(model) / Rf(test) with the load level. The linear regression that is calculated on all the points shows that the safety level is nearly constant; it increases very slightly with the load level.

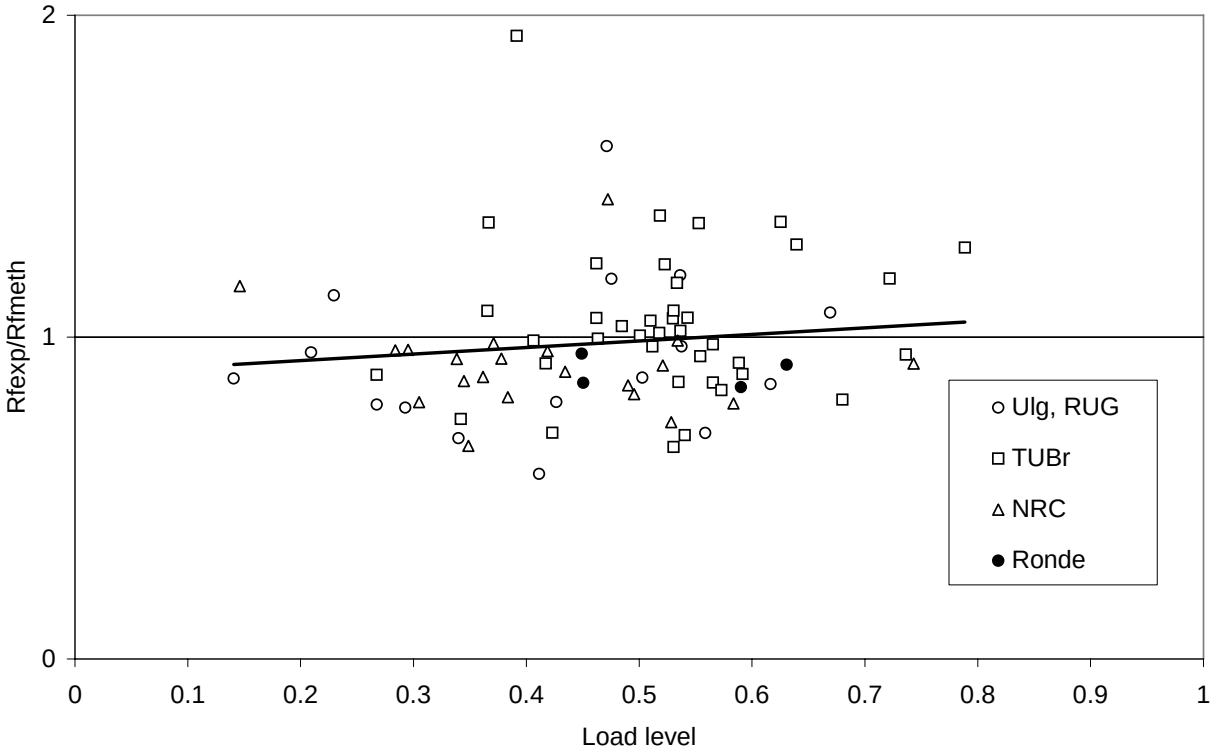

Figure 2

Figure 3 shows the evolution of the ratio Rf(model) / Rf(test) with the concrete cover. The linear regression that is calculated on all the points shows that the safety level is nearly constant; it decreases very slightly with the cover.

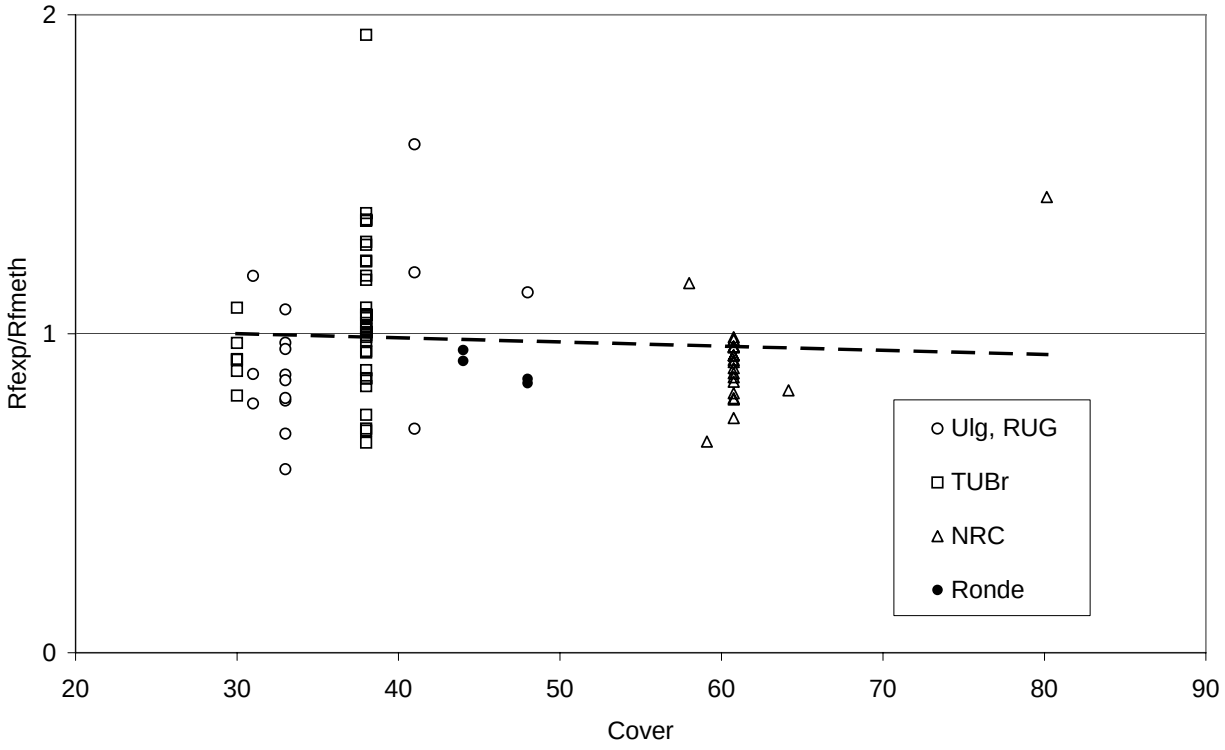

Figure 3

Figure 4 shows the evolution of the safety level with the dimension of the section b'. The linear regression that is calculated on all the points shows that the safety level is nearly constant; it decreases very slightly with b'.

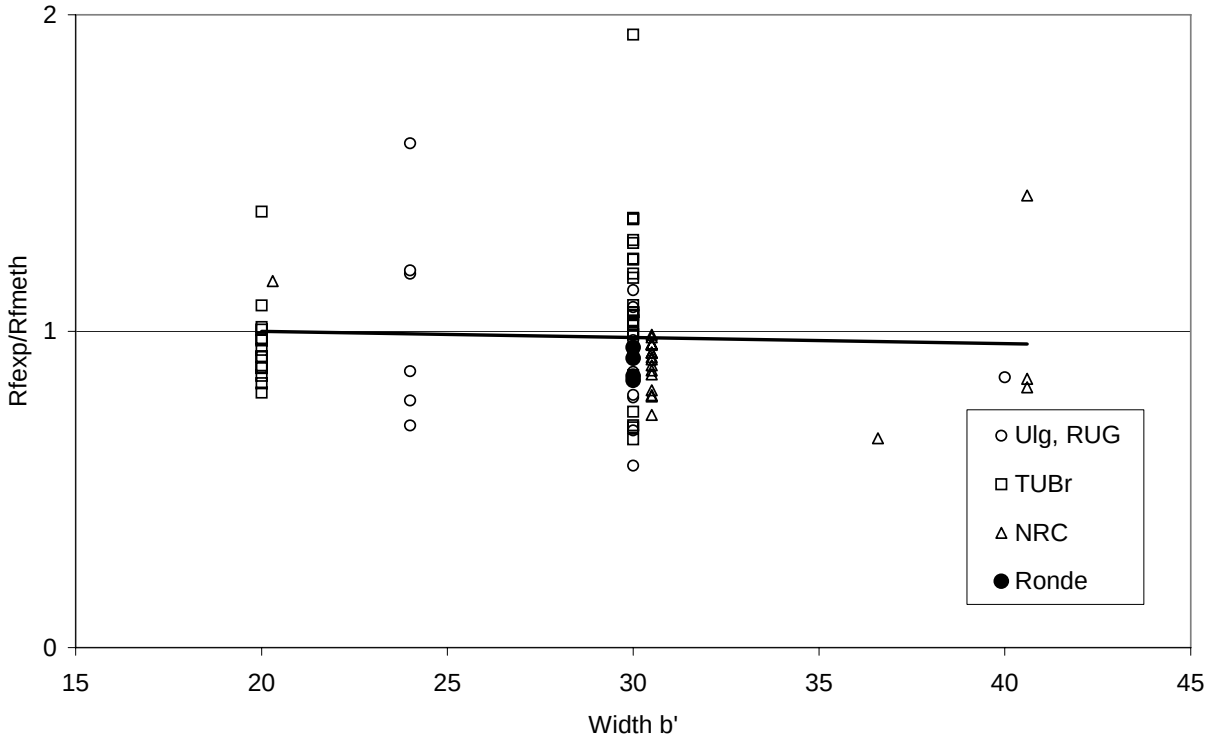

Figure 4

Figure 5 shows the evolution of the ratio Rf(model) / Rf(test) with the buckling length. The linear regression that is calculated on all the points shows that the safety level is nearly constant; it increases slightly with L.

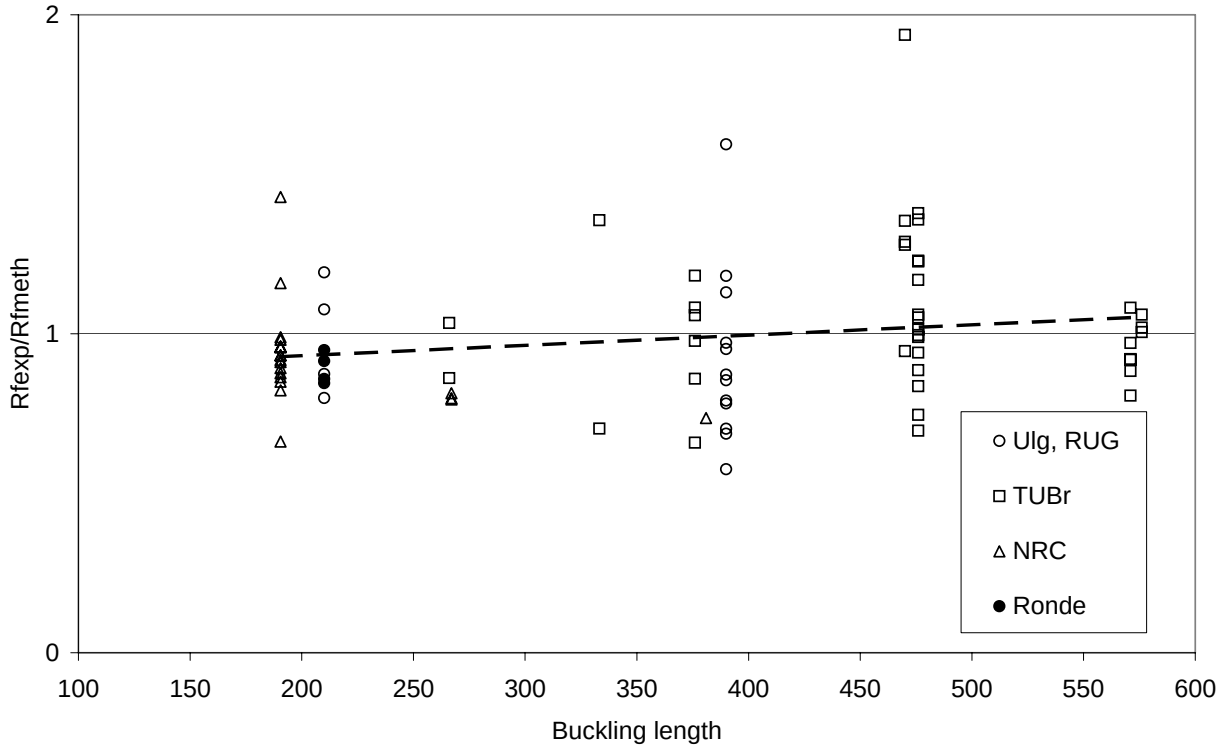

Figure 5

BDA 5.3 2004-07-05

Comparison of Belgian simplified calculation methods and ENV 1992-1-2 Tabulated data to circular column test results

This document has been prepared by Professors Franssen and Dotreppe. Method 1 is Belgian NAD1 and Method 2 is Belgian NAD2, which is not included in EN 1992-1-2, see also BDA 5.1.

FIRE TESTS AND CALCULATION METHODS FOR CIRCULAR CONCRETE COLUMNS

Franssen, J.-M. & Dotreppe, J.-C.
University of Liege, Belgium

Abstract

The introduction sets the scene of the present paper, i.e. the extensive research works performed at the university of Liege in order to derive acceptable calculation methods for the fire design of concrete columns. It is explained that all previous works have been based on square or rectangular cross sections, for which corner spalling was observed very often, whereas circular section are nowadays becoming more and more popular.
In order to examine the influence of the circular shape on the behaviour under fire conditions, an experimental research study has been performed recently at the University of Liege. This paper describes the test procedure, the observations made and the values obtained for the fire resistance. Theoretical methods have been developed for a quick, safe and efficient design of concrete columns under fire conditions. These methods have been applied successfully to the recently tested circular columns.

Key words: *concrete, columns, fire resistance, fire tests, calculation method, spalling, circular section.*

1. Introduction

The behaviour of reinforced concrete columns under fire attack is generally satisfactory. However, sudden spalling is sometimes observed; in such cases, failure may occur prematurely and fire resistance may be reduced substantially. Despite this phenomena, concrete columns must be properly and safely designed under fire conditions. Different approaches can be used in order to design a concrete structure in case of fire:

- Experimental tests has been the first method to be used, but it is limited to simple elements, and it is time consuming and expensive.

- Numerical modelling is nowadays the most sophisticated tool that is available.
- Simple calculation methods are necessary for application to most simple cases in everyday practice.

In fact, the three approaches are related, not so much for their application, but certainly during the creation of the different tools, see figure 1: numerical modelling relies on experimental tests for validation, whereas simple calculation methods are based on the knowledge gained from numerical modelling and are also supposed to yield results that are in good agreement with experimental results.

It is not easy to simulate the behaviour of concrete structures under fire conditions, and moreover consulting engineers do not always have the required kind of numerical tool at their disposal. In order to proceed to a quick and efficient design, it is important to elaborate simplified methods based on analytical formulations. These types of methods are also proposed in FIP-CEB Recommendations and in the European prestandard ENV 1992-1-2 (Eurocode 2-1-2), but they are more appropriate to beams and slabs than to columns.
This is why, in everyday practice, the design of simple concrete columns submitted to fire is traditionally realised by using tabulated data. This procedure has been appearing for long in the FIP/CEB Recommendations dealing with this matter (1). More recently the European Commission for Standardisation (CEN) has published Eurocode 2-Part 1-2, in which various tables of this type are proposed to the designers.

Several research studies have been performed in Belgium, and more particularly at the University of Liege on the fire resistance of concrete columns. It has been quickly realized from comparisons with results of experimental tests that the tabulated data proposed in ENV 1992-1-2 was not satisfactory and, furthermore, had a tendency to yield unsafe results, see Figure 2.

These research studies were thus undertaken in order to improve the calculation methods for the design of concrete columns under fire situations.

In one of them (3) the main parameters affecting the behaviour of reinforced concrete columns at elevated temperatures and their influence on the fire endurance have been examined. This experimental study has been performed at the Universities of Liege and Ghent in Belgium.

As a result, two alternative simplified calculation methods were developed in Liege for the determination of the fire resistance of column subjected to the standard ISO fire. To this purpose, not only the test results from Liege and Ghent have been used (3), but also experimental results from the Technical University of Braunschweig (4) and from the N.R.C. Fire Research Station in Ottawa (5). These two methods are briefly described in (6), while the second (more elaborate) one is developed in detail in (7).

Another experimental investigation has been subsequently performed at the University of Liege on spalling of concrete columns (8,9). With this study and the experimental results obtained in the preceding research works (3), it has been possible to derive conclusions regarding various parameters influencing this phenomenon.

As a whole, 21 test results from N.R.C., 39 from Braunschweig, 24 from Ghent and 4 from Liege were considered in these research works, i.e. a total of 88 test results on full scale columns. Yet, all the preceding tests and studies have been made on columns with square or rectangular cross sections. Due to the development of new types of framework, circular concrete columns are now cheap and easy to build, and they are progressively more and more used. However very few tests under fire conditions have been made on columns with this type of cross section.

In order to examine the influence of the circular shape on the behaviour of concrete columns at elevated temperatures, an experimental study has been performed recently at the University of Liege. The two main questions for which an answer was sought are:

1. Are the circular sections less prone to spalling, due to the fact that there is no corner in a circular section and that corner spalling in the rectangular sections is usually the first observed spalling?
2. Are the calculation methods that have been developed for rectangular sections still valid in the case of circular section?

This paper describes first the elements tested, the experimental procedure and the observations made during the tests. Conclusions are drawn regarding spalling phenomena and design methods for circular concrete columns.

2. Experimental program

2.1 Description of specimens

Four columns with circular cross section (diameter 300 mm) and a length of 2100 mm have been tested.

Two columns are reinforced with 6 ϕ 20 longitudinal bars (A_s/A_c = 2.67%) and two with 6 ϕ 12 (A_s/A_c = 0.96%). For each specimen the transversal reinforcement is realised with ϕ 8 circular stirrups with a spacing of 100 mm until 400 mm from the supports, and a spacing of 200 mm in the central part.

The concrete cover is c = 30 mm on the stirrups and c = 38 mm on the main bars, i.e. for the longitudinal bars an axis distance a = 44 mm for ϕ 12 bars and a = 48 mm for ϕ 20 bars.

The material qualities are C 60 siliceous for concrete and S 500 for the steel reinforcing bars.

2.2. Experimental procedure

The columns have been tested in one of the furnaces of the Fire Test Laboratory. The length of the columns was limited by the height of the furnace.

The concrete characteristics have been evaluated according to the Belgian standards. Quality C 60 was obtained without adding ultra fine particles.

Each column was simply supported at the ends, which give a slenderness of 28. The furnace is provided with an external frame specially designed to apply forces. Specimens are loaded by means of two double-effect (compressive and tensile) hydraulic jacks. Several thermocouples were placed in each column before casting of concrete in order to measure the temperature evolution.

The temperature in the furnace varied according to standard ISO 834 (very similar to the ASTM 119). The elongation of the columns and the temperature in the thermocouples were recorded every minute during the tests. The compression force was applied first and measured continuously in order to check that its variation during the fire test was negligible. The column aspect was examined basically every 15 minutes, unless spalling was noticed.

2.3. Test results

The test results are summarised in Tables 1 and 2.

3. Simplified calculation methods for design

As already mentioned two alternative simplified calculation methods have been developed.

The first one is a very simple model (6) which gives values well in agreement with experimental results. Referring to the classification of EC2-1-2 (2), it can be considered as a level 1 method (same as tabulated data). The basic equation is given hereafter.

$$R_f = 120\left(\frac{R_{f,\eta}+R_{f,a}+R_{f,L}+R_{f,b}+R_{f,n}}{120}\right)^{1.8} \quad (1)$$

where

$$R_{f,\eta} = 83\left(1.00-\eta_{fi}\right) \quad , \qquad \eta_{fi} = N_{d,fi}/R_d \quad (2)$$

$$R_{f,a} = 1.60\left(a-30\right) \quad , \qquad a = \text{axis distance in mm} \quad (3)$$

$$R_{f,L} = 9.60\left(5-L\right) \quad , \qquad L = \text{buckling length in m} \quad (4)$$

$$R_{f,b} = 0.09\,b \quad , \qquad b = \text{Dimension of the section in mm} \quad (5)$$

$$R_{f,n} = 12 \quad \text{if more than 4 long. bars are present, 0 otherwise} \quad (6)$$

This method has been used to evaluate the fire resistance of the 4 circular columns. As can be seen in Table 3, it gives values in good agreement with experimental results, though a little bit too conservative. Figure 3 shows a graphic presentation of the comparison between results obtained with this method and the experimental test results.

The second model is more elaborate (6) (7) and can be considered as a simplified calculation method (level II according to EC2-1-2). This method has been applied to the 4 circular columns ; the approach and the results are presented hereafter.

In this model, the ultimate load capacity of the heated column is expressed as a fraction of the plastic crushing load of the section :

$$N_u(t) = \chi^{MN}(\lambda)\, N_{pl}(t) \quad (7)$$

with t : time

λ : slenderness ratio at 20°C

$N_{pl}(t)$ is the plastic load of the section at time t :

$$N_{pl}(t) = \gamma(t)\,(\beta_1(t)\, N^c_{pl} + \beta_2(t)\, N^s_{pl}) \quad (8)$$

with N^c_{pl} the plastic load of the concrete core at 20°C,

N^s_{pl} the plastic load of the steel reinforced at 20°C.

$\beta_1(t)$ and $\beta_2(t)$ represent the diminution of the plastic loads with time.

$\gamma(t)$ is a function which takes into account spalling of concrete occurring at the beginning of the fire :

$$\gamma(t) = 1 - 0.3\, t \geq 0.85 \quad (9)$$

$\chi^{MN}(\lambda)$ is the buckling coefficient :

$$\chi^{MN}(\lambda) = \frac{\chi(\lambda)}{\varphi(\lambda)} \quad (10)$$

$\chi(\lambda)$: buckling coefficient for an axial load

$\varphi(\lambda)$: non linear amplification term due to the eccentricity of the load.

When applying the values proposed in (7) to the circular columns it was observed that the theoretical results were too conservative. The analysis of the discrepancies between theoretical and experimental results led to the following considerations.

- Despite the particular shape of the columns, surface spalling was observed in the four tests, see Figure 4. This means that the reduction coefficient $\gamma(t)$ of equation (3) taking account of spalling should also be applied for circular columns.
- The calibration of equations (7) to (10) has been based on test results on columns with a rectangular cross-section and with a length situated between 3 and 4 m for almost all the elements. A new calibration for a length of approximately 2 m was realised. This led to the following new formulation for the buckling coefficient $\chi(\lambda)$ appearing in equation (10), the amplification coefficient $\varphi(\lambda)$ remaining unchanged. Figure 5 shows a graphic presentation of equations (11) to (13)

$$\chi(\lambda) = 1 \qquad \lambda \leq 20 \qquad (11)$$

$$\chi(\lambda) = \left[1 + \frac{70-\lambda}{200}\right].0.80.\left(\frac{20}{\lambda}\right)^{0.7\left(\frac{\lambda}{70}\right)\left(\frac{225-c}{200}\right)^5} \qquad 20 < \lambda < 70 \qquad (12)$$

$$\chi(\lambda) = 0.80.\left(\frac{20}{\lambda}\right)^{0.7\left(\frac{\lambda}{70}\right)\left(\frac{225-c}{200}\right)^5} \qquad 70 < \lambda \qquad (13)$$

in which c : concrete cover (to the longitudinal reinforcement)

In order to show the adequacy of this new formulation, the ratio N_u (formula)/N_u (test) has been calculated for the 4 columns. N_u (formula) is the maximum axial load according to the theoretical formulation, and N_u (test) is the load applied during the test. The fire resistance is the one measured during the test.

It can be noticed that the new formulation leads to safe, though rather conservative, values for design purposes, see table 4. Additional studies will be performed to examine whether a particular formulation should be derived for $N_{p\ell}$, equation (8), in case of circular columns.

4. Conclusions

1) Observations made during experiments show that surface spalling was noticed between 20 and 60 minutes of fire test. The circular shape of the cross-section does not prevent the occurrence of this phenomenon.
2) No explosive spalling occurred with the high strength concrete C 60 used here.
   This corroborates research studies made previously (7) (8) (10). This type of spalling is essentially observed in concrete densified by means of ultra fine particles such as silica fume.
3) The diameter of the longitudinal reinforcement ϕ 12 or ϕ 20 had no significant influence on surface spalling.
4) Despite surface spalling phenomena, the values obtained for the fire resistance are relatively high.
   An increase of the load level leads to a significant decrease of the fire resistance.
5) Two simplified calculation procedures developed previously at the University of Liege have been used to evaluate the ultimate capacity of the 4 columns at elevated temperature.
   In order to take account of the short length of the specimens, a new formulation has been proposed for the buckling coefficient used in the second method.
6) With this new formulation, both methods lead to acceptable and safe values for design purposes.

5. References

1. CEB, “Fire design of concrete structures in accordance with CEB/FIP Model Code 90”. *Bulletin d'Information du Comité Euro-International du Béton* (208) Lausanne, 1991.
2. EC2-1.2, “Eurocode 2 : Design of concrete structures – Part 1.2 : General rules - Structural fire design”, European prestandard ENV 1992-1.2, CEN, Bruxelles, 1995.
3. Dotreppe, J-C., Franssen, J-M., Bruls, A., Baus, R., Vandevelde, P., Minne, R., Van Nieuwenburg, D. and Lambotte H., “Experimental research on the determination of the main parameters affecting the behaviour of reinforced concrete columns under fire conditions”, Magazine of Concrete Research 49, 179, Thomas Telford Ltd, London, (1997), 117-127.
4. Hass, R., “Practical rules for the design of reinforced concrete and composite columns submitted to fire”, Technical Report 69, T.U. Braunschweig, 1986, in german.

5. Lie, T.T. and Woollerton, J.L., “Fire resistance of reinforced concrete columns-test results”, Technical Report 569, NRCC, Ottawa, 1988.
6. Dotreppe, J-C. and Franssen, J-M., “Fire attack on concrete columns and design rules under fire conditions” in 'Computational and Experimental Methods in Mechanical and Thermal Engineering', Proceedings of an International Symposium, Ghent, May 1998, Academia Press, Ghent, (1998); 219-223.
7. Dotreppe, J-C., Franssen, J-M. and Vanderzeypen, Y., “Calculation method for design of reinforced concrete columns under fire conditions”, ACI Structural Journal 96 (1), (1999) 9-18.
8. Aldea, C-M., Franssen, J-M. and Dotreppe, J-C., “Fire tests on normal and high strength reinforced concrete columns”, in 'Fire Performance of High Strength Concrete', Proceedings of an International Workshop, Gaithersburg, NIST-National Institute of Standards and Technology, Gaithersburg, (1997), 109-124.
9. Dotreppe, J-C., “Influence of concrete quality on spalling of short columns submitted to fire conditions”, in 'Challenges for Concrete in the next Millenium' (2), Proceedings of the XIIIth FIP Congress, Amsterdam, May 1998, D. Stoelhorst & G.P.L. den Boer Ed, Amsterdam, (1998), 219-223.
10. Hertz, K.D., “A survey of a system of methods for fire safety design of traditional concrete constructions”, in 'Structures in Fire', Proceedings of the First International Workshop, Copenhagen, June 2000, J-M. Franssen Ed, Univ. of Liege, (2000), 283-292.

Table 1 : Load applied and fire resistance obtained for the 4 columns

Colum	Main reinforcement	Load applied (kN)	Load applied / Design strength N_{ud}	Fire resistance (min)
C1	6 ϕ 12	1260	0.59	156
C2	6 ϕ 12	1770	0.83	131
C3	6 ϕ 20	1450	0.57	187
C4	6 ϕ 20	1900	0.75	163

Table 2 : Main observations during the tests

Column	Time (min)	Observations
C1	25	sloughing off of concrete in many places of the external layer
C2	20	large cracks (mainly longitudinal)
	29	sloughing off of concrete of almost the whole external layer
C3	34	large cracks at the bottom of the column
	60	a few moments later sloughing off of concrete at the same place significant increase of the damage
C4	30	large cracks at the bottom of the column
	38	a few moments later sloughing off of concrete at the same place significant increase of the damage

Table 3 : Fire resistance values (method 1)

Column	Theoretical fire resistance Method 1 (min)	$R_{f,m1}/R_{f,test}$
C1	126	0.81
C2	91	0.7
C3	141	0.76
C4	113	0.7

Table 4 : Comparison between theoretical (method 2) and experimental results

Column	N_u(formula)/N_u(test)
C1	0.79
C2	0.65
C3	0.58
C4	0.5

Figure 1: relationship between the 3 approaches for design

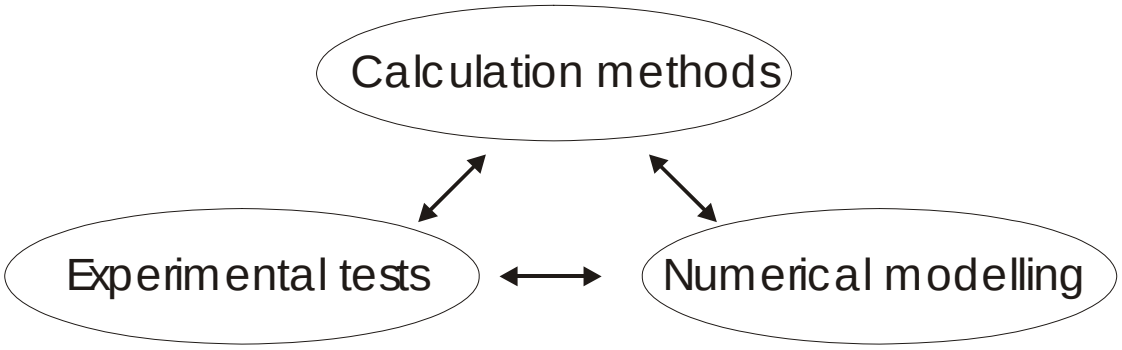

Figure 2: comparison between test and ENV 1992-1-2

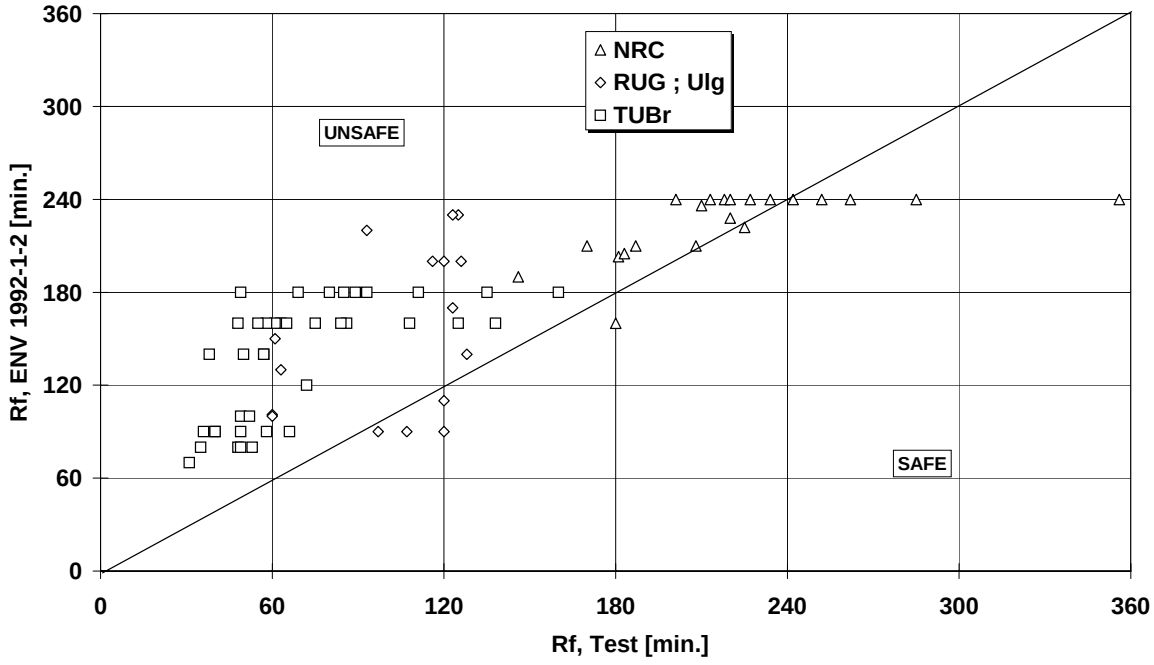

Figure 3: comparison between test and method 1

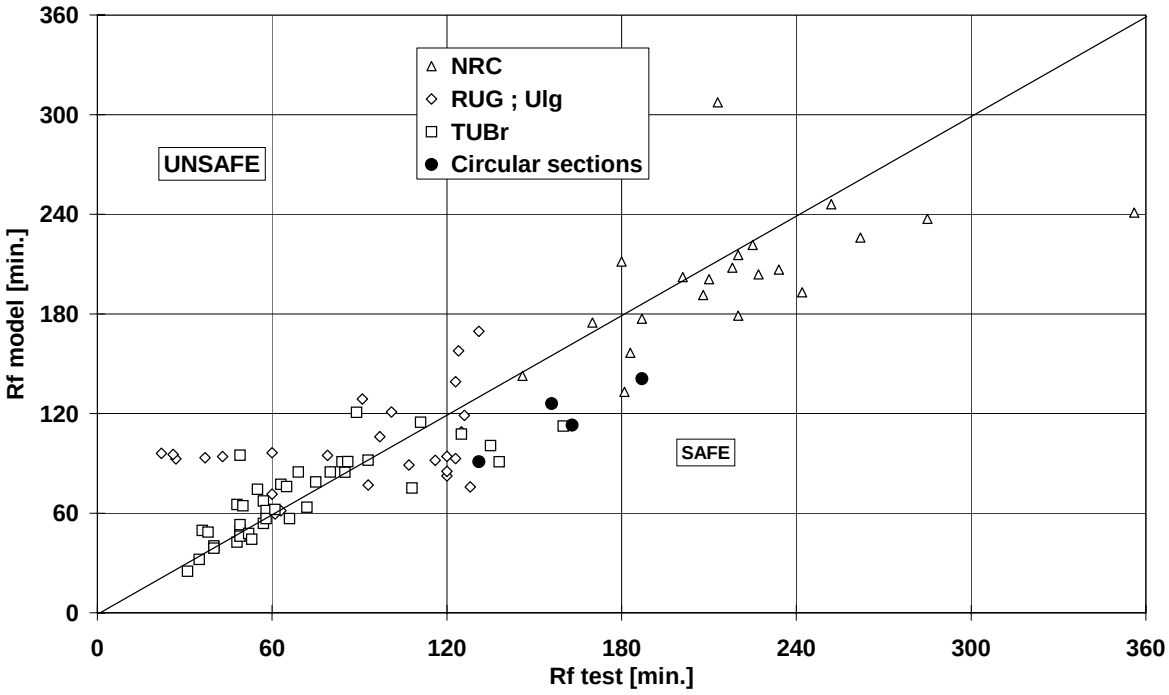

Fig. 5 : Buckling coefficient versus slenderness ratio

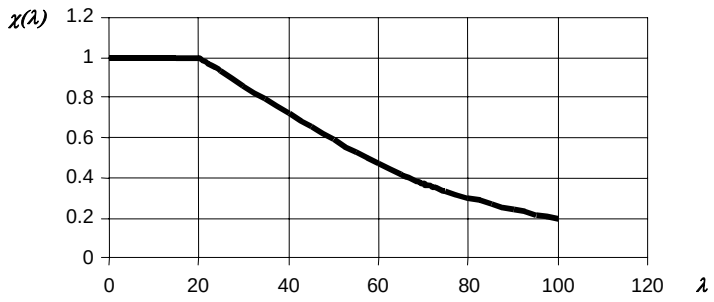

Fig. 4: spalling in column C1 as observed after the test

Univ.-Prof. em. Dr.-Ing. Dr.-Ing. E. h. KARL KORDINA
Institut für Baustoffe, Massivbau und Brandschutz

TECHNISCHE UNIVERSITÄT
BRAUNSCHWEIG

CEN/TC 250/SC 2/PT 1-2 Doc N 35

ABSTRACT

Flat slabs under fire
Redistribution of the internal forces and punching tests.

The German Research Association (Deutsche Forschungsgemeinschaft) has sponsored 1990 - 1992 investigations on the behaviour of flat slabs under fire, which have been carried out in the Institut für Baustoffe, Massivbau und Brandschutz of the Technical University of Braunschweig; the following report demonstrates the results. The investigations show the redistributions of bending moments and column loads of flat slabs under fire compared with the cold state and should clear the necessary capacity in punching shear under fire as well. The redistribution of the internal forces must be studied by finite-elements-calculations only; however, punching has been investigated in 10 fire tests on slabs with dimensions usual in practice. This tests link up with 4 tentative tests, which have been carried out in the Special Research Department 148 "Behaviour of Structural Members in Fire" in 1986.

A short report in German was published in Bautechnik 70 (1993), part 11.

Key words: Flat slab, fire, internal forces, punching

1 Distribution of internal forces

Fire exposure intensifies the risk of cracking and reduces the concrete strength f_c and also the modulus of elasticity E_c. High concrete stress around points of support, in particular at the fire-exposed underside of the slab, in addition reduce the flexural stiffness. It remains to be clarified whether or not any variations in the flexural stiffness need to be accounted for. Numerical assessment, however, suggests that local variations in flexural stiffness only have a minor influence on the distribution of internal forces. As at normal temperature and design load conditions already the flexural stiffness has to be assumed to go down in the cracked state to about 65% [1], the reduction coefficient $\beta_T = (EI)_T/EI)_0$ has to be expected to be in the order of 0.25 in the event of a fire.

Fire tests performed on continuous bending elements in reinforced concrete revealed that as a result of the temperature-induced moment of restraint due to ISO-834 fire exposure the moment at support rises within a period of 20 - 30 minutes until the top reinforcement above the column, which is affected by the fire to a much lesser degree, starts yielding. This observation can be explained by moment redistribution. The ensuing yield moment remains almost constant for another 10 to 15 minutes before it gradually declines. Failure of the element occurs after 90 minute ISO-834 fire exposure in the area of positive bending moment in the span, unless fire protection measures

beyond normal temperature design have been taken for this area. It should be noted that such behaviour in the event of a fire presupposes adequate ductility of the column reinforcement and rotation capacity of the column cross section.

Primarily, the objective was to render calculable that temperature-induced moment of restraint M_T that tends to change the moment distribution prevailing under design load conditions in the cold state until the column reinforcement starts yielding (Fig. 1). In evaluating tests on strips of continuous reinforced-concrete slabs, the difference in the moment at support between M_q at the commencement of the fire test and the measured yield moment was used to infer the reduction in stiffness β_T and the linearized temperature gradient ΔT [6]. From temperature curves for reinforced-concrete slabs of different thickness, obtained through measurement and calculation, the linearized temperature gradients were at least by approximation determined for 30 minute ISO 834 fire exposure. The inherent scatter is shown in Fig. 2.

Fig. 1

Fig. 2

It appears from Fig. 2 that for reinforced-concrete slabs, about 20 cm thick, the temperature gradients ΔT given are still fairly reliable, although clear deviations remain possible. These would be attributable to differences between temperature readings and calculation, or the actual concrete moisture and the mineralogical properties of the aggregates used. Above and beyond that linearization of the temperature gradient by necessity also implies a

considerable degree of uncertainty and remains somewhat arbitrary. Uncertainty increases, the greater the slab thickness.

The moments of restraint of prestressed-concrete structures were analysed in a similar way. Table 1 lists the values $\beta_T \cdot \Delta T$ determined by approximation for reinforced-concrete and prestressed-concrete slabs (pretensioned, unbonded) together with ΔT for a number of slab thicknesses.

Table 1

Basically, values β_T 0.2 and $\beta_T \leq 0.5$ appear to be probable for fire-exposed reinforced-concrete and prestressed-concrete slabs, respectively, as flexural members of this kind will under the conditions considered here always be in a cracked state, where prestress inevitably proves to have a bracing effect.

The product $\beta_T \cdot \Delta T = (EI)_T \times \Delta T/(EI)_0$ was used to determine the temperature-induced moments of restraint on the basis of the theory of elasticity. Shown in Fig. 3 are characteristic results of the bending moment distribution after 30 minute ISO-834 exposure for a column strip and a field strip, which were established for a flat slab in reinforced concrete, 20 cm thick, comprising 16 square bays of 6.0 m span. The detailed test report includes a large number of additional graphs for the moment distributions determined for different fire scenarios.

Fig. 3

Obviously, the present study cannot aim to present a comprehensive and realistic picture of how the internal forces will be distributed in flat slabs in the event of a fire, covering the period up to the point when plastic hinges

appear above the columns. For the time being, the numerical basis required for this purpose cannot be defined with the necessary accuracy. The effects a fire will have on the temperature-induced moments of restraint and the column loads - which essentially are only determined by $\beta_T \cdot \Delta T$ and the column distance ratio l_x/l_y - can hence only be assessed in an approximative and global approach.

The following conclusions could be drawn:

– The temperature-induced moments of restraint remain unaffected by the column distance and are determined by $\alpha_T \cdot \Delta T$, $\beta_T = J_T/J_0$ and the square of the slab thickness rather than the column distance ratio l_x/l_y. An estimate for the temperature-induced moments of restraint can be made with the aid of expression

$$m_x \approx m_y \approx \alpha_T \cdot \beta_T \cdot E_c \cdot h^2 \cdot \Delta T/10$$

for the slab strip 1 m wide. It goes without saying that the boundary conditions of the slab strip need to be taken into account. Such an approximative approach produces an **upper** limit, for which the lower deviation is generally not found to be more than 15%. The changes any deviations from the edge ratios of a square slab field produce remain within the limits of accuracy that can be achieved by this approximative approach [8].

– The reinforcement determined from cold design of reinforced-concrete slabs for column strips within the area of negative moments, and in particular for the area above the points of support, will also cover the temperature-induced moments of restraint for

these areas in a fire. It should be noted, however, that the areas of negative moments will then extend into the spans in a similar way as it may be observed for linearly supported continuous beam and slab systems. The difference in the case considered here is, however, that areas of positive moments will rarely be found to occur. It follows that it is absolutely necessary to provide the column strips with a top continuous reinforcement having a cross section which is at least 20% of what has been found to be required above the points of support in the cold state.

Negative temperature-induced moments of restraint also occur in the internal strips within the span, which also appear to call for a minimum top reinforcement. Same need, however, not be made an absolute requirement as under normal conditions negative moments tend to occur within the spans alone from the live loads carried, which as a consequence mean adequate top reinforcement across the column strips, but also in the span. Also, the in-plane "disc compressive stresses" that occur in the event of a fire will raise the moment capacity.

– Flat slabs in prestressed concrete reveal during the first phase of a fire a clearly higher flexural rigidity than slabs in reinforced concrete. The temperature-induced moments of restraint rise to higher levels by comparison and may after a shorter fire exposure than is observed for reinforced-concrete slabs produce plastic hinges above points of support. It is important to provide within the spans a top steel reinforcement, which may be weak

(0.3%), relatively strong top reinforcing steels being provided near points of support. This is to account for negative moments near points of support also in the situation of a tension member returning to the bottom end of the slab. The top-end continuous minimum steel reinforcement to be made a requirement for the column strips should be designed for 20% the numerically required total tensile force above the columns.

A minimum continuous top reinforcement provides flat slabs with a substantial capacity margin, in particular in a fire, as it allows a tension membrane to form, once the cross sections should fail due to bending.

– Column loads increase considerably under fire. For the slab system considered here, with a slab density of h = 20 cm, the load was found to increase for the first inside corner column by 70% of the column load, composed of dead weight + live load (g + p = 10 kN/m²) (partial load factor γ_F = 1.0). Consideration was here given to the fact that at normal temperature this column has to support a load from g + p which is higher by about 25% than that for any other inside column. The increase in the load imposed was found to be between 20% and 45% for the next inside columns of the first row (running in parallel with a free edge), and ≤ 15% for all the other columns. This column load increase, substantial in some cases, can be explained by the fact that with, say, four adjacent spans (corner slab, two adjacent edge slabs and one inside slab) subjected to partial fire attack, same try to deflect towards the

fire-exposed side, which means downwards, but are prevented from doing so by the first inside corner column so that the latter has to absorb the above high additional loads due to restraint.

2 Fire tests

To date, the data available on the structural behaviour of supporting areas of point-supported reinforced-concrete slabs (flat slabs) under fire are scarce. Fire tests conducted (and evaluated) in the period 1991/1993 were to cast some light on the complex factors influencing this problem. Information is also available from four tentative tests carried out under the Special Research Scheme 148 (SFB 148) in 1986 [5], and from investigations made into the question of the redistribution of internal forces [7].

2.1 Test procedure

Test objects were reinforced-concrete slabs of identical geometry, which differed, however, in the reinforcement pattern:

- slab dimensions 2.50 m × 2.50 m × 0.20 m
- loaded circular section D = 2.20 m, r = 1.10 m
- central column stub 0.25 m × 0.25 m × 0.40 m
- graded top bending tension reinforcement (in BSt 500/550):
  low level of reinforcement = 0.564%
  high level of reinforcement = 1.54 %
  using slab designations P 0.5 and P 1.5, resp.
- Each reinforcement level did either include or not include shear reinforcement (slab designations

with stirrup / w/o stirrup, resp.), which, to facilitate assembly, was provided in the form of continuously cranked stirrups (cf. Fig. 4).

Fig. 4

– At the time of testing, the compressive strength of the concrete was f_c = 33 to 51 N/mm².

– At the time of testing, the slabs were 88 to 178 days old, their moisture content was however still so high (4.0% by weight) that liquid water covered the slab surface during the test, which did not evaporate until towards the end of the test.

– Temperature development in the furnace according to ISO temperature/time curve.

The 10 tests can be classified as follows:

P0.5 / w/o stirrup - tests 1, 7, 9
P0.5 / with stirrup - tests 2, 10
shear reinforcement 4.52 cm²
P 1.5 / w/o stirrup - tests 3, 5, 6, 8
(with fire-resistant slab)
P1.5 / with stirrup - test 4
shear reinforcement 6.78 cm²

The SFB 148 tentative tests used four reinforced-concrete slabs, 150 mm thick, 1.75% reinforcement without shear reinforcement, but also with a loaded circular area D = 2.2 m (f_c 38 N/mm²).

The test set-up is shown in Fig. 5. The test load is applied by a tubular-piston jack positioned above the load frame. Load transmission is by means of a (heat-insulated) tension member, which runs through a sheath inside the specimen and is anchored to the underside of the column stub. The load frame serves to uniformly transmit the force of the jack - via 16 radially arranged displaceable

Fig. 5

points of load application - to the specimen.

Test evaluation started from the following measured data:

- Analyses of additional specimen to determine the material properties of concrete and steel.
- Temperatures across the slab cross section.
- Specimen deflection under load, both in the cold state and under fire exposure.
- Steel strain within the bending tension and shear reinforcement.
- Cracking and fracture line pattern at the top of the slab and within the slab cross section.

The test procedure was varied to reflect the test objective. The initial load was established to be $0.7 \times V_{Rd,1}$ and $0.7 \times V_{Rd,3}$, respectively (acc. to EC2, part 1, 1991) and was applied to the specimen before commencing with the fire test. The test procedure is illustrated in Fig. 6.

Fig. 6

2.2 Test results

From the many test data and readings obtained, only some of the main findings can be presented here; they are listed in table 2. For further information, reference is made to the final report.

Table 2

- In all the 14 experiments, a punching cone was found to form, which however differed in the top diameter (varying between 1.28 and 1.86 m for the slabs 20 cm thick). The slab underside was found to spall in tests 3, 4 and 7-10, the spalling depth averaging 50 mm.
- The angle of the failure cone averaged 32°.
- Cracking at the slab top occurred already after loading in the cold state with all the specimen

that included shear reinforcement (tests 2, 4, 10) and in test 7 (raised initial load). This went along with more intensive deflections and higher steel strain values than was observed with the specimen that were subjected to a lower initial load and did not have any shear reinforcement. To enter the shear reinforcement in the computation at 100% the stirrup steel tensile force, as is the case in EC2, Part 1, was found to be too high an assumption [2], [3].

– The loading level was raised during the first 30 minutes with a view to the expected redistribution of internal forces in the event of a fire. The risk of spalling intensified as the loading level was increased during the first phase of the test. Application of a fire-resistant slab in test 8 proved to be a successful countermeasure.

– In fire tests 1 - 10 (slab thickness h = 200 mm) deflections were found to be directed against the load action for the whole test period. This means that the thermally induced deformation dominated, which was directed downwards in the test. Although the tentative tests A-D of SFB 148, using slabs h = 150 mm thick, at first revealed a similar deformation behaviour, the direction of the deflection was reversed as from test minute 30, after which it followed the direction of loading.

– In tests 2, 4, 7, and 10, the yield limit of the bending tension reinforcement was clearly exceeded; in the remaining tests it was not reached until towards the end of the experiment.

– Fig. 7 illustrates the rupture loads, related to the design load currently in use in Germany, $V_{Rd,1}$ and $V_{Rd,3}$, respectively (EC2, Part 1, 1993 with $\tau_{Rd} = 1.2 \cdot 0.09 \cdot f_{ck}^{1/3}$ and $V_{Rd,1} = \tau_{Rd} \cdot (1.6\text{-}d)(1.2 + 0.4\ \rho_L,\%) \cdot \quad \cdot d)$ [4]. Although the limited number of experiments made does not permit of any statistical evaluation, tendencies can still be made out. In tests 2, 4 and 10, the ratios entered consider a reduced load-bearing component of the shear reinforcement with $\sum 0.50 \cdot A_{sw} \cdot f_{yd} \cdot \sin\alpha$.

– According to EC2, Part 10 (now ENV 1992-1-2), the fire resistance time has to be determined for a loading level of $\gamma_F = 1.0$. This by approximation corresponds to $0.7 \cdot V_{Sd}$ or $0.7 \cdot V_{Rd}$. It is apparent from Fig. 7 that the fracture loads of the slabs 15 cm and 20 cm thick were not lower than V_{Rd} in the fire test, which means that also column loads increased as a result of restraint under fire can be carried at an order of $0.3 \cdot V_{Rd}$.

Fig. 7

Literature

[1] *Grasser, E.; Thielen, G.:* Hilfsmittel zur Berechnung der Schnittgrößen und Formänderungen in Stahlbetontragwerken, Heft 240, Schriftenreihe DAfStb.

[2] EC 2, Teil 1, Abschn. 4.3.4 Durchstanzen, Gl. (4.58).

[3] *Kordina, K.; Nölting, D.:* Tragfähigkeit durchstanzgefährdeter Stahlbetonplatten, Heft 371, Schriftenreihe DAfStb.

[4] Deutscher Ausschuß für Stahlbeton: Ausschuß „Bemessung und Konstruktion", Beschluß April 1993.

[5] *Kiel, M.:* Brandversuche zum Durchstanzen von Flachdecken. Arbeitsbericht SFB 148, Sign.: AC 7057 (1984–86, 1B), Technische Informationsbibliothek Hannover.

[6] *Kordina, K.; Wesche, J.:* Stahlbeton-Durchlaufkonstruktionen unter Feuerangriff. Versuchsbericht 30-0025 (1979), iBMB der Technischen Universität Braunschweig, unveröffentlicht.

[7] *Krampf, L.:* Untersuchungsbericht „Punktgestützte Platten unter Brandangriff", Institut für Baustoffe, Massivbau und Brandschutz, Technische Universität Braunschweig (1987), unveröffentlicht.

[8] *Hotzler, H.:* Untersuchungen über die Biegemomente und Durchbiegungen in punktgestützten Platten. Veröffentlichung in Vorbereitung.

[9] *Kordina, K.:* Zum Tragsicherheitsnachweis gegenüber Schub, Torsion und Durchstanzen nach EC2, Teil 1, Beton- und Stahlbetonbau, ~~in Vorbereitung~~. 1994, H. 4

Author of this paper:
~~Autor dieses Beitrages:~~
Univ.-Prof. em. Dr.-Ing. Dr.-Ing. E.h. Karl Kordina, Institut für Baustoffe, Massivbau und Brandschutz, TU Braunschweig, Beethovenstraße 52, 38106 Braunschweig

Table 1 Stiffness in bending of flat slabs after 30 min ISO fire

Reinforced concrete slabs	h cm	ρ_s %	ρ_p [1] %	β_T	ΔT K	$\beta_T \cdot \Delta T$ K
	20	0,5 1,5	- -	0,20 0,23	180	36 40
	30	0,5 1,5	- -	0,20 0,23	130	26 30
Prestressed-concrete slabs	22[2]	1,02	0,68 (0,27)	0,68	170	114
	35	0,3	0,43 (0,16)	0,20	110	54

1) related to reinforcing steel content with σ_{cp}/f_{yd} and $\sigma_{cp} = N_{cp}/A_c$ to EC, Section 4.3.4.5; in brackets A_p/A_c in %.

2) Very high degree of reinforcing and prestressing steel by comparison

Table 2: Results of the fire tests-summary

Number of test		1	2	3	4	5	6	7	8	9	10	A	B	C	D
Material prop. $f_{c,cube}$	N/mm²	55	55	61	61	42	42	63	63	53	53		47	45	
f_{cc}	N/mm²	45	45	51	51	33	33	53	53	43	43	39	39	37	37
τ_{RD} *)	N/mm²	0,38	0,38	0,40	0,40	0,35	0,35	0,41	0,41	0,38	0,38	0,37	0,37	0,36	0,36
f_{yd}	N/mm²					435								435	
Longit.reinf.	%	0,56	0,56	1,54	1,54	1,54	1,54	0,56	1,54	0,56	0,56	1,75	1,75	1,75	1,75
Shear reinf. A_{sw}	cm²	-	4,52	-	6,78	-	-	-	-	-	4,52	-	-	-	-
Effect. height	mm	d_m = 167										d_m = 120			
Critical perimeter	mm	U_m = 2575										U_m = 2130			
Column cross sec.	mm	250/250										250/250			
Diam. failure cone	m	1,35	1,51	1,86	1,85	1,38	1,38	1,70	1,52	1,30	1,45				
V_{RD1}	kN	334	334	448	448	392	392	360	460	334	334	264	264	260	260
Shear reinf. **)	kN	-	98	-	148	-	-	-	-	-	98	-	-	-	-
$V_{Rd} = V_{RD1} + V_{sw,ef}$	kN	334	432	448	596	392	392	360	460	334	432	264	264	260	260
Duration of test	min	120	120	27	17	90	90	29	70	90	22	14	8	180***)	92***)
Initial load	kN	229	372	330	520	232	238	404	334	227	359	287	287	260	160
Failure load $V_{T,f}$	kN	492	475	550	810	386	380	500	568	410	460	345	360	>>250	>>260
$V_{T,f}/V_{Rd}$	-	1,48	1,10	1,23	1,36	0,99	0,97	1,39	1,23	1,23	1,07	1,31	1,37	>1,0	>1,0

*) $\tau_{RD} = 1,2 \cdot 0,09 \cdot f_{ck}^{1/3}$

**) $\Sigma\ 0,50 \cdot A_{sw}\ f_{yd} \cdot \sin\alpha$

***) Test finalized before failure

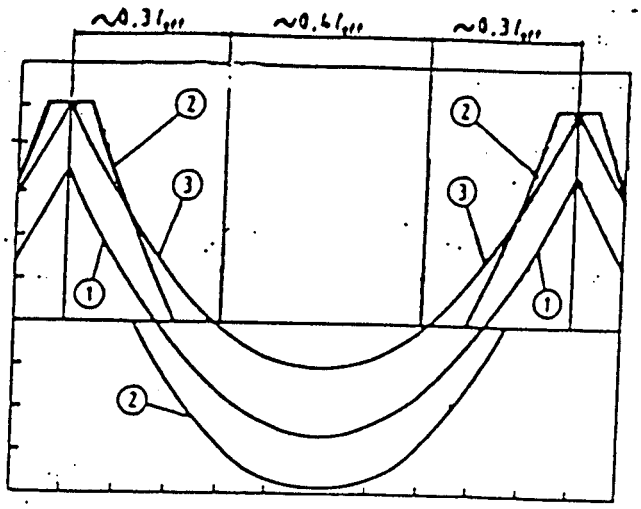

Explanation:

(1) Diagram of bending moments for the actions in a fire situation at $t = 0$
(2) Envelop line of acting bending moments to be resisted by tensile reinforcement according to ENV 1992-1-1
(3) Diagram of bending moments in fire conditions

Fig. 1. Moment redistribution in a continuous concrete beam under fire until yielding in the upper reinforcement over the middle support

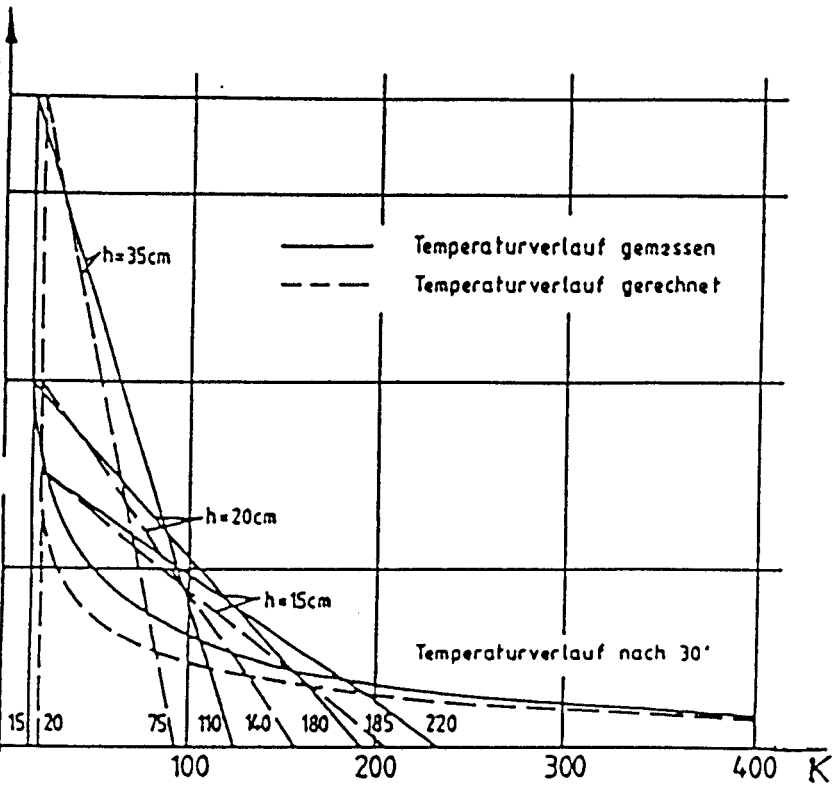

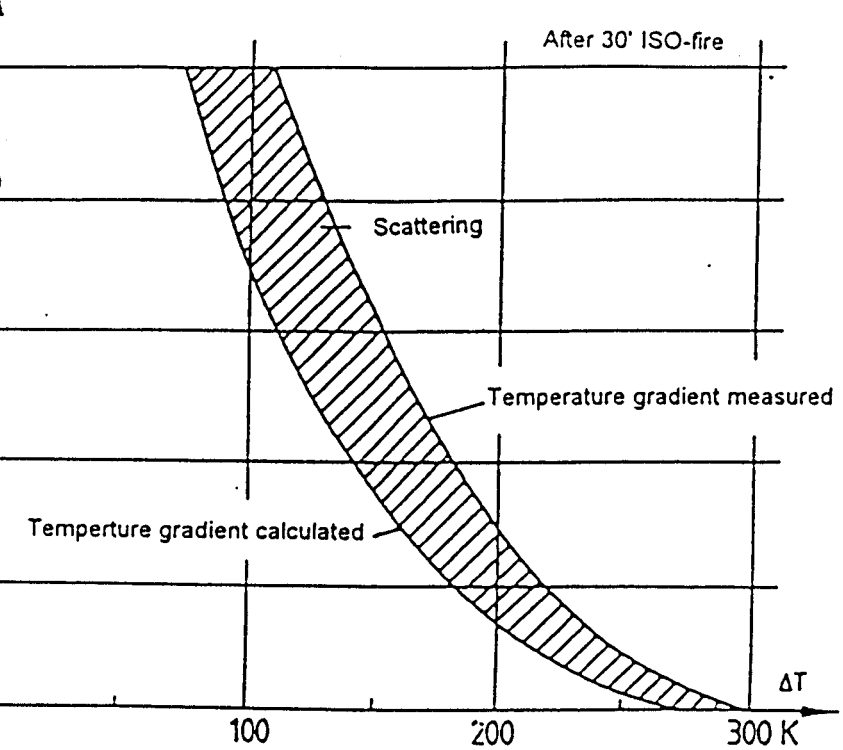

Fig. 2. Linear temperature gradients after 30 min ISO-fire

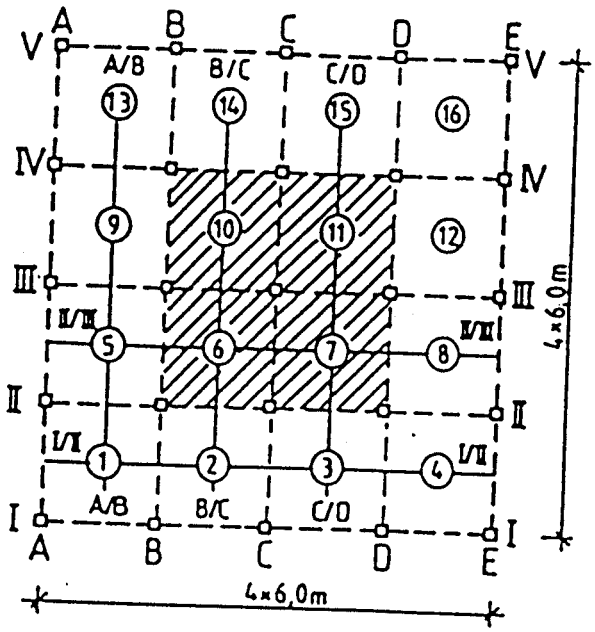

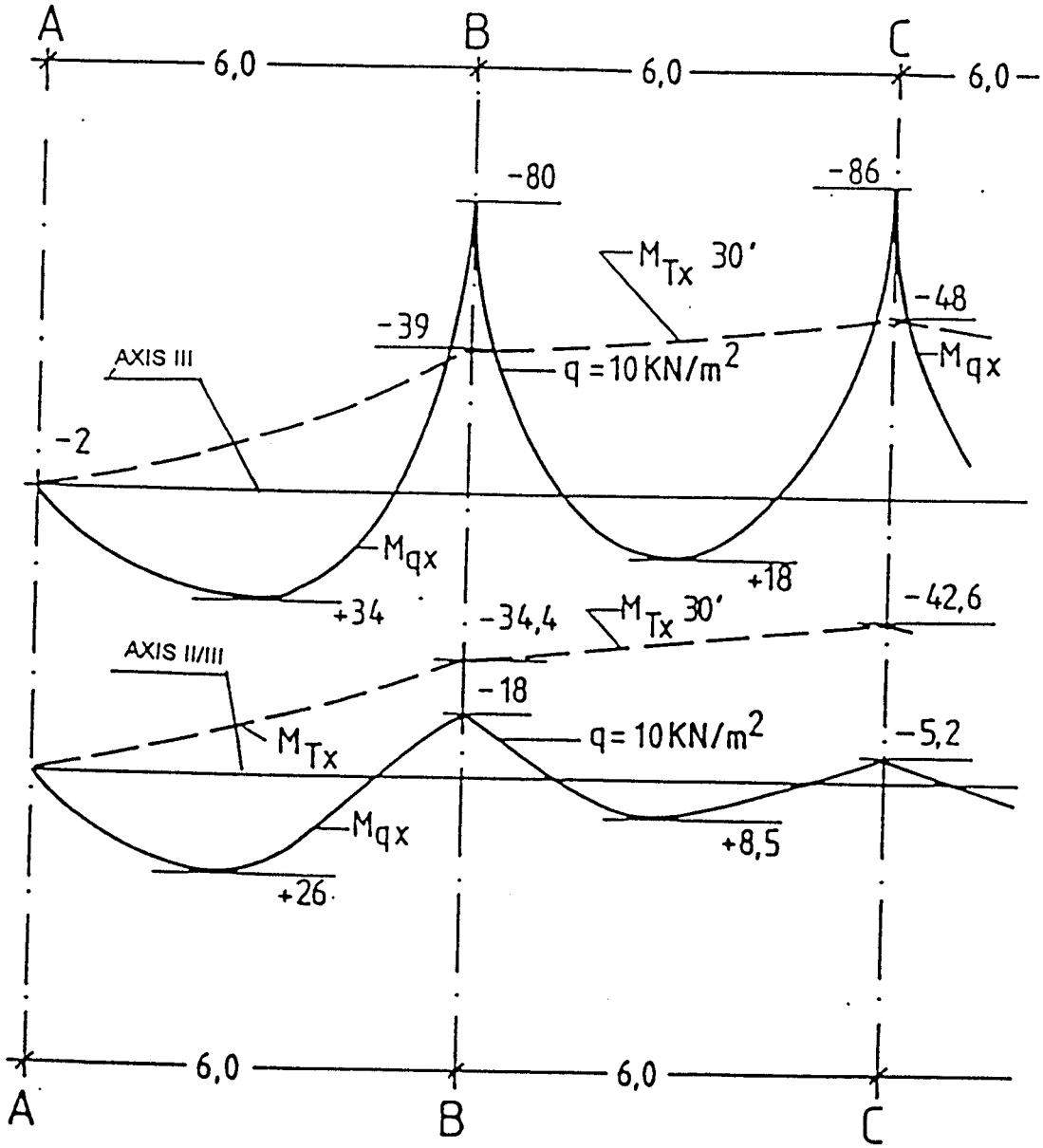

Fig. 3. Moment-distribution after 30 min ISO-fire in a column-strip and a field-strip; flat slab with 16 square fields, 20 cm thick; 4 internal fields heated

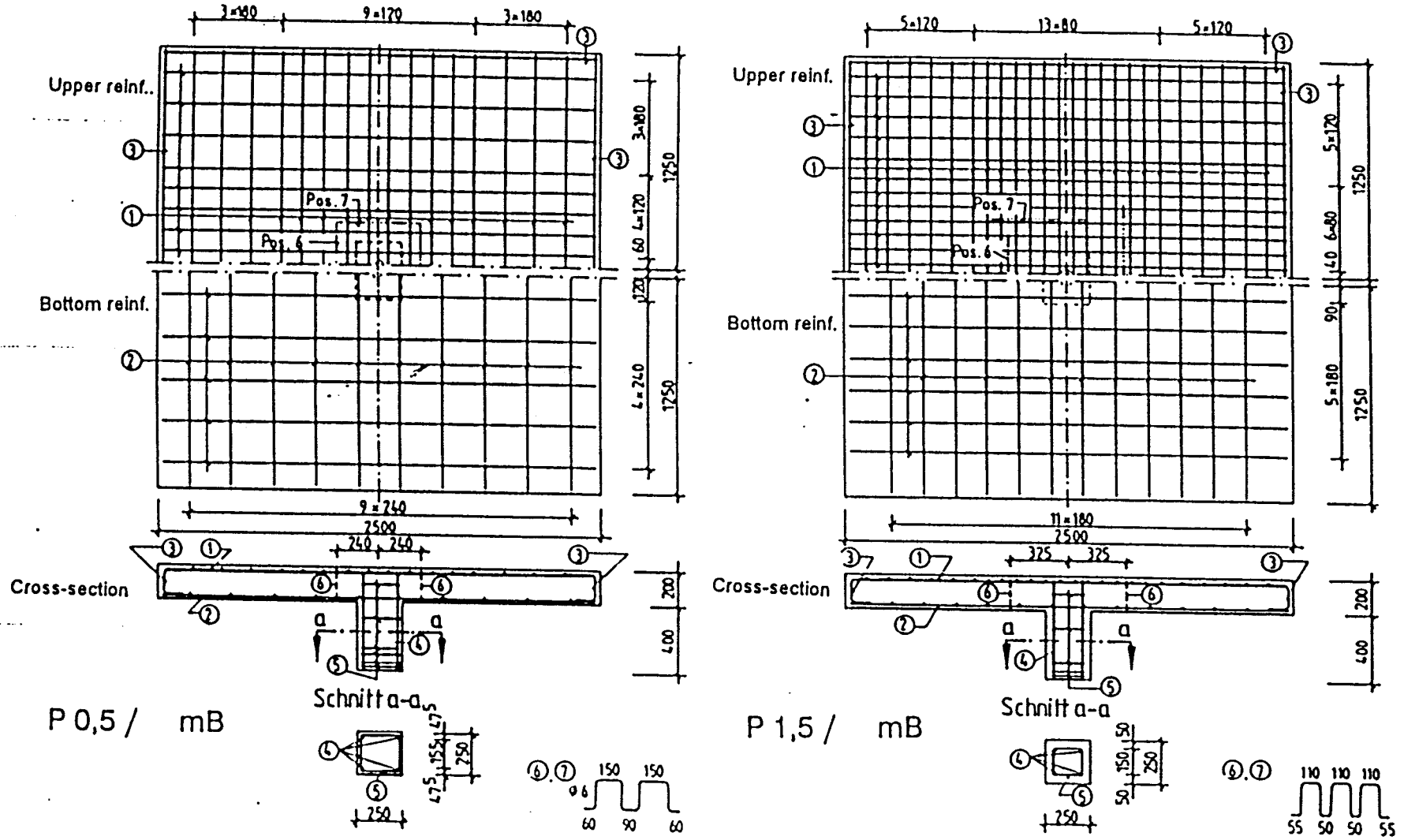

Fig. 4. Detailing of the reinforcement

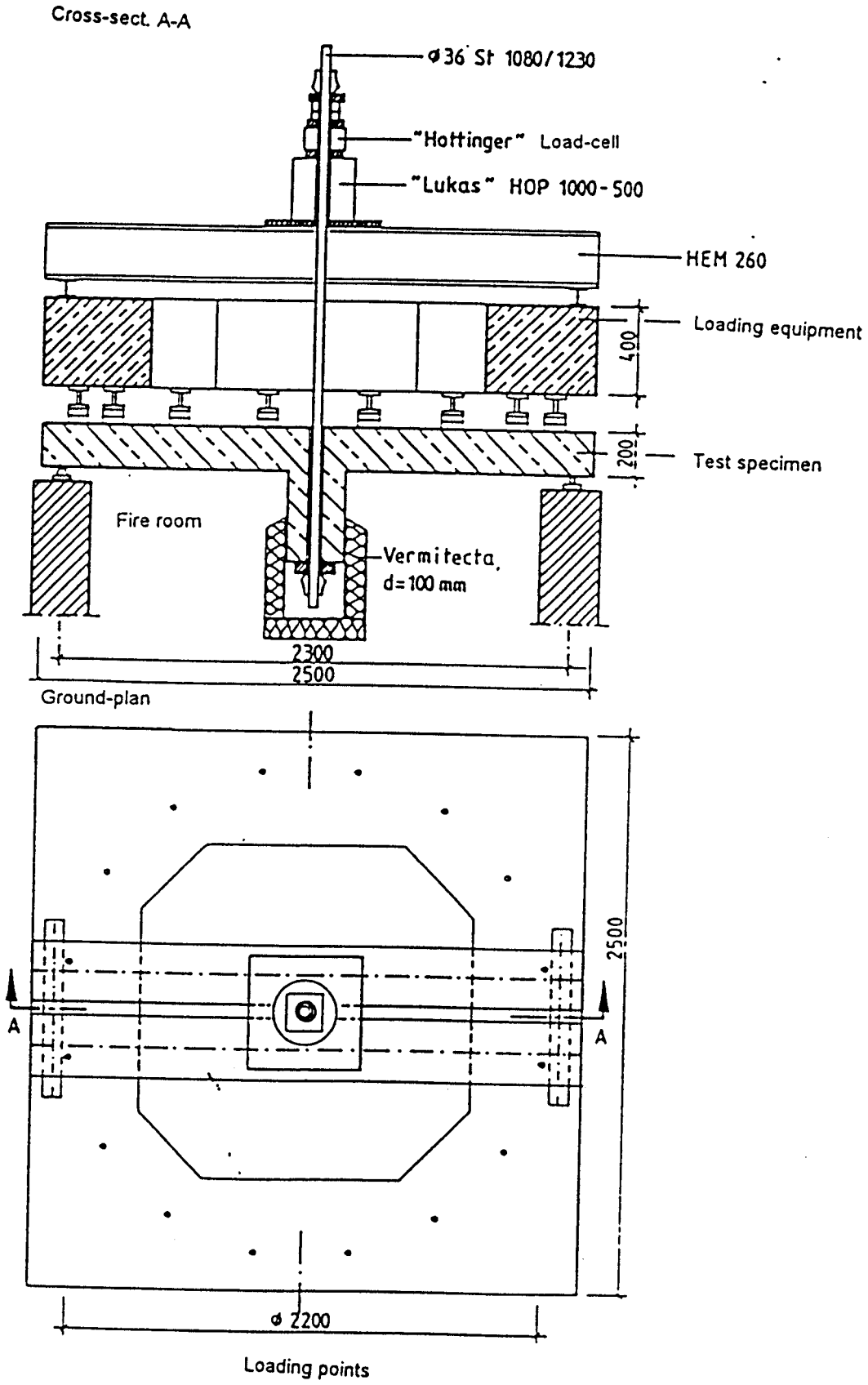

Fig. 5. Test set-up

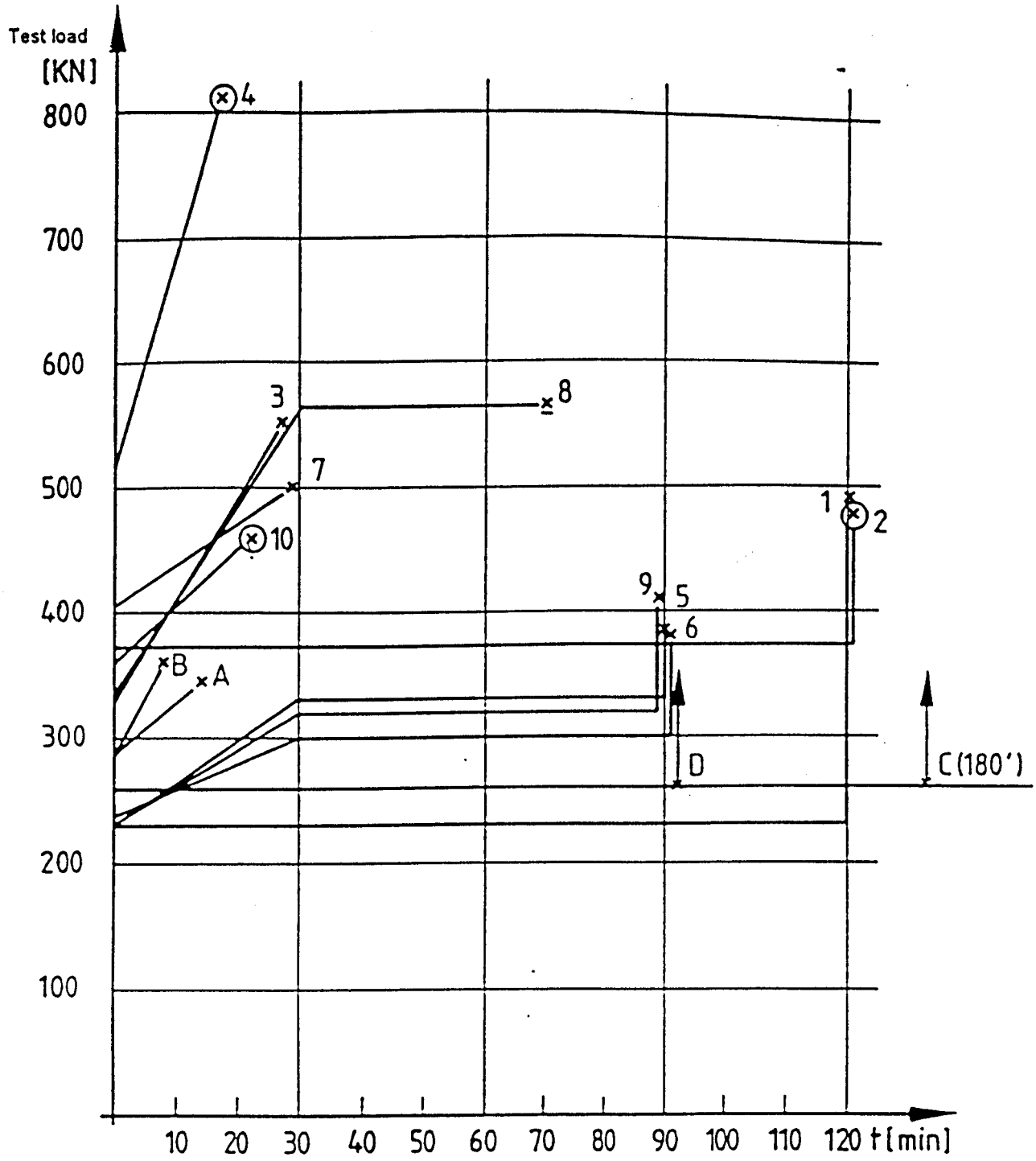

⊕ with shear reinf. $V_{shear} = 0,5 \cdot A_{sw} \cdot f_{yd}$

± with fire protecting plate d = 20 mm

\+ without shear reinf.

Fig. 6. Test procedure

Fig. 6

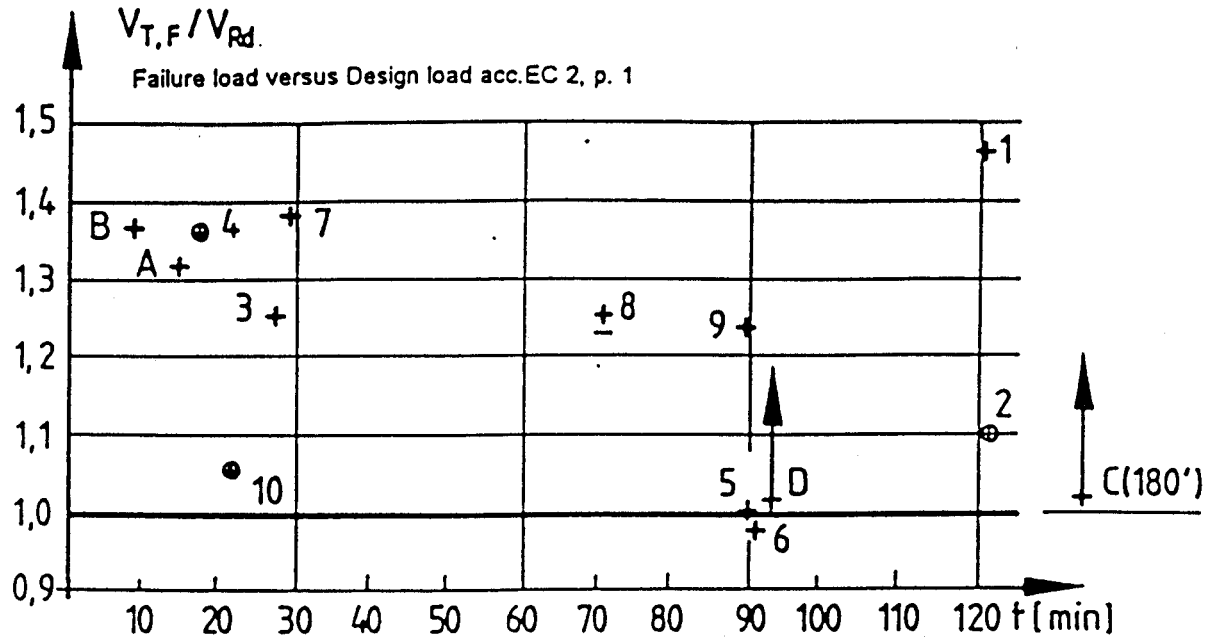

⊕ with shear reinf. $V_{shear} = 0,5 \cdot A_{sw} \cdot f_{yd}$

± with fire protecting plate d = 20 mm

\+ without shear reinf.

Fig. 7. Relation failure loads under fire versus design loads V_{Rd1} and V_{Rd3} resp. (acc. EC 2, part 1) with $\tau_{RD} = 1,2 \cdot 0,09 \cdot f_{ck}^{1/3}$

Bild 7

Mechanical behaviour of HPC at high temperature

Pierre PIMIENTA, Izabela HAGER

ABSTRACT

This paper describes results of an experimental program carried out by the Centre Scientifique et Technique du Batiment within the framework of the French National Project BHP 2000. Compression tests were carried out at high temperature (120, 250, 400 and 600 °C) on normal strength concrete and three high performance concretes (HPC). Samples were heated until test temperature at a heating rate of 1°C/min. 104 mm x 320 mm cylindrical specimens were equipped with a deformation measure device allowing determining stress/strain curves. The relative compressive strength of the 3 HPC at the different temperatures were, either in good agreement, or, in certain cases, lower than those determined on HPC by Diederichs and al and Castillo and Durrani. Modulus of elasticity determined on the 3 HPC decreased regularly from 20 °C to 600 °C.

1. Introduction

The numerous researches carried out on High Performances Concretes (HPC) allowed, during these last years, an important development of the use of this new material. Main properties of the HPC are well known today. This is not however the case for their properties at high temperatures. Indeed, even if numerous research data are available, results are often contradictory and unexplained. One of the weak points of the material is its hazard of spalling.

We present in this paper the results of an experimental program carried out by the Centre Scientifique et Technique du Batiment within the framework of the French National Project BHP 2000. Our experimental procedure was based on RILEM recommendation [1]. Compression tests were carried out at 120, 250, 400 and 600 °C on normal strength concrete and three high performance concretes (HPC). They were carried out at high temperature and not after cooling. Compressive strength and modulus of elasticity were deduced from stress/strain curves. Results were compared with those determined within the framework of two researches, which were realised on HPC by Diederichs and al [2] and Castillo and Durrani [3].

More complete information on the main physical mechanisms and chemical reactions within the cement paste and the aggregates that could be at the origin of the observed behaviour at different temperature can be found in [2, 4, 5].

Pierre PIMIENTA, Centre Scientifique et Technique du Bâtiment, France
Izabela HAGER, Centre Scientifique et Technique du Bâtiment, France and Ecole Polytechnique of Cracow, Poland

2. Mix proportions

Four concrete compositions were tested: M30C, M75C, M75SC, M100C. The number indicates the expected average strength of concrete. C and SC indicate the nature of aggregates: respectively calcareous and silico-calcareous. Tests on concretes M75C and M75SC aimed to determine the influence of nature of aggregates
The mix proportions of M30C, M75SC, M75C and M100C are given in the table 1. Cement paste content of M75SC was higher to that of M75C in order that M75SC strength be equivalent to that of M75C. M75C and M100C were designed for the French National Project BHP 2000.

Materials (kg/m^3)	**M30C**	**M75C**	**M75SC**	**M100C**
Cement CEM I 52,5 PM CP of St Vigor		360	450	377
Cement CEM II 32,5 R (L)	350			
Boulonnais calcareous sand 0/5	401	442		439
River Seine sand 0/4	401	435		432
Boulonnais calcareous aggregate 5/12,5	514	465		488
Boulonnais Calcareous Aggregate 12,5/20	514	579		561
Bouaffles silico-calcareous sand 0/5			615	
La Brosse silico-calcareous aggregate 5/12,5			726	
La Brosse silico-calcareous aggregate 12,5/25			504	
Densified silica Fume (DM)		22	45.1	37.8
GT Superplasticizer from Chryso		9	12.25	12.5
Retarding Chystard from Chryzo		2.5	3.1	2.6
Water	181	136	148	124
water/(cement + SF) ratio	**52 %**	**36 %**	**30 %**	**30 %**

Table 1: Mix proportions

3. Testing procedure

As written before, our experimental procedure was based on RILEM recommendation [1]. Compression tests were carried out on heated samples. Samples were tested non sealed and were not submitted to preliminary load. Test temperatures were 20 °C, 120 °C, 250 °C, 400 °C and 600 °C. 3 cylinders were tested at each temperature. Compressive strength on 28 days water cured samples were determined on 160 mm x 320 mm cylinders.

Test specimens consisted of 104 mm x 320 mm cylinders. The size of test specimens is the result of a compromise. Size must be important enough in order that the material homogeneity can be acceptable. This must, in particular, be connected with the maximal size of aggregates (here 20 and 25 mm). In another hand, a too important cylinder size can lead to too high temperature and moisture heterogeneity during the heating of samples. In order to reduce this heterogeneity, heating rate was chosen low: 1°C/min. The length/diameter ratio is equal to 3 and not 2 as usual. Indeed, the contact with the compression apparatus platens tends to cool the end of test cylinder. Length/diameter ratio is then increased in order that the central area of samples is longer.

Specimens were demoulded 2 days after casting, then cured in waterproof bags during 5 days at 20°C ± 2 °C. They were then stored in a climate room (20°C ± 2 °C/ RH 50% ± 5 %). Age of specimens at the time of the tests was between 125 and 335 days. During the period of drying, the surfaces of test cylinders were ground. For each concrete, the moisture content was determined on other similar samples by drying them at 105°C until mass stabilisation. The determined moisture contents were the following: M30C: 2,4%, M75C: 2,8%; M75SC: 3,2%; M100C: 2,8%.

Test specimens were heated in an electric oven at 1°C/min. After reaching desired temperature, stabilisation length was the following: 2 hours (tests at 120 °C) and 1 hour (tests at 250, 400 and 600 °C). Specimens were then removed from the oven, wrapped with ceramic fibre insulator and then equipped with a deformation measure device allowing determining the deformation in the central area of the cylinders. The specimens were surrounded by two rings 10 cm from each other. The rings were connected to the samples by 3 steel points. 3 transducers located at 120 degrees measured the relative displacement of the rings.
The evolution of temperature fields between the removal of the oven and the end of the compression test was measured on samples equipped wit K thermocouples. Decline of temperature was considered low enough.

4. RESULTS OF THE TEST AND DISCUSSION

4.1 Stress/deformation curves

Determined stress - strain curves at the different temperatures on the 4 concretes are plotted in Fig. 1. We can observe, and this is an important result, that the 3 curves determined at each temperature and for each concrete present a weak dispersion. This result allows checking that test procedures can be reproduced.
From this results we determined the evolution of compressive strength and modulus of elasticity. These results are analysed hereafter.

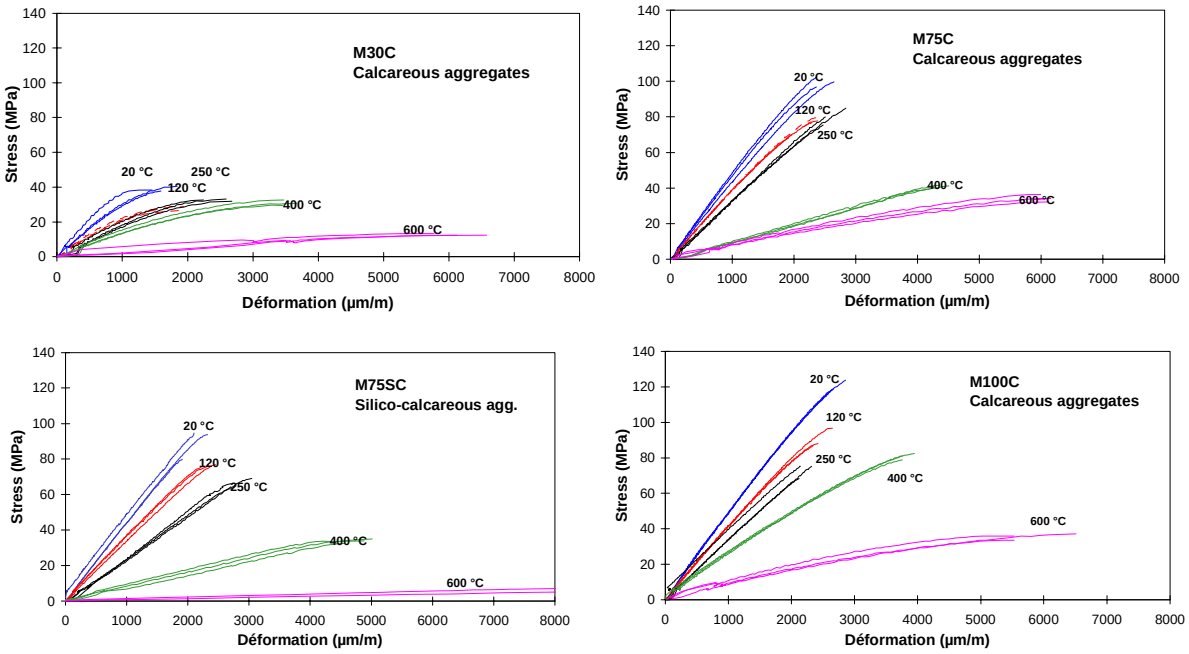

Fig. 1: Stress – strain curves of the concrete M30C, M75C, M75SC and M100C at different temperatures

4.2 Compressive strength

Compressive strength results are listed in Table 2. Relative compressive strengths are listed between brackets. Mean values are written in bolt police.
28 days water cured 160 x 320 mm cylinders and air cured 104 x 320 mm cylinders tested at 20 °C compressive strength present some discrepancies. However age, samples dimension and cure condition are different and should explain this difference. 28 days water cured 160 x 320 mm cylinders are higher to the expected nominal values. The compressive strengths of M75C are respectively for example equal to 107 MPa (160 x 320mm) and 100 MPa (104 x 320 mm). However, we decided to maintain the designation adopted by the French National Project BHP 2000. Compressive strengths difference between the two concretes M75C and M75SC is equal to 10 MPa. Although this difference is not unimportant, the influence of the nature of aggregates on the behaviour of the HPC will be discussed on the basis of the results obtained on these 2 concretes.

The evolutions of the mean values of the relative compressive strength are plotted versus temperature in Fig. 2. Results obtained by Diederichs and al [2] and Castillo and Durrani. [3] are plotted too. As in the present study, tests presented by these authors were carried out at elevated temperature and not after cooling.

	28 days water cured strength (MPa)	Compressive strength (MPa) and relative strength (%) (between brackets)				
		T = 20°C	T = 120°C	T = 250°C	T = 400°C	T = 600°C
M30C	37.3	41.7	27.6 (70,2)	32.5 (82,8)	29.8 (75,9)	12.4 (31,5)
	37.9	38.4	28.7 (73,2)	33.2 (84,6)	32.6 (83,1)	12.4 (31,5)
	36.4	37.7	26.5 (67,5)	33.1 (84,3)	31.1 (79,2)	13.3 (33,9)
	37.2	**39.3**	**27.6 (70,3)**	**32.9 (83,9)**	31.2 (79,4)	**12**.7 (32,3)
M75C	111.4	96.7	77.7 (77,9)	75.4 (75,6)	41.6 (41,7)	36.4 (36,5)
	105.3	102.9	78.6 (78,7)	80.0 (80,2)	41.3 (41,7)	34.3 (34,4)
	103.7	99.6	77.1 (77,3)	84.9 (85,1)	40.2 (40,3)	32.3 (32,3)
	106.8	**99.8**	**77.8 (78,0)**	**80.1 (80,3)**	**41.1 (41,2)**	**34.3 (34,4)**
M75SC	87.6	93.7	76.7 (85,8)	63.4 (83,1)	32.4 (42,5)	6.3 (8,3)
	94.8	79.9	75.8 (84,8)	69.1 (90,6)	33.9 (44,4)	7.4 (9,7)
	94.2	94.7	76.3 (85,3)	66.1 (86,7)	34.9 (45,8)	
	92.2	**89.4**	**76.3 (85,3)**	**66.2 (86,8)**	**33.7 (44,2)**	**6.9 (9,0)**
M100C	112.0	119.4	96.7 (80,1)	68.4 (56,7)	78.9 (65,4)	37.1 (30,7)
	112.0	119.0	88.6 (73,4)	75.3 (62,3)	82.6 (68,4)	33.6 (27,8)
	114.5	123.8	87.0 (72,1)	75.5 (62,5)	80.9 (67,0)	36.0 (29,9)
	112.8	**120.7**	**90.8 (75,2)**	**73.**1 (60,5)	**80.8 (66,9)**	**35.6 (29,5)**

Table 2: compressive strength and relative compressive strength (between brackets) at different temperatures

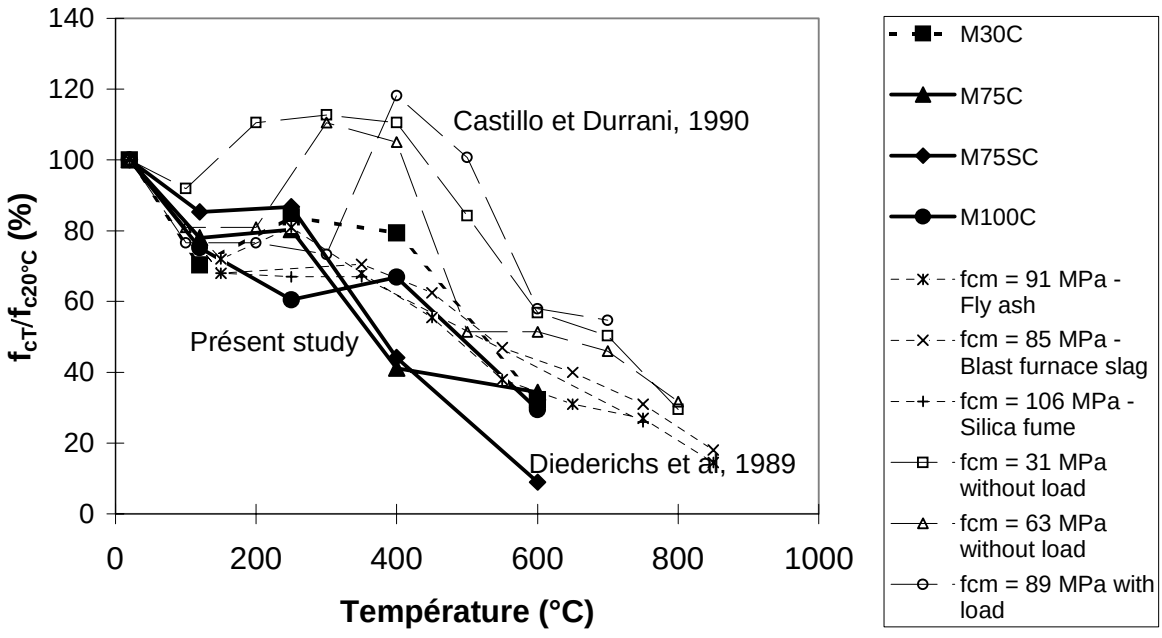

Fig.2: relative compressive strength vs. temperature

A general observation of Fig. 2 shows that the relative strength determined on the 3 HPC are in rather good agreement with those obtained by by Diederichs and al [2]. They are generally lower than those determined by Castillo and Durrani [3].

At 120 °C, the relative strength of the 3 concretes M30C, M75C and M100C containing calcareous aggregates are between 70 and 80 %. Relative strength of M75SC is equal to 85 %. These values are lower than those generally observed on normal strength concretes. At this temperature, codes, as the French "Document Technique Unifie", consider that relative strength is equal to 100 %. However, different authors observed that concrete can present a minimum in strength at 80 – 100 °C. This behaviour is attributed to the role of warmer, less viscous and dilated evaporable water (Khoury, [5]). Values determined at 120 °C on the 3 HPC are in good agreement with those obtained by Diederichs and al [2] and Castillo and Durrani [3]. These authors proposed several mechanisms that could explain the weakest relative strength of HPC. Diederichs and al suggested, for example, that their lower stress difference between cement paste and aggregates and their higher vapour pressure at this temperature could reduce the relative strength of HPC.
The influence of the aggregate nature on the strength of the 2 concretes M75C and M75SC is little significant. At 120 °C, only differences of aggregates thermal deformation and bonding between aggregates and cement paste should be able to explain mechanical behaviour differences between these two concretes.

At 250 °C free water (not chemically bounded) is removed from the material. At this temperature, we can observe that relative strength of M30C, M75C and M75SC are very closed from each others (between 80 and 90 %). These values are lower than that considered by codes for normal strength concrete. For example, French "Document Technique Unifie", considers that relative strength is equal to 100 % until 250 °C. However values between 80 and 90 % have been obtained on normal strength concrete. The obtained values on these 3 concretes are in rather good agreement with those obtained by Castillo and Durrani.

Tests on normal strength concrete and HPC at temperatures higher than 350°C show that strength generally decrease regularly to reach approximately 20 % at 850 °C. Many reasons can be at the origin of this decrease: chemical reactions, differential deformation between cement paste and aggregates, decrease of cement paste and aggregates bonding, cracks development, porosity increase, etc [2, 3, 4, 5]. At 400 °C, strength determined on the 3 HPC are lower than that determined on M30C. The last ones are in good agreement with those considered by codes. Relative strength of M100C increases between 250 °C to 400 °C. As at 250 °C, it is in rather good agreement with the result obtained by Diederichs and al on the 106 MPa HPC. The relative strengths of M75C and M75SC drop to 40 - 45 %. Therefore, at 250 and 400 °C, the relative strength of the 2 HPC do not seem sensitive to the nature of the calcareous and silico-calcareous aggregates.

At 600 °C, the relative compressive strengths of 3 concretes containing calcareous aggregates M30C, M75C and M100C, converge to 30 - 35 %. These values are slightly lower than those obtained by Diederichs and al. Samples of M75SC containing silico-calcareous aggregates were already cracked at the exit of the oven and before compression test. This behaviour is certainly due to the cleaving of flint rocks contained in these aggregates. Relative compressive strength of M75SC is very low (< 10 %).

4.3 Modulus of elasticity

The modulus of elasticity were determined by calculating the slopes between the origin and the points corresponding to: 500µm/m (20, 120, 250°C), 1000µm/m (400°C) and 4000µm/m (600°C). Results are listed in Table 3. Relative modulus of elasticity is listed between brackets. Mean values are written in bolt police. The evolutions of the mean values of the relative modulus of elasticity are plotted versus temperature in Fig. 3. Results obtained by Diederichs and al and Castillo and Durrani are plotted too.

Results show that modulus of elasticity of our 4 concretes decrease continuously from 20 C to 600 °C. Values at 600 °C are lower or equal to 15 %. M75SC present the smaller value (lower than 2 %).
Obtained values are again in rather good agreement with those determined by Diederichs and al.

	Modulus of elasticity (GPa) and relative modulus of elasticity (%) (between brackets)				
	T = 20°C	T = 120°C	T = 250°C	T = 400°C	T = 600°C
M30C	33.6	26.8 (74)	16.8 (47)	13.5 (37)	25.6 (7)
	42.7	24.0 (67)	22.5 (62)	10.0 (28)	23.7 (7)
	31.9	22.4 (62)	18.0 (50)	13.3 (37)	30.4 (8)
	36.1	**24.4 (68)**	**19.1 (53)**	**12.3 (34)**	**26.6 (7.4)**
M75C	48.3	40.7 (86)	33.8 (71)	9.4 (20)	7.3 (15)
	49.8	38.2 (80)	31.5 (66)	9.0 (19)	6.6 (14)
	44.3	39.6 (83)	31.7 (67)	10.1 (21)	6.3 (13)
	47.5	**39.5 (83)**	**32.3 (68)**	**9.5 (20)**	**6.8 (14.2)**
M75SC	45.0	34.0 (70)	23.1 (47)	6.9 (14)	0.6 (1)
	44.1	37.7 (77)	21.5 (44)	9.4 (19)	0.8 (2)
	53.4	38.1 (78)	22.0 (45)	8.5 (17)	
	48.8	**36.6 (75)**	**22.2 (45)**	**8.3 (17)**	**0.7 (1.4)**
M100C	52.2	41.2 (81)	33.9 (67)	26.9 (53)	7.3 (14)
	50.5	41.4 (81)	32.5 (64)	27.1 (53)	7.3 (14)
	49.8	41.9 (82)	33.8 (66)	26.4 (52)	8.1 (16)
	50.8	**41.5 (82)**	**33.4 (66)**	**26.8 (53)**	**7.6 (15)**

Table 3: modulus of elasticity and relative modulus of elasticity (between brackets) at different temperatures

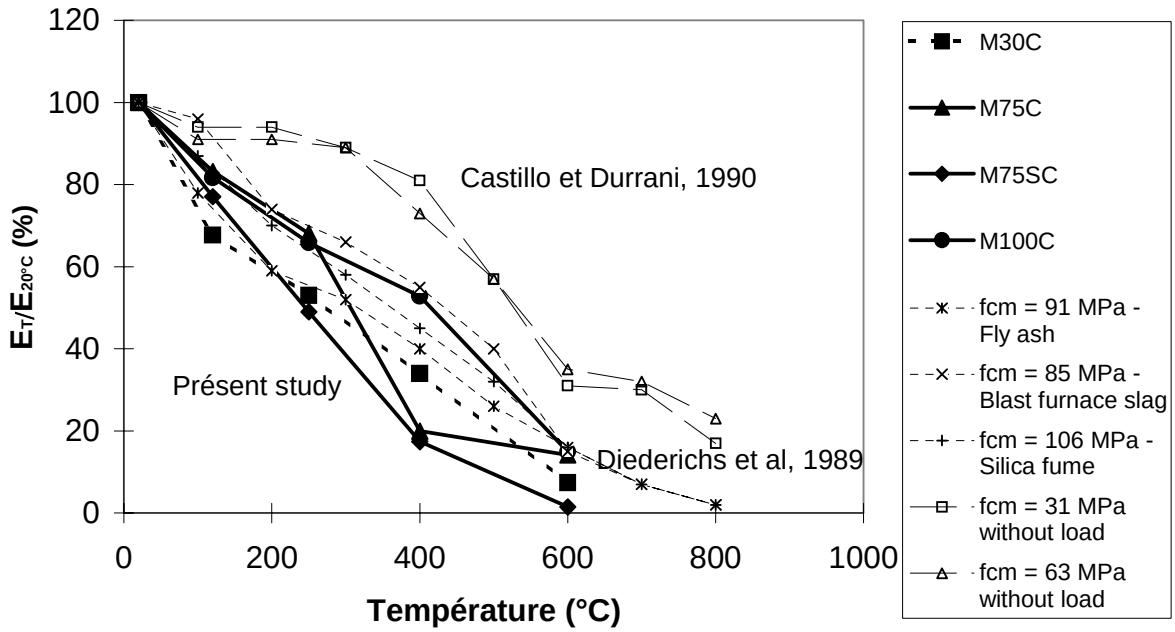

Fig.3: relative modulus of elasticity vs. temperature

5. Conclusions

Compression test have been carried out on 3 HPC and a normal strength concrete at 120, 250, 400 and 600 °C. Tests have been carried out on the bases of the RILEM recommendations. We observed that the 3 curves determined at each temperature and for each concrete present a weak. Relative compressive strength and modulus of elasticity of the 3 HPC at the different temperatures are in rather good agreement with those determined by Diederichs and al. They are generally lower than those determined by Castillo and Durrani. Relative strength are generally lower than that considered for normal strength concrete in codes like the French "Document Technique Unifie".

References

[1] RILEM. Compressive strength for service and accident conditions. Materials and structures. 28, p.410-414. 1995.

Izabela HAGER, Centre Scientifique et Technique du Batiment, France and Ecole Polytechnique of Cracow, Poland

[2] DIEDERICHS U., JUMPPANEN U. M. AND PENTALLA V. 1992. Behaviour of high strength concrete at elevated temperatures. Espoo 1989. Helsinki University of Technology, Department of structural Engineering, Report 92 p 72.

[3] CASTILLO C. ET DURRANI A. J. 1990. Effect of transient high temperature on high-strength concrete. ACI Materials Journal. Jan-Feb 1990, pp 47-53.

[4] JAHREN P.A. 1989. Fire resistance of high strength/dense concrete with particular reference to the use of condensed silica fume - A review. Proc. of Trondheim (Norway) 1989 Conference, pp 1013-1049.

[5] KHOURY G.A. 1992. Compressive strength of concrete at high temperatures: a reassessment. Magazine of Concrete Research. 44, n° 161, pp 291-309.

BDA 6.2

CEN/TC 250/SC 2/PT 1-2 Doc N 171

TUNNEL FIRE SAFETY

Kees Both
TNO, the Netherlands

SUMMARY

In forthcoming years, public and private transport in Europe requires large investments in infra-structural works. A significant part of the infra-structural works will consist of tunnels and other underground structures. Such structures have specific safety aspects. The safety of underground structures like tunnels, is a point of increasing concern, both in Europe and elsewhere.
Main reason is the increasing road and rail traffic and increasing tunnel lengths. New innovative safety measures have to be defined to avoid an increasing incident frequency in tunnels and to avoid increasing consequences of the incidents both in terms of causalities and material damage, including traffic obstruction.
This paper briefly reviews the various aspects involved in the assessment of the structural integrity. Results of extensive research into three major infra-structural works are be presented: the fire safety of the tunnels in the High Speed Link, Betuweroute and the Western Scheld tunnel in the Netherlands. The results incorporate full scale fire tests investigating the structural integrity of high strength concrete tunnel linings.

INTRODUCTION

In the Netherlands, a large number of tunnel projects is currently being undertaken, a.o. (1) the Betuweroute, (2) the High Speed Link and (3) the Westerschelde tunnel.

Ad (1) The Betuweroute is a 160 km double track freight railway linking the Port of Rotterdam directly to the European hinterland [1].
Tunnels and covering (to a total of 20 km) include:
- Botlek: double bore 1.9 km tunnel
- Barendrecht covering: 1.5 km long covering both the tracks of the Betuweroute and the High Speed Line - a total of nine tracks
- Pannerdensche Canal Tunnel
- Sophia rail tunnel: double bore 7.8 km tunnel

Ad (2) In the High Speed Link from Amsterdam to Paris, the Dutch track has a large amount of civil engineering constructions covering tunnels, bridges and viaducts. The most important tunnel is the Green Hart tunnel: a single bore 15 m diameter 8km long tunnel [2].

Ad (3) The Westerschelde tunnel is a double bore 6.5 km long tunnel. Every 250 m, a connecting tunnel provides access from one tube to the other [3].

Besides these tunnel projects, bored subway tunnels and stations are planned in Amsterdam (North-South Line) and a rail system connecting major cities in the Western urban area (Randstad Rail). Also south of Rotterdam, the Benelux tunnel crossing is extended with an second immersed tunnel, comprising a separate road and subway section.

A key issue is that sections of the above tunnels were to be constructed in water bearing soil, and the survivability of the tunnel linings with regard to their structural integrity following a potential severe fire, was of particular concern.

In the Netherlands, traditionally, tunnels were of the immersed type. The (normal weight) concrete quality for these types of tunnels is rather low (strength class up to C30). In the event of a fire, passive fire protection is applied on the roofs of the tunnel, extended to 1.0m over the walls. The main purpose of the passive fire protection is to limit the temperature rise of the (sagging) reinforcement in the roof, and thus prevent the premature collapse of the roof (development of a sagging plastic moment) and -as a consequence- leakage of the tunnel. This is schematically illustrated in Figure 1. Note that the walls are largely unprotected. The reason is that wall-reinforcement needs no or very little protection in thick walls.

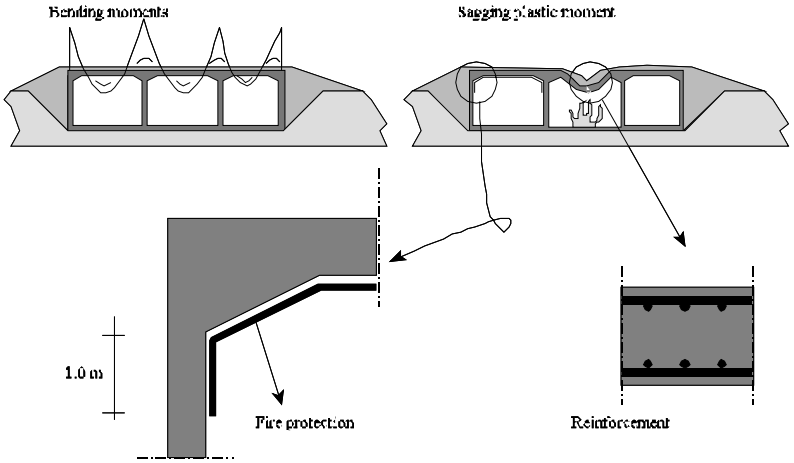

Figure 1 Protection of roofs and upper parts of the walls of immersed tunnels to limit the probability of structural collapse of the roofs in the case of fire.

Recently, another tunnelling technique is becoming popular in the Netherlands: bored tunnelling. Up to now, these tunnels are designed with segmented reinforced concrete linings. The reinforcement in the segments mainly functions during handling and during boring (jack pressures). After completion, the reinforcement in the segments is in fact obsolete; at least, the reinforcement is not there to take tension forces in sagging moment regions, because the concrete will be in compression (in ring direction). Another difference with respect to immersed tunnelling is that higher concrete strength classes are commonly applied (C50 and beyond). It is well known that -generally speaking- high strength concrete is more prone to so-called thermal spalling. Under thermal spalling is understood the sudden explosive disintegration of fire exposed concrete. Thermal spalling can be attributed to the combination of moisture clogging and stress clogging inside the concrete. The main function of the passive fire protection is therefore -only- to prevent explosive concrete spalling.

The behaviour of concrete under fire exposure is determined by the properties of the aggregates and the cement matrix, its moisture content, pore structure and loading, in addition to the rate of heating and maximum temperatures attained.

The occurrence of thermal spalling depends on several factors, such as:

- the temperature development at the exposed side and consequently the occurrence of thermal stresses due to (partial) restraint of thermal expansion;
- external forces leading to (compressive) stresses in the concrete element;
- concrete composition and material properties (permeability, porosity, thermal expansion coefficients of its constituents, thermal conductivity, specific heat, compressive strength, fracture energy, etc.), as well as the (free) moisture contents (important in this respect are therefore also the compaction and curing conditions).

The above indicates that in general the concrete cube or cylinder strength determined 28 days after concrete casting has only little direct relation to the sensitivity of the concrete to thermal spalling.

For the assessment of the damage level due to thermal spalling for concrete tunnel linings which in service life may be exposed to severe fires, up to now, no adequate design guidance is at hand. In some tunnel projects, limitations are given to the concrete cube or cylinder strength, but as mentioned above that is only a (small) part of the story. Consequently, experiments are needed to approve certain solutions.

Mitigating measures against spalling focus at the first and latter influencing factors indicated above. In this paper, the results are described of recent full scale fire tests. In section 2, mitigating measures aiming at reducing the heat flow into the tunnel lining are discussed. In section 3, mitigating measures aiming at improving the lining resistance to spalling are described. Conclusions are presented in section 4.

THERMAL INSULATION OF THE TUNNEL LINING

Thermal

As mentioned earlier, most tunnels in the Netherlands were of the immersed type. In most cases, thermal insulation was provided by placing a board type material inside the formwork, prior to concrete casting of the tunnel. In road tunnels through which hazardous goods may be transported (except for e.g. LPG), the Dutch Ministry of Transport requires the structural integrity to be assessed on the basis of a severe 2 hour hydro-carbon fire, with maximum temperatures reaching 1350 ^{0}C (the so-called RWS fire).

The Dutch Ministry of Transport had commissioned to TNO to investigate the effect of the moisture content in the concrete of typical Dutch immersed tunnel concrete (340 kg/m^3 CEM III; river gravel aggregate; wcf 0.5) on the sensitivity to thermal spalling, under RWS fire conditions. Fire tests on unloaded concrete slabs, protected with 27 mm calcium silicate board (Promatect-H) indicated that with relatively high moisture content in the concrete (some 6% by weight), in combination with low moisture content in the insulation material (some 3% by weight), no spalling occurred [4]. Previous tentative research on test specimens cannibalised from existing tunnels in the Netherlands in the winter time, as well as laboratory

tests indicated that the equilibrium moisture content of typical insulation materials is in the order of magnitude of 4-5 % by weight [5].

For the Westerschelde tunnel, the tunnel lining is made of -relatively- high strength concrete segments (C50-60; the concrete mix comprised CEM I (310 kg/m^3), river gravel (Rheinkies) and 80 kg/m^3 fly ash; wcf 0.36) with a thickness of 0.45 m and a width of 2 m. The tubes have a diameter of some 11 m. The tunnel is to be designed such that it can withstand the effects of the RWS fire, since it is open for the transportation of hazardous goods. RWS fire tests were conducted on full scale loaded segments. The loading, representative for the ground- and water pressure after completion of the tunnel, is applied by means of an internal pre-stressing system such that an overall uniform compressive stress (in ring direction) of some 12 N/mm^2 is achieved [6]. Results of the tests on protected tunnel segments are presented in Figure 2, in terms of measured concrete surface temperatures. The results of three tests are presented: with 23, 27 and 44 mm of calcium silicate board material (Promatect-H). Thermal spalling is indicated by the sudden sharp increase in temperatures; it occurred after some 30, 60 and 119 minutes of fire exposure. The later the onset of spalling, the more violent it appeared to be; also the thickness of the first pieces of concrete that spalled seemed to increase as the onset of spalling occurred in later stages of the fire.

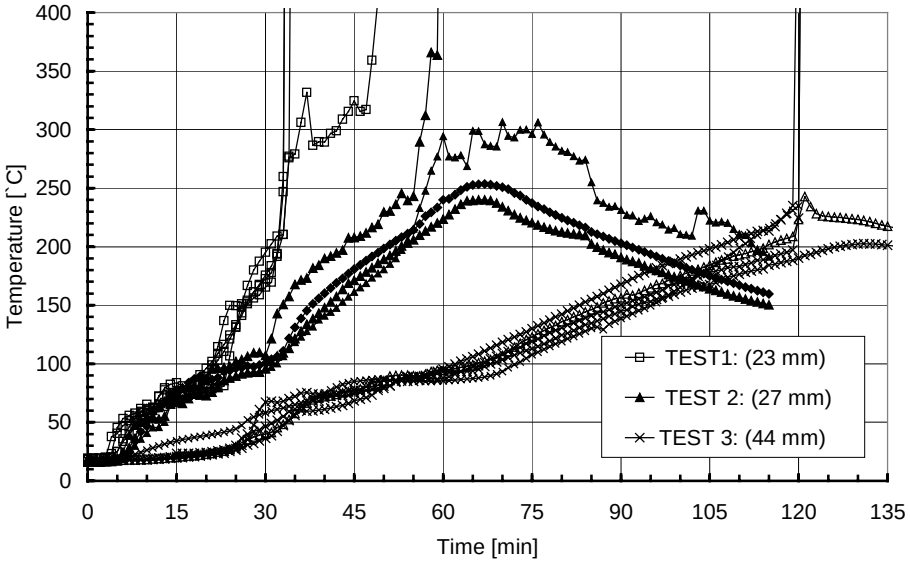

Figure 2 Results of RWS fire tests in terms of measured concrete surface temperatures: influence of board thickness.

From this Figure it becomes apparent that for the investigated cases, thermal spalling already occurs at temperature levels at the concrete surface ranging from some 160-220 ^{0}C. Note that the moisture contents of the concrete were some 4% by weight and for the board some 3% by weight.

The relevance of the moisture content in the insulation material was demonstrated in a fourth fire test for the Westerschelde tunnel project, on a similar loaded tunnel segment, protected with 51 mm layer of a cementitious vermiculite spray mortar (Fendolite MII). The moisture content was some 18% by weight. Apart from the insulation system, the test specimens and test arrangement was equal to the “Promatect-H” tests. Due to the unrealistically high moisture content in the insulation material [5], temperatures at the concrete surface did not rise above 100 ^{0}C within 2 hours of RWS fire exposure. After that period, temperatures gradually

increased up to nearly 300 ^{0}C during additional 3 hours of heating at 1200 ^{0}C, without any spalling [7]. Apparently the thermal gradients and heating rates in the concrete remained below critical levels.
Additional fire tests were performed with lower moisture contents in the Fendolite (some 4% by weight). Three tests, with a test arrangement identical to the "Promatact-H" tests, were performed: one with 42 mm and two with 45 mm. In the test with 42 mm, violent thermal spalling occurred after 170 minutes of fire exposure [8]. Due to the scatter in results, it is however extremely difficult to make conclusions about critical combinations of heating rate, thermal gradient and actual temperature level at the concrete surface, for this particular concrete and the applied external loading conditions. It is even more difficult to extrapolate to other concretes and other loading conditions and tunnel segment geometries.

Therefore, the Dutch Ministry of Transport also commissioned TNO to investigate the above mentioned assumption that the walls of immersed tunnels could be unprotected. For that purpose, a model was made of a part (2x2x0.8m) of an external wall of an immersed tunnel. The upper part of the test specimen (700 mm) was protected with Promatect-H (27 mm). External loading in compression was applied to a level of 10 MPa.

During the test on the loaded test specimen, no significant spalling occurred, only superficial damage occurred in the unprotected area.

The test underscores [9] that the hypothesis of unprotected walls (with the Dutch immersed tunnel concrete!) is justified; i.e. the structural integrity of the walls is not seriously affected in RWS fire conditions.

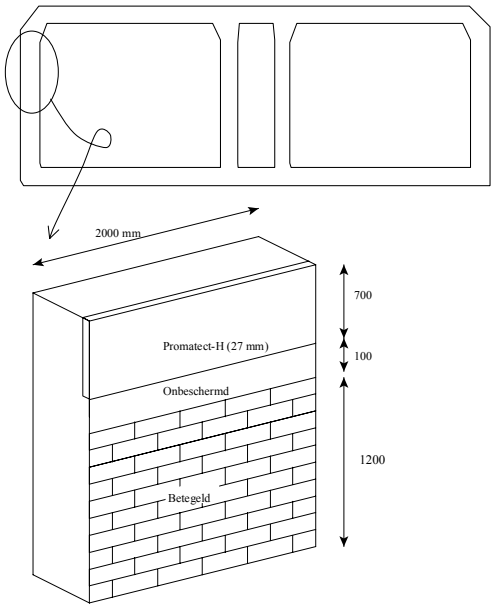

Figure 3 Test arrangement for wall of an immersed tunnel.

Effect of anchors

Anchorage systems used to suspend e.g. ventilators from the crown of the tunnel may cause problems. It is beyond the scope of this paper to address the failure mechanisms of the anchorage systems. However, in this paper, the adverse effect of the "heat leakage" into the concrete is discussed. It was found during tests for the Westerschelde tunnel that a sufficiently large heat leakage could invoke thermal spalling, despite the protection of the concrete surface with an insulation system. The separate fire tests were performed on loaded tunnel segments of running dimensions, under RWS fire conditions (for concrete mix details and the test arrangements and loading conditions, refer to the above mentioned "Promatect-H" tests). The tunnel segments were protected with 45 mm Fendolite MII (moisture content some 4% by weight); the anchorage systems were loaded to a realistic level at the onset of the fire tests, with a view to create realistic boundary conditions. The research is ongoing, but already revealed that for the investigated cases, anchorage systems with unprotected single M8 and M10 bolts, protruding the Fendolite MII, the risk of thermal spalling did not significantly increase. However in the case of an anchorage system based on M16 bolts and a

partly unprotected T- or L-steel plate (for suspension of ventilators), thermal spalling, reducing the structural integrity to an unwanted level, may indeed occur. Research is now focussing on improvement of the ventilator anchorage system, a.o. by reducing the area of unprotected steel. To that end, 3D FEM simulations were made to optimise the anchorage system with respect to heat leakage [10,11]. Some typical results are plotted in Figure 4. In that Figure, the temperature distribution after 2 hours of fire exposure for the bolt (for practical reasons modelled as a square bolt) and the steel T-plate are plotted.

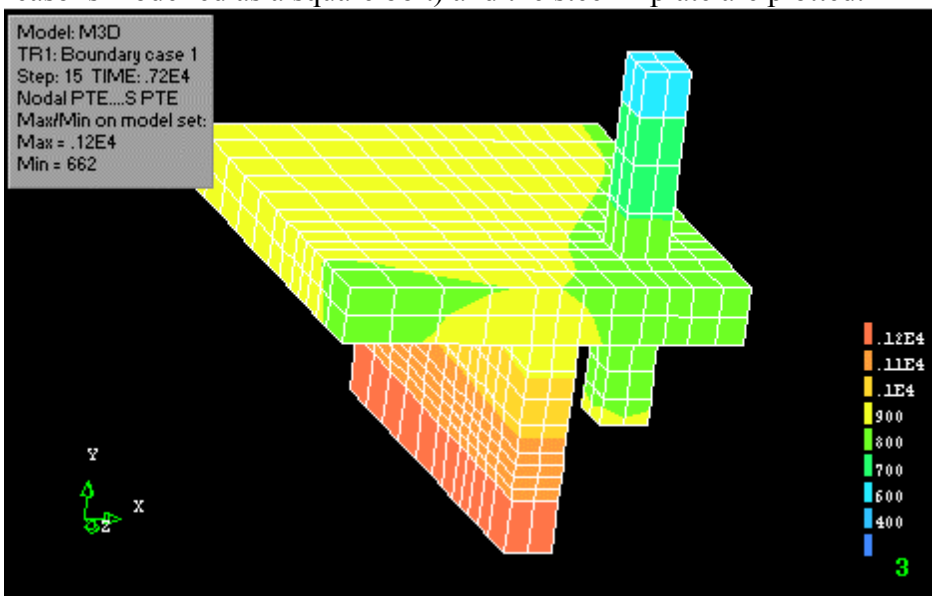

Figure 4 FEM simulation of penetration of heat via steel plate and M16 bolt.

Sprinkler ??

In the Betuwe route, the safety concept prepared by the Dutch Ministry of Internal Affairs, prescribes a sprinkler system in the tunnels to be built. TNO was asked to prepare indicative tests, with a view to determine any positive effect of the sprinkler on the structural integrity of the concrete lining in the event of a severe hydro-carbon fire which could not be extinguished by the sprinkler system. Indeed by means of hand calculations one could show that even a thin water-film on the concrete surface would be able to absorb the energy released from a severe hydro-carbon fire to such an extend that concrete surface temperatures would not exceed 100 ^{0}C. It is generally felt that the risk of loss of structural integrity due to thermal spalling is negligible at such low surface temperatures. A picture taken during the test is given in Figure 5.

Indicative fire tests on unloaded tunnel segments of running dimensions for the Botlek rail tunnel (concrete mix unknown) have shown that the hypothesis of water cooling of the concrete surface may indeed work. It is noted specifically that the tests were not meant to demonstrate the effectiveness of the sprinkler system with respect to its primary function: prevent fire spread from one tanker-wagon to the other [12].

Figure 5 “Sprinkler fire test”.

Based on the anchorage tests performed for the Westerschelde tunnel, it must be realised that even a small heat leakage may cause the onset of thermal spalling, which may lead to partial loss of functionality of the sprinkler system. Further research into this item is therefore highly recommended.

IMPROVING RESISTANCE OF CONCRETE TUNNEL LININGS TO THERMAL SPALLING

As an alternative to external mitigating measures, one could think of internal measures. In principle, there are three options to improve the resistance to thermal spalling:

1 increase the permeability (preferably during fire, to avoid durability problems);
2 increase the fracture energy;
3 decrease differences in thermal expansion coefficients between aggregates and matrix.

The advantage of improving the resistance of the tunnel lining is that also in the construction phase additional structural fire safety is obtained.

As an alternative to these three options, one might consider composite steel-concrete tunnel linings. A limited number of such tunnel linings were actually used (in the USA and in Japan). In the Netherlands a desk study was performed as part of a feasibility study for the second Coen tunnel near Amsterdam. Because of the fact that the desk study showed that the composite steel–concrete lining was less cost-effective, further research was temporarily cancelled [13].

The theory behind thermal spalling in concrete tunnel linings is not yet fully developed. It is however felt by the majority of researchers that the development of high vapour pressures is a key factor. Mitigating measures have aimed at increasing the permeability at elevated temperatures by adding low-melt point polypropylene fibres to the concrete mix (option 1).

Polypropylene fibres

In the international literature on thermal spalling, the application of low-melt fibres in the concrete mix has been reported as a possible measure to prevent or limit thermal spalling. However, some researchers have serious doubts as to the actual effect of the fibres as well as the practical application. For that reason, the Dutch Ministry of Transport commissioned TNO to investigate on the basis of indicative tests the effect of polypropylene fibres on the fire behaviour of concrete slabs. Two different fibres were tested on unloaded slabs (1.5x1.5x0.35m; moisture content some 4% by weight), under RWS fire conditions, using the Westerschelde tunnel concrete mix design: test specimen 1 had 2 kg/m^3 monofilament fibres (type “23", length 12 mm, diameter 18 μm) test specimen 2 had 2 kg/m^3 fibrillated fibres (type 12-60F, length 12 mm, diameter 60 μm). The test results showed that with monofilament the damage was only superficial, whereas with fibrillated fibres, the damage extended the whole heated surface and locally some 35 mm had spalled off [14].

The positive results with monofilament fibres lead to further research on loaded tunnel segments. For that purpose, 4 additional tests were performed with the same concrete mix, on loaded Westerschelde tunnel segments with running dimensions. The external loading amounted to 6 MPa; RABT-ZTV fire conditions were applied, with the modification that the gas temperatures after reaching 1200 ^{0}C were kept constant at that level up to 120 minutes. In

the 4 test specimens, the following dosages of fibres was used: 0, 1, 2 and 3 kg/m^3. It was found that the fibres had no significant effect on the compressive strength (some 60 MPa after 28 days) nor on the moisture content (4% by weight).

The results of the fire tests are presented below in terms of measured spalling depths [15].

Table 1 Recorded spalling depths (mm).

	0 kg/m^3	1 kg/m^3	2 kg/m^3	3 kg/m^3
Average	95	37	32	7
Minimum	5	0	0	0
Maximum	265	95	90	25
Standard deviation	65	26	29	8
Characteristic	203	80	79	20

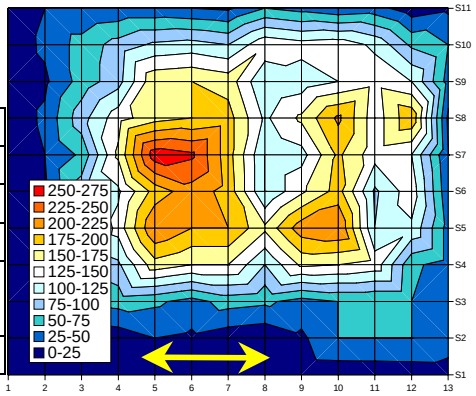

Figure 6 Spalling depths test 1 (0 kg/m^3)

From the point of view of structural integrity in fire, the test results suggest for the investigated cases the following conclusions:

- without any measures, the structural integrity can not be maintained;
- the thermal spalling seems to be controllable using polypropylene fibres;
- usage of polypropylene fibres to maintain structural integrity in fire deserves further attention in research programmes so as to be able to optimise in dosage and fibre type for different applications (loading and heating conditions, concrete mix, …);
- the workability of the mortar and durability of the concrete are items for further research.

Steel fibres

As thermal spalling is in fact a concrete cracking process, another way of mitigating damage could be by introducing steel (fibre) reinforcement (option 2). One must realise however that due to restraint to thermal expansion a complex stress situation occurs, with compressive stresses in the concrete close to the heated surface and tensile stresses further away from the heated surface. This situation may become critical reinforcement allows the development of large tensile forces.

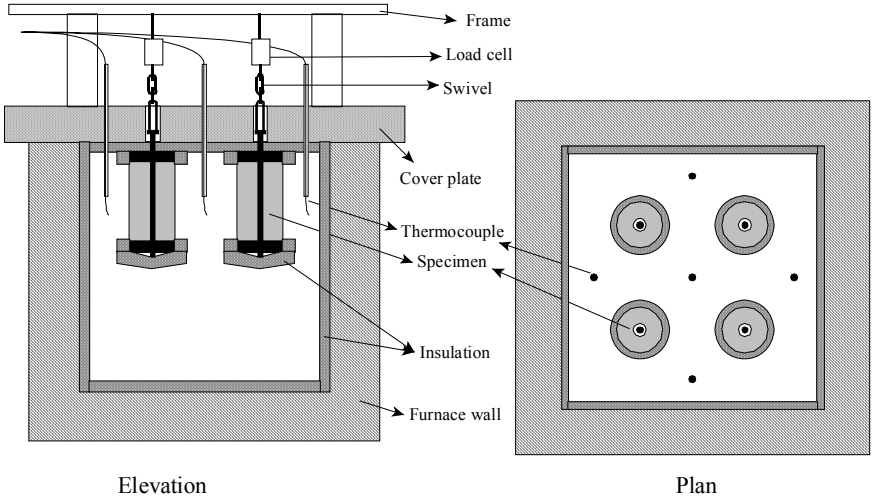

Figure 7 Test arrangement cylinder tests.

Results of recent tests have suggested however that by adding steel fibres, spalling could be stopped. In a study commissioned by ITM, TNO first performed indicative fire tests to select the most appropriate mix (with and without polypropylene and steel fibres; C30 and C50 concrete). The polypropylene fibres

where of the coarse fibrillated type, to an amount of 900 gr/m^3. For the steel fibres, 50 kg/m^3 was used. The indicative tests were done using 235 mm diameter, 500 mm long, cylinders, which were pre-stressed to 17 MPa. In the indicative cylinder tests, ting conditions where according to the German RABT-ZTV standard (hydro-carbon), with a modification that the maximum temperatures where kept constant at 1200 ^{0}C for 2 hours. The test set-up was as depicted in Figure 7. By determining the weight loss, the spalling (rate) could be monitored during the fire tests. From the indicative tests it became apparent that the fibrillated fibres (at an amount of 900 kg/m^3), for the investigated cases, could not significantly improve the resistance to thermal spalling [16]. On the other hand, the steel fibres did enhance the fire performance. It was therefore decided, also on the basis of other practical reasons, to select the C50 mix for further investigation.

For that purpose, large scale segments were cast, with a thickness of 450 mm, for a tunnel with an internal diameter of 9 m. The tunnel segments were loaded to a ring stress level of 15 MPa. The test was duplicated with a view to investigate the scatter in results.
The damage results were: average spalling depth of some 30 mm and standard deviation of some 20 mm (yielding a characteristic spalling depth of some 60 mm). The main conclusion was that although spalling was not completely prevented, the spalling seemed “controllable” by applying steel fibres. After cooling down, cores were taken from the test specimens to be used in microscopic analysis . This analysis revealed an additional layer of un-spalled, yet, damaged concrete of some 50 mm. This means that during after a severe hydrocarbon fire of the RABT-ZTV type, some 110 mm must be considered as lost. For the investigated case, this was considered as feasible [17].

Additional problems arise due to the fact that by adding fibres, either steel and or polypropylene, the workability and/or the durability of the concrete may be adversely affected. Recent research aims therefore at combining fibres with other measures to improve for instance frost-resistance. It is considered of vital importance that a proper numerical model is developed, allowing to investigate the physical mechanisms and its relative importance, resulting finally in adequate combinations of mitigating measures. The Dutch concrete industry is preparing plans to investigate such a “cocktail” approach.

NOMINAL FIRE CURVES FOR THE ASSESSMENT OF THE STRUCTURAL INTEGRITY OF TUNNEL LININGS

A realistic fire description can not be done in terms of nominal temperature time curves. Indeed a large number of factors would influence the temperature distribution in tunnels (ventilation, thermal inertia of the lining, fuel type and distribution, fire spread to other objects (cars, trains, ...), effects of active measures like sprinklers, etc.). The main factor is felt to be the fuel type and its distribution (area) inside the tunnel, since these will determine to a large extent the heat release rate (MW). In design, to determine for each tunnel a realistic fire description is an impossible task, and design would be hampered.

For structural design therefore, simplifications can and should be made, as is also done for e.g. buildings. For buildings, the fire safety is assessed by a "classification system" based on the ISO curve. The required fire resistance times (at 30, 60, 90, 120, 180, 240 min) depend e.g. on the "value", the height and complexity and use of the building and are primarily meant to allow for egress of occupants and intervention of the fire brigade.

In the Netherlands, a deterministic 2h 300 MW pool fire scenario (representative for a leaking crashed 50 m^3 petrol tanker) was agreed upon for immersed concrete tunnels through which limited hazardous goods are allowed to be transported, and a scale 1:2 test was developed to determine the effect of thermal insulation on the temperature development in the concrete linings. The tests indicated that, with an insulated ceiling gas temperatures could reach 1200-1400 ^{0}C. The curve extracted from these tests is the so-called RWS fire.
It should be noted that above 1100-1200 ^{0}C, a significant number of ordinary building materials will disintegrate and would therefore be inappropriate to perform a thermal insulating function in higher temperature regimes.

For concrete tunnel linings, the RWS and the newly proposed (by PIARC) "modified hydro carbon fire" denoted as HCM fire ($(T(t) = 1280 * (1 – 0.325*\exp(– 0.167*t) – 0.675*\exp(– 2.5*t) + 20)$) will produce very similar safety levels, since the penetration of heat will be very similar and as also in the first minutes both curves rise very quickly, the effect of such fire scenarios will be similar as regards concrete spalling. Technically, the choice seems therefore rather arbitrary.

Both the RWS and HCM curve are hydro-carbon fires; whereas e.g. the ISO-834 curve is a cellulosic fire, which shows a much slower increase, and would not reach (only after very long fire exposure times) temperatures in excess of 1200 ^{0}C. This means that by applying an ISO fire scenario, the risk of concrete spalling is underestimated in the case of tunnels through which hydro-carbons are allowed to be transported. The suggestion is to use only one fire curve (RWS or HCM) and vary in exposure time to underscore differences in "economic value" of the tunnel and length of the tunnel (ease for fire brigade to intervene; and for long underwater tunnels also for the safety of end-users!).

Finally, it is a good idea to try to distinguish in fire exposure times. Although the recent fires have shown fire exposure times can be much longer than 2 h. If reinstatement and retrofitting at acceptable costs is an issue for a certain tunnel, than it would be wise to -besides an RWS/HCM requirement of 2 h- also to consider requiring sufficient resistance to longer fire exposure times (at lower temperatures), up to say 4 to 8 h, especially for long tunnels and single bore tunnels for which it will be difficult for the fire brigade to reach the fire zone.

CONCLUSIONS

If the structural integrity in and after fires in tunnels is a point of concern, e.g. in the case that tunnels are located in water bearing soil, or when part(s) of the tunnel structures are used to maintain evacuation and rescue routes and ventilation channels, there are a number of options to maintain the integrity.
In the case of concrete tunnel linings, loss of integrity due to thermal spalling is a point of concern in the case that severe hydro-carbon fires can and must be expected in the tunnel.
In this paper the most current options to maintain the structural integrity during hydro-carbon fires are discussed on the basis of results obtained in large scale fire tests:

- application of passive fire protection by using thermal insulation;
- improving the resistance to thermal spalling by adding polypropylene and or steel fibres to the concrete;
- application of sprinklers.

The project organisations of the large tunnel projects currently undertaken in the Netherlands have commissioned TNO to investigate these options. It appeared from the tests that in all

cases thermal spalling can be prevented or limited to acceptable levels; it is however premature to draw general conclusions for other situations (other concrete mixes, other heating and loading conditions etc.). The main reason is that the thermal spalling mechanism is only qualitatively understood and still not fully quantitatively. Further research in this area is highly recommended; the alternative is costly full scale testing for every tunnel project and consequently limited possibilities to investigate alternative mitigating measures. Finally research is recommended with a view to be able to determine the positive secondary effect of sprinklers on a more realistic scale.

FUTURE

Obviously, the structural integrity is only one out of many issues to be dealt with in the case of fires in tunnels. It is beyond the scope of this paper to address these issues. The European Commission has however emphasised the relevance of addressing all issues related to fires in tunnels. In fact three projects are recently granted in the scope of the 5th Framework Programme (the EU research and development programme): a thematic network (Fire In Tunnels – FIT) and two R&D projects (Durable and Reliable Tunnel Structures – DARTS; cost-effective, sustainable and innovative UPgrading methods for fire safety in existing TUNnels - UPTUN). In these projects, a.o. human factors and active suppression systems will be investigated and evaluated. FIT and DARTS have started this year; UPTUN is likely to start by the end of this year, or early next year. In all projects, active dissemination is dealt with in dedicated tasks or work-packages, which no doubt will be brought to the attention of all those interested in future conferences and seminars.

REFERENCE LIST

1 www.betuweroute.nl
2 www.hslzuid.nl
3 www.westerscheldetunnel.nl
4 C. Both, et al, “Brawat II: spalling behaviour of a wet concrete slab with river gravel aggregate, protected with a dry Promatect-H, under RWS fire conditions”, TNO report 99-CVB-R2155, 1999.
5 Castenmiller, C.J.J., "The hygroscopic equilibrium moisture content of Fendolite M2 spray cementitious vermiculite mortar", TNO report 1999-BT-BK-R0203, 1999.
6 Both, C., “Experimental research into passive fire protection measures for the Westerschelde tunnel, on the basis of the RWS fire; part 1 Promatect-H”, TNO report 99-CVB-R0001, 1999.
7 Both, C., "Experimental research into passive fire protection measures for the Westerschelde tunnel, on the basis of the RWS fire; part 2 Fendolite MII", TNO report 99-CVB- R1478, 2000.
8 Both, C., "Experimental research into passive fire protection measures for the Westerschelde tunnel, on the basis of the RWS fire; part 3 additional tests with Fendolite MII", TNO report 99-CVB- R1478, 2000.
9 Both, C., “Brawat 3: research into the spalling behaviour of a wall in an immersed tunnel, loaded in compression”, TNO report 2001-CVB-R03264, 2000.
10 Wolsink, G.M., “Ministry of Transport, Memo, Penetration of heat through thermal insulation of the Westerschelde tunnel, caused by the ventilator anchorage system”, 2001.

11 Both, C., “FEM simulation of anchorage system”, TNO memo-report, 19-04-2000.
12 Berg, G. van den, et al, “Indicative fire tests Betuweroute tunnels”, TNO report 2000-CVB-R01106, 2000.
13 Both, C, et al, “Tunnel linings in steel and composite steel-concrete”, Bouwen met Staal (Building in Steel) number 157, 2000.
14 Both, C., et al, “Brawat II: spalling behaviour of an unprotected wet concrete slab with river gravel aggregate and polypropylene fibres, under RWS fire conditions”, TNO rapport 99-CVB-R2154, 1999.
15 Both, C. “Indicative experimental determination of the structural behaviour of loaded tunnel segments with Monofilament polypropylene fibres, on the basis of the RABT-ZTV fire”, TNO report 2000-CVB-R00702, 2000.
16 Fellinger, J.H.H. and Both, C, “Small scale fire tests in determining the sensitivity to spalling of concrete samples of various mixtures subjected to RWS heating curve” , TNO report 97-CVB-R1463, 1997.
17 Both, C., “Experimental determination of the behaviour of loaded B65 (C50) steel fibre concrete tunnel segments for the Hubertus tunnel on the basis of the RABT-ZTV fire”, TNO report 99-CVB-R1097, 1999.